

Print ISSN : 2395-1990

Online ISSN : 2394-4099

www.ijsrset.com



First International Conference on Smart Technologies, Communication & Robotics

ICSCR- 2023

Date : 20th and 21st July, 2023

Organised by

Department of Electronics and Communication Engineering,
East Point College of Engineering and Technology,
Jnana Prabha Campus, Virgonagar Post, Avalahalli,
Bangalore, Karnataka, India

VOLUME 10, ISSUE 10, JULY-AUGUST-2023

**INTERNATIONAL JOURNAL OF SCIENTIFIC
RESEARCH IN SCIENCE,
ENGINEERING AND TECHNOLOGY**

Scientific Journal Impact Factor : 8.154

Email : editor@ijsrset.com Website : <http://ijsrset.com>

**First International Conference on Smart Technologies,
Communication & Robotics
20th & 21st July 2023**

Organized by

Department of Electronics and Communication Engineering, East Point
College of Engineering and Technology, Jnana Prabha Campus, Virgonagar
Post, Avalahalli, Bangalore, Karnataka, India

In association with

International Journal of Scientific Research in Science, Engineering and
Technology

Print ISSN : 2395-1990 Online ISSN : 2394-4099
Volume 10, Issue 9, November-December-2023

Published By

Technoscience Academy



GENERAL CHAIR

DR YOGESH G S
HOD & PRINCIPAL, EPCET

ORGANIZING CHAIRS

DR ANITA R
DR CHANDRAPPA D N
ASSOCIATE PROFESSOR

COORGANIZING CHAIR

DR K HARSHAVARDHANA REDDY
ASSOCIATE PROFESSOR



**Dedicated to our
Beloved
Honorable
Founder Chairman**

**Late Dr. S.M. Venkatpathi
Hon. Founder Chairman ,EPGI
Bengaluru (1955-2017)**



Smt.B.L Ramadevi Venkatpathi

**Chairperson,
East Point Group of Institutions, Bengaluru,
Karnataka, India**



It is indeed our pleasure and privilege to host the First International conference on Smart Technologies, Communication & Robotics 20th-21st July 2023 at EPCET, Bangalore.

This conference provides a platform which brings Academicians and Research Scholars from across the country under one platform to discuss about their latest research ideas, results, potential applications in the areas of Electronics & Communication Engineering.

I extend my best wishes to entire organizing team and committee members in bringing out this proceeding on the occasion of the International conference. I extend my greetings and best wishes to all the participants and wish this conference a grand success.

Sri. S. V Pramod Gowda

**CEO,
East Point Group of Institutions, Bengaluru,
Karnataka, India**



It is a great pride to host the First International Conference on “Smart Technologies, Communication & Robotics” 20th-21st July 2023 at EPCET, Bengaluru.

The emerging technologies are the key to future socio-economic growth of any developing country and today's challenge is to build cost effective solutions using recent technological developments.

This conference offers a platform for Research scholars, Faculty and Students to present and discuss their latest research ideas which will go a long way in enriching the knowledge to generate new ideas and solutions for the upcoming challenges.

I wish the participants of this conference to come out with new inventions and innovative ideas which will contribute for the advancement of global technology. I wish all the success to the conference.

Sri. S. V Rajiv Gowda

**CEO,
East Point Group of Institutions, Bengaluru,
Karnataka, India**



It is a great pride to host the First International Conference on "Smart Technologies, Communication & Robotics" 20th-21st 2023 at EPCET, Bengaluru.

The emerging technologies are the key to future socio-economic growth of any developing country and today's challenge is to build cost effective solutions using recent technological developments.

This conference offers a platform for Research scholars, Faculty and Students to present and discuss their latest research ideas which will go a long way in enriching the knowledge to generate new ideas and solutions for the upcoming challenges.

I wish the participants of this conference to come out with new inventions and innovative ideas which will contribute for the advancement of global technology. I wish all the success to the conference.

Dr Prakash S
Senior Vice President,
East Point Group of Institutions, Bengaluru,
Karnataka, India



I am happy to know that Department of Electronics and Communication Engineering is organizing the First International conference on "Smart Technologies, Communication & Robotics " 20th-21st July 2023 at EPCET, Bangalore.

The Conference provides an open forum for scientists, Researchers and Engineers to exchange the information on innovations and research advancements in the areas of Electronics and Communication Engineering, I hope that this conference will go a long way in enriching the knowledge and it will generate new ideas among the Researchers.

I appreciate the efforts and dedication of the organizing committee for organizing this Conference and I hope the deliberations would benefit all the students and faculty.

I wish this conference a great success

Dr Yogesh G S

**Principal & HOD ECE,
East Point College of Engineering & Technology,
Bengaluru, Karnataka, India**



I am happy to know that Department of Electronics and Communication Engineering is organizing the First International conference on "Smart Technologies, Communication & Robotics" 20th-21st July 2023 at EPCET, Bangalore.

The Conference provides an open forum for scientists, Researchers and Engineers to exchange the information on innovations and research advancements in the areas of Electronics and Communication Engineering, I hope that this conference will go a long way in enriching the knowledge and it will generate new ideas among the Researchers.

I appreciate the efforts and dedication of the organizing committee for organizing this Conference and I hope the deliberations would benefit all the students and faculty.

I wish this conference a great success

DEPARTMENT VISION

The Department aspires to be a center of excellence in Electronics and Communication Engineering to develop competent and ethical professionals through holistic development.

DEPARTMENT MISSION

- To impart quality education and provide a conducive environment for innovation and Research.
- To develop skills to meet scientific, technological, and socio- economic needs.
- To inculcate professional ethics, teamwork, leadership qualities, and lifelong learning.

INDUSTRIAL ADVISORY COMMITTEE

Dr. Vikram T. G.

Embedded Staff Engineer II and Scientist, Enercon Technologies, Pennsylvania, USA.

Mr Soumen Das

Scientist F, LRDE, DRDO, Bengaluru.

Dr. Rajeev Kamal

Sr. Solution Engineer, Samsung, (IT&D), INDIA

Mr Dinesh

Principal Engineer, Microchip, Bengaluru.

Dr K Vishwanath

Sr. Software Engineer, Accenture Pvt Ltd, Bengaluru.

Mr Bhanuprakash Dixit B S

Associate Manager, CoreEL Technologies, Bengaluru.

ACADEMIC ADVISORY COMMITTEE

Dr. Radurakanth Sollapur

Professor & Chair of Quantum Electronics, Friedrich Schiller University Jena, Germany.

Dr. Muralidar Kulkarni

Professor, Dept. of ECE, NITK Surathkal, Mangalore.

Dr. Basavraj Talawar

Professor, Dept. of CSE, NITK Surathkal, Mangalore.

Dr. Hariprasad S. A

Director - Faculty of Engineering & Technology, Jain University, Bengaluru.

Dr. S. G. Hiremath

Professor, Dept. of ECE, EWIT, Bengaluru.

ORGANIZING COMMITTEE

Dr Anita R

Associate Professor, Department of ECE, EPCET

Dr Chandrappa D N

Associate Professor, Department of ECE, EPCET

CO-ORGANIZING COMMITTEE

Dr K Harshavardhana Reddy

Associate Professor, Department of ECE, EPCET

ABOUT INSTITUTE

East Point College of Engineering and Technology (EPCET) is a renowned institution established in 1999 by M. G. Charitable Trust in Bangalore. Affiliated to Visvesvaraya Technological University (VTU), approved by AICTE & Accredited by NBA, EPCET offers a wide range of undergraduate and postgraduate programs in disciplines such as Artificial Intelligence and Data Science, Computer Science and Engineering, Information Science and Engineering, Electronics and Communication Engineering, Mechanical Engineering, and Civil Engineering. With a strong faculty team of over 150+ members, including Ph.D. holders, EPCET is committed to providing quality education and research opportunities to its more than 2000 students. The college emphasizes industry collaborations and offers accredited programs with Industry- Institute integrated learning initiatives through partnerships with leading companies like Salesforce, UiPath, VMware, AWS, Texas Instruments, ARM University, CISCO. EPCET boasts state-of-the-art infrastructure with modern classrooms, well-equipped laboratories, and a Wi-Fi-enabled library housing a vast collection of books and technical journals. The college actively encourages faculty participation in seminars and conferences, fostering a culture of continuous learning and keeping up with industry trends. The college campus provides a vibrant environment for student development, offering opportunities for intercollegiate sports activities, cultural events, and student clubs. EPCET's multi-college campus facilitates interdisciplinary interactions among students from various fields, fostering a holistic educational experience. EPCET is dedicated to preparing students for successful careers by offering internships in reputed industries and ensuring a high job placement rate, with graduates securing positions in esteemed companies like VMware, Cognizant, Infosys, and more. The college also promotes entrepreneurship, with several alumni successfully establishing their own start-ups. With its ambitious vision and mission, EPCET continuously adapts to newer concepts in teaching, learning, and student assessments. The college aims to enhance students' satisfaction levels through a holistic approach to education, focusing on academic excellence, industry relevance, and overall student development. Join East Point College of Engineering and Technology and unlock your potential for a successful career in the dynamic world of technology.



ABOUT THE DEPARTMENT

The Department of Electronics and Communication Engineering (ECE) started in the year 1999 with 60 intake, with the idea of endowing young people with the necessary technical knowledge and professional skills needed to address the challenges in the rapidly growing field of Electronics and Communication Engineering and promoting research in this area. Currently, the Department offers B.E in Electronics and Communication Engineering with an intake of 120 students, M.Tech in VLSI Design and Embedded Systems with an intake of 16 students. The major areas of faculty expertise of the department include Digital Electronics and Communication Systems, Optical Communication and Networks, Signal Processing, Image Processing, Power Electronics, Microwaves, VLSI and Embedded Systems. The department houses a Research Center affiliated to Visvesvaraya Technological University. The department is involving in wide range of research activities supported by grants received from LRDE-DRDO, VGST and KSCST. The department has industry collaboration under Industry Institute Integrated Learning Program (IIILP) such as Cisco Network Academy, ARM University Program, Texas Instruments Innovation Lab to name a few.

Email Phone

info@eastpoint.ac.in +91 72042 29999
admissions@eastpoint.ac.in

Address :Jnana Prabha, East Point Campus, Virgo Nagar Post, Avalahalli, Bengaluru-560049,
Karnataka

<https://www.epcet.ac.in>

CONTENTS

Sr. No	Article/Paper	Page No
1	Machine Learning based Agriculture Bot Dr. Pradeep Kumar N S, Mr Suhas S K, Dr. Girish H, Mr B C Divakara, Mrs.K Revathi, Mrs. Swetha C S	01-08
2	Deep Learning Techniques for Detection of Deepfakes Deshagouni Manasa, Vasudev Dehalwar	09-18
3	IOT Based Vehicle Accident Prevention and Detection System Using Raspberry-Pi Rahul Devnath Tiwari, P. P. Tasgaonkar	19-29
4	Scalable Design and Implementation IP for Advanced Extensible Interface (AXI) Protocol Kaveri A. Sangamnerkar, Yogita D. Kapse, Nilima R. Kolhare	30-35
5	A GSM-Based System for Vehicle Collision Detection and Alert Dr. Pradeep Kumar N S, Suhas S K, Dr. Girish H, Mrs. Dhivya Karunya S, Mrs. K Revathi, Mrs. K Gayathiri	36-44
6	Design and Analysis of Parallel Slotted Multiband Microstrip Patch Antenna for Wireless Applications Sreenvas Naik, Kiran Kumar K , Arun Kumar G, Chandrappa D N	45-51
7	Performance Analysis of Fiber Optic Link Using Hybrid Dispersion Compensation Technique Balgopal Raju, Tusharkant Panda	52-58
8	Effect of the Slot and Dielectric Materials on The Performance of Rectangular Microstrip Antenna Anita R, Jayanthi Kumari T. R, Yogesh G.S	59-76
9	A Short-circuit Model Based on Artificial Neural Network and Artificial Bee Colony Algorithm for SiC MOSFETs Dr. Rajesh L, Praveen Kumar K C, Malini V L, Kavitha A	77-84
10	IOT based Contactless Temperature using Raspberry Pi Anushree N R, Nilu Mishra, Kavitha L, Dr. Nandini V L	85-93
11	Blackfin Processor Boom to Embedded System Nilu Mishra, Anushree N R, Kavitha L, Chaitali Darode	94-99
12	Selection of Suitable Filter Parameters for Denoising Breast Thermograms Using Anisotropic Diffusion Filter Vijaya Madhavi M, Vetrikani R, Malini V L	100-107
13	Sign Language Recognition System based on posture using Seer pipe Radhamani R, Praveen Kumar K C	108-116
14	Energy Conservation through Energy Audit in LT2 Consumers Avinash B C, Kiran Kumar Kommu, Rajesh K	117-124

Machine Learning based Agriculture Bot

Dr. Pradeep Kumar N S¹, Mr Suhas S K², Dr. Girish H³, Mr B C Divakara³, Mrs.K Revathi³, Mrs. Swetha C S³

¹Professor, Department of ECE, SEACET, Bengaluru, India

²Associate Professor, Department of ECE, Cambridge Institute of Technology, Bengaluru, India

³Assistant Professor, Department of ECE, SEACET, Bengaluru, India

ABSTRACT

Diseases on plants cause significant damage and economic losses in crops. Subsequently, reduces the diseases on plant by early diagnosis results in substantial improvement in quality of the product. Incorrect diagnosis of disease and its severity leads to inappropriate use of pesticides. The goal of proposed system is to diagnose the disease by using image processing and artificial intelligence techniques on images of plant leaf. This system is divided into two phases, in first phase the plant is recognized on the basis of the features of leaf, it includes preprocessing of leaf images, and feature extraction followed by ANN based training and also classification for recognition of leaf. In second phase the classification of disease which is present in the leaf is done, this process includes K- Means based segmentation of defected area, feature removal of defected portion and the ANN based classification of disease.

Keywords : Artificial Neural Networks (ANN), Conventional Neural Networks (CNN), Artificial Intelligence (AI).

I. INTRODUCTION

In Agriculture sector plants or crop cultivation have seen fast development in both the quality and quantity of food production, however, the presence of destructive insects and diseases on crops especially on leaves has hindered the quality of agricultural goods. If the presence of pests on crops and leaves is not checked properly and the timely solution is not provided then the quality and quantity of food production will be reduced, which results in upsurge in poverty, food insecurity and the mortality rate . This severe effect can disturb any nation's economy especially of those where 70% of the inhabitants rely on the products from the agricultural sector for their livelihood and endurance. One of the major problems for agriculturists is to lessen or eradicate the growth of pests affecting crop yields. A pest is an organism that spreads disease, causes damage or is a nuisance.

The most frequent pests that affect plants are aphids, fungus, gnats, flies, trips, slugs, snails, mites and Caterpillars. Pests lead to sporadic outbreaks of diseases, which lead to famine and food shortage. According to H. Al-Hiary et al in most of the countries farmers are used to detect pests manually through their observation of naked eyes, which requires continuous monitoring of the crop stem and leaves, which is a difficult labor intensive, inaccurate and expensive task for large farms. Further the early detection of diseases

on plants is really required as a very small number of diseased leaves can spread the infection to the whole batch of fruits and vegetables and thus affects further storage and sales of agriculture products. This effect of plant diseases are very destructive as a lot of farmers were discouraged to the point where some decided to give up the work of crop cultivation. There is therefore a need to identify these diseases at an early or superior stage and suggest solutions so that maximum harms can be avoided to increase crop yields. The applications like plant recognition, crop yield estimation, soil quality estimation etc. With the existence of massive volume of plant species and their use in various fields, the quality of agricultural products has become a major issue in agriculture sector.

Image processing technique such as machine vision system has been proven to be an effective automated technique. Image processing based artificially intelligent computer vision techniques can reduce the computational time and as a result, the automated leaf disease detection can be made much faster.

In future, the farmer can obtain a consolidated view of the farm along with decision support statistics for planning purposes. In the field of agriculture digital image processing techniques have been established as an effective means for analyzing purposes in various agricultural applications like plant recognition, crop yield estimation, soil quality estimation etc.

The problem of efficient plant disease protection is closely related to the problems of sustainable agriculture and climate change In India, Farmers have a great diversity of crops. Various pathogens are present in the environment which severely affects the crops and the soil in which the plant is planted, thereby affecting the production of crops .Various disease are observed on the plants and crops .The main identification of the affected plant or crop are its leaves. The various colored spots and patterns on the leaf are very useful in detecting the disease. The past scenario for plant disease detection involved direct eye observation, remembering the particular set of disease as per the climate, season etc. These methods were indeed inaccurate and very time consuming.



Fig 1: AGROBOT

II. LITERATURE SURVEY

The Design of General Purpose Autonomous Agricultural Mobile-Robot:

“AGROBOT” Halil Durmuş Burak Berk Üstündağ in 2015, Purpose of this work is to increase the production efficiency in agricultural field by developing a mobile autonomous robot which has the capability of processing and monitoring field operations like spraying remedies for precision farming, fertilization, disease diagnosis, yield analysis, soil analysis and other agricultural activities.

A Low Power IoT Network for Smart irrigation:

Soumil Heble, Ajay Kumar, et al. in 2018, `proposed a low- power, low-cost IoT network for smart agriculture. For monitoring of the soil moisture content, they have used an in- house developed sensor.

Performance Analysis of Multipurpose AGROBOT:

Sharif Ullah Al- Mamun, Md. Rabiul Islam, Arpita Hoque in2019, The goal of the AGROBOT projectis the implementation of a robotic system for agricultural operations such as plowing the field, sowing seeds, spraying fertilizers, nutrition deficiency and controlled use of fertilizers and pesticides. The agricultural scientists are experimenting to replace tractor driven mechanization with robotic agriculture by introducing “AGROBOT”.

Machine Vision and Machine Learning for Intelligent Agrobots:

A review Bini D, Pamela D, Shajin Prince in2020, A machine vision-based Agrobots along with artificial intelligence provides unmanned ground vehicle and unmanned aerial vehicle to navigate the path and to implement the agricultural task for minimizing labour and increasing quality food production.



Fig 2: Demo model of AGROBOT

Components Required

Hardware Requirements

- Raspberry Pi
- Motor Driver
- Raspberry Pi Camera
- Johnson's motors
- Nodemcu
- Lead acid battery

Software Requirements

- Anaconda
- Arduino IDE
- Raspberry Pi OS

Machine Learning Approach

A Convolutional Neural Network (ConvNet/CNN) is a Deep Learning algorithm which can take in an input image, assign importance (learnable weights and biases) to various aspects/objects in the image and be able to differentiate one from the other. The pre-processing required in a ConvNet is much lower as compared to other classification algorithms. While in primitive methods filters are hand-engineered, with enough training, ConvNets have the ability to learn these filters/characteristics.

The architecture of a ConvNet is analogous to that of the connectivity pattern of Neurons in the Human Brain and was inspired by the organization of the Visual Cortex. Individual neurons respond to stimuli only in a restricted region of the visual field known as the Receptive Field. A collection of such fields overlap to cover the entire visual area.

The objective of the Convolution Operation is to extract the high-level features such as edges, from the input image. ConvNets need not be limited to only one Convolutional Layer. Conventionally, the first ConvLayer is responsible for capturing the Low-Level features such as edges, color, gradient orientation, etc [2]. With added layers, the architecture adapts to the High-Level features as well, giving us a network which has the wholesome understanding of images in the dataset, similar to how we would. Image recognition also known as classification is the first step done here. It is the process where an image is given to the neural network as an input and an output with a label for that image is expected. This is called as "feature extraction", which is a vital ability of any neural network to extract minute details from an object.

Working Module

The working module is shown in the below fig 3. The plant is first captured by the camera which is connected to the raspberry pi. The captured image is processed in the raspberry pi4 model. The raspberry pi can be considered as minicomputer[1]. The raspberry pi is programmed to detect whether the plant is healthy or it is infected by a disease. If the plant is said to be infected, then which type of disease the plant is suffering from is also checked, using different machine learning algorithms and the datasets. The raspberry pi compares the input data with the standard data provided in the dataset and hence the disease is detected from which the plant is suffering. The raspberry pi camera takes the image as the input. The raw input is

then sent to the raspberry pi for processing the image. An image is made up of pixels arranged in a form of square matrix, a two-dimensional view having coordinates as x and y.

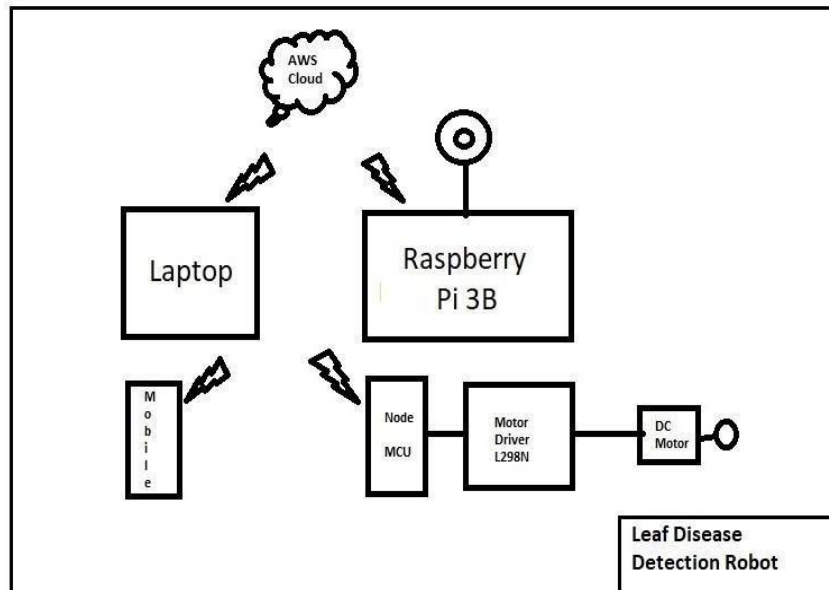


Fig 3: Block Diagram of working Module

The agrobot will survey the crop by scanning the image of the crop through the raspberry pi camera. The camera takes the image as input for raspberry pi and starts with the pre- processing which include the elimination of the undesirable distortions from the image. The raspberry pi then extracts the features of the image and proceed with the classification of the image as a normal or abnormal one [4].

If the image is classified to be normal then the crop is not infected whereas if the image is classified as abnormal then it detects the disease with which the plant is suffering. The classification is done by using the machine learning algorithms which checks the feature extracted image with the training dataset whose prediction accuracy is checked by the test dataset [3] as soon as the disease is detected.

Image Aquisition

The images are obtained using the digital camera that is connected to the Latte panda as shown in fig 4. The images captured are subjected to further preprocessing. For each observation of an individual leaf, we systematically varied the following image factors: perspective, illumination, and background. We captured two perspectives per leaf in-situ and in a non- destructive way: the top side and the back side, since leaf structure and texture typically substantially differ between these perspectives. If necessary, we used a thin black wire to arrange the leaf accordingly [5].



Fig 4: Image Acquisition

Image Preprocessing

The images obtained from the camera are subjected to preprocessing for increasing the quality of the images. The preprocessing steps may include color transformation, noise removal, histogram equalization, green masking etc as shown in fig 5. Here we use the technique of color transformation for increasing the quality of the image .Conversion of RGB image into Grey and also HSI to increase the quality .

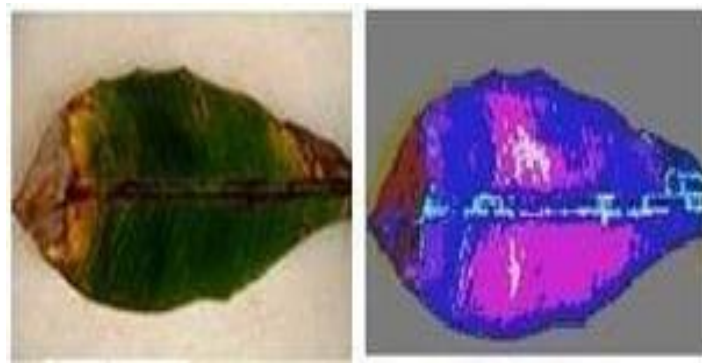


Fig 5 : Image preprocessing

Image Segmentation

Image segmentation are of many types such as clustering, threshold, neural network based and edge based. In this implementation we are using the clustering algorithm called mean shift clustering for image segmentation. This algorithm uses the sliding window method for converging to the center of maximum dense area. This algorithm makes use of many sliding windows to converge the maximum dense region.



Fig 6: Image segmentation

Applications

Some of the applications includes

- Weed control, Planting and Seeding and soil analysis
- Used in Horticulture: to transport potted plants in a greenhouse or outdoor setting.
- Fruit plucking robots
- Bug Vacuum

Conclusion

India is a global agricultural power house where the most of the farmers are failed to implement new strategies from the containment of the leaf disease. Leaf disease is a wide spread infectious disease which affects the whole crop on the fields by spreading. To overcome this problem faced by farmers in leaf disease recognition. We are using robotics that is agricultural surveillance robot which will help farmers to clear out their problems regarding the leaf disease by the working process as discussed in this paper which will ever reduce the man power and also time and helps the farmers to spray the pesticides on time so that they can overcome the loss faced by them due to leaf disease. Also these robots go way ahead for the future use. The robot is controlled by using android application.

In the proposed system, the leaf disease detection was only constricted to a specific disease in the proposed system. The number of diseases to be identified can be extended for more diseases in future with the development of the robot. In future the robot can be integrated with another machine learning . It can also be fixed with another camera that can be used for navigational purpose and later robot will be trained to navigate through the entire field and later it is allowed to move independently and take actions.

References

- [1] G. Eason, B. Noble, and I. N. Sneddon, "On certain integrals of Lipschitz-Hankel type involving products of Bessel functions," *Phil. Trans. Roy. Soc. London*, vol. A247, pp. 529–551, April 1955. (references) M. Sardogan, A. Tuncer and Y. Ozen, "Plant Leaf Disease Detection and Classification Based on CNN with

- LVQ Algorithm," 2018 3rd International Conference on Computer Science and Engineering (UBMK), 2018, pp. 382-385.
- [2] D. Bini, D. Pamela and S. Prince, "Machine Vision and Machine Learning for Intelligent Agrobots: A review" 2020 5th International Conference on Devices, Circuits and Systems (ICDCS), 2020, pp. 12- 16.
- [3] G. M. Sharif Ullah Al- Mamun et al., "Performance Analysis of Multipurpose AGROBOT," 2019 IEEE International WIE Conference on Electrical and Computer Engineering (WIECON-ECE), 2019, pp. 1-4.
- [4] H Durmuş, E. O. Güneş, M. Kırıcı and B. B. Üstündağ, "The design of general purpose autonomous agricultural mobile-robot: "AGROBOT"," 2015 Fourth International Conference on Agro- Geoinformatics (Agro- geoinformatics),2015,pp.49-53.
- [5] N G. Kurale and M. V. Vaidya, "Classification of Leaf Disease Using Texture Feature and Neural Network Classifier," 2018 International Conference on Inventive Research in Computing Applications (ICIRCA),2018,pp. 1-6.

Deep Learning Techniques for Detection of Deepfakes

Deshagouni Manasa*, Vasudev Dehalwar

Computer Science Engineering Department, Maulana Azad National Institute of Technology
Bhopal, India

ABSTRACT

There have been ground-breaking developments in machine learning and artificial intelligence thanks to science and information technology development. With the widespread use of social media comes the issue of Deepfakes, which has led to a rise in digital media content that has been altered or fabricated. The manipulated videos and photographs pose a severe risk to people's safety and privacy, which may also have catastrophic ramifications for a country's politics, religion, and social cohesion. Humans can spot image forgeries like face swapping, but Generative Adversarial Networks (GAN) can create images that are tough to detect even by humans; identifying such pictures and videos is a real challenge. Deep learning techniques are gaining popularity for detecting face swaps. Thus for stopping political unrest, blackmail we need smart algorithms to combat fake videos. In this paper, we suggest some deep learning models for detecting deepfakes videos to classify them accurately as real or fake.

Index Terms : Deepfakes, Classification, Deep Learning, Convolution Neural Networks, ResNet50, InceptionResnetV2 , M2model.

I. INTRODUCTION

The use of cell phones has multiplied with the emergence of technology. The use of videos and photographs on social media has increased due to social networks' growth. A survey found that every day, around a million images are shared online. The excessive usage of images on online platforms has given rise to various techniques for altering digital information utilizing Photoshop, among others.

In a narrow definition, deepfakes (stemming from "deep learning" and "fake") are created by techniques that can superimpose face images of a target person onto a video of a source person to make a video of the target person doing or saying things the source person does. This constitutes a category of deepfakes, namely face-swap. In a broader definition, deepfakes are artificial intelligence-synthesized content that can also fall into two other categories, i.e., lip-sync and puppet-master. Lip-sync deepfakes refer to videos that are modified to make the mouth movements consistent with an audio recording. Puppet-master deepfakes include videos of a target person (puppet) who is animated following the facial expressions, eye and head movements of another person (master) sitting in front of a camera (Agarwal et al., 2019) While some deepfakes can be created by traditional visual effects or computer-graphics approaches, the recent common underlying mechanism for deepfake creation is deep learning models such as autoen coders and generative adversarial networks (GANs), which have been applied widely in the computer vision domain. These models are used to examine facial expressions and movements of a person and

synthesize facial images of another person making analogous expressions and movements. Deepfake methods normally require a large amount of image and video data to train models to create photo-realistic images and videos. Deep learning methods called generative adversarial networks (GANs) [1] can create fake photos and videos that are difficult for a person to distinguish from the real ones. These models produce faked images and videos after training on a data set. For those deepfake media, this form of deepfake model needs a sizable amount of training data. The model may produce more credible and realistic photos and movies with an enormous data collection. In reality, the widespread availability of films featuring presidents and Hollywood celebrities on social media might aid people in creating plausible rumours and false information that could have a significant negative impact on our society.

Fake images and videos including facial information generated by digital manipulation, in particular with DeepFake methods, have become a great public concern recently. The very popular term “DeepFake” is referred to a deep learning based technique able to create fake videos by swapping the face of a person by the face of another person. This term was originated after a Reddit user named “deepfakes” claimed in late 2017 to have developed a machine learning algorithm that helped him to transpose celebrity faces into porn videos. In addition to fake pornography, some of the more harmful usages of such fake content include fake news, hoaxes, and financial fraud. As a result, the area of research traditionally dedicated to general media forensics, is being invigorated and is now dedicating growing efforts for detecting facial manipulation in image and video part of these renewed efforts in fake face detection are built around past research in biometric anti-spoofing and modern data-driven deep learning.

Fake news has been spreading at an alarming rate recently, and videos of a million hours or more in length are being shared widely on social media, endangering civilization. Although there has been an impressive development in identifying image forgeries, finding faked films is still tricky. Many imagebased algorithms can't be used directly on videos because of compression. The majority of current video research is concentrated on re-encoding [2] and re-capturing [3] [4], although video detection is still challenging.

Face-swapping videos have been created using deep learning algorithms. A robust method for capturing and recreating facial expressions is deepfake. The creation of adult content was the main application of this technique.



Fig. 1. Deepfake manipulation [5]

Technologies based on artificial intelligence have been developed to find tampering [6] [7]. Convolution Neural Networks are being used to address the problem because they perform remarkably well in photos. Generative Adversarial Networks (GAN) have been used to create imitations of real videos and other content. Thus, a new category of movies known as “DeepFake” videos has been created as a result of the usage of Variational Autoencoder and Generative Adversarial Networks (GANs) [1].

Deepfake videos, which are produced using the image modification program Abode, are simpler to make and have a more realistic appearance than traditional Hollywood movies. Face swapping is made possible in film by using deep learning techniques on various video samples. The results are more realistically represented the more significant the sample sizes. The general public, particularly women, are now victims of deepfakes, and the bulk of these victims are portrayed in porn. In a post, Washington claimed that face photos and pornographic images were expertly combined and shared on social media without the consent of any outside parties. Deep learning techniques have proved to be quite successful in image forensics in recent years. Many researchers in the field of image forensics, eg. Barni et al. used deep learning algorithms for detection of changes in images due to JPEG compression. For the identification of deepfake movies, various techniques are used because identification of deepfakes necessitates the extraction of complex features; therefore, a good number of fake and real videos are required for training purposes. FaceForensics++ [8], Deepfake Detection Challenge (DFDC) [9] and Celeb-DF [5] are a few of the data.

II. RELATED WORKS

Li and Lyu et al. [10], suggested machine learning method for detection of deepfake videos. They offer an approach that pits one machine learning methodology against another. Convolutional neural networks (CNN) were trained with real and fake images. CNN networks were utilised in the experiment, with result accuracies ranging from 84 to 99%. The precision of the results acquired by their method was excellent. Ricard Durall et al. [11] proposed a technique for identifying deepfakes. Their method relied on frequency response and then used a simple classifier. The technique produced excellent results with only a few training samples and high accuracy compared to prior methods. The author generated their datasets by integrating available datasets such as Faces-HQ to obtain high-face-resolution photos. After only ten high-resolution photos, the approach obtained a classification accuracy of about 100%. The videos demonstrate how their technique yields excellent outcomes.

Tackhyun Jung et al. [12] proposed an architecture using the DeepVision algorithm to detect blinking pattern changes, a spontaneous movement, to identify Generative Adversarial Networks (GAN) generated deepfakes. The human eye pattern is thought to differ from one person to the other based on the person's biology and physical state. The pattern is determined by factors such as sex. Deepfakes can be recognised using algorithms that track significant difference in the blinking patterns of human eyes.

Xin Yang et al. [13] introduced a novel technique for detecting altered or fraudulent photos or videos. Deepfakes are generated by splicing the region of interest in the face of the source image, that creates inconsistencies that can be identified when 3D postures of heads are acquired from face photographs, according to the method. Experiments were carried out to demonstrate the approach, and a classification system based on the concept was developed. An SVM classifier that incorporates features found on this cue is used for evaluation.

Haya R Hashan and Khaled Salah et al. [14] presented a technique and broad framework for tracking the computerised items back to their source using Ethereum smart contracts. In the keen agreement, hashes from the interplanetary document framework (IPFS) are used to store advanced data and metadata. Their method is based on the fact that if the digital content to be tracked down to a reliable origin, the chances are that it is authentic.

David Guera et al. [15] demonstrated a method for automatically detecting fake films. The technique utilized a Convolutional Neural Network for extracting features. The features or aspects gathered are used for training a recurrent neural network. The method showed a good classification accuracy. Hany Farid et al and Shruti Agarwal [16] suggested a technique for detecting tampered films based on the motion of the mouth(visemes) is most

consistent with spoken phenome. Mismatches of a phoneme can thus be used to identify changes in time and location. The proposed approach proved reliable and effective in detecting deepfakes.

Darius Afchar et al. [17] proposed a method for effectively detecting face alteration in films, focusing on the Face2Face and Deepfake techniques for creating believable forged videos. The researchers utilised a deep learning method to develop two networks concentrating on the image's mesoscopic properties. They put rapid networks to the test on a dataset produced from films. Deepfake detects more than 98% of the time, according to the tests.

Yuezun Li, Siwei Lyu and Ming-Ching Chang et al . [18] suggested a model which focuses on identifying the blinking pattern of eyes in video films, which is an involuntary response of human beings that is not well addressed in the generated fake videos. The algorithm was tested on eye-blinking dataset and has shown great results in detection of DeepFake movies.

Mohit Patel, Aaryan Gupta et al. [19] discussed various transfer learning methods for detecting deep fake videos. In the study, they forwarded a technique for extracting and detecting a person's face from videos and then utilising them to extract features. Based on the extracted features, the model classifies them as fake or real. The features were extracted using pretrained models like VGG, MobileNet, ResNet etc. For the classification task, they used a random forest classifier. The accuracy achieved by the model was around 90% in classifying deepfakes.

A. Dataset used in our study

The dataset used in our study has been taken up from Kaggle deepfake detection challenge. The Facebook Deepfake detection challenge initially released the dataset.

For the study, we have taken 800 videos of training data. The JSON file contain real and fake videos labels. The frames were extracted from the videos, and they were used for training the model. The dataset is in the form of videos, with over one lakh clips taken from various paid actors and generated using a variety of GAN-based methods.

Deepfakes are a recent off-the-shelf manipulation technique that allows anyone to swap two identities in a single video. In addition to Deepfakes, a variety of GAN-based face swapping methods have also been published with accompanying code. To counter this emerging threat, we have constructed an extremely large face swap video dataset to enable the training of detection models, and organized the accompanying DeepFake Detection Challenge (DFDC) Kaggle competition. Importantly, all recorded subjects agreed to participate in and have their likenesses modified during the construction of the face-swapped dataset. The DFDC dataset is by far the largest currently and publicly available face swap video dataset, with over 100,000 total clips sourced from 3,426 paid actors, produced with several Deepfake, GAN-based, and non-learned methods. In addition to describing the methods used to construct the dataset, we provide a detailed analysis of the top submissions from the Kaggle contest. We show although Deepfake detection is extremely difficult and still an unsolved problem, a Deepfake detection model trained only on the DFDC can generalize to real "in-the-wild" Deepfake videos, and such a model can be a valuable analysis tool when analyzing potentially Deepfaked videos.

III. PROPOSED METHODOLOGY

In our proposed methodology we took the dataset from Kaggle deepfake detection challenge, the videos are labelled as fake and real. The region of interest in identifying deepfake images



Fig. 2. Frames of videos

is the face so we have used Dlib face detector. The frames from the input videos are taken at various instances and then they are saved as images. The frames are captured at different instances of time. The images are labelled as real and fake. The labelled images are fed into the training model and the model is trained for certain number of epochs. The model have different layers in which the input data is fed like different convolution, pooling layers and the final layers are dense layers in the models. The features from the input images are extracted and are used for training the model. The dataset is divided for 70% training data and 30% testing data. We have used M2, Modified InceptionResnetV2, Modified Resnet50 model. The model trained is now used on the testing data.

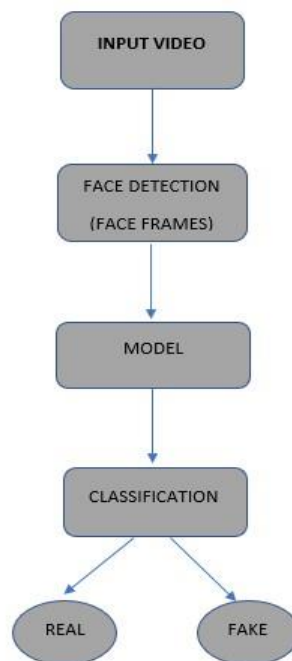


Fig. 3. Proposed Methodology

IV. DEEP LEARNING MODELS

A. Convolution Neural Networks

In neural networks, Convolutional neural network [20] is a neural networks to do the image recognition and image classifications, Object detections, etc.

There are majorly three types of layers:

- Convolutional Layer: the input neurons are connected to hidden neurons in the hidden layers; certain neurons can be left without being connected to the next layer's hidden layer(dropout).
- Pooling Layer: is used for reducing the dimensions of the features extracted either by using min, max, or average Pooling. In a neural network, there can be several pooling layers
- Fully Connected layer: these are the final layers of the neural network. Output from the previous layers or the pooling layers are flattened and then fed into these layers. The proposed architecture is given below, and there are several convolution layers, max-pooling layers and some dense layers are added at the end of the model consisting of one twenty eight neurons in the first and one neuron at the last layer of the model.

Layer	Parameters	Activation
Input		
Rescaling		
Conv2D	16x3x3	ReLU
Max Pool	2x2	
Conv2D	32 x 3 x 3	ReLU
Max Pool	2 x 2	
Conv2D	64x3x3	ReLU
Max Pool	2x2	
Conv2D	32x3x3	ReLU
Max Pool	2x2	
Flatten		
Dense		ReLU
Dense		Sigmoid

Fig. 4. M2 model

B. RESNET50

ResNet-50 [21] is a convolutional neural network with fifty layers.

It is a variation of Resnet with forty-eight Convolutional layers, one max pool layer and one average pool layer. Architecture of resnet50: The first layer is produced using a convolution using 64 distinct kernels, each having a size of 7x7, and a stride of 2. There is a max pooling layer of stride 2 in the next step. This is followed by a convolutional layer using a 1x1,64 kernel, a 3x3,64 kernel, and finally a 1x1,256 kernel. These layers are repeated three times to create a total of nine layers. Following a layer of 3 x 3,128 and a layer of 1 x 1,512 kernel, we see a convolution of 1 x 1,128 once more. These layers are repeated four times for a total of twelve layers.

This is followed by a convolution with a 1 x 1,256 kernel, two further convolutions with 3 x 3,256 kernel, and finally a third convolution with a 1 x 1,1024 kernel. These three layers are then repeated six times in total to give us eighteen layers. These layers were repeated three times, giving us a total of nine layers. Then, there is a convolution of kernel 1 x 1,512, followed by two further convolutions of 3 x 3,512 and 1 x 1,2048. Following this, there is average pooling, followed by a layer with 1,000 nodes that is fully connected, and finally, a softmax function that yields one layer.

In the proposed model, we modified the Resnet50. We have added a global average pooling layer, and we have added three dense layers. In the first dense layer of one twenty eight neurons have relu activation function. In the

second dense layer of sixty-four neurons have relu activation function, and in the last dense layer of one neuron we have used the sigmoid activation function.

Layers of the model
Resnet50
GolbalAveragePooling2D
Dense layer
Dense layer
Dense layer

Fig. 5. Modified Resnet50 architecture

InceptionResnet V2

The Inception-ResNet-v2 [22] architecture is a convolutional neural architecture that expands on the Inception family of architectures while also including residual connections. It is a variant of Inception and ResnetV2 architectures. The 164-layer network can recognise images into one thousand object categories including animals, mice, pencils .

A hybrid inception module was proposed, inspired by ResNet's performance. Inception ResNet is divided into two versions: v1 and v2.

The cost of Inception-ResNet v1 is comparable to that of Inception v3 in terms of computing. The cost of InceptionResNet v2 is comparable to that of Inception v4 in terms of computing. They have various stems.

In the proposed model, we modified the InceptionResnetV2. We have added a global average pooling layer and one Dropout layer of 20 % and three dense layers. In the first layer, we used dense layer of two fifty six neurons having relu activation function, in the second layer, we used dense layer one of twenty eight neurons having relu activation function and in the last dense layer we used a sigmoid activation layer.

V. ANALYSIS OF RESULTS

The models were trained for 25 epochs and the batchsize was taken as 32, thus the testing accuracies that we achieved are given in the table 1 below.

The models were able to achieve good accuracy. The classification accuracy for M2model, InceptionResnetV2, ResNet50 is

Layers of the model
InceptionResnetV2
GolbalAveragePooling2D
Dropout
Dense layer
Dense layer
Dense layer

Fig. 6. Modified InceptionResnetV2 architecture

TABLE I. COMPARATIVE ANALYSIS

MODEL	Accuracy
M2 model	92%
InceptionResnetV2	96%
Resnet50	96.5%

92%, 96%, 96.5%, The best classification accuracy obtained is for modified Resnet50. The confusion matrix was obtained for M2 model, Modified InceptionResnetV2, Modified Resnet50 where df label represents deepfake image and real label represents real image. The Modified model has InceptionResnetV2, Resnet50 as it's first layers and the new model was made adding global average pooling layer and few dense layers, it can be seen that M2 model which has few convolutional and pooling layers also achieves good accuracy.

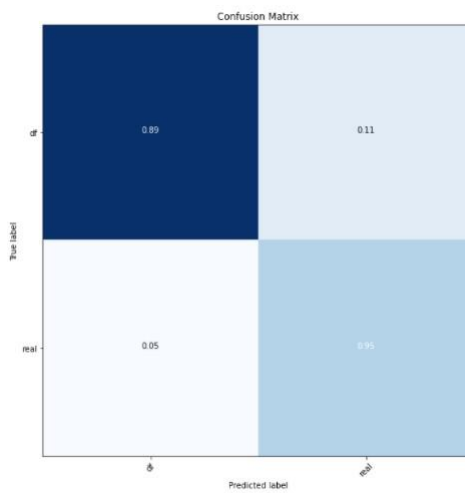


Fig. 7. Confusion matrix of M2 implementation

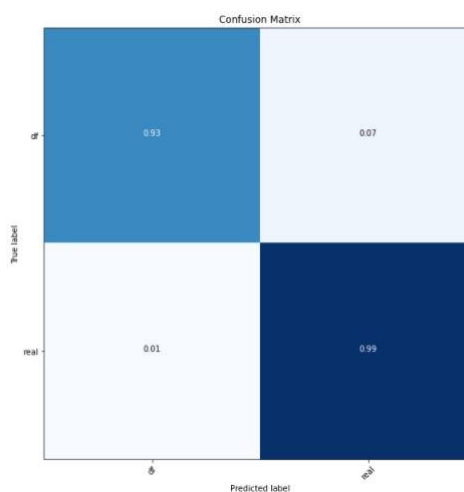


Fig. 8. Confusion matrix of InceptionResnetv2 implementation

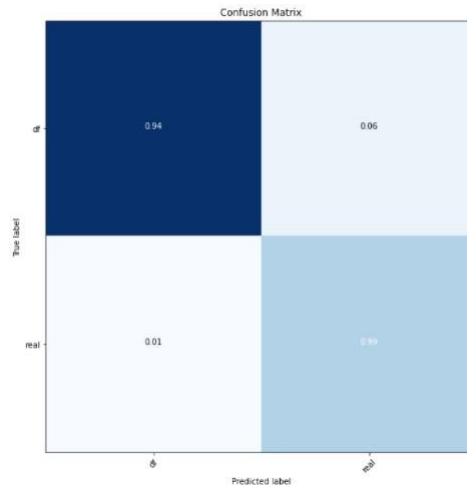


Fig. 9. Confusion matrix of Resnet50 implementation

VI. CONCLUSION

The proposed method above uses various models. The different architecture used helped us in detection of deepfakes. The use of models like modified InceptionResnetV2, modified Resnet50 helped us in achieving good accuracy of detection. It can be seen that the M2 model also accomplishes a good classification accuracy of 92% whereas by using modified models we can achieve best accuracy of 96.5%. In future we would be gathering more data from various sources including compressed ones for making our model more efficient.

REFERENCES

- [1] I. Goodfellow, J. Pouget-Abadie, M. Mirza, B. Xu, D. Warde-Farley, S. Ozair, A. Courville, and Y. Bengio, "Generative adversarial nets," *Advances in neural information processing systems*, vol. 27, 2014.
- [2] W. Wang and H. Farid, "Exposing digital forgeries in video by detecting double mpeg compression," in *Proceedings of the 8th workshop on Multimedia and security*, pp. 37–47, 2006.
- [3] W. Wang and H. Farid, "Detecting re-projected video," in *International Workshop on Information Hiding*, pp. 72–86, Springer, 2008.
- [4] J.-W. Lee, M.-J. Lee, T.-W. Oh, S.-J. Ryu, and H.-K. Lee, "Screenshot identification using combing artifact from interlaced video," in *Proceedings of the 12th ACM workshop on Multimedia and security*, pp. 49–54, 2010.
- [5] Y. Li, X. Yang, P. Sun, H. Qi, and S. Lyu, "Celeb-df: A largescale challenging dataset for deepfake forensics," in *Proceedings of the IEEE/CVF Conference on Computer Vision and Pattern Recognition*, pp. 3207–3216, 2020.
- [6] H. Farid, "Image forgery detection," *IEEE Signal processing magazine*, vol. 26, no. 2, pp. 16–25, 2009.
- [7] J. A. Redi, W. Taktak, and J.-L. Dugelay, "Digital image forensics: a booklet for beginners," *Multimedia Tools and Applications*, vol. 51, no. 1, pp. 133–162, 2011.
- [8] A. Rossler, D. Cozzolino, L. Verdoliva, C. Riess, J. Thies, and M. Nießner, "Faceforensics++: Learning to detect manipulated facial images," in *Proceedings of the IEEE/CVF International Conference on Computer Vision*, pp. 1–11, 2019.
- [9] B. Dolhansky, J. Bitton, B. Pflaum, J. Lu, R. Howes, M. Wang, and C. C. Ferrer, "The deepfake detection challenge (dfdc) dataset," *arXiv preprint arXiv:2006.07397*, 2020.

- [10] Y. Li and S. Lyu, "Exposing deepfake videos by detecting face warping artifacts," *arXiv preprint arXiv:1811.00656*, 2018.
- [11] R. Durall, M. Keuper, F.-J. Pfrendt, and J. Keuper, "Unmasking deepfakes with simple features," *arXiv preprint arXiv:1911.00686*, 2019.
- [12] T. Jung, S. Kim, and K. Kim, "Deepvision: deepfakes detection using human eye blinking pattern," *IEEE Access*, vol. 8, pp. 83144–83154, 2020.
- [13] X. Yang, Y. Li, and S. Lyu, "Exposing deep fakes using inconsistent head poses," in *ICASSP 2019-2019 IEEE International Conference on Acoustics, Speech and Signal Processing (ICASSP)*, pp. 8261–8265, IEEE, 2019.
- [14] H. R. Hasan and K. Salah, "Combating deepfake videos using blockchain and smart contracts," *Ieee Access*, vol. 7, pp. 41596–41606, 2019.
- [15] D. Guera and E. J. Delp, "Deepfake video detection using recurrent neural networks," in *2018 15th IEEE international conference on advanced video and signal based surveillance (AVSS)*, pp. 1–6, IEEE, 2018.
- [16] S. Agarwal, H. Farid, O. Fried, and M. Agrawala, "Detecting deepfake videos from phoneme-viseme mismatches," in *Proceedings of the IEEE/CVF Conference on Computer Vision and Pattern Recognition Workshops*, pp. 660–661, 2020.
- [17] D. Afchar, V. Nozick, J. Yamagishi, and I. Echizen, "Mesonet: a compact facial video forgery detection network," in *2018 IEEE International Workshop on Information Forensics and Security (WIFS)*, pp. 1–7, IEEE, 2018.
- [18] Y. Li, M.-C. Chang, and S. Lyu, "In ictu oculi: Exposing ai created fake videos by detecting eye blinking," in *2018 IEEE International Workshop on Information Forensics and Security (WIFS)*, pp. 1–7, IEEE, 2018.
- [19] M. Patel, A. Gupta, S. Tanwar, and M. Obaidat, "Trans-df: a transfer learning-based end-to-end deepfake detector," in *2020 IEEE 5th international conference on computing communication and automation (ICCCA)*, pp. 796–801, IEEE, 2020.
- [20] L. Alzubaidi, J. Zhang, A. J. Humaidi, A. Al-Dujaili, Y. Duan, O. AlShamma, J. Santamaría, M. A. Fadhel, M. Al-Amidie, and L. Farhan, "Review of deep learning: Concepts, cnn architectures, challenges, applications, future directions," *Journal of big Data*, vol. 8, no. 1, pp. 1–74, 2021.
- [21] S. Targ, D. Almeida, and K. Lyman, "Resnet in resnet: Generalizing residual architectures," *arXiv preprint arXiv:1603.08029*, 2016.
- [22] C. Szegedy, S. Ioffe, V. Vanhoucke, and A. A. Alemi, "Inception-v4, inception-resnet and the impact of residual connections on learning," in *Thirty-first AAAI conference on artificial intelligence*, 2017.

IOT Based Vehicle Accident Prevention and Detection System Using Raspberry-Pi

Rahul Devnath Tiwari¹, P. P. Tasgaonkar²

¹Department of E&TC College of Engineering, Pune, India

²Professor, Department of E&TC College of Engineering, Pune, India

ABSTRACT

The pace of our life has accelerated due to the transit system thanks to continual technological advances. Accidents are still a major problem, especially on the highways where they often result in fatalities and have catastrophic consequences for the victims. Innovative smart city systems are highly desired to avert such accidents. A self-driving autonomous car is created in this study to be used in accident prevention applications. The working prototype is totally managed by a Raspberry Pi that integrates smart sensors for automation and ADXL345 for accident detection. The Raspberry Pi is used because it has a faster processing speed than other microcontrollers and is excellent for creating software applications. Accident Utilizing a Pi-camera and an IR sensor, prevention is carried out by alerting the driver about nearby cars when their distance from one another exceeds a threshold value, and if it violates a limit, the vehicle will stop automatically. Additionally, a Wi-Fi connection is successfully established using the Thing Speak platform for real-time monitoring of the system online.

Index Terms : Raspberry-Pi, IR Sensor, Thingspeak Cloud, ADXL345, Smart City ,API, IOT.

I. INTRODUCTION

As number of vehicles are rising day by day, with increase in population, so are the road accidents. About 80 percent of the accidents occurrence end up in losing lives. According to the survey which was conducted by the research agency [1], about 1.25million people die every year whereas 3,287 deaths happen every day. National expressways or highways have been made to cut down the travelling cost between the cities. But, the major thing which misses out is to manage the traffic which eventually causes deadly accidents. A total of [8] 280 accidents happened between 1st January-2016 to 31st December-2017 on expressways as per the accident researchers which was published on July-2018. These involved 218 road users (193 vehicles and 25 pedestrians) and 443 victims out of which 65 were lethal, 105 were serious and 129 suffered minor injuries, which invoked a thought of doing something in order to decrease the accidents and also monitor it 24x7, throughout the year. This system described will monitor the accidents continuously by the help of internet of things using various protocols. So, if in case accident happens, it will be immediately informed to nearby authorities and accordingly necessary actions can be taken. We can see that with each passing year, the number of accidents keep on rising.

Year	Total Accidents	Fatal	Fatal (In %)	Killed
2015	5,01,423	1,46,133	26.3	1,46,133
2016	4,80,652	1,50,785	28.3	1,50,788
2017	4,64,210	1,47,913	29	1,47,913
2018	4,67,044	1,51,417	29.5	1,51,417
2019	4,49,002	1,51,113	30.7	1,51,113
2020	3,66,128	1,31,714	33	1,31,714

Fig. 1. Major parameters Contributes to road accidents.

As we can see that with each coming years the number of accidents is keep on rising. Also number of people killed in the accidents are going up so, we need some system or technology which can help in decreasing the number of accidents. The concept of “Smart city” is introduced for development of urban cities. Smart means something which is more technology oriented makes life easier and more efficient. The major contribution of “smart city” is to make the life of people more comfortable, easy and sustainable. There are so many smart technologies which can be used at wide range of areas such as transportation, healthcare, aviation etc. With the IoT this idea is more achievable. Transportation plays an essential role for any city to be smart. In this paper the main focus would be to eradicate the amount of accidents happening in a city for safety of the citizens. Smart transportation mainly consists of infrastructures, AI based (artificial intelligence) based traffic control and management systems aiming to transform sustainable and green system. Major areas on which smart transportation supports are:

- a. Smart Automobile.
- b. Smart Infrastructure.
- c. Intelligent Transport System.
- d. Sustainable fuels.

The paper starts by describing the standalone, lightweight and smart detection system in the current scenario which can be implemented in a Smart City. A brief discussion on the Past approaches is present in Section II. A brief methodology and block diagram is described in Section-III. Hardware requirements has been also discussed in Section- IV. Finally results are present in Section-V. At the end final conclusion has been given in Section-VI.

II. LITERATURE REVIEW

A lot of research has been done till date to detect the accident and later on notification is sent to emergency medical services.

In [2] this author has present eye blink monitor technique for accident detection which alerts during drowsiness states. A system which depends on psychological state of focus and eye movement are helpful in alerting driver during drowsiness state. There will be no effect during an ordinary movement of the eyes. In [3]

this author has designed a speed automatic detection system which detects the speed of a vehicle. In case over speed happens a mail will be send to toll plaza and fine will be imposed. Here Doppler effect has been employed for ensuring the speed of a vehicle. And if over speed happens the image of a vehicle is taken and license will be removed using DIP method. In [4] this author proposed a system that notifies emergency contacts like police, ambulance when accident happens. The system uses mamdani fuzzy logic based on a support taken from programmed smartphone and the information will be stored to data centre. Data is taken with the help of accelerometer, gyroscope sensors that is attached to different side of the vehicle. However, the hardware system has excessive sensors which was not compact enough. In [11] author has used a function which is programmable oriented and developed a Software Network(SDN) in order to improve the quality of services in IOV network which is very important while vehicle reports the accident to each other. In [12] have discussed about VCA (vehicle cloud access) problem that has been modelled with the help of evolutionary gaming and have given two important algorithms based on the EG-VCA and QL-VCA.

In [13] author has used detection based system which is due to collision by using a smart phone and different sensors like accelerometer, gyroscope, magnetometer in order to reduce the false alarms occurs in the system. In [5] author has employed a shock sensor and geographical location is sent when the accident occurs. Additional information such as full name, email, phone number etc. are being send to the public safety organization. Main drawback of this system is passenger need to pre-register its vehicle information which is currently not possible. In [6] on-board diagnostic system has been implemented and acceleration data is used for accident detection. But implementation of OBD in each vehicle is not possible. An alert is generated along with email notification with the help of Message queuing telemetry transport(MQTT). With the help of ultrasonic and accelerometer sensor data will be received and stored on Iot platform Losant [7]. Real time accident detection algorithm is used with the help of RFID is shown in [9] which collects a lot of information such as speed, number of passengers inside the vehicle etc. Also multiple sensors have been used at different corner of the vehicle which make this method less compact. In [14] author has mentioned about IR sensor which is interfaced with Arduino board also 16*2 counter is used to count the vehicles at the turning point to improve the accuracy of the road.

III. PROPOSED METHODOLOGY

1. Hardware arrangement

Fig demonstrates the electronic components necessary to create a smart, autonomous automobile. The Raspberry Pi Microcontroller is used in the model to provide control and offer interface between several sensors, including ADXL-345, IR, alcohol, gas, and alcohol sensors. To enable viewing of data on the cloud, a Wi-Fi module is interfaced with the board. Additionally, Pi-Camera is employed to record high definition images and videos for real-time monitoring. Hardware setup is shown in Figure 2. The Raspberry Pi, Motor Driver (L293d), and 9V battery are included. Battery is utilised to power the circuit, and L293D is interfaced with the board. The motor driver is essential for managing the speed of a DC motor. It is an integrated circuit (IC) or circuit that supplies energy to the car's motor. The speed of a motor is directly correlated with the voltage applied to its terminals. As a result, when the voltage of the motor varies, the vehicle's speed also does. The motor driver receives a pulse width modulation (PWM) signal from the Raspberry-Pi board. The reference signal is used to control the motor's speed. The used DC motor spins at a speed of 1000RPM.

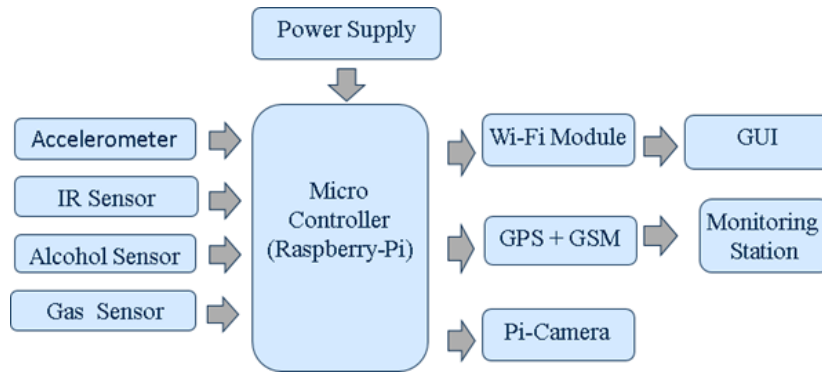


Fig. 2. Architecture of proposed model.

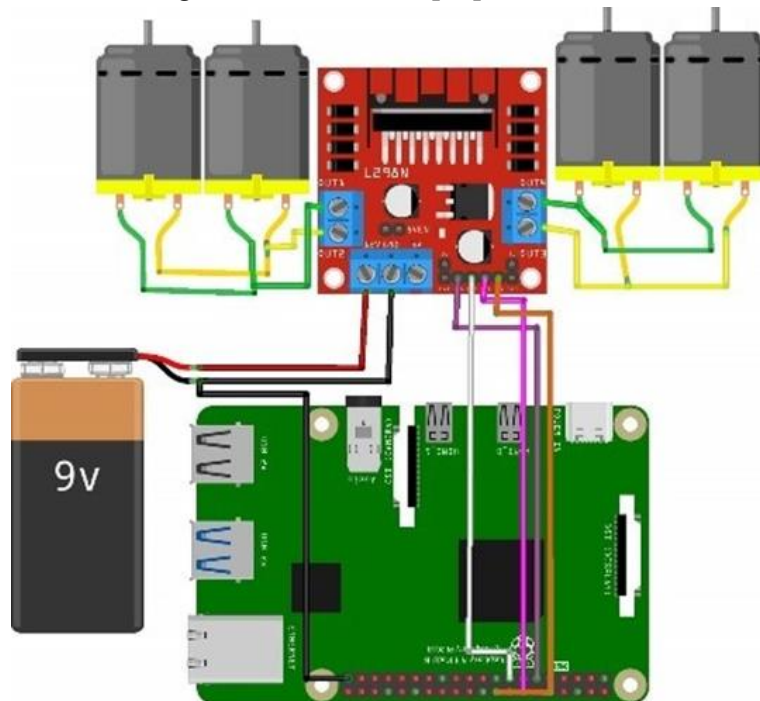


Fig. 3. hardware setup.

2.Sensors

A. Accelerometer

A sensor which measures acceleration of an object or body when it is in rest state that helps in accident detection. It acquires data from the 3 axial components along with three different orthogonal axis. The acceleration can be calculated from three equations given below:

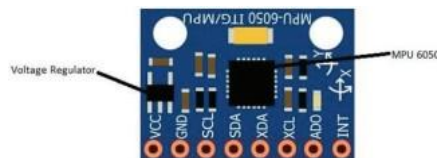


Fig. 4. Accelerometer

$$A = (V_i - V_f)/T \quad (1)$$

$$A = (2(D - V_i T))/T^2 \quad (2)$$

Where V_i = Initial velocity.

V_f = Final velocity

T = Time taken during acceleration.

D = Distance travelled.

Suppose 3-axis accelerometer is mounted on a device in the gravitational field, and undergoing acceleration a . It will generate output G which is given by:

$$G = R(F - a) \quad (3)$$

Where R is the rotational matrix defines the orientation of the device with respect to the earth. F is a gravitational force and a is acceleration. Whenever a running vehicle is dropped from a certain height the orientation of the vehicle changes. In such case gravitation of a vehicle changes with respect to X , Y and Z axis. And declaration due to the impact will be distributed to more than one axis. Therefore, it is very difficult to detect the precision of the declaration. To address this problem absolute linear acceleration is calculated with the help of X , Y and Z axis. ALA is calculated by:

$$ALA = \sqrt{(x^2 + y^2 + z^2)} \quad (4)$$

Where X , Y , Z are the deceleration at x -axis, y -axis, and z -axis. When a vehicle is collided with an object or any other solid object at the speed of 30km/h, the intensity of declaration always crosses 5g.

B. Alcohol sensor

The presence and quantity of alcohol vapours in the air are detected by an alcohol sensor, also referred to as an alcohol gas sensor or alcohol detector. It is frequently employed in alcohol detection systems, industrial safety applications, and breathalyser equipment. If a drunk person take air near the sensor, then it detects the ethanol in his breathe and output is generated passed on the alcohol concentration. In case the driver is in dunked state notification will be send to the owner's number and buzzer will lit up The analog output pin of alcohol sensor is connected to pin number 37 i.e. GPIO 26.

C. Pi-Camera

The camera module created especially for use with the well- known single-board computer Raspberry Pi is referred to as the "Pi Camera". A special CSI (Camera Serial Interface) connector is used to link the Pi Camera modules to the Raspberry Pi board. For the direct connection of camera module to raspberry-pi CSI port is use. Raspbian, the official operating system for the Raspberry Pi, often comes with the essential software drivers and libraries pre-installed or is readily installable.



Fig. 5. Pi-camera.

D. IR sensor

A sensor that detects and measures infrared radiation that is emitted by things or substances in its range of vision is known as an infrared (IR) sensor. In the model we have used this device to detect any obstacle present, according to the location of the obstacle the car will move in a particular direction. Based on each gas's distinct infrared absorption properties, IR sensors are used to identify, quantify, and measure its existence and quantity. IR sensor can be interfaced with Raspberry-Pi by using software drivers and libraries. The analog output pin of IR sensor is connected to pin number 16 i.e. GPIO 23.

E. Motor Driver(L293D)

The L293D device is a quadruple which produces high current Half-H. It is designed to produce bidirectional drive currents up to 600mA at a voltage from 4.5v to 36v. four Dc motor with 1000rpm is attached to 4 wheel of the car. The motor driver is essential for managing the speed of a DC motor. It is an integrated circuit (IC) or circuit that supplies energy to the car's motor. The speed of a motor is directly correlated with the voltage applied to its terminals. As a result, when the voltage of the motor varies, the vehicle's speed also does. The motor driver receives a pulse width modulation (PWM) signal from the Raspberry-Pi board. The reference signal is used to control the motor's speed.

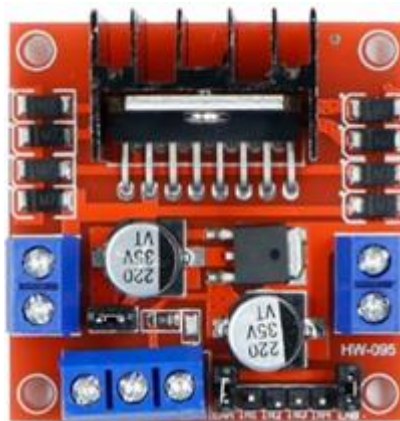


Fig. 6. Motor-driver IC(293d).

F. GPS/GSM

GSM/GPS is also installed on the device. GPS helps in track the location of vehicle. In our proposed methodology we used to find the current location of the device if accident occurs. When the microcontroller receives the signal from accident location it will request the current location to the GPS. GSM is a device helps in mobile communication. The notification will be sent via GSM to nearby hospitals and nearby police station whenever any mishap take place. There is a SIM installed inside the GSM that is used for communicating purpose with the date and time. Whereas GPS helps to trace the location of particular vehicle if in case something happens. Both GSM/GPS is interfaced with Raspberry-Pi.

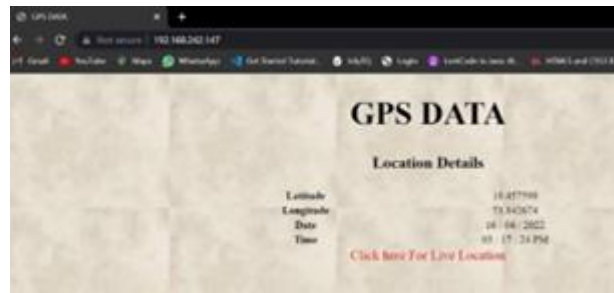


Fig. 7. Shows the location with Date and Time.

G. Raspberry Pi (3A)

It is equipped with a quad-core, 1.2GHz Broadcom BCM2837 processor, which has enough processing capacity for a variety of applications. The board's 512MB of LPDDR2 SDRAM enables multitasking and the use of numerous software programmes. With built-in Wi-Fi (802.11n) and Bluetooth 4.2 connectivity, the Raspberry Pi 3 Model A enables wireless communication and IoT projects without the need for extra adapters. It contains a 40-pin GPIO header that enables the board to be expanded by connecting different sensors, modules, and peripherals. A 5V power supply can be used to power the board using a micro USB port.

IV. CLOUD (THING SPEAK)

The IoT is a system that connects things together. The things generally consist of operating systems and ability to connect with internet or any other neighbouring things. It is a platform which provides various exclusively services build for IoT applications. It has the capabilities to collect various data in real-time, visualized in the forms of charts has the ability to create apps and plugins for collaborating with social networks, web services, APIs. The main elements of thing speak is 'channel'. It stores the data that we send to thing speak. It comprises of Multiple fields in that any kind of data can be stored. Multiple location field for storing latitude, longitude and various types of elevation. This are very important while tracking a device which is in moving condition. Status field is used to describe the short message in the channel. Thing speak has a unique key through which data is secured that is a API. Every user id that is created has a different API key.

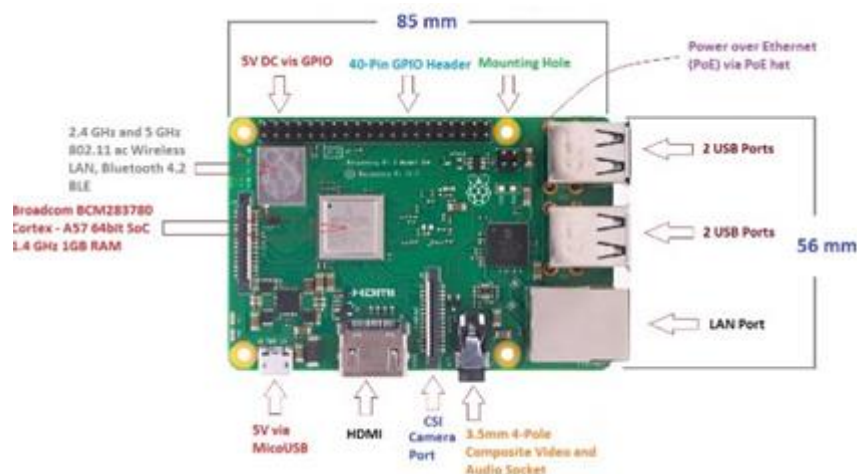


Fig. 8. Raspberry-Pi(3A).



Fig. 9. Axis-wise real time Accelerometer records on Thing speak.

Fig.3. shows the accelerometer readings on Cloud (Think speak) We can set up thresholds in Think Speak to set off alerts or notifications based on specific circumstances. For instance, we may enable Think Speak to send an email or push notice whenever the acceleration exceeds a predefined threshold in any axis. This function is helpful for identifying noteworthy events or unusual behaviour recorded by the ADXL345. The angle will start off at zero degrees and can increase all the way to 360 degrees in any direction. If the vehicle crosses the accelerometer threshold value in either direction, an accident is deemed to have occurred. The X-axis and Y-axis threshold values are 250 and 300, respectively. Depending on the vehicle's orientation, we can see various values on the display. As can be seen in Figure 3, if X is initially set to 255 but Y and Z are practically negligibly 0, then the car has been raised from the back. In contrast, if Y increases and X and Z are almost zero, the vehicle is lifted from the front. An alert will be produced and essential steps can be done if it lifts over a certain threshold. We can conclude an accident has happened if the variance at the various axes is quite large within a short period of time.

'Thing Speak' will be used to continuously monitor this system. All the real time data will be stored on the cloud and if the accident occurs, the spike will be seen on the terminal depending on the threshold value. The data could be monitored from anywhere around the world and can be accessed by anyone. Using this technique, emergency services can be easily alerted when the accident occurs.

V. EXPERIMENTS AND RESULTS

A. Device Prototype



Fig. 10. Prototype of Smart accident detection and prevention system.

B. Result Discussion:



Fig. 11. LCD Display for Obstacle Detection.

Fig.10. Shows the response of system when the obstacle is detected. The obstacle detection is carried out with the use of IR sensor Module. The Pi-Camera simultaneously captures the real time images of the obstacle detected. The image which is captured by the P-camera is processed with the help of image processing techniques.



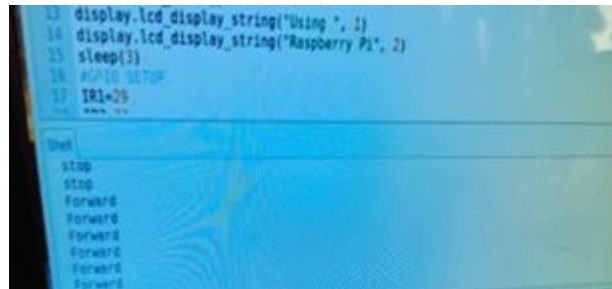
Fig. 12. LCD Display to stop vehicle .



Fig. 13. LCD display for obstacle location.

On similar lines, Fig.11. and Fig.12. depicts the stopping of vehicle on detection of obstacle. The IR sensor detects the precise location of obstacle and displays a message "Left side obstacle on road" on LCD.

Fig.14. Shows the code output generated in shell script. The code tells about the status of the vehicle whether moving forward, stop ,left, or right.



```

13 display lcd_display_string("Using ", 1)
14 display lcd_display_string("Raspberry Pi", 2)
15 sleep(3)
16 #GPIO SETUP
17 IR1=20
18
19
20
21
22
23
24
25
26
27
28
29
30
31
32
33
34
35
36
37
38
39
40
41
42
43
44
45
46
47
48
49
50
51
52
53
54
55
56
57
58
59
60
61
62
63
64
65
66
67
68
69
70
71
72
73
74
75
76
77
78
79
80
81
82
83
84
85
86
87
88
89
90
91
92
93
94
95
96
97
98
99
100
101
102
103
104
105
106
107
108
109
110
111
112
113
114
115
116
117
118
119
120
121
122
123
124
125
126
127
128
129
130
131
132
133
134
135
136
137
138
139
140
141
142
143
144
145
146
147
148
149
150
151
152
153
154
155
156
157
158
159
160
161
162
163
164
165
166
167
168
169
170
171
172
173
174
175
176
177
178
179
180
181
182
183
184
185
186
187
188
189
190
191
192
193
194
195
196
197
198
199
200
201
202
203
204
205
206
207
208
209
210
211
212
213
214
215
216
217
218
219
220
221
222
223
224
225
226
227
228
229
230
231
232
233
234
235
236
237
238
239
240
241
242
243
244
245
246
247
248
249
250
251
252
253
254
255
256
257
258
259
260
261
262
263
264
265
266
267
268
269
270
271
272
273
274
275
276
277
278
279
280
281
282
283
284
285
286
287
288
289
290
291
292
293
294
295
296
297
298
299
300
301
302
303
304
305
306
307
308
309
310
311
312
313
314
315
316
317
318
319
320
321
322
323
324
325
326
327
328
329
330
331
332
333
334
335
336
337
338
339
340
341
342
343
344
345
346
347
348
349
350
351
352
353
354
355
356
357
358
359
360
361
362
363
364
365
366
367
368
369
370
371
372
373
374
375
376
377
378
379
380
381
382
383
384
385
386
387
388
389
390
391
392
393
394
395
396
397
398
399
400
401
402
403
404
405
406
407
408
409
410
411
412
413
414
415
416
417
418
419
420
421
422
423
424
425
426
427
428
429
430
431
432
433
434
435
436
437
438
439
440
441
442
443
444
445
446
447
448
449
450
451
452
453
454
455
456
457
458
459
460
461
462
463
464
465
466
467
468
469
470
471
472
473
474
475
476
477
478
479
480
481
482
483
484
485
486
487
488
489
490
491
492
493
494
495
496
497
498
499
500
501
502
503
504
505
506
507
508
509
510
511
512
513
514
515
516
517
518
519
520
521
522
523
524
525
526
527
528
529
530
531
532
533
534
535
536
537
538
539
540
541
542
543
544
545
546
547
548
549
550
551
552
553
554
555
556
557
558
559
560
561
562
563
564
565
566
567
568
569
570
571
572
573
574
575
576
577
578
579
580
581
582
583
584
585
586
587
588
589
590
591
592
593
594
595
596
597
598
599
600
601
602
603
604
605
606
607
608
609
610
611
612
613
614
615
616
617
618
619
620
621
622
623
624
625
626
627
628
629
630
631
632
633
634
635
636
637
638
639
640
641
642
643
644
645
646
647
648
649
650
651
652
653
654
655
656
657
658
659
660
661
662
663
664
665
666
667
668
669
670
671
672
673
674
675
676
677
678
679
680
681
682
683
684
685
686
687
688
689
690
691
692
693
694
695
696
697
698
699
700
701
702
703
704
705
706
707
708
709
710
711
712
713
714
715
716
717
718
719
720
721
722
723
724
725
726
727
728
729
730
731
732
733
734
735
736
737
738
739
740
741
742
743
744
745
746
747
748
749
750
751
752
753
754
755
756
757
758
759
760
761
762
763
764
765
766
767
768
769
770
771
772
773
774
775
776
777
778
779
780
781
782
783
784
785
786
787
788
789
790
791
792
793
794
795
796
797
798
799
800
801
802
803
804
805
806
807
808
809
810
811
812
813
814
815
816
817
818
819
820
821
822
823
824
825
826
827
828
829
830
831
832
833
834
835
836
837
838
839
840
841
842
843
844
845
846
847
848
849
850
851
852
853
854
855
856
857
858
859
860
861
862
863
864
865
866
867
868
869
870
871
872
873
874
875
876
877
878
879
880
881
882
883
884
885
886
887
888
889
890
891
892
893
894
895
896
897
898
899
900
901
902
903
904
905
906
907
908
909
910
911
912
913
914
915
916
917
918
919
920
921
922
923
924
925
926
927
928
929
930
931
932
933
934
935
936
937
938
939
940
941
942
943
944
945
946
947
948
949
950
951
952
953
954
955
956
957
958
959
960
961
962
963
964
965
966
967
968
969
970
971
972
973
974
975
976
977
978
979
980
981
982
983
984
985
986
987
988
989
990
991
992
993
994
995
996
997
998
999
1000

```

Fig. 14. Automatic Moving code snapshot.

IV.CONCLUSION

Road deaths in India are among the highest in the world, and they are steadily increasing over time. Therefore, a mechanism that can lower fatalities across the nation is required. To prevent such accidents, innovative smart city solutions are widely desired. In this project, a self-driving autonomous car is built with the help of a Raspberry Pi and various sensors are interfaced for use in accident prevention applications. The paper includes results and a prototype. Additionally, sensor data is uploaded to think speak and is accessible for real-time monitoring.

V. REFERENCES

- [1]. S. Sarker, M. S. Rahman and M. N. Sakib, "An Approach Towards Intelligent Accident Detection, Location Tracking and Notification System," 2019 IEEE International Conference on Telecommunications and Photonics (ICTP), 2019, pp. 1-4, doi: 10.1109/ICTP48844.2019.9041759.
- [2]. Arjun K., Prithviraj and Ashwitha A. (2017), "Sensor Based Application for Smart Vehicles", International Journal of Latest Trends in Engineering and Technology, 8 (1), pp. 526-532.
- [3]. Rangan P. R. (2017), "Vehicle Speed Sensing and Smoke Detecting System", International Journal of Computer Science and Engineering, pp. 27-33
- [4]. A. Ali and M. Eid, "An automated system for accident detection," in I2MTC'15, 2015, IEEE, pp 1608-1612
- [5]. P. Nath and A. Malepati, "IMU based Accident Detection and Intimation System," in Proc. IEMENTech'18, 2018, IEEE, pp 1-4.
- [5]. P. Nath and A. Malepati, "IMU based Accident Detection and Intimation System," in Proc. IEMENTech'18, 2018, IEEE, pp 1-4.
- [6]. Prasanth P. and Karthikeyan U. (2016), "Effective Tracking of Misbehaviorial Driver Over Speed Monitoring With Emergency Support", International Journal of Advanced Research Computer Technology, 5 (10), pp. 2527-2529

- [7]. H. M. Sherif, M. A. Shedid, and S. A. Senbel, "Real Time Traffic Accident Detection System using Wireless Sensor Network," in Proc. SoCPaR'14, 2014, IEEE, pp 59-64.
- [8]. Report by J.P. Research India Pvt Ltd, Mumbai-Pune expressway Road accident study.
- [9]. P. Fabian, A. Rachedi, and C. Gue'guen, "Programmable objective function for data transportation in the Internet of Vehicles," Trans. Emerg. Telecommun. Technol., vol. 31, no. 5, 2020, Art. no. e3882, doi.
- [10]. T. Mekki, I. Jabri, A. Rachedi, and M. Ben Jemaa, "Vehicular cloud networking: Evolutionary game with reinforcement learning-based access approach," Int. J. Bio Inspired Comput., vol. 13, no. 1, pp. 45-58, 2019, doi.
- [11]. J. Smolka and M. Skublewska-Paszowska, "A method for collision detection using mobile devices," in Proc. 9th Int. Conf. Human Syst. Interact. (HSI), 2016, pp. 126-132, doi.
- [12]. R. K. Kodali and S. Sahu, "MQTT Based Vehicle Accident Detection and Alert System," in ProiCATccT'17, 2017, IEEE, pp 186-189.
- [13]. N. T. S. A. Wadhahi, S. M. Hussain, K. M. Yosof, S. A. Hussain and
- [14]. V. Singh, "Accidents Detection and Prevention System to reduce Traffic Hazards using IR Sensors," 2018 7th International Conference on Reliability, Infocom Technologies and Optimization (Trends and Future Directions) (ICRITO), Noida, India, 2018, pp. 737-741, doi: 10.1109/ICRITO.2018.8748458.
- [15]. J. Singh et al., "IR Sensor Based Accident Prevention System for Hilly Areas," 2023 International Conference on Disruptive Technologies (ICDT), Greater Noida, India, 2023, pp. 786-789, doi: 10.1109/ICDT57929.2023.10150715.
- [16]. M. Kumar, A. Kant, P. Kaktan, R. Bishnoi and K. Upadhyay, "Arduino Based System to Prevent Vehicle Accidents," 2021 International Conference on Design Innovations for 3Cs Compute Communicate Control (ICDI3C), Bangalore, India, 2021, pp. 140-144, doi: 10.1109/ICDI3C53598.2021.00037.
- [17]. V. Kinage and P. Patil, "IoT Based Intelligent System For Vehicle Accident Prevention And Detection At Real Time," 2019 Third International conference on I-SMAC (IoT in Social, Mobile, Analytics and Cloud) (I-SMAC), Palladam, India, 2019, pp. 409-413, doi: 10.1109/I-SMAC47947.2019.9032662.
- [18]. P. D. R. Dewmin, P. S. H. Yapa, S. D. Lokuge, M. G. N. M. Pemadasa and N. Amarasena, "License Detection and Accident Prevention System," 2022 4th International Conference on Advancements in Computing (ICAC), Colombo, Sri Lanka, 2022, pp. 381-386, doi: 10.1109/ICAC57685.2022.10025352.
- [19]. G. Ravindra, M. V. Rao and V. S., "Sensor Assisted Ghat Road Navigation and Accident Prevention," 2022 International Conference on Automation, Computing and Renewable Systems (ICACRS), Pudukkottai, India, 2022, pp. 1402-1407, doi: 10.1109/ICACRS55517.2022.10029037.
- [20]. R. Mounika, S. Hussian. Sk and L. Venkateshwara Kiran, "A Novel Approach for Accident Prevention Using IOT," 2019 International Conference on Vision Towards Emerging Trends in Communication and Networking (ViTECoN), Vellore, India, 2019, pp. 1-5, doi: 10.1109/ViTECoN.2019.8899717.
- [21]. L. Rupesh, A. Jain, S. Sarda, S. Gupta, S. I. Sajeesh and D. Palanisamy, "IoT and Cloud Based Integrated System for Accident Reporting and Vehicular Health Monitoring," 2018 Fourth International Conference on Research in Computational Intelligence and Communication Networks (ICRCICN), Kolkata, India, 2018, pp. 23-26, doi: 10.1109/ICRCICN.2018.8718699.

Scalable Design and Implementation IP for Advanced Extensible Interface (AXI) Protocol

Kaveri A. Sangamnerkar, Yogita D. Kapse, Nilima R. Kolhare

Department of E&TC, COEP Technological University, Pune, Maharashtra, India

ABSTRACT

The VLSI industry for semiconductors has undergone a transformation thanks to System-on-Chip technology. Recently, semiconductor hobbyists have been using a revolutionary approach, primarily over the past ten years, to integrate millions of ICs onto a silicon wafer. The on-chip communication is made possible by the communication protocols, which are crucial. AXI is a high-performance and efficient protocol that facilitates point-to-point transfers and interconnections. AXI is the most used AMBA protocol because of its distinct channel-wise distribution and hand-shaking. A scalable design for the Advanced Extensible Interface (AXI4.0Lite) protocol, a part of AMBA architecture, that provides control between the channel signals of protocol is presented in this work for master and slave configuration. It facilitates a simple and practical way to connect multiple IP cores in a system-on-chip or FPGA architecture, particularly for peripheral or control register access. The design is represented on the Intel Quartus Prime Lite 20.0 using Verilog for hardware description.

Keywords—VLSI, AXI, AMBA, System-on-Chip, communication, protocol, scalable

I. INTRODUCTION

The AXI is a part of Advance Microcontroller Bus Architecture (AMBA) developed by ARM. The AMBA makes it possible to design with a wide range of integrated and directly usable processing units and peripherals on the System on Chip. As opposed to other AMBA protocols like APB and AHB, the AXI provides substantially greater performance and throughput, making it a commonly used and acknowledged standard for constructing on-chip communication IPs. A subset of the AXI4 protocol called AXI4.0 Lite is frequently used in applications with defined burst lengths. AXI4-Lite's simplicity aids in lowering the interface's overall latency. Time-sensitive applications can benefit from its ability to communicate quickly and effectively between the master and slave modules. In this version of AXI, the data length is likewise expected to be fixed at 32 or 64 bits. The protocol, as depicted in Fig. 1, essentially establishes communication between its Masters and Slaves/Memory by using the Handshaking mechanism. The construction of a scalable architectural design for the AXI4.0 Lite Protocol employing sophisticated Verilog as a Hardware Description Language is the main emphasis of this work. State Machine (FSM) concepts are used to create an easy-to-understand and implement design that facilitates control between different protocol signals. For each of the master and slave's channels, a design is

created. Additionally, FPGA implementation of the synthesizable design is also carried out for hardware verification of the design functionality.

A. The AXI4.0 Basic Structure.

The protocol establishes communication between the master and slave using a handshaking approach. To execute the read/write transactions, the AXI protocol primarily consists of five communication channels, as depicted in fig. 1. They are listed as follows:

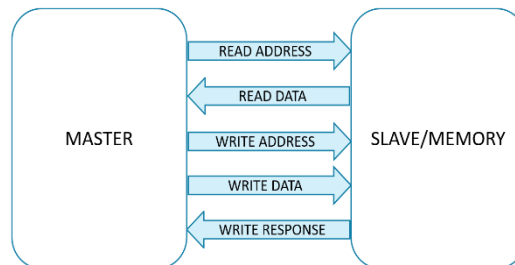


Fig. 1. Basic Structure of AXI.

Write Address Channel is specifically used by Master to know the address in slave on which the data is to be written. This channel includes the valid (AWVALID), ready (AWREADY), address (AWADDR) and protect (AWPROT). Write Data Channel enables the Master to write into the memory/slave. The signals that function within this communication channel are valid (WVALID), ready (WREADY), data (WDATA) and strobe (WSTRB). Write Response Channel helps the slave to send a response to the master after the data write operation has taken place. The signals that are directed within this channel are valid (BVALID), ready (BREADY) and response (BRESP). Read Address Channel employs its signals to read address from slave from which the data is to be read. The signals in this channel are valid (ARVALID), ready (ARREADY), address (ARADDR) and protect (ARPROT). Read Data Channel is utilised by the slave to read from the master with signals valid (RVALID), ready (RREADY), data (RDATA) and response (RRESP).

B. Signals in AXI4.0 Lite

a) The AXI is operational based on signals and controls between them. The protocol has two global signals clock (ACLK) and negedge reset (ARESETn). These signals are globally provided to all the channels for synchronisation and orderly operations. Valid signal is initiated by the master or slave depending on who is initiating the transaction. When the receiving segment is ready for the transaction, it sends back the ready signal. This enables reduction of power consumption. In order to read address from the slave or to write address, separate address signals are enabled. To read and write specific data within the master and slave channels, data signals are employed. If the channel wants to ensure if the read transaction is successful or a failure after the exchange of ready and valid signals, a response signal is generated. The responses are OKAY, EXOKAY, SLVERR and DECERR. 'Protect' is a special feature of AXI4.0 Lite. Due to this signal, secured reads and writes are carried out. Various values denote different access permissions such as unprivileged access, secure access, data access etc. 'Strobe' is also an exclusive feature of AXI4.0 Lite. It is used to mask particular bits of the write data channel and is used to enable the write action for specific desired bits.

TABLE I. SIGNALS OF AXI4.0 LITE PROTOCOL

Global Inputs	Write Address Channel	Write Data Channel	Write Response Channel	Read Address Channel	Read Data Channel

ACLK	AWVALID	WVALID	BVALID	ARVALID	RVALID
ARESETn	AWREADY	WREADY	BREADY	ARREADY	RREADY
	AWADDR	WDATA	BRESP	ARADDR	RDATA
	AWPROT	WSTRB		ARPROT	RRESP

II. RELATED WORK

A novel approach of the design for real time micro-architecture for interconnects has been devised by Zhe Jiang [1]. This design finds applications in highly integrated SOCs for higher throughputs. A performance-based comparison of various AMBA on chip communication protocols is presented by Anurag Shrivastava[2]. The protocols AMBA 2.0, AMBA3.0, AMBA4.0 AHB and AXI were compared based on performance, power consumption, speed and other design parameters in this work. Arun C G has proposed an Interface for Single Master and Singular slave has been designed for various burst operations[3]. The design is verified for functionality using the Universal Verification Methodology (UVM). Verification of all important features of five channels of AXI has been carried out by M Prasanna Deepu[4]. System Verilog has been used as a verification language for a coverage driven report. AXI protocol specifications were studied with the help of specification guide provided by ARM Limited[6]. Neethika[7], has designed a network on chip interface for AXI protocol with further PLD prototype.

III. PROPOSED METHODOLOGY

A design establishing control between the master and slave is proposed in this work that essentially uses the state machine algorithms as a basis of control and communication. The channels of AXI for the master and slave have been designed, each as a controlling unit state machine with various states through which the transfer mechanism takes place. These states are controlled by the signals of AXI included in that particular channel. The master and slave are further integrated together in the AXI top level entity.

A. Handshaking Mechanism.

The protocol obeys a handshaking mechanism that ensures a secure communication with reduction of power loss. A signal is passed from the master to slave and the slave returns back an acknowledgement to master so as to notify the receipt of signal from the master and vice versa. This process ensures that the data bits are transmitted and there's no loss of bits in between the channel.

B. Control Unit

The channels are designed as state machines whose states are controlled and determined by various signals of the protocol. The state table and state diagrams for each channel fsm is formed based on the signal enabling conditions and the design is developed accordingly.

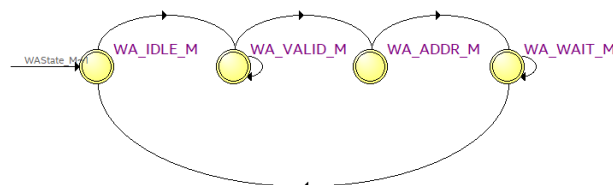


Fig. 2. State Diagram for Write Address Channel of Master.

Fig. 2 shows the state diagram for write address channel FSM of master which transitions from the idle state to the valid state if the address to be written is ready (awaddr > 32'h0) else it remains in the idle state. Going ahead, if the ready signal is received (awready), then the FSM moves ahead to the write address state, else it remains in the same state. Once the desired address is written, the FSM moves to the wait state till it gets the write response channel's valid signal (BVALID). If it is not received, the FSM continues to be in the wait state. In similar fashion, depending on the signal dependencies, all other read and write channels are also designed for functionality by determining its proper state tables and state diagrams.

C. Field Programmable Gate Array

The Field Programmable Gate Array (FPGA) is a user fabricated IC that can be programmed and tailored in the user defined way to perform specific required functions. An FPGA's main building blocks are CLBs; the complex logic blocks. They are made up of flip-flops, registers, and a matrix of adjustable logic elements (LEs) or lookup tables (LUTs). To implement desired logic operations or digital circuits, these CLBs can be designed. A network of programmable interconnect resources, including routing channels and programmable switches, connects the CLBs together. The signal connections between various CLBs and I/O (Input/Output) blocks are made possible by these interconnect resources. Any Logic circuit can be designed and implemented on FPGA for a hardware display and verification of its functionality. The AXI4.0 Lite design is implemented on the FPGA for hardware proven results. The user-defined configuration bitstream is stored in the configuration memory of FPGAs, which are programmable hardware. To identify the FPGA's functioning, the configuration memory is loaded upon power-up or reconfiguration.

IV. RESULTS

The design modules for Master, Slave and a top module integrating them together were created and the RTL Schematic and simulations for the same were recorded and observed.

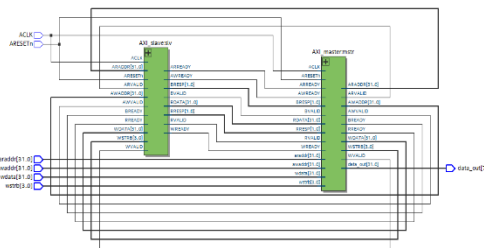


Fig. 3. RTL Design for AXI top.

As shown in Fig. 4, the master and slave modules are integrated into a top module 'AXI top' with all the interconnecting signals and the RTL is generated.

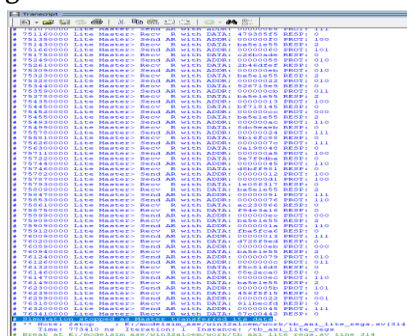


Fig. 4. Transcript outcomes for transaction.

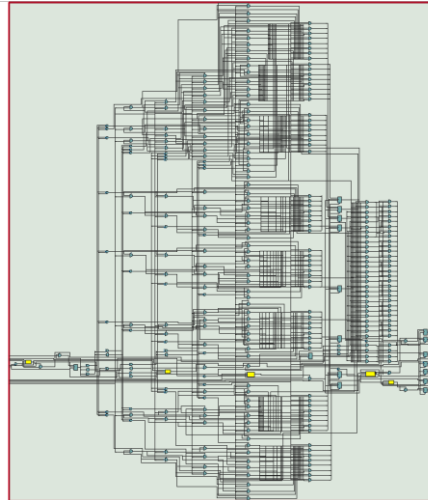


Fig. 5. RTL Design for AXI slave.

Fig. 4 shows the transcript snapshot that is taken once the simulation is stopped after the data transfer of Master is completed.

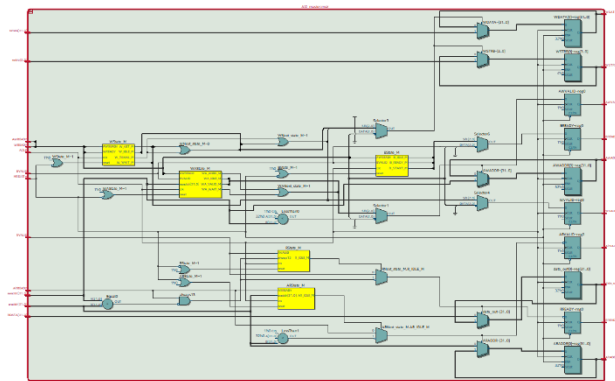


Fig. 6. RTL Design for AXI master.

Fig. 5 and 6. shows the RTL generated for master and slave of AXI. We can see that both the RTL consists of five FSMs, one for controlling each channel transactions, further interconnected by input and output decoders, integrated together to form a synthesizable RTL design for Master and Slave.

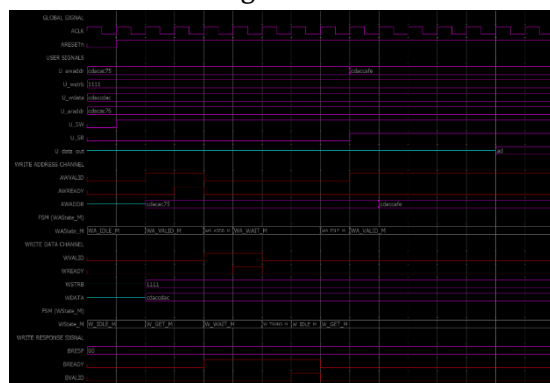


Fig. 7. Simulation result for AXI master.

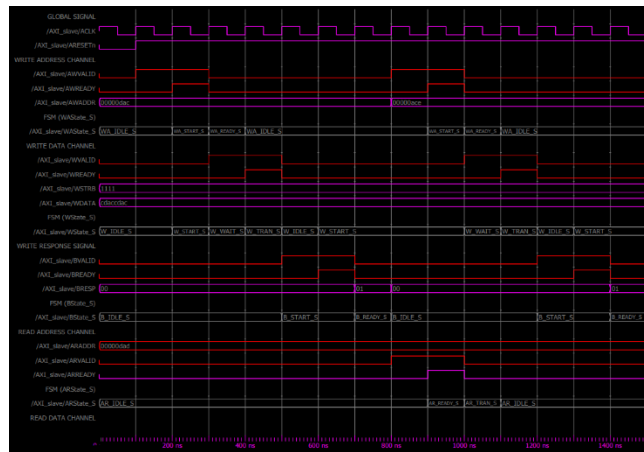


Fig. 8. Simulation result for AXI slave.

As seen in Fig. 8 and Fig. 9, the simulation for master and slave channels is generated, one can see that the ready signals are turned high on the next cycle of valid signals and the FSMs vary in the various states according to the signals.

V. CONCLUSION AND FUTURE SCOPE

The design for AXI4 Lite is thus developed for all its channels and the functionality is checked from the simulation results. The scalable design for AXI4.0 Lite can be utilized for the on-chip communication for establishment of on chip communication. The parameterized design makes it scalable for all existing and further AXI versions. The functionality can further be implemented and verified using the Field Programmable Gate Arrays (FPGA) for all existing and further AXI versions. The functionality can further be implemented and verified using the Field Programmable Gate Arrays (FPGA).

REFERENCES

- [1]. Zhe Jiang, Kechen Yang, Nathan Fisher, Ian Gray, "AXI-IC RT : towards a real-time AXI-interconnect for highly integrated SOCs," IEEE Transaction in Computers, 2023.
- [2]. Anurag Shrivastava, G.S. Tomar, Ashutosh Kumar Singh, "Performance Comparison of AMBA bus-based system-on-chip communication protocol," International Conference on Communication Systems and Network Technologies, 2011.
- [3]. Arun C G, Suganya .S, "Constrained random verification of burst operation in AXI-4," International Interdisciplinary Humanitarian Conference for Sustainability (IIHC), 2022.
- [4]. M. Prasanna Deepu, R. Dhanabal, "Validation of transactions in AXI Protocol using System Verilog," International conference on microelectronic devices, circuits and systems, 2017.
- [5]. Vazgen Melikyan, Stepan Harutyunyan, "UVM verification IP for AXI," IEEE East-West Design & Test Symposium (EWDTS), 2021.
- [6]. "AMBA AXI and ACE Protocol Specification," ARM IHI 0022H.
- [7]. Neethika Tidala, "High Performance Network On Chip using AXI4 protocol interface on an FPGA", Proceedings of the 2nd International conference on Electronics, Communication and Aerospace Technology (ICECA 2018).

A GSM-Based System for Vehicle Collision Detection and Alert

Dr. Pradeep Kumar N S¹, Suhas S K², Dr. Girish H², Mrs. Dhivya Karunya S³, Mrs. K Revathi³, Mrs. K Gayathiri³

¹Professor, Department of ECE, SEACET, Bengaluru, India

²Associate Professor, Department of ECE, Cambridge Institute of Technology, Bengaluru, India

³Assistant Professor, Department of ECE, SEACET, Bengaluru, India

ABSTRACT

Road accidents is one of the severe problems that leads the deaths of innocent pupil surrounding the world. India is currently at the highest of the list of road fatalities. This is a very severe problem that needs to be resolved to save the lives of many injured in the accident. With regards to WHO surveys and findings, more than 50% of people die each year from road accidents. Most of them suffer from cyclists due to head injuries. In the event of an accident, rescue of a person is delayed, so the proposed study aims to address this issue by building an automated system that alerts family members and nearby hospitals in the event of an accidents increase. In this work, we will introduce an accident prevention system with a vehicle accident detection function. This increases the chances of reducing the number of daily accidents on the road. At the same time, in the event of an accident, the system will locate it and automatically notify those who can respond immediately. Global Positioning System & # 40; GPS & # 41; and Global System for Mobile Communication (GSM) technology have built an Arduino-based system. Accelerometers are also used to measure the amount of vehicle speed and pitch when the vehicle collides with something. If the speed of the car exceeds the speed limit or falls.

Keywords— GPS, GSM, Accelerometer, Arduino

I. INTRODUCTION

The automobile industry's production has risen steadily over the world in recent years. Annually, millions of automobiles are manufactured. As a result of the increased traffic, the number of accidents is also rising. Because of a lack of competent treatment, many people have died in traffic accidents.[1] This accident on the highways and in a distant location has resulted in a large number of deaths and is a danger to society. The number of automobiles on the road is increasing faster than the economy and population. Road accidents and deaths, particularly among two-wheelers, are on the rise at an alarming rate.

Most crash fatalities are due to lack of prompt medical attention on highways and other roads. Accident site emergency medical facilities can further reduce fatalities. Hence the idea of an alarm system that recognizes the accident and its severity, alerts a nearby medical center, and brings an ambulance or medical assistance to the scene of the accident.

The proposed system will check if an accident has occurred and determine the extent of injury to the victim/driver. If the accident is determined to be serious, locate the nearest medical center and report the

accident. The exact location is transmitted via the victim's mobile phone so emergency services can reach the scene without delay. The system also sends messages to friends and relatives to inform them of the incident.

In recent years, studies on accident detection/alarm systems have been actively conducted. [2] In this topic, research presented a model with two main modules. The purpose of this system is to track the location of the vehicle using a GPS receiver and send that information to the owner's mobile phone via his SMS. Another prototype proposes a method to identify traffic accident victims and provide assistance more quickly. Here, a low-cost alert system is proposed to provide immediate medical assistance to accident victims by alerting the local medical assistance center with the exact location of the accident and patient details via SMS.

However, many if paramedics receive timely crash information, despite numerous attempts by different government and non-governmental groups around the world through various initiatives to raise awareness of the problem. Life should have been saved. A study by Virtanen et al. Shows that 4.6% of accident fatalities could be prevented only if rescue services were available at the time of the accident. Therefore, efficient automated accident detection with automatic notification of rescue services, including information about the location of the accident, is a fundamental requirement for saving valuable lives.

II. LITERATURE REVIEW

A This paper proposes to use a GPS receiver's capabilities to monitor a vehicle's speed, detect an accident based on the monitored speed, and broadcast the location and time of the accident using GPS data processed by a micro-Controller to the Alert Service Centre through the GSM network [1]. The interval between starting to brake and coming to a complete stop is greater at high speeds. [3] The square of speed determines braking distance. As a result, the chances of avoiding a collision decrease. A speedometer can also be used to detect speed reductions in automobiles, but it requires an analogue to digital converter to do so. As a result, a GPS is utilized to track the vehicle's speed at all times.

The vehicle speed is calculated at every instance by GPS. If there is decrease in new speed values then it raises an ALARM for accident detection. Then 10 secs will be given to abort the emergency Else the emergency is sent to Alert Service Centre and plot the location of accident by the GSM number received. There after rescuing the individual. This study proposes to use the features of accelerometers to collect data and identify accidents. It then sends the location of the accident, determined by the GPS data processed by the microcontroller, over the GSM network to the nearest hospital available on the network to alert the family. [4] If the angle is greater than 46 degrees and less than -46 degrees, the car will roll over. The weight and center of gravity of the vehicle, in addition to the rolling and pitching limit frequency values, have a decisive effect on rollover. When the threshold is reached, the notification mechanism is activated to alert the family and the nearest hospital to the rollover.

In addition, a GPS tracker is used to record false assumptions from the captured GPS data. The notification system shares information with family emergency contacts and the nearest hospital. When the detection threshold is reached, the notification system becomes active. The location is identified by GPS.

In this study, the function of the piezoelectric sensor is used to identify the accident based on the voltage generated by the collision, and the GPS data processed by the microcontroller is used to alert the location and time of the accident on the GSM network.

We suggest reporting to the service centre. Piezoelectric sensors generate a DC voltage that is proportional to the impact of the vehicle. When the voltage exceeds a certain value, the sensor is triggered.

The GPS module determines the latitude and longitude and is forwarded as a message to the rescue service via the GSM module. Another GSM module receives the message. Map created by Google. [5] Receive detailed SMS from the accident site. As a result, the coordinates change slightly. An OFF switch is also available if necessary to avoid false alarms.

Table 1: Comparison between Research Paper

	Research/Technical Paper	process	Advantage
Approach1	Accident Detection using GPS and GSM Technology.	Detects Accident and location is sent over GPS to mobile through GPS.	Just detects the location of accidents and alerts to the mobile.
Approach2	Accident Detection through GPS, GSM and Accelerometer.	Detects the location of accident by detecting the changes in the orientation levels of accelerometer	Detects the collision by the accelerometers.
Approach3	Read time detection using vibration sensor	Detects the accident by collision by voltage generated through sensors by collision	Sending of location To near-by hospitals through network.

III. METHODOLOGY

We presented this accident detection and alarm system project in order to protect the driver's life in all types of accident situations. We utilized an Arduino UNO to connect a GPS GY6MV2 receiver and a GSM module SIM 800L in our model. The X and Y axis co-ordinates of the car will be captured by the MEMS Accelerometer, and the GSM SIM 800L will send a notification message to the family members' registered contact numbers. [6] The GPS module continuously records the vehicle's latitude and longitude. If the mishap is minimal and does not necessitate notifying family members and requesting an emergency, we will use a reset button to stop the message from being sent.

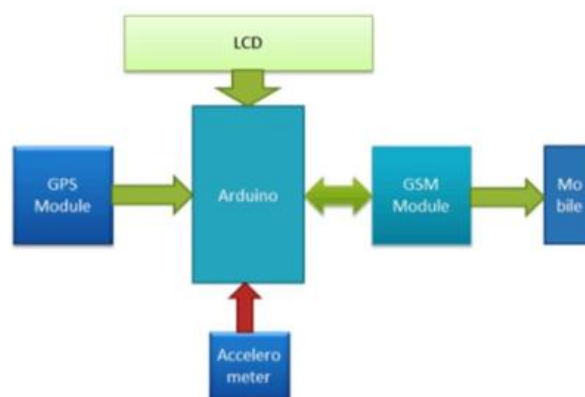


Fig 1. Block Diagram of the Accident Alert system

In Figure 1 shows an accident warning system from GPS modules, GSM modems, accelerometers to Arduino miniature controllers. The GPS module endlessly identifies the location of an accident as its perimeter and longitude. The accelerometer gets the X and Y coordinates of the vehicle, and when the coordinates exceed the

limit, the miniature controller sends a signal. The miniature controller activates the SIM 800L GSM module and sends notifications to family members.

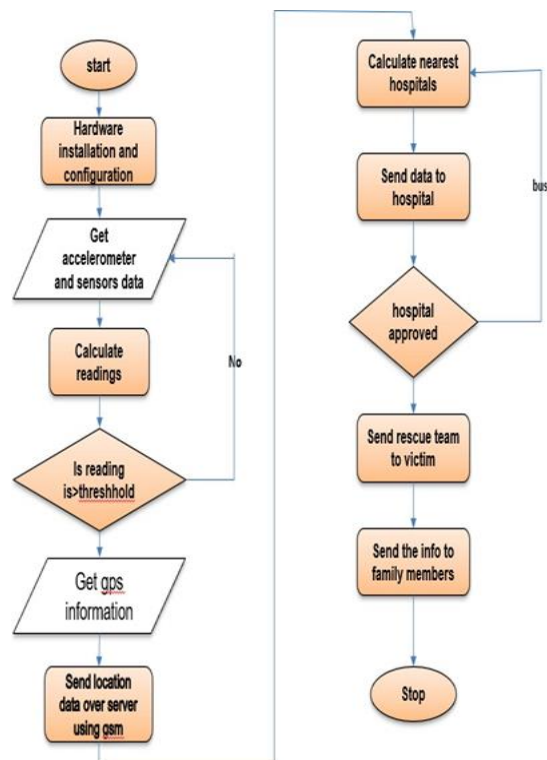


Fig 2. Flow chart

Monitors vehicle speed and detects sudden drops in vehicle speed. An Arduino UNO is used as the controller and reads the values from the accelerometer. An accelerometer detects if the axis is falling. When the Arduino observes a sudden change in vehicle speed. Read your current location from GPS module and send it to your mobile number via SMS via GSM module. [7] The Arduino will buzz before sending his SMS, and after 30 seconds it will buzz and he will send the SMS. However, if the passenger is not in danger, they can press the "I'm fine" button. This is done to avoid situations that lead to erroneous and accidental rescues.

System Implementation

The proposed system can be extremely useful in detecting automobile crashes, and when one occurs,[8] it will send a text message to family, hospitals, and police stations, among other places, in order to provide medical assistance to passengers as promptly as possible. The system is built on a microcontroller and interacts with a variety of sensors and modules, including an accelerometer, limit switch, GPS system, and GSM module. The accelerometer and limit switch are crucial components in this system for detecting the accident. The Arduino UNO board is chosen as a microcontroller device in this system since it is readily available and simple to implement. The next section goes through the many aspects of the proposed plan.

Arduino

The Arduino UNO board is used as a microcontroller device in this setup. The Arduino board is currently being used in a variety of IoT-based applications due to its ease of integration with a variety of devices (such as

sensors, different modules, etc.). The Arduino platform was used for the programming portion. [9] It comes with an Integrated Development Environment that allows it to communicate with a variety of devices. A programming language, such as C, is an open-source software that can be used to interface with the Arduino hardware and upload any program over USB.

Accelerometer

The acceleration is measured using an accelerometer, which is an electromechanical device. It can be dynamic (moving or vibrating) or static (still) (such as the constant force of gravity). The accelerometer is a transducer that detects the movement of an item by measuring the acceleration imparted. The ADXL335 Accelerometer, a three-axis accelerometer, is employed in this system. [10] It's a low-profile MEMS sensor that's made up of micro-machined structures on a silicon wafer suspended by a poly-silicon spring. It calculates the object's coordinates in relation to the earth using gravitational pull. It has two supply pins and three analogue pins for the three axes. It is mostly used for car-crash detection, scrolling, and other similar tasks.

GPS System

This module is extremely useful for tracking the location of an accident using the GPS system. This information can also be utilized to track the vehicle's speed, which is very useful in predicting the likelihood of an accident. The NEO 6M GPS module was utilized to track the vehicle's location in this system. The main advantage of this module is that it can easily be combined with the Arduino module, that it is simple to operate, and that it responds quickly, which is very helpful for sending the location to a specified number in order to receive assistance as soon as possible. There are 27 satellites orbiting the earth, and three of them are used to track the location.

GSM Module

A GSM module is a type of circuit that allows a mobile device to communicate with a GSM system. The most significant portion of this module is the modem, which is powered by the power supply circuit and used to connect to the network and send messages.[11] GSM-based communication systems are extremely useful for transmitting information to the police station, family members, hospitals, and other locations. The information on the Arduino board has been relayed in this system. To send/receive texts and make/receive phone calls to the predefined person, we utilize the GSM module SIM900A, which is attached to the Arduino board. The module operates at 3A power supply and uses Dual-Band 900 MHz and 1800 Mhz. Both limit switches are used in this system.

IV. RESULTS AND DISCUSSIONS

An experimental arrangement for vehicles has been devised in this work to continually relay the location when an accident happens. The experiment is carried out here different angles, and to double-check the correctness of the measurements. It is tried numerous times at the place with the time delay. From the data and observations gathered from the projected some findings are obtained using the model. The system keeps track of everything. The longitude and latitude of the locations where the car is parked Creating a virtual

environment necessitates unintentional observation. Environment. We have taken the following steps in this experiment.

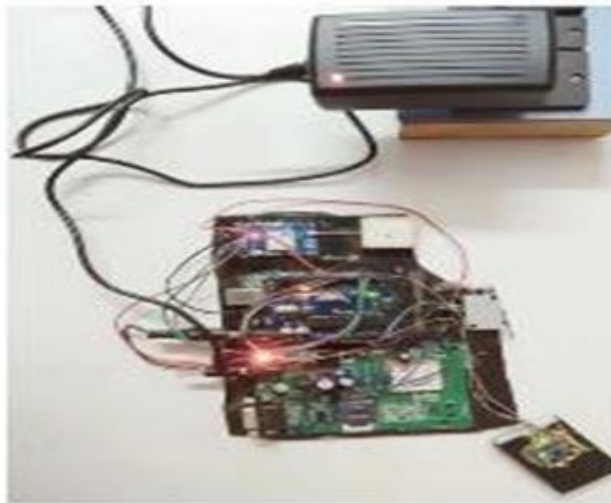


Fig 3: Experimental setup

We must ensure that the connection between Arduino and GSM is formed. There are two ways to achieve it: one is to link the TX pin of the GSM module to the RX pin of the Arduino, and the other is to connect the RX pin of the GSM module to the TX pin of the Arduino

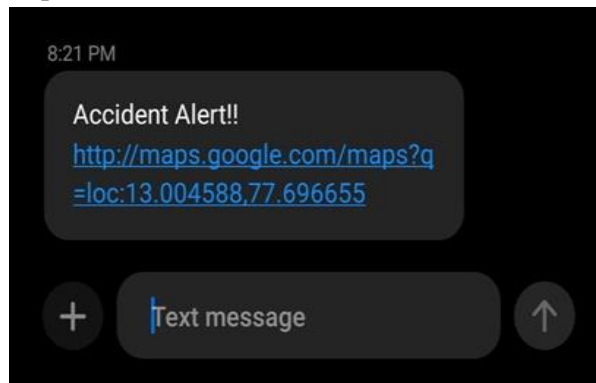


Fig 4: Output of GSM Module When Accident Occurs Receiving accident location message



Fig 5: Hardware Model of Accident Alert System

When our vehicle is struck from the front by another vehicle, we are said to be involved in a front accident. When our vehicle is struck from the left side by another vehicle, it is considered a left accident. The X and Y coordinates of our car will be detected by the MEMS Accelerometer.

When our vehicle is struck from the right side by another vehicle, it is considered a right accident. Our vehicle's X and Y coordinates will be detected by the MEMS Accelerometer. When our vehicle is hit from behind by another vehicle, it is considered a back accident. Our vehicle's X and Y coordinates will be detected by the MEMS Accelerometer.

The second method is to choose two Arduino pins that are PWM enabled (Pin 9, 10). It makes use of Arduino's software serial library, and once connected, data may be sent immediately to GSM.

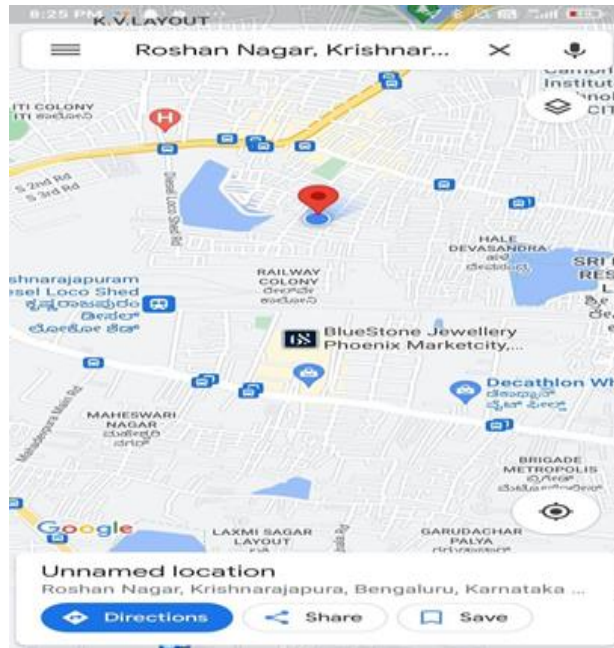


Fig 6: Receiving accident location message with google map link

In order to reduce accidents, we proposed this system that uses a GSM module to send warning messages to accident families and a GPS modem to continuously record the location of the accident site. Send the latitude and longitude of the accident site. When a vehicle collides with another vehicle, an ADXL335 MEMS accelerometer is used to detect the axis change. The MEMS accelerometer gets the X&Y axis values.

The proposed technique helps to reduce the number of people killed in car accidents. With the help of the proposed methodology, it detects the accidents that have occurred using the GPS module, determines the location of the accident and sends an alarm message using a GSM module to travel to the location of a medical emergency accidents happen all the time, and they can save people's lives. The death rate is reduced as a result of this feature accident- related deaths and injuries can be reduced.

V. CONCLUSION

We have created a mechanism to detect accidents. The proposed system handles accident detection and warning. It identifies the exact latitude and longitude of the accident vehicle and sends this information to the nearest emergency service. Arduino helps send messages to various components in the system. The direction of the accident is monitored by an accelerometer and the vehicle rollover is determined by the gyroscope. The data will be sent to the registered phone number via the GSM module. Locations are provided via a GPS

tracking system and cover the geographic coordinates of the entire area. Due to the popularity of vehicles, traffic accidents and road breakdowns are also increasing. People's lives are at stake. This is a direct result of our country's inability to access major issues.

II. REFERENCES

- [1] T Kalyani, S Monika, B Naresh, Mahendra Vucha, Accident Detection and Alert System, IJITEE, March 2019.
- [2] Parag Parmar, Ashok M. Sapkal, Real time detection and reporting of vehicle collision, IEEE, 2020.
- [3] Md. Syedul Amin, Jubayer Jalil, M.B.I. Reaz, Accident Detection and Reporting System using GPS, GPRS and GSM Technology, IEEE, 2019
- [4] Gowshika B, MadhuMitha, G, Jayashree, Vehicle accident detection system using GPS, GSM modem, IRJET
- [5] Sayanee Nanda, Harshada Joshi, Smitha Khairnar, An IOT Based Smart System for Accident Prevention and Detection, IEEE, 2018.
- [6] Norsuzila Yaacob, Ainnur Eiza Azhar, Azita Laily Yusofl, Suzi Seroja Sarnin, Darmawaty Mohd Ali and Ammar Anuar, Real Time Wireless Accident Tracker using Mobile Phone, IEEE
- [7] S. Sonika, Dr. K. Sathyasekhar, S. Jaishree, Intelligent accident identification system using GPS, GSM modem, DARCCE,
- [8] Girish H, Iot operated wheel chair, IJER, Vol-5, ISSN: 2347-5013, may 2016.
- [9] Girish H, Sridhar S, Bharath H, Vishvesh V, Gowtham K V, "IOT based transformer power theft detection and protection", IJER, Vol-5, ISSN: 2347-5013, may 2016
- [10] Girish H. "Intelligent Traffic Tracking System Using Wi-Fi." International Journal for Scientific Research and Development 8.12 (2021): 86-90.
- [11] GIRISH H , "Internet of Things Based Heart Beat Rate Monitoring System", © September 2022 | IJIRT | Volume 6 Issue 4 | ISSN: 2349-6002 IJIRT 156592 INTERNATIONAL JOURNAL OF INNOVATIVE RESEARCH IN TECHNOLOGY 227
- [12] A. Devipriya, H. Girish, V. Srinivas, N. Adi Reddy and D. Rajkiran, "RTL Design and Logic Synthesis of Traffic Light Controller for 45nm Technology," 2022 3rd International Conference for Emerging Technology (INCET), 2022, pp. 1-5, doi: 10.1109/INCET54531.2022.9824833.
- [13] Girish H, Shashikumar D R, "A Novel Optimization Framework for Controlling Stabilization Issue in Design Principle of FinFET based SRAM", International Journal of Electrical and Computer Engineering (IJECE) Vol. 9, No. 5 October 2019, pp. 4027~4034. ISSN: 2088-8708, DOI: 10.11591/ijece.v9i5.pp.4027-4034
- [14] Girish H, Shashikumar D R, "PAOD: a predictive approach for optimization of design in FinFET/SRAM", International Journal of Electrical and Computer Engineering (IJECE) Vol. 9, No. 2, April 2019, pp. 960~966. ISSN: 2088-8708, DOI: 10.11591/ijece.v9i2.pp.960-966
- [15] Girish H, Shashikumar D R, "SOPA: Search Optimization Based Predictive Approach for Design Optimization in FinFET/SRAM", © Springer International Publishing AG, part of Springer Nature 2019 Silhavy (Ed.): CSOC 2018, AISC 764, pp. 21–29, 2019. https://doi.org/10.1007/978-3-319-91189-2_3.

- [16] Girish H, Shashikumar D R, “Cost-Effective Computational Modelling of Fault Tolerant Optimization of FinFET-based SRAM Cells”, © Springer International Publishing AG 2017 R. Silhavy et al. (eds.), Cybernetics and Mathematics Applications in Intelligent Systems, Advances in Intelligent Systems and Computing 574, DOI 10.1007/978-3-319-57264-2_1.
- [17] Girish H, Shashikumar D R, “A Survey on the Performance Analysis of FinFET SRAM Cells for Different Technologies”, International Journal of Engineering and Advanced Technology (IJEAT) ISSN: 2249 – 8958, Volume-4 Issue-6, 2016.
- [18] Girish H, Shashikumar D R, “Insights of Performance Enhancement Techniques on FinFET-based SRAM Cells”, Communications on Applied Electronics (CAE) – ISSN: 2394-4714, Foundation of Computer Science FCS, New York, USA .Volume 5 – No.6, July 2016 – www.caeaccess.org
- [19] Girish H, Shashikumar D R, “DESIGN OF FINFET”, International Journal of Engineering Research ISSN: 2319-6890) (online), 2347-5013(print) Volume No.5 Issue: Special 5, pp: 992-1128, doi: 10.17950/ijer/v5i5/013 2016.

Design and Analysis of Parallel Slotted Multiband Microstrip Patch Antenna for Wireless Applications

Sreenvas Naik¹, Kiran Kumar K², Arun Kumar G³, Chandrappa D N⁴

¹Faculty, Department of Engineering, University of Technology and Applied Sciences, IBRI, OMAN.

²Assistant Professor, Dept. of ECE, East Point College of Engineering & Technology, Bangalore, Karnataka, India.

³Professor & HOD, Dept. of ECE, JSS Academy of Technical Education, NOIDA, Uttar Pradesh, INDIA.

⁴Associate Professor, Dept. of ECE, East Point College of Engineering & Technology, Bangalore, Karnataka, India

ABSTRACT

In this research article, we introduce a multiband- microstrip slotted antenna specifically designed for wireless communication applications. Microstrip patch antennas are extensively engaged due to their advantageous characteristics, including flexibility, robustness, compact size, lightweight nature, narrow radiation beam, and ease of installation and fabrication. Our proposed antenna is developed using a lossy FR-4 substrate with a permittivity of 4.3. It comprises a patch with four narrow slits and a ground plane, designed to generate a range of frequencies centered at 5.2 GHz, 9.33 GHz, and 12.038 GHz. To validate our design, we conducted simulations utilizing the CST MICROWAVE STUDIO software. These simulations enable us to analyze the performance behavior of the antenna across the desired frequency bands.

Keywords - microstrip, Multiband, Patch.

I. INTRODUCTION

Microstrip patch antennas are comprehensively utilized in various applications due to their appealing characteristics, such as a low profile, lightweight design, cost-effectiveness, compatibility with modern printed circuit technology, and integration capabilities with MMIC (Monolithic Microwave Integrated Circuit) design [1-3]. These features have made microstrip patch antennas popular in radar systems, microwave communication, and space communication. The construction of microstrip antennas involves a thin metallic strip, known as a patch, positioned above a ground plane. A dielectric sheet, referred to as the substrate, separates the strip patch and the ground plane. The resonating patch can be designed in various shapes, such as circular, square, elliptical, rectangular, or any other desired configuration [5- 7].

To achieve a smaller antenna size, we employ substrate materials with high dielectric constants [4]. Our primary objective is to enhance the operating bandwidth while simultaneously reducing the overall size of the antenna. The proposed antenna consists of a substrate with a height of 1.67mm and a dielectric constant of 4.3. To evaluate its performance, simulations are conducted using the CST MICROWAVE STUDIO software.

Wireless communication applications often necessitate antennas that can operate at multiple frequencies. Given its compact size, affordability, and lightweight nature, this antenna proves suitable for various applications such as radar communication, satellite TV communication, and K-band microwave communication. Simplicity is the major advantages of the proposed antenna. Its straightforward design allows for easy implementation and fabrication, thereby reducing manufacturing costs and time.

THE ANTENNA DESIGN

The antenna is structured using three layers, namely the patch, substrate, and ground. All dimensions are quantified in millimeters to ensure precise measurements. The planned antenna is integrated onto a FR-4 lossy dielectric sheet, which forms an essential part of its composition.

A. Wideband Microstrip Antenna

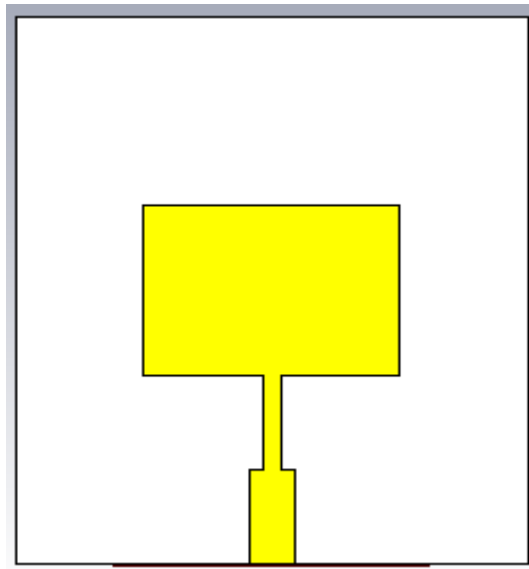


Fig.1: Basic patch antenna

The figure 1 illustrates a basic patch antenna designed to generate a single frequency. The essential formulas for calculating the width and length of such antennas are detailed below [1].

$$w = \frac{1}{2f_r \sqrt{\mu_0 \epsilon_0}} \sqrt{\frac{2}{\epsilon_r + 1}} = \frac{c}{2f_r} \sqrt{\frac{2}{\epsilon_r + 1}} \quad \dots\dots\dots(1)$$

$$L = \frac{c_0}{2f_r \sqrt{\epsilon_{reff}}} \quad \dots\dots\dots(2)$$

$$\epsilon_{reff} = \frac{\epsilon_r + 1}{2} + \frac{\epsilon_r - 1}{2} \left[1 + \frac{12h}{w} \right]^{-\frac{1}{2}} \quad \dots\dots\dots(3)$$

Patch	17.88X 13.51
Height of the substrate	1.60
QWT line width	1.27
QWT line length	7.45
Feed line width	3.16
Feed line length	7.41

I. The antenna results

$$\frac{\Delta L}{h} = \frac{0.412(\epsilon_{reff} + 0.3) \left(\frac{w}{h} + 0.264 \right)}{(\epsilon_{reff} - 0.258) \left(\frac{w}{h} + 0.8 \right)} \dots\dots\dots(4)$$

Where

L_{eff} = Effective patch length

c = Free space Velocity of light

f_r = Operating resonating frequency ϵ_r = Dielectric constant

h = Substrate thickness

The projected antenna underwent analysis and optimization using CST MWS software, resulting in the achievement of a tri-band patch slot antenna design. In this design, the first- band resonates at 5.10 GHz, with a reflection coefficient of -17.20 dB and a -10 dB bandwidth of 0.32 GHz. The second- band operates at 9.33 GHz, with a reflection coefficient of -21.90 dB and a -10 dB bandwidth of 1.002 GHz. Lastly, the third-band resonates at 12.03 GHz, with reflection coefficient of -23.053 dB and a bandwidth of 1.2942 GHz. The figure 3 showcases plot of reflection coefficient against frequency, providing a visual representation of the antenna's performance. The antenna basic parameters include a dielectric constant of $\epsilon_r=4.3$, a substrate height of $h=1.6\text{mm}$, and a resonating frequency of $f_r=5.2\text{GHz}$. The employed substrate material is FR-4 lossy.'

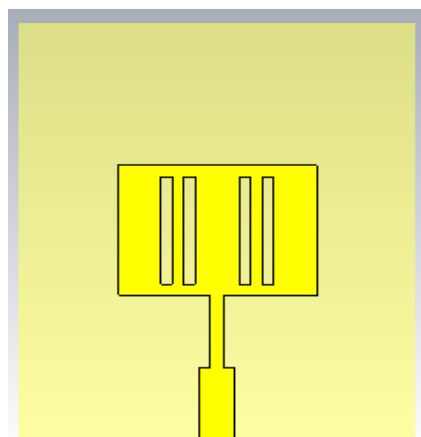


Fig.2: Geometry of the antenna with slots

Slots are introduced on the patch, where each slot is having length of 10.0 mm and width of 1.0 mm as shown in figure2.

Table 1: Dimension of antenna structure

Parameters	Dimensions
Ground	35.7X 27.02
Substrate material	35.7X 27.02

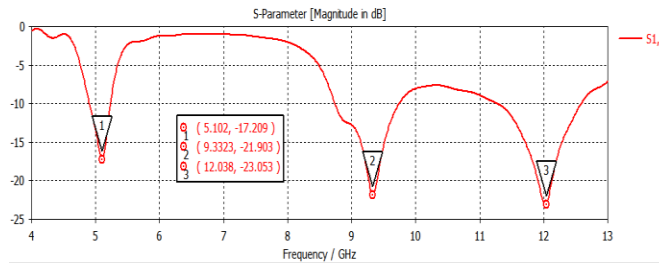


Fig.3: The return loss graph

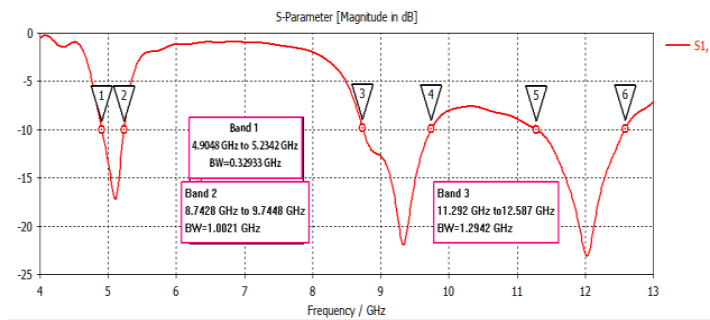


Fig.4: The bandwidth graph

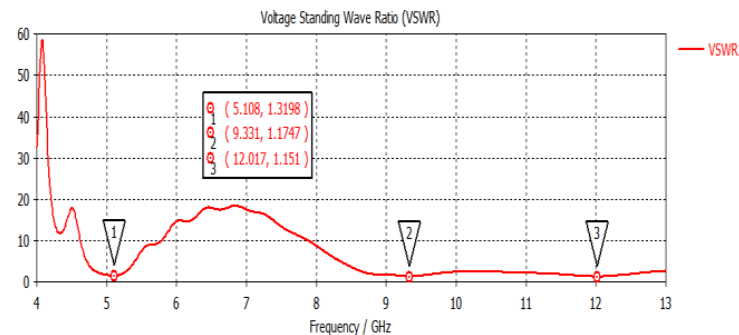


Fig.5: The VSWR graph

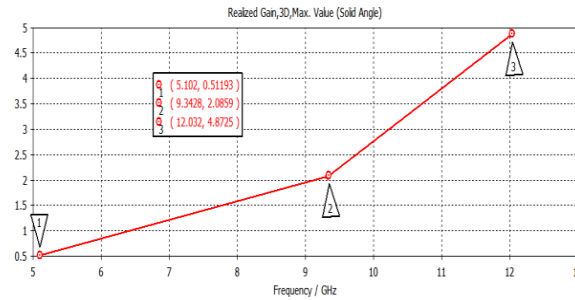


Figure 6: The gain plot

The projected antenna patterns have been thoroughly investigated. Figures 7, 8, and 9 depict the 2D patterns at 5.10 GHz, 9.33GHz, and 12.03 GHz. These patterns demonstrate the simulated total-field patterns, illustrating excellent wideband radiation characteristics at these radiating frequencies. To provide a more comprehensive view, figure 10, 11, and 12 showcase the 3D patterns specifically for the resonant frequencies of 5.10 GHz, 9.33GHz, and 12.03 GHz, respectively. These visual representations further highlight the antenna's radiation behavior at different frequencies.

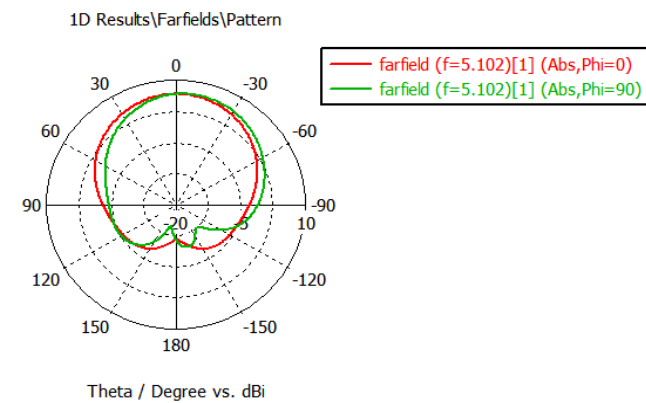


Fig.7: E and H-Planes at 5.10 GHz

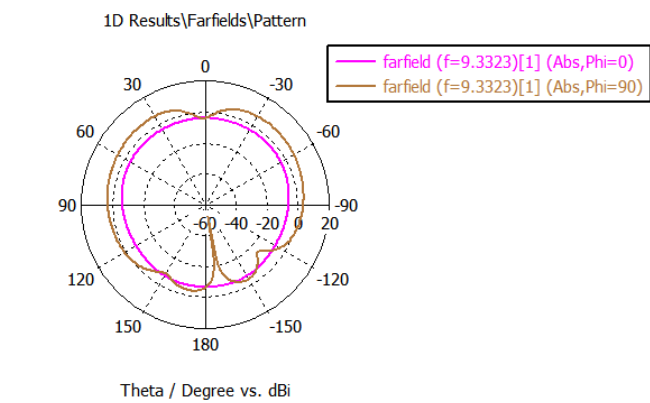


Fig.8: E and H-Planes at 9.33 GHz

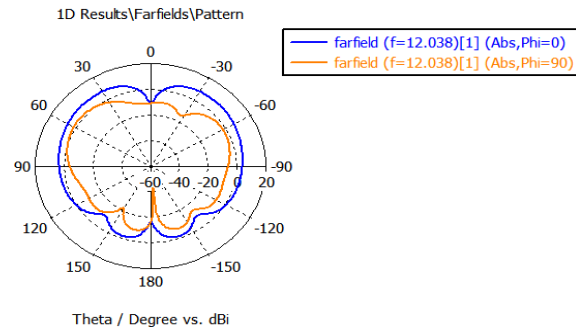


Fig.9 : E and H-Planes at 12.03 GH

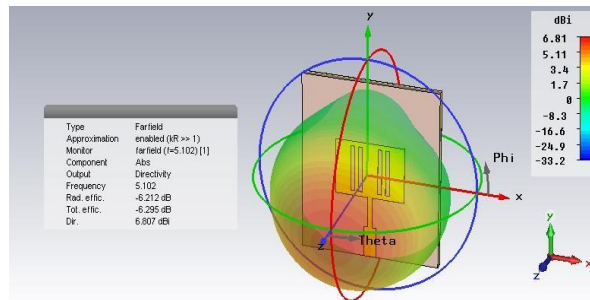


Figure 10: 3D pattern at 5.10 GHz

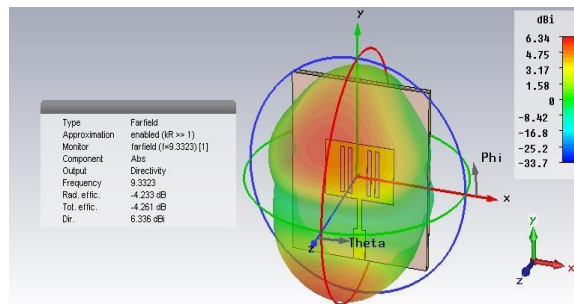


Fig.11: 3D pattern at 9.33 GHz

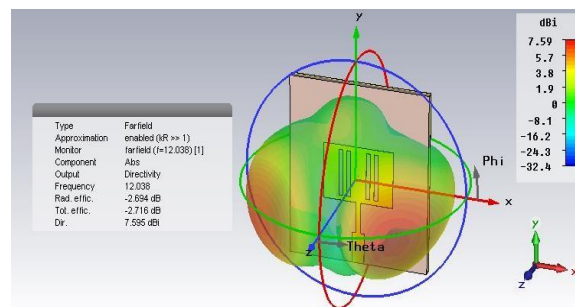


Fig. 12: 3D pattern at 12.03 GHz

The antenna gain provides an indication of its efficiency and directional capabilities. For the projected antenna, gains of 0.51193 dB, 2.0859 dB, and 4.8725 dB have been obtained at frequencies of 5.10 GHz, 9.33 GHz, and 12.038

GHz, respectively. These gain values illustrate the antenna's ability to focus and direct radiation in specific directions, thereby enhancing its overall performance.

TABLE II:
The antenna Performance

Parameters	Simulated results		
	5.108GHz	9.3323GHz	12.038GHz
Return Loss (dB)	-17.209dB	- 21.903dB	-23.053dB
Gain (dB)	0.51193	2.0859	4.8725
Directivity(dB)	6.807	6.33	7.59
Radiationefficiency	-6.21dB	-4.23dB	-2.29dB

II. CONCLUSION

The objective is to design, construct and simulate multi-band patch slotted antenna which operates in three distinct bands. The antenna design incorporates the microstrip feeding technique, and to achieve its functionality, the patch includes the insertion of four narrow slits. The antenna yields the following outcomes: The first-band resonates at 5.10 GHz, with a reflection coefficient of -17.20 dB and -10 dB bandwidth of 0.32 GHz. This band is appropriate for many applications, comprising mobile communication, wireless LAN, and radar communication. The second-band operates at 9.33 GHz, with a reflection coefficient of -21.90 dB and -10dB bandwidth of 1.002 GHz. This band is appropriate for satellite communication. The third-band operates at 12.03 GHz, with a reflection coefficient of -23.05 dB and -10dB bandwidth of 1.29 GHz. This band is appropriate for satellite and radar communications. The projected antenna displays minimum reflection loss and better gain at the frequencies of

5.10 GHz, 9.33 GHz, and 12.03 GHz, enabling its effectiveness in the desired frequency ranges.

II. REFERENCES

1. Rajendra Soloni, Rajappa H S and Chandrappa D N "Design and analysis of multiband reconfigurable microstrip patch antenna with switchable element" in Advances in Computing, Communications and Informatics (ICACCI), IEEE, 13-16 Sept. 2017, DOI: 10.1109/ICACCI.2017.
2. Chandrappa D.N., Mrs.Vani R.M. and P.V. Hunagund "Design and Implementation of Slotted Reconfigurable Microstrip Antenna for Wireless Application", International Journal of Electronics and Communication Engineering. ISSN 0974-2166 Volume 6, Number 3 (2013), pp. 233-239

3. Chandrappa D.N, P.A.Ambresh, P.V.Hunagund., "Design of compact reconfigurable multy frequency microstrip antennas for wireless applications" International Journal of Advanced Research in Computer and Communication Engineering (IJARCCE), Vol. 2, Issue 9, September 2013.
4. Chandrappa D N, Ambresh P A, Vani R M, P V Hunagund., "Multi-slots Reconfigurable MicrostripAntenna with Capacitive Loading Technique"., International Journal of Innovative Research in Computer and Communication Engineering, Vol. 2, Issue 1, Jan. 2014
6. Rekha D C, Rajappa.H.S, RajendraSoloni and Chandrappa.D.N "Design of dual band microstrip patch antenna for RFID" International Journal for Research Trends and Innovation, Volume 2, Issue 5, pp 253-257, 2017.
7. Jobins George and Shehana Pareeth "Multiband Microstrip patch Antenna using parallel slots for wireless applications" International Conference on Electrical, Electronics, and Optimization Techniques(ICEEOT) – 2016, pp 3614-3619, 2016.
8. J. H. Kim and C. G. Christodoulou, "A simple reconfigurable microstrip antenna for wideband applications," *2010 IEEE Antennas and Propagation Society International Symposium*, Toronto, ON, 2010, pp. 1-4

Performance Analysis of Fiber Optic Link Using Hybrid Dispersion Compensation Technique

Balgopal Raju¹, Tusharkant Panda^{2*}

¹PG Scholar, Dept. of ECE, GIET University, Gunupur

²Assistant Professor, Dept. of ECE, GIET University, Gunupur

ABSTRACT

Optical fibers are widely used for data transmission over longer distances with higher data rates. Fiber optic system suffers from various distinctive losses, non-linear effects and dispersion which degrades the signal quality. Among them, dispersion is the most significant signal deteriorating factor. There are many ways through which one can reduce dispersion but some of the most efficient techniques are using a Dispersion compensating fiber (DCF), Fiber Bragg grating (FBG) or Electronic dispersion compensation (EDC) techniques etc. In this project we have used both DCF and FBG together for reducing dispersion for long distance transmission with high data rate with suitable components. This hybrid model transmits signal over a distance of 360km with data rate 20Gbps. This paper also shows comparison between different techniques used for compensating dispersion which are mentioned above. The results obtained are analysed by considering Q-factor and BER as determining parameter.

I. INTRODUCTION

There is a significant development in Optical fiber communication technologies on invention of glass fibers and lasers in 1960s. Earlier, the attenuation in fiber communication was too high and in the range of > 1000 dB/km but in 1970, there was drastic improvement in the attenuation (to 20 dB/km). The fiber loss went below 1 dB/km on development of GaAsP lasers for data transmission in early 1980's. The transmission speed in graded index multimode fibers went up to 44.7 Mb/s over a distance of 23.3km and up to 274 Mb/s up to distance of 7.5 km without using repeaters [1,2].

Dispersion is the primary barrier to long-distance transmission in multi-mode fibers. To address this issue, single mode fibers were developed in 1981. Later, single mode in GaAsP semiconductor lasers were developed. These lasers have a wavelength of 1550 nm and can operate at 2 Gb/s, allowing repeater spacing to be increased to 130 km. The systems can currently transmit data at a 100 Gb/s bit rate up to a distance of more than 1000 km. The scientific and technological development in this field has been so fast and advanced that optical fiber communication system is already in the fifth generation within a period of about 25 years [3].

Attenuation loss in optical fiber is minimum and optimum at the wave length of 1550 nm [4,5]. Hence, the main limiting factor is the dispersion loss and this factor can be compensated or minimized using different techniques like use of DCF and FBG [6]. Each of these methods have their own limiting factors, hence we

propose a hybrid model which includes the advantageous features of DCF and FBG techniques. Through this hybrid model we can be able to send signals with high data rate over a long distance.

DISPERSION COMPENSATION

Dispersion compensation means canceling the effect of dispersion in fiber optic communications. The purpose is to avoid the widening of input pulses and/or the signal distortion in optical fiber communications. In optical communication, the broadening of the signals can occur. If each symbol would be broadened, there might be the case of overlapping between the symbols/signal [7].

By using fibre segments with various designs or other optical components, the effect of dispersion in fibre communication can be reduced [8]. Long dispersion-shifted fibre pieces or chirped fibre Bragg gratings are both possible components of dispersion compensation modules (DCMs). When compared to other dispersion compensation strategies, the fibre gratings are extremely compact and have low insertion losses [9,10].

A typical single mode fibre has a dispersion value of approximately +16–17 ps/nm/km at 1550 nm. To handle or control this quantity of dispersion coefficient, a particular kind of DCF with a negative value of dispersion coefficient is utilized inside the module. Such compensating fibers have a dispersion coefficient that ranges from -30 to -300 ps/nm/km.[11]

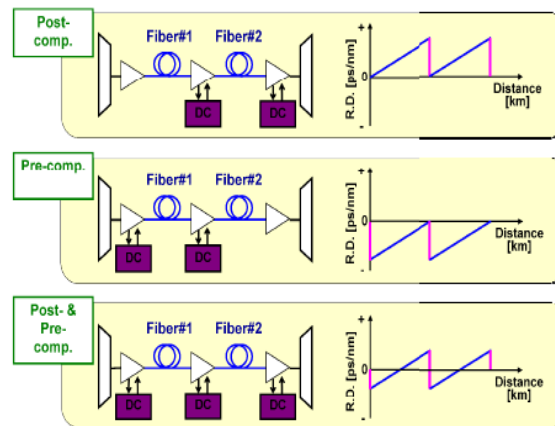


Fig 1: Different types Dispersion Compensating Fiber (DCF)

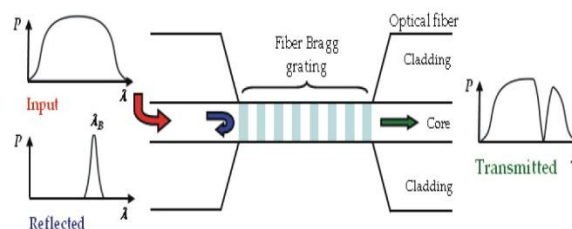


Fig 2: Systematic diagram of FBG

SIMULATION SETUP

Optisystem software is an ingenious and developing tool which helps us to simulate and test almost all kind of optical links. Here all the simulation setup was designed using Optisystem 19.0 simulation software. For the simulation setup we have used the following components-

The PRBS Generator: A Pseudo Random Sequence of binary data is generated by this single port device in accordance with various operating modes. The bit order is intended to mimic the properties of random data.

NRZ Pulse Generator:

It is a two-port device, with binary input delivered to the input port and electrical output provided by the output port. This model can generate pulses with various edge shapes depending on the parameter Rectangle shape.

CW Laser:

CW Laser is a single port device which provide continuous wave optical signal.

M-Z Modulator:

The Mach-Zehnder modulator is an interferometric-based intensity modulator. It is made up of two 3 dB couplers coupled by two equal-length waveguides. Depending on the voltage used, the various routes can result in both positive and negative interference at the output. The output intensity can then be modulated in accordance with voltage at that point [12].

Optical Fiber:

The optical signal is sent through optical fibre. It is a clear, malleable fibre made of plastic or glass. The three layers are core, cladding, and jacket, with jacket serving as the optical fiber's protective outer layer and core serving as the innermost layer in which the signal is conveyed [13,14].

EDFA:

An optical repeater with two ports uses an erbium-doped fibre amplifier to boost optical signal power.

Photodetector PIN:

Photodetector is a two-port device used to reciprocate the received optical signal into electrical.

Optical Filter:

It is a two-port device which only allows a particular wavelength of light signal to pass through it. Here we have used two optical filter i.e., Band pass Gaussian Filter and Low pass Gaussian Filter.

BER analyzer:

BER analyzer provides the result for the whole simulation setup.

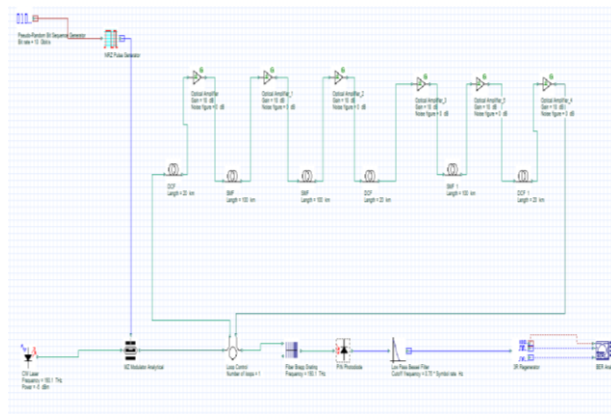


Fig 3: Simulation setup for hybrid model

SIMULATION PARAMETERS:

Parameters	SMF	DCF
Reference Wavelength	1550nm	1550nm
Distance	100 Km	20 Km
Dispersion	16.75ps/nm/km	85ps/nm/km
Attenuation	0.2 dB/km	0.5 dB/km

SYSTEM DESCRIPTION

To examine the effects of dispersion, an SMF of length 100 km in three stage is used in this simulation. In order to create a system with great performance, there are three stages where DCFs of 20 km each are employed in between the link for research while trying to recover the dispersed signal. Over various permutations and combinations, the DCF and SMF are used in various ways [15].

The following list includes the component parameters utilized in the simulation process:

The transmitter part of this simulation setup includes a Mach-Zehnder modulator. One of the input ports is connected to a CW laser, while another input port is connected via a band pass Gaussian filter, NRZ pulse modulator, and a series of pseudo random bit sequence generators.

The transmitter section's output port is linked to a channel that has optical fibre, EDFA, and DCF.

The receiver part, which includes a photodetector PIN, low pass Gaussian filter, electrical attenuator (which attenuates the electrical signal), and electrical equalizer, is then linked to the channel. Utilizing the BER Analyzer and eye diagram analyzer, the setup's outcome can be discovered.

RESULTS AND ANALYSIS

Here simulation is carried out in 4 stages. First simulation is carried out for the simulation setup described in the simulation setup section without using any dispersion compensation technique. The result is noted down for the same. Simulations are carried out then for the same simulation setup using DCF and FBG as compensator separately. Here the length of the fiber and data rate are kept constant to have a fare comparison. Finally the system is designed with both DCF and FBG together as dispersion compensator. The corresponding output is recorded through BER analyzer.

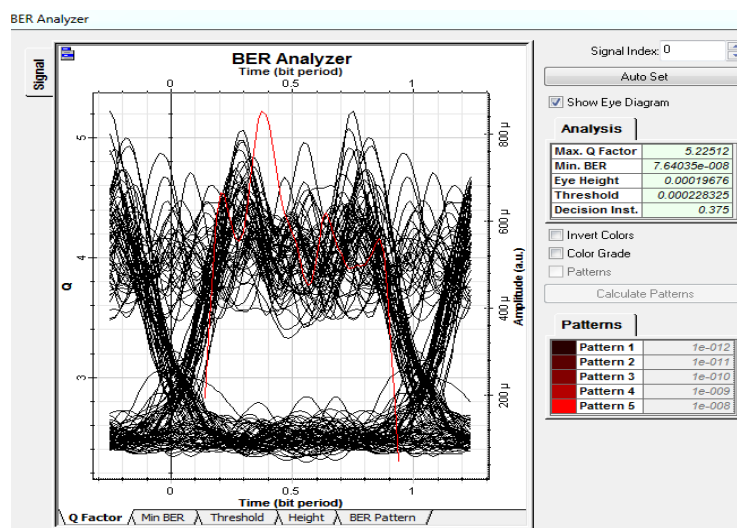


Figure 4: Eye Diagram without using any dispersion compensator

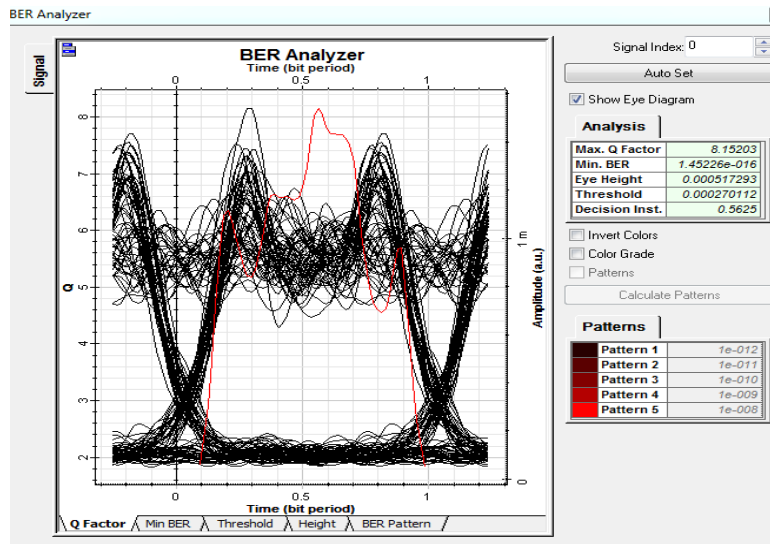


Figure 5: Eye Diagram with FBG as dispersion compensator

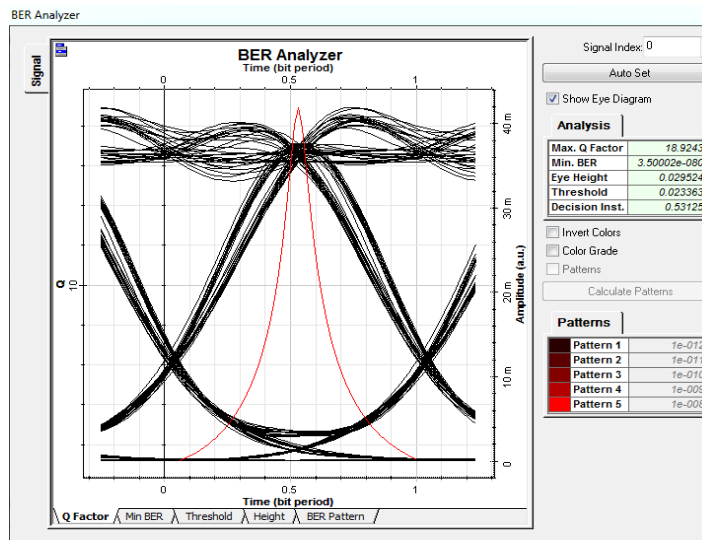


Figure 6: Eye Diagram with DCF as dispersion compensator

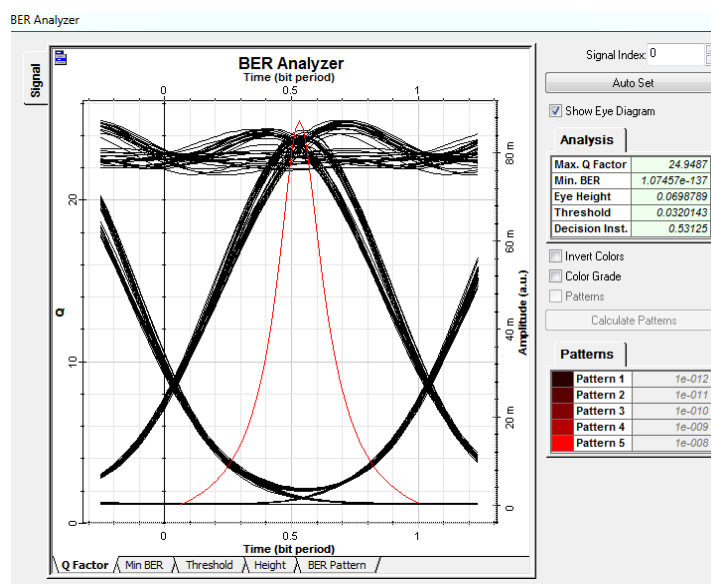


Figure 7: Eye Diagram with Hybrid Dispersion compensator

It can be observed that the system performance varies significantly with use of dispersion compensators. Figure 4 shows the eye diagram for the case when no dispersion compensator is used. Here the Q factor obtained is merely 5.2. This suggests that transmission of data for the specified length of the fiber isn't possible as the Q factor is well below the cutoff mark. Similarly figure 5 shows the eye diagram when only FBG is used in post configuration as dispersion compensator. It can be observed that the Q Factor is just above the cutoff mark and the BER is satisfactory. Similarly figure 6 shows the eye diagram when DCF is used in symmetrical configuration as dispersion compensator. This also shows satisfactory result with Q-Factor of 18.92 and a small bit error rate. Figure 7 shows the eye diagram of the proposed hybrid dispersion compensation technique that contains both FBG and DCF as dispersion compensator. Here DCF is used in symmetrical configuration and FBG is used in post configuration. The Q Factor here is maximum and the bit error rate is minimum among all configurations.

CONCLUSION

Performance of any fiber optic link transmitting optical signal at greater data rate is bound to be affected by attenuation and dispersion. The effect of attenuation is minimized to a large extent with advancement in the field of optical amplifier, optical modulator and availability of advanced Lasers operating at 1550 nm. Compensating the effect of dispersion still remains a critical task. In this thesis we have tried to design a hybrid dispersion compensating module comprising of both DCF and FBG as dispersion compensator. The results shows this module performs way better than using DCF and FBG alone as dispersion compensator. The design of this module is quite simpler and can be used at any length with appropriate calculation of the length of DCF.

II. REFERENCES

- [1]. A.J. Antos and D.K. Smith, Design and Characterization of Dispersion Compensating Fiber based on the LP-01 mode, *Journal of Lightwave Technology*, vol. 12, issue no.10pp. 1739-1745, October, 1994.
- [2]. J. M. Tang and K.A. Shore, 30-Gb/s Signal Transmission Over 40-km Directly Modulated DFB-Laser-Based Single-Mode-Fiber Links Without Optical Amplification And Dispersion Compensation, *Journal of Lightwave Technology*, IEEE, vol. 24, issue no. 6,pp. 2318-2327, June, 2006.
- [3]. Elham Jasim Mohammad, Gaillan H. Abdullah, Soliton Optical Fibers Super continuum Generation Near the Zero Dispersion, *International Journal of Industrial Engineering Research and Development (IJIERD)*, Volume 4, Issue 1, January - April (2013), pp. 52-58
- [4]. N.K. Kahlon and G.Kaur Various Dispersion Compensation Techniques for optical system: A Survey, *Open Journal of Communications and Software*, vol.1, issue no. 1, pp. 64-73, May, 2014.
- [5]. Ashwini Sharma, Shalini Sharma, Inder singh, Suman Bhattacharya, "Simulation and analysis of dispersion compensation using proposed hybrid model at 100 Gbps over 120km using SMF" *International Journal of Mechanical Engineering and technology (IJMET)* vol 8, issue 12Dec2017.
- [6]. A.B. Dar and R.K. Jha, *Chromatic dispersion compensation techniques and Characterization of Fiber Bragg Grating for Dispersion Compensation*, Springer, February, 2017
- [7]. Mishra, P., Panda, T., Rout, S.S., & Palai, G. (2020). Investigation of a 16 channel 40 Gbps varied GVD DWDM system using dispersion compensating fiber. 2020 International Conference on Computer Science, Engineering and Applications (ICCSEA), 1-5.

- [8]. S. Kumar, A. K. Jaiswal, Er. M. Kumar, and Er. R. Saxena, "Performance Analysis of Dispersion Compensation in Long Haul Optical Fiber with DCF," IOSR Journal of Electronics and Communication Engineering (IOSR-JECE), Vol. 6, No. 6, pp. 19-23, Jul.-Aug. 2013.
- [9]. T. K. Panda, P. Mishra, K. C. Patra and N. K. Barapanda, "Investigation and performance analysis of WDM system implementing FBG at different grating length and data rate for long haul optical communication," 2017 IEEE International Conference on Power, Control, Signals and Instrumentation Engineering (ICPCSI), Chennai, India, 2017, pp. 483-488, doi: 10.1109/ICPCSI.2017.8392343.
- [10]. Y.W. Song, Z. Pan, S.M.R.Motaghian Nezam et.al, Tunable Dispersion Slope Compensation for 40-Gb/s WDM Systems Using Broadband Non channelized Third Order Chirped Fiber Bragg Gratings, Journal of Lightwave Technology, IEEE, vol. 20, issue no. 12, December, 2002.
- [11]. Deepika Prajapati, Dhyanendra Parashar, Study of Dispersion Curves in M-Type Triple Clad Single Mode Optical Fiber, International Journal of Electronics and Communication Engineering & Technology (IJECET), Volume 6, Issue 4, April (2015), pp. 28-33
- [12]. Mir Zayed Shames, Md. Surat-E-Mostafa, Imtiaz Ahmed, Signal Quality of Dispersion Managed Quasi-Linear High Bit Rate Optical Transmission System, International Journal of Electronics and Communication Engineering & Technology (IJECET), Volume 4, Issue 3, May – June, 2013, pp. 108-114
- [13]. A. S. Verma, A. K. Jaiswal, and M. Kumar, "An Improved Methodology for Dispersion Compensation and Synchronization in Optical Fiber Communication Networks," International Journal of Emerging Technology and Advanced Engineering, Vol. 3, No. 5, pp. 769- 775, May 2013.
- [14]. Y. Zhou, Y. Shao, Z. Wang, C. Li, J. Zhou, and W. Ma, "Research on Dispersion Compensation of 40 Gb/s Optical Duo-Binary Coded Transmission System," Optics and Photonics Journal, 2016, Vol. 6, pp. 190-195, Aug. 2016.
- [15]. S. S. Muduli, L. Padhy, S. Polei, and T. Panda, "Performance Analysis of a High-Speed Optical Transmission System Using Various Pulse Generator", SPAST Abs, vol. 1, no. 01, Oct. 2021.

Effect of the Slot and Dielectric Materials on ThePerformance of Rectangular Microstrip Antenna

Anita R¹, Jayanthi Kumari T. R², Yogesh G.S³

¹Associate Professor, Dept of ECE, EPCET, Bangalore

²Professor, Dept of ECE, EPCET, Bangalore

³Principal, Dept of ECE, EPCET, Bangalore

ABSTRACT

This paper discusses the analysis of a rectangular microstrip antenna for different dielectric materials. The rectangular microstrip antenna is designed to operate at 2.4GHz. The rectangular microstrip antenna is designed and simulated using HFSS. The rectangular microstrip antenna is designed with FR4 substrate in which the different dielectric materials such as Mica, Teflon, rubber, paper, solid polymer material are integrated into an FR4 substrate. The rectangular microstrip antenna with different dielectric materials are fabricated and the results are experimentally verified. The results have shown that the performance of the antenna is improved in terms of return loss by -36.79 dB for the paper dielectric material and the gain is improved by 4.51 dB for the Teflon dielectric material.

Keywords—Rectangular Microstrip, Dielectric Materials, FR4 Substrate

I. INTRODUCTION

Due to the demand of wireless communication technology the demand has increased significantly for low profile and broad band antennas. Hence microstrip antennas have been used widely in wireless communication due to their light weight, low profile, low cost and ease of fabrication and excellent compatibility with planar integrated circuits and even non planar surfaces. In recent years, as the demand of the small systems have increased, small size antennas at low frequency have drawn much interest from researchers [1], [2]. Nowadays, microstrip patch antenna has become very popular and is widely used in many areas like in mobile communication, Wi-Fi and WiMAX applications.

The main disadvantage of the microstrip antenna is its narrow bandwidth. To increase the performance of a microstrip patch antenna there are several methods like increasing the thickness of substrate, using low dielectric substrate, using of various impedance matching and feeding techniques [3].

The selection of dielectric material is based on the following parameters: relative Dielectric Constant or permittivity, Height of the substrate material, Loss Tangent. Selection of dielectric material with appropriate dielectric constant is important as it has a major role in antenna performance. It directly affects gain, bandwidth, shift in operating frequency, radiation loss [4]. Also dielectric constant controls the fringing field

which is the main cause of radiation in microstrip patch antenna. The lower will be ϵ_r , the wider will be the fringes which in turns results into the better radiation and also increased bandwidth and efficiency[5].

In this paper, the rectangular microstrip antenna is designed with different dielectric materials. The substrate is considered as FR4 and a slot is made on the FR4 substrate into which the different dielectric materials are integrated inside into the substrate. The effect of the dielectric materials on the performance of antenna is analysed in terms of return loss, bandwidth, gain.

II. DESIGN OF RECTANGULAR MICROSTRIP PATCH ANTENNA

A. Design parameters:

The proposed rectangular microstrip patch antenna is designed with FR4 substrate. The patch has the dimensions of 28.33 mm x 37.26 mm. The ground plane has the dimensions of 67.5 mm x 65.5 mm. The substrate height is taken as 1.6 mm. A slot of 28.33 mm x 37.26 mm is made on the FR4 substrate and different different dielectric materials such as Mica, Teflon, rubber, paper, solid polymer material with permittivity of 5.7, 2.1, 3, 3.1, 3.2 are integrated into FR4 substrate. The feed used for the rectangular microstrip antenna is microstrip line feed with a length of 22.65 mm and a width of 1.2 mm. Fig 1 shows the designed rectangular microstrip patch antenna.

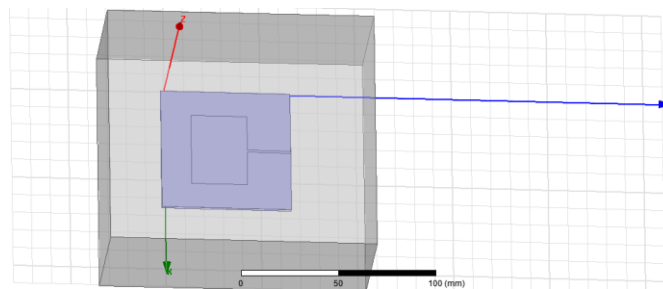


Fig 1. Rectangular microstrip antenna

B. Design of Length and Width of patch:

Depending on the relative permittivity, operating frequency the width and length of the patch are determined. the desired length and width can be found out by using following equations:

The effective dielectric constant of the microstrip patch antenna is calculated from,

$$\epsilon_{eff} = \frac{\epsilon_r + 1}{2} + \frac{\epsilon_r - 1}{2} \left(\frac{1 + \frac{12h}{w}}{\sqrt{1 + \frac{12h}{w}}} \right)$$

(1)

The actual Width (W) of patch:

$$W = \frac{C}{2f_r} \sqrt{\frac{2}{\epsilon_r + 1}} \quad (2)$$

$$C = \frac{1}{\mu_0 \epsilon_0} \quad (3)$$

Where,

μ_0 is the Permeability

ϵ_0 is the Permittivity

C is the Velocity

ϵ_r is the Dielectric constant

f is the resonant frequency

The actual length of the patch (L):

$$L = \frac{c}{2f_r \sqrt{\epsilon_{eff}}} - 2\Delta L \quad (4)$$

$$L_{eff} = \frac{c}{2f_r \sqrt{\epsilon_{eff}}} \quad (5)$$

$$L = L_{eff} - 2\Delta L \quad (6)$$

Where,

ΔL is the Line extension

II. RESULTS AND DISCUSSION

The rectangular microstrip patch antenna is designed to operate at 2.4 GHz. The parametric analysis of the rectangular microstrip antenna is carried out by considering different dielectric materials such as mica, Teflon, rubber, paper, solid polymer which are integrated on to the FR4 substrate. A slot is made on the FR4 substrate and the dielectric materials are integrated on to it one by one and the performance of the antenna in terms of return loss, gain, bandwidth, VSWR is measured.

I. Effect of mica on the performance of antenna:

The rectangular microstrip patch antenna is designed with FR4 substrate of permittivity 4.4. A slot of 28.33 x 37.26 mm are made on the FR4 substrate and the slot is filled with mica which has a dielectric constant of 5.7. The dimension of mica is taken as 28.3mm x 37.26mm. The ground plane has the dimension of 67.5mm x 65.5mm. The rectangular microstrip patch antenna is designed and simulated using HFSS. The fabricated rectangular microstrip antenna with slot on the FR4 substrate is shown in fig2. The performance of the antenna is measured in terms of return loss, bandwidth, gain and VSWR.

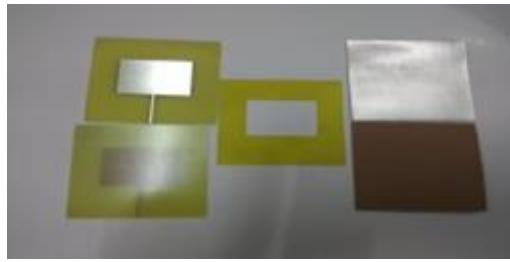


Fig2.Fabricated rectangular microstrip with slot on FR4 substrate

Fig2(a) shows the return loss plot of the rectangular microstrip antenna with mica as the dielectric material.

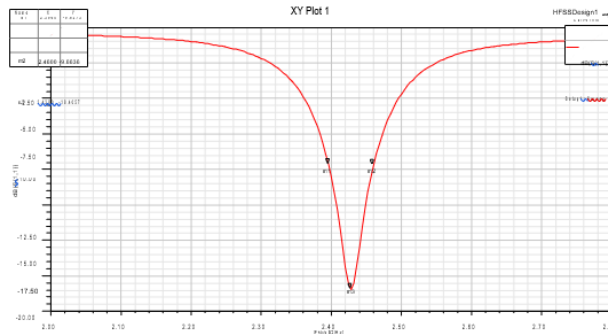


Fig2(a).Return loss plot of rectangular microstrip antenna with mica as dielectric material

From fig2(a), we can observe that the return loss of rectangular microstrip antenna with mica as dielectric material is obtained as -18.4057 dB. The bandwidth is obtained as 64 MHz. Fig2(b) shows the 3D radiation pattern of the rectangular microstrip antenna with mica as the dielectric material.



Fig 2(b) 3D radiation pattern of rectangular microstrip patch antenna with mica as dielectric material

From fig2(b), we can observe that the gain of the rectangular microstrip antenna with mica as dielectric material is obtained as 3.888 dB. Fig 2(c) shows the electric field distribution of rectangular microstrip antenna with mica as dielectric material.

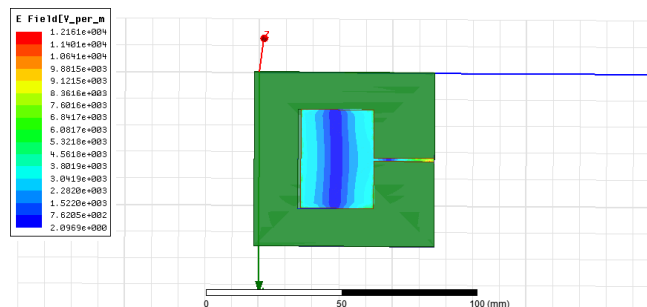


Fig.2©Electric Field distribution of rectangular microstrip antenna with mica as dielectric material

From fig 2©,we can observe the field distribution from the rectangular microstrip antenna with mica as dielectric material.

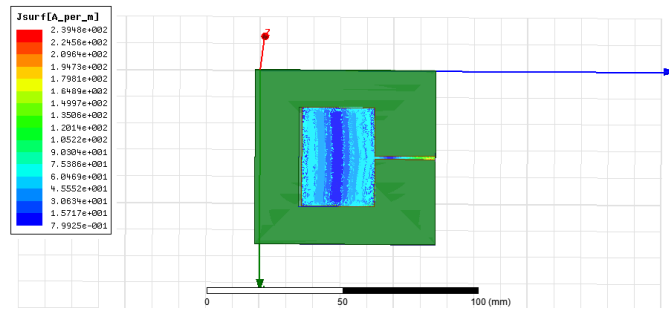


Fig.2(d)surface current distribution of rectangular microstrip with mica

Fig 2(d) shows the surface current distribution of rectangular microstrip antenna with mica as dielectric material.

From Fig 2(d),we can observe the uniform current distribution across the patch in a rectangular microstrip antenna with mica as the dielectric material.Fig 2(e) shows the VSWR plot of the rectangular microstrip antenna with mica as the dielectric material

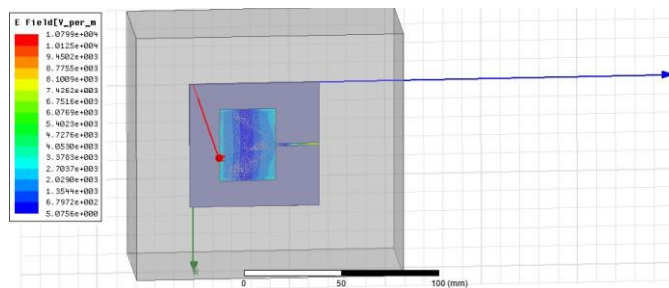


Fig.2(e)VSWR plot of rectangular microstrip with mica as dielectric material

From fig 2(e),we can observe that the VSWR of the rectangular microstrip antenna with mica as dielectric material is obtained as 1.2731.Fig 2(f) shows the 2D radiation pattern of the rectangular microstrip antenna with mica as the dielectric material.

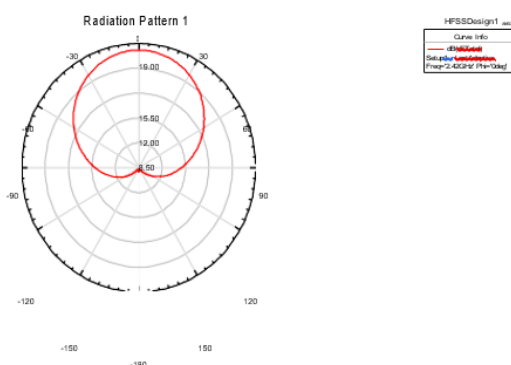


Fig.2(f) 2D radiation pattern of rectangular microstrip with mica as dielectric material

From fig 2(f),we can observe that the maximum power is radiated from the rectangular microstrip antenna with mica as the dielectric material.

II. Effect of Teflon on the performance of antenna:

The rectangular microstrip antenna is designed by considering FR4 substrate with a permittivity of 4.4. A slot is made on the FR4 substrate and filled with teflon material of dielectric constant 2.1. The performance of the rectangular microstrip antenna is analysed in terms of return loss, gain, bandwidth and VSWR. The rectangular microstrip antenna with teflon material is fabricated and the experimental results are also verified. A Conducting strip is placed on the teflon material and the dc voltage is applied. The performance of the antenna with teflon material is analysed by applying voltage and without applying voltage. Fig3(a) shows the fabricated rectangular microstrip antenna with teflon material and the experimental set up to measure the return loss of the antenna.



Fig 3(a) Experimental setup to measure the return loss of rectangular microstrip antenna with teflon material

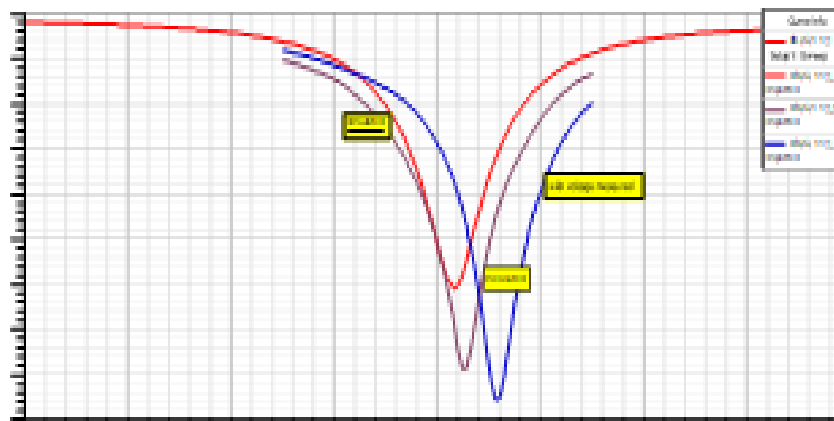


Fig 3(b) Simulated and measured return loss plot of rectangular microstrip antenna with teflon material

From fig 3(b), we can observe that the return loss of the simulated rectangular microstrip antenna with teflon material is -10.1293 dB. The measured return loss of the rectangular microstrip antenna with teflon material is found to be -19.71 dB. When the voltage is applied to the teflon material, the return loss is measured as -20.418 dB. The bandwidth of the simulated rectangular microstrip antenna with teflon material is 56 MHz. The bandwidth of the measured rectangular microstrip antenna with teflon material is obtained as 75 MHz. When the voltage is applied, the measured bandwidth is 79.5 MHz. The resonant frequency of the simulated rectangular microstrip antenna with teflon material is 2.4160 GHz. The resonant frequency of the measured rectangular microstrip antenna with teflon material is 2.4285 GHz. When the voltage is applied, the resonant frequency is shifted from 2.4160 GHz to 2.4600 GHz. This

shows that the antenna can be used as a frequency reconfigurable antenna which finds its application in wireless communication. Fig 3(c) shows the electric field distribution of rectangular microstrip antenna with teflon material.

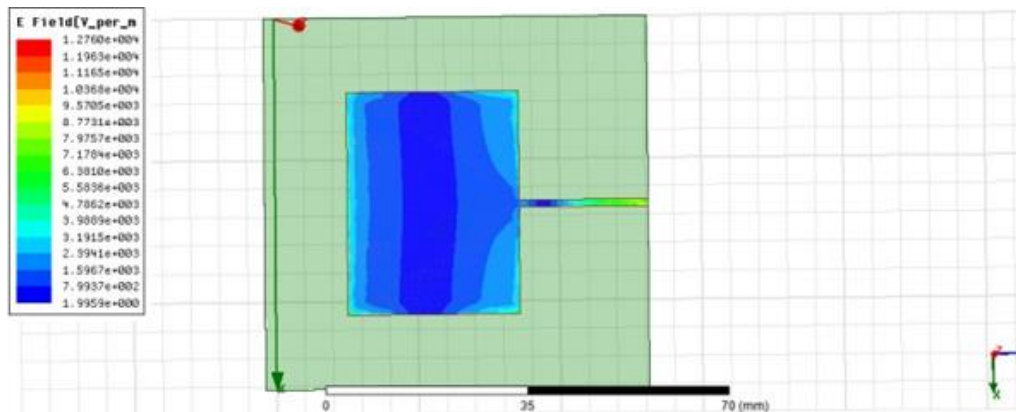


Fig.3© Electric Field distribution of rectangular microstrip antenna with teflon material

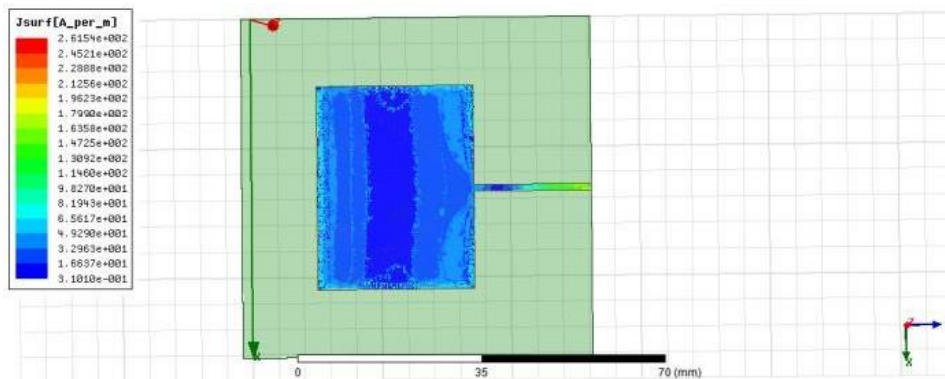


Fig 3(d) shows the surface current distribution of rectangular microstrip antenna with teflon material.

Fig.3(d) surface current distribution of rectangular microstrip antenna with Teflon material

From fig 3(d), we can observe that there is a uniform current distribution across the patch of a rectangular microstrip antenna with Teflon material. Fig 3(e) shows the 3D radiation pattern of the rectangular microstrip antenna with Teflon material.



Fig.3(e)3D radiation pattern of rectangular microstrip antenna with Teflon material

Fig 3(f) shows the 2D radiation pattern of the rectangular microstrip antenna with Teflon material.

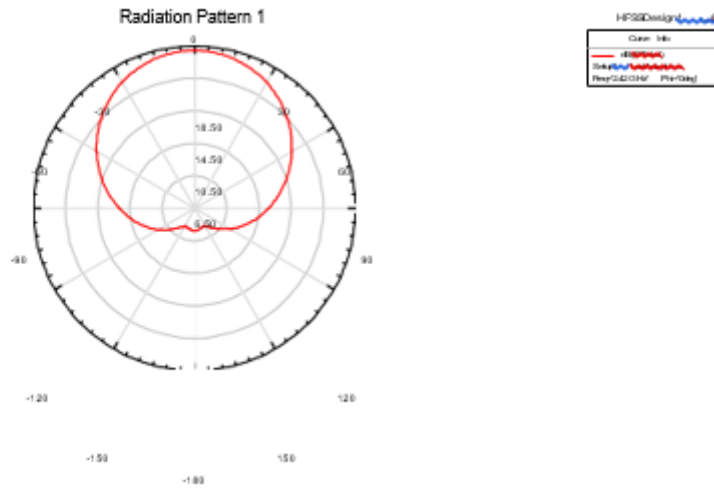


Fig.3(f) 2D radiation pattern of rectangular microstrip antenna with Teflon material

From fig 3(f),we can observe that the maximum radiation is obtained from the rectangular microstrip antenna with Teflon material.

III. Effect of paper on the performance of antenna:

The rectangular microstrip antenna is designed with FR4 substrate which has a dielectric constant of 4.4.A slot is made on the FR4 substrate and filled with paper as dielectric.The dielectric constant of paper is 3.1.Fig 4(a) shows the return loss plot of the rectangular microstrip antenna with paper material.

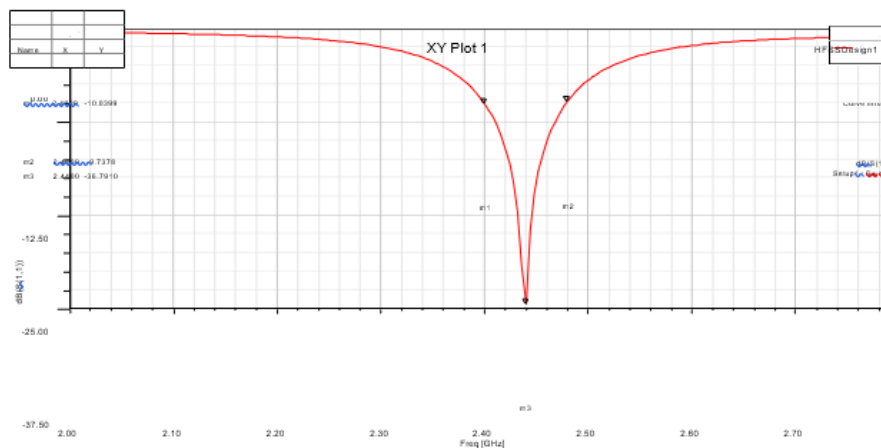


Fig.4(a)Return loss plot of rectangular microstrip antenna with paper material

From fig 4(a),we can observe that the return loss of the rectangular microstrip antenna with paper material is -36.79 dB.The bandwidth of the rectangular microstrip antenna with paper material is obtained as 80 MHz.Fig 4(b) shows the 3D radiation pattern of the rectangular microstrip antenna with paper material.



Fig.4(b)3D radiation pattern of rectangular microstrip antenna with paper material

From fig 4(b), we can observe that the gain of the rectangular microstrip antenna with paper as dielectric material is obtained as 2.6864 dB. Fig 4(c) shows the 2D radiation pattern of rectangular microstrip antenna with paper as dielectric material.

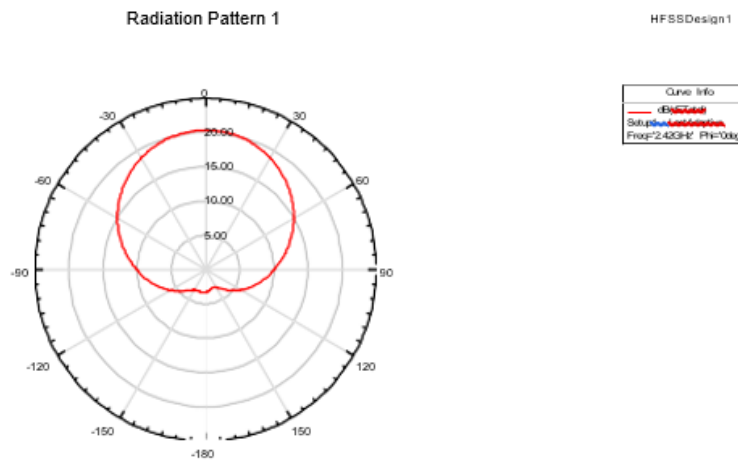


Fig.4(c) 2D radiation pattern of rectangular microstrip antenna with paper material

Fig 4(d) shows the VSWR plot of the rectangular microstrip antenna with paper as the dielectric material.

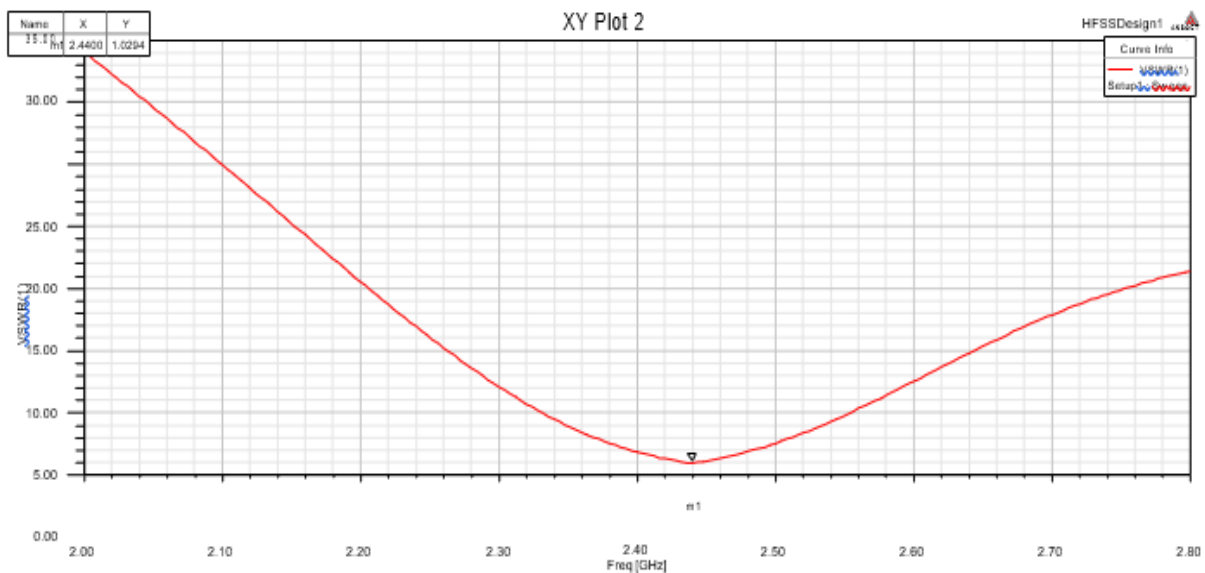


Fig.4(d) VSWR plot of rectangular microstrip antenna with paper material

From fig 4(d), we can observe that the VSWR of the rectangular microstrip antenna with paper as dielectric material is obtained as 1.0294. Fig 4(e) shows the electric field distribution of the rectangular microstrip antenna with paper as the dielectric material.

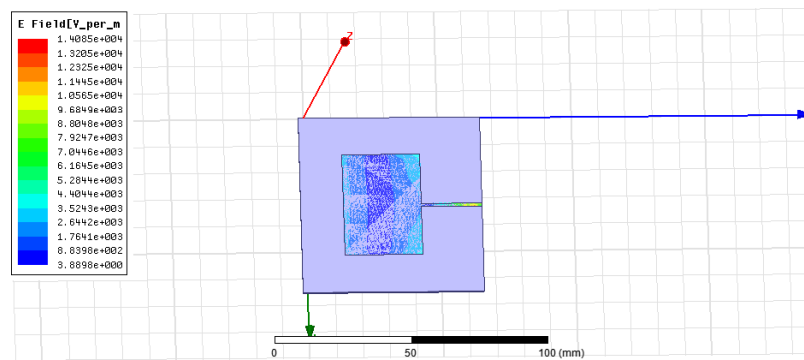


Fig. 4(e) Electric field distribution of rectangular microstrip antenna with paper material

Fig 4(f) shows the surface current distribution of rectangular microstrip antenna with paper material.

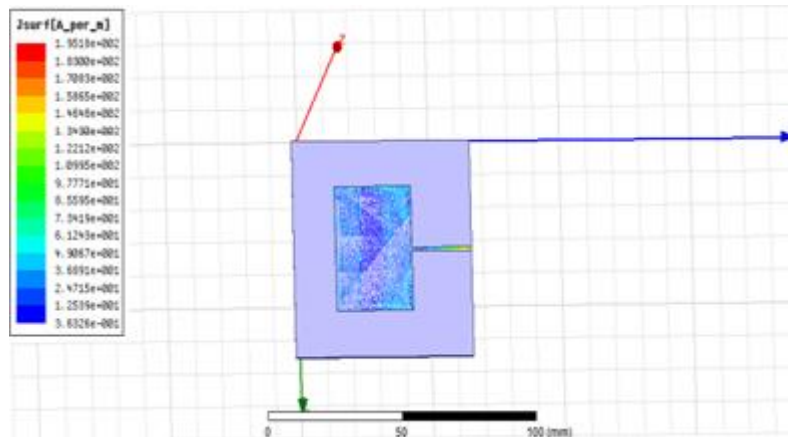


Fig.4(f) Surface current distribution of rectangular microstrip antenna with paper material

From fig 4(f), we can observe that there is a uniform current distribution across the patch of a rectangular microstrip antenna with paper material.

IV. Effect of rubber on the performance of antenna:

The rectangular microstrip antenna is designed by considering an FR4 substrate which has a dielectric constant of 4.4. A slot is made on the FR4 substrate and filled with rubber dielectric material which has a dielectric constant of

3. Fig 5(a) shows the return loss plot of the rectangular microstrip antenna with rubber as the dielectric material.

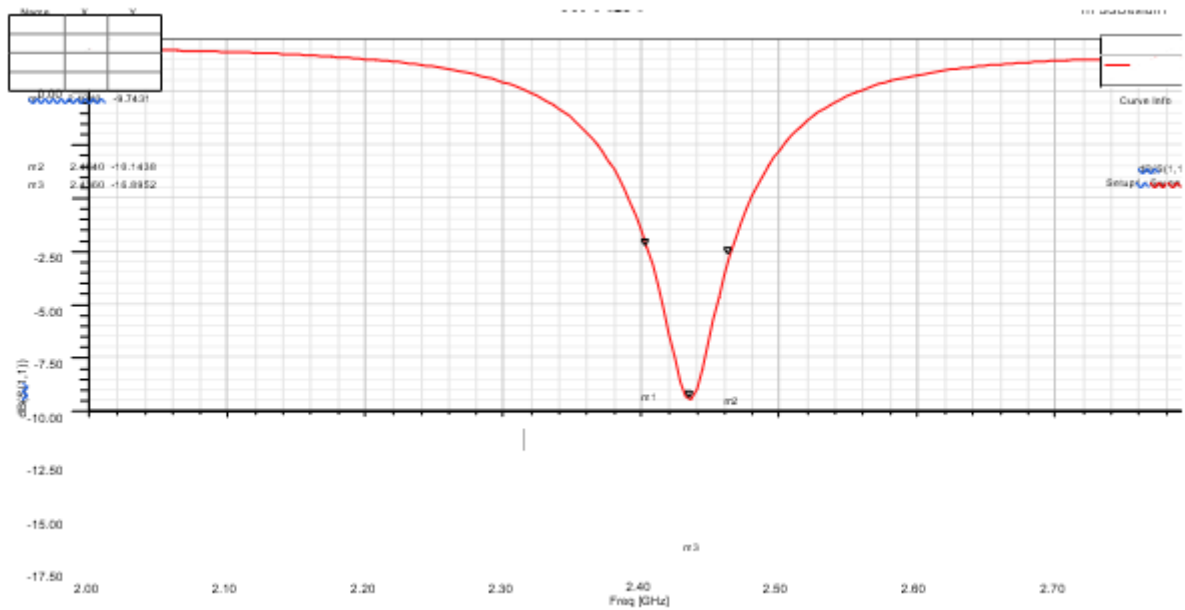


Fig.5(a)Return loss plot of rectangular microstrip antenna with rubber material

From fig 5(a),we can observe that the return loss of the rectangular microstrip antenna with rubber material is -16.89 dB.The bandwidth of the rectangular microstrip antenna with paper material is obtained as 60 MHz.Fig 5(b) shows the 3D radiation pattern of the rectangular microstrip antenna with rubber material.



Fig.5(b)3D radiation pattern of rectangular microstrip antenna plot with rubber material

From fig 5(b), ,we can observe that the gain of the rectangular microstrip antenna with rubber as dielectric material is obtained as 4.2007 dB.Fig 5(c) shows the VSWR plot of rectangular microstrip antenna with rubber as dielectric material.

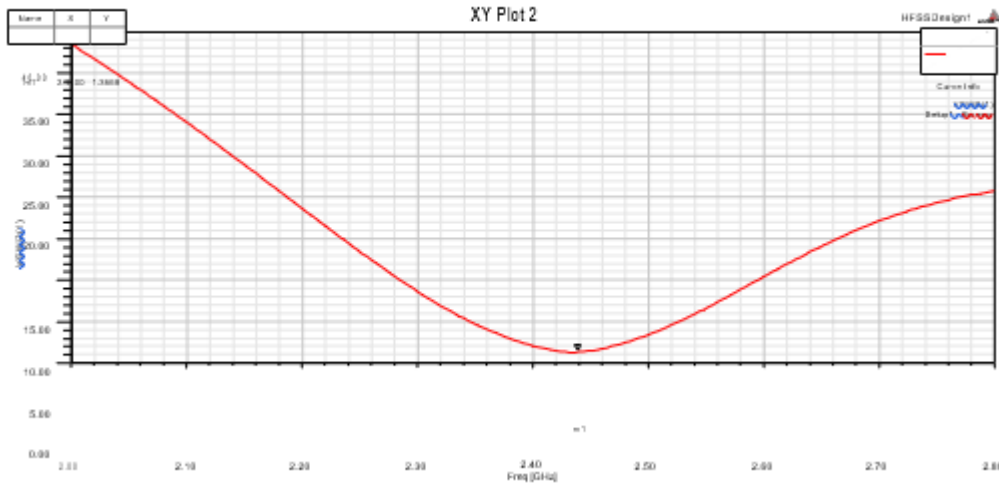


Fig.5©VSWR plot of rectangular microstrip antenna with rubber material

From fig 5(c),we can observe that the VSWR of the rectangular microstrip antenna with rubber as dielectric material is obtained as 1.3568.Fig 5(d) shows the 2D radiation pattern of the rectangular microstrip antenna with paper as the dielectric material.

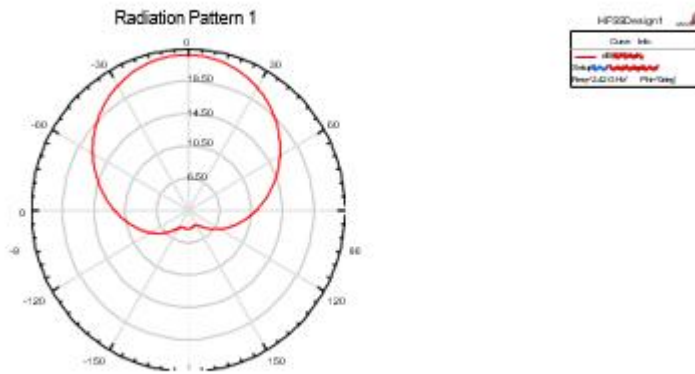


Fig.5(d)2D radiation pattern of rectangular microstrip antenna with rubber material

From fig 5(d),we can observe that the maximum radiation is obtained from the rectangular microstrip antenna with rubber material.Fig 5(e) shows the electric field distribution of rectangular microstrip antenna with rubber as dielectric material.

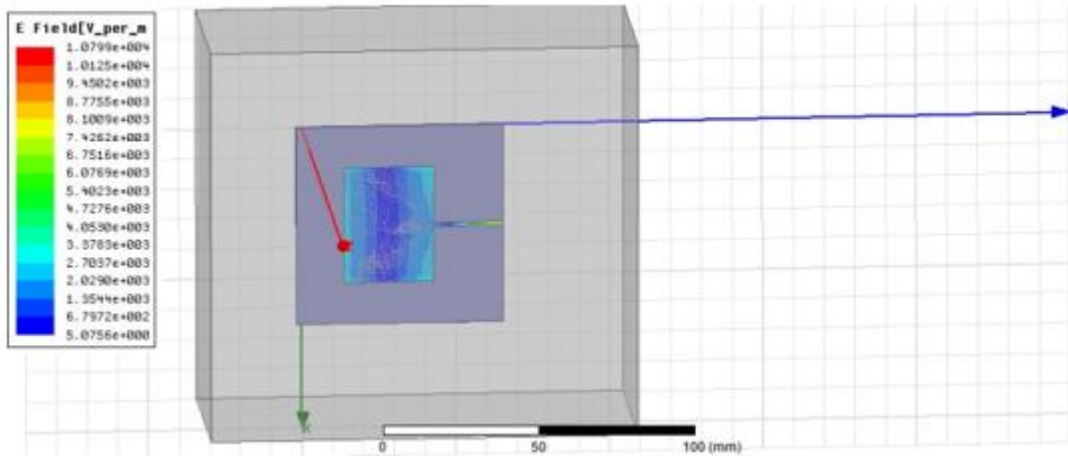


Fig.5(e)Electric Field distribution of rectangular microstrip antenna with rubber material

Fig 5(f) shows the surface current distribution of rectangular microstrip antenna with rubber material.

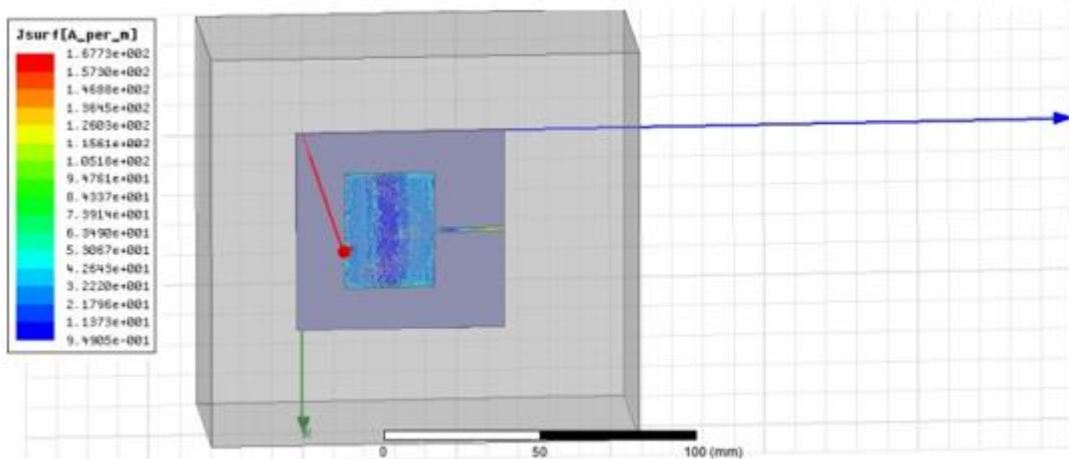


Fig.5(f)Surface current distribution of rectangular microstrip antenna with rubber material

From fig 5(f),we can observe that there is an uniform current distribution across the patch of a rectangular microstrip antenna with rubber material.

V. Effect of polyster on the performance of antenna:

The rectangular microstrip antenna is designed by considering an FR4 substrate which has a dielectric constant of 4.4.A slot is made on the FR4 substrate and filled with polyster dielectric material which has a dielectric constant of 3.2.Fig 6(a) shows the return loss plot of the rectangular microstrip antenna with polyster as the dielectric material.

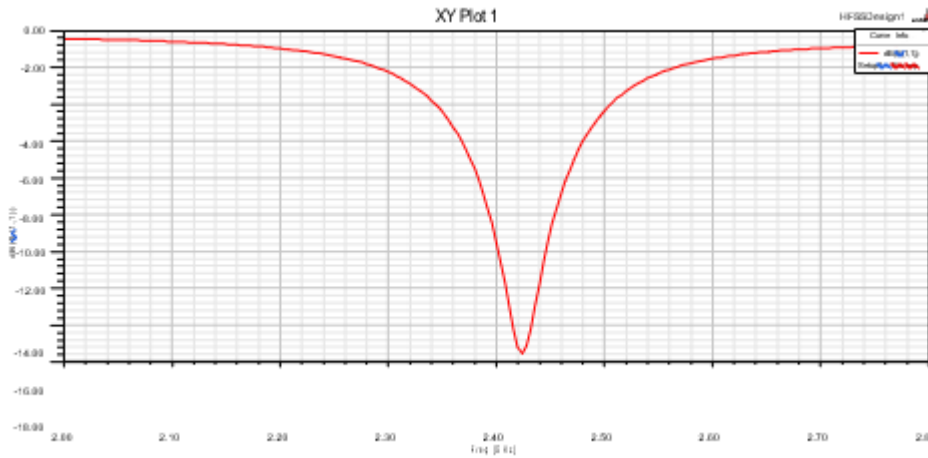


Fig.6(a)Return loss plot of rectangular microstrip antenna with polyster material

From fig 6(a),we can observe that the return loss of the rectangular microstrip antenna with polyster material is

- 17.51 dB.The bandwidth of the rectangular microstrip antenna with polyster material is obtained as 64 MHz.Fig 6(b) shows the 3D radiation pattern of the rectangular microstrip antenna with polyster material.



Fig.6(b)3D radiation pattern of rectangular microstrip antenna with polyster material

Fig 6(c) shows the 2D radiation pattern of the rectangular microstrip antenna with polyster as the dielectric material.

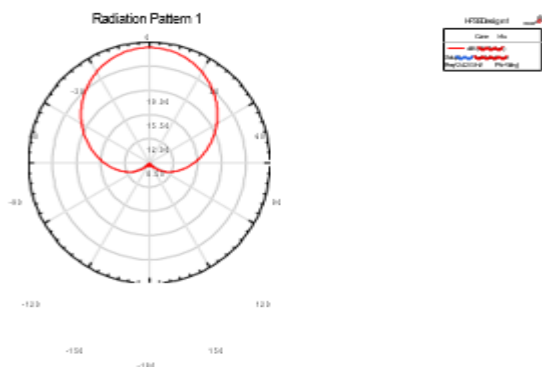


Fig.6©2D radiation pattern of rectangular microstrip antenna with polyster as dielectric material

Fig 6(d) shows the electric field distribution of rectangular microstrip antenna with polyster as dielectric material.

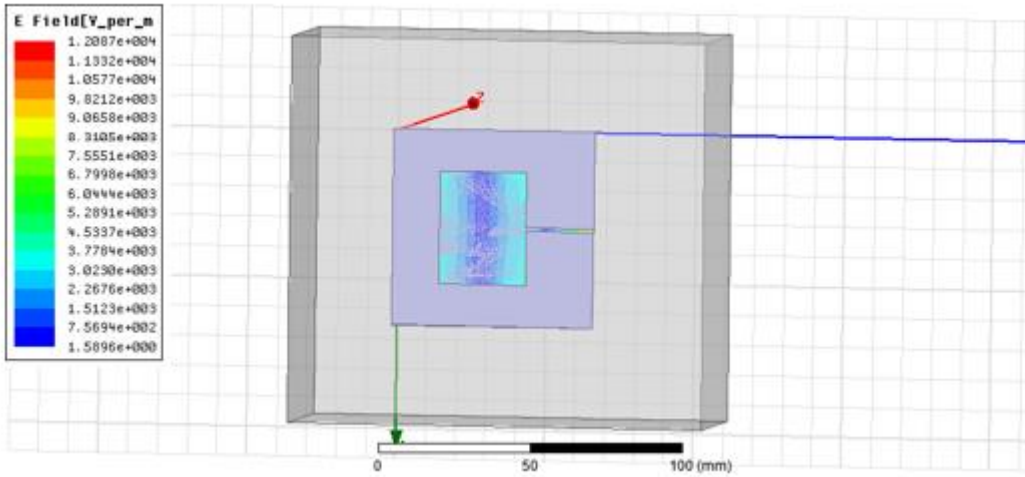


Fig.6(d) Electric Field distribution of rectangular microstrip antenna with polyster material

Fig 6(e) shows the surface current distribution of rectangular microstrip antenna with polyster dielectric material.

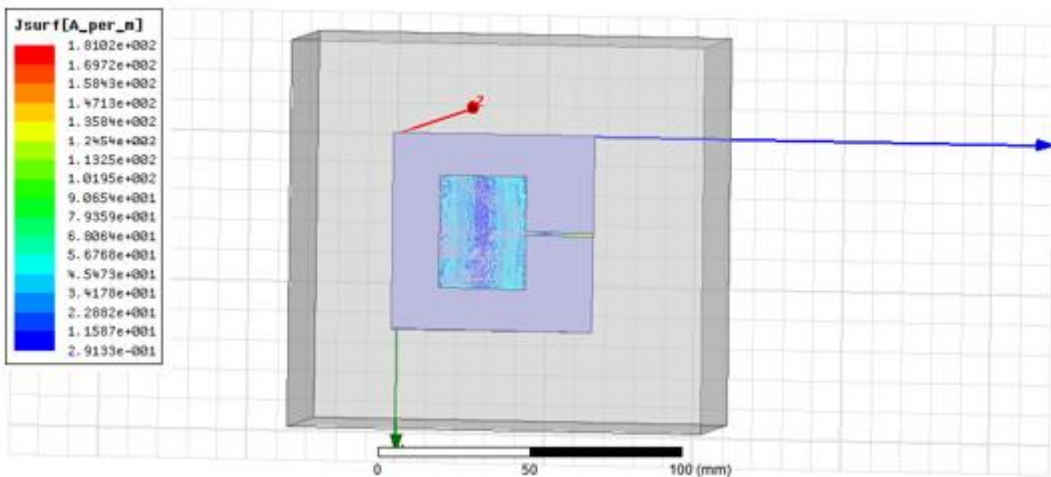


Fig.6(e)Surface current distribution of rectangular microstrip antenna with polyster material.

From fig 6(e),we can observe that there is an uniform current distribution across the patch of a rectangular microstrip antenna with polyster material

Table 1. shows the results obtained for different dielectric materials.From the results ,we can observe that when the paper material is integrated inside the FR4 substrate,the return loss is obtained as -36.79 dB .The gain of the antenna is increased to 4.351 dB when the Teflon material is digged inside the FR4 substrate and the bandwidth is also improved to 79.5 MHz.Since the loss of Teflon material is less and to improve the gain of the microstrip antenna,Teflon material can be used.

Table1.Results obtained for different dielectric materials

Sl. no	Name of the substrate	Dielectric constant	Return loss (dB)	Gain(dB)	Bandwidth(MHZ)	VSWR
1	Mica	5.7	-18.405	3.888	64	1.2731
2	Teflon	2.1	-20.4184	4.351	79.5	1.0294
3	Paper	3.1	-36.79	2.686	80	1.0294
4	Rubber	3	-16.89	4.2007	60	1.3568
5	Polyster	3.2	-17.516	4.0364	64	1.3226

Fig 7. Shows the return loss plot for different dielectric materials.

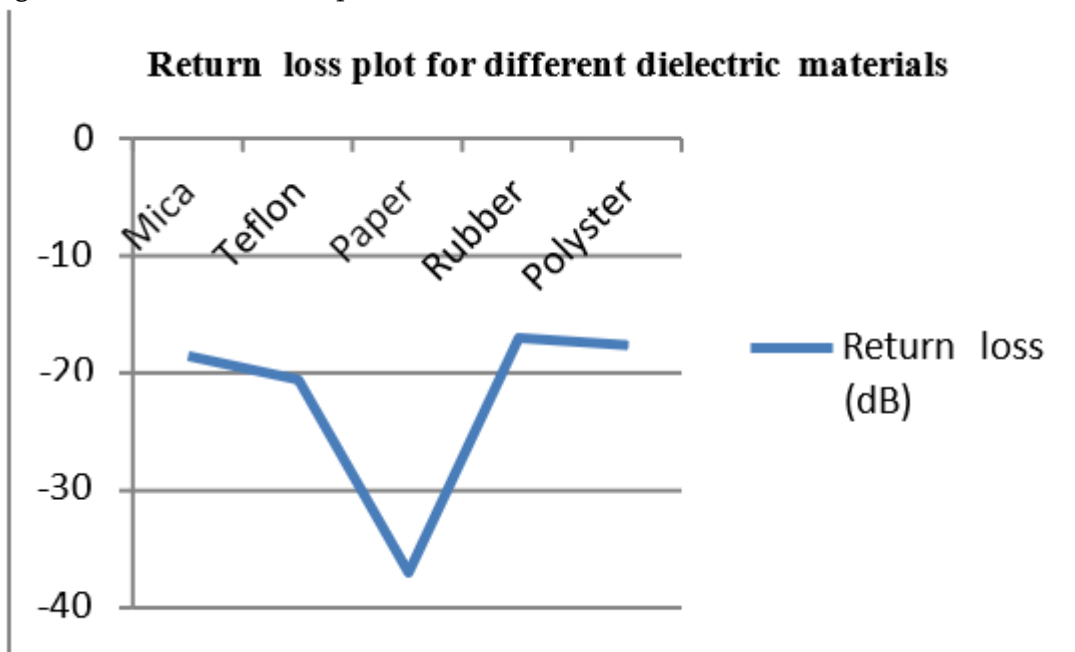


Fig 7. Return loss plot for different dielectric materials.

Fig 7. Shows the return loss obtained for different dielectric materials. From the graph, we can observe that the return loss obtained for paper is -36.79 dB which shows an improved performance, whereas the return loss obtained for rubber material is -16.89 dB which is not showing good performance compared to paper material.

Fig.8. shows the gain obtained for different dielectric materials.

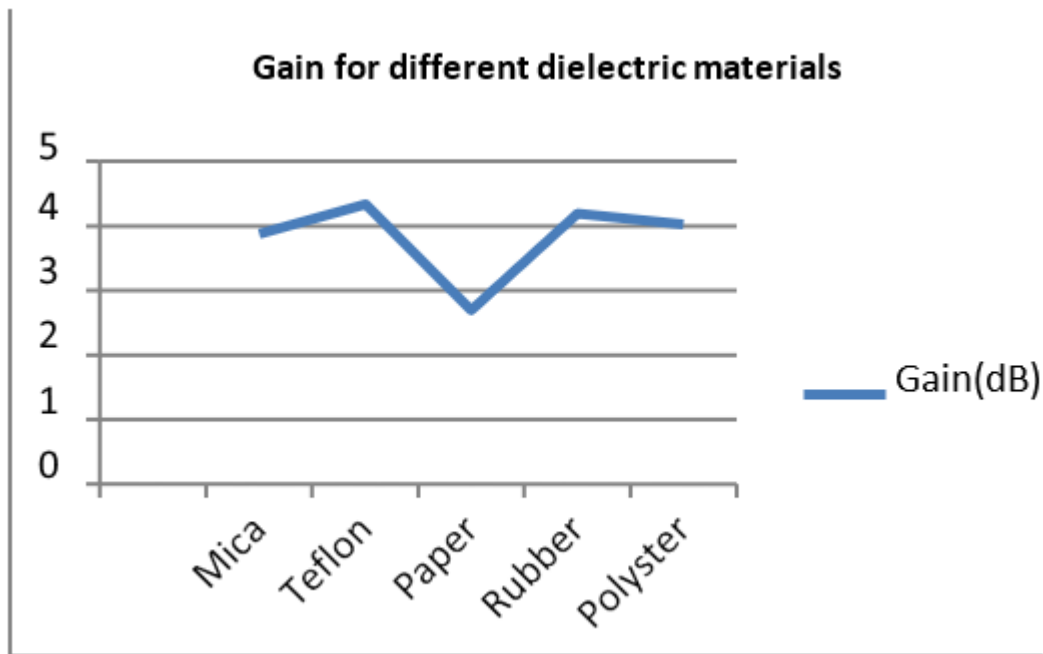


Fig 8. Gain plot for different dielectric materials

From fig 8, we can observe that the gain obtained for Teflon material is 4.351 dB, whereas the gain obtained for paper material is 2.686 dB. This shows that the performance of the antenna can be improved in terms of gain by considering Teflon material and the performance of the antenna can be improved in terms of return loss by considering paper as dielectric material.

IV. CONCLUSION

The rectangular microstrip patch antenna is designed at an operating frequency of 2.4 GHz. The rectangular microstrip antenna is designed and simulated using HFSS. The rectangular microstrip antenna is analysed by integrating different dielectric materials such as mica, Teflon, paper, rubber, polyster inside FR4 substrate. The rectangular microstrip antenna with different dielectric materials are fabricated and the experimental results are verified. The results show that the gain of the antenna is improved by considering a Teflon material which is obtained with a gain of 4.351 dB. The performance of the antenna is improved in terms of return loss by considering paper as dielectric material. The rectangular microstrip antenna with Teflon material can be considered for wireless applications as the loss of Teflon material is less compared to other dielectric materials.

III. REFERENCES

- [1]. Mrinmoy Chakrabortya , Biswarup Ranab , P.P. Sarkarc , Achintya Dasd, " Design and Analysis of a Compact Rectangular Microstrip Antenna with slots using Defective Ground Structure", Science direct, pp 411-416, 2012
- [2]. Indrasen Singh, Dr. V.S. Tripathi, Micro strip Patch Antenna and its Applications: a Survey, Indrasen Singh et al, Int. J. Comp. Tech. Appl., Vol 2 (5), 1595-1599.

- [3]. Md. Moidul Islam, Raja Rashidul Hasan, Md. Mostafizur Rahman, Kazi Saiful Islam, S.M. Al-Amin,” Design & Analysis of Microstrip Patch Antenna Using Different Dielectric Materials for WiMAX Communication System”, International Journal of Engineering and Science, vol.4, issue 1, 2016, pp 19-24
- [4]. Vivek Hanumante, Sahadev Roy; “Comparative Study of Microstrip Patch Antenna Using Different Dielectric Materials,” 9th International Conference On Microwaves, Antenna, Propagation & Remote Sensing ICMARS-2013
- [5]. Vivek Hanumante , Panchatapa Bhattacharjee , Sahadev Roy , Pinaki Chakraborty , Santanu Maity,” Performance Analysis of Rectangular Patch Antenna for Different Substrate Heights”, International Journal of innovative research in Electrical, Electronics, Instrumentation and Control Engineering vol 2, Issue 1, January 2014

A Short-circuit Model Based on Artificial Neural Network and Artificial Bee Colony Algorithm for SiC MOSFETs

Dr. Rajesh L, Praveen Kumar K C, Malini V L, Kavitha A

ABSTRACT

A short-circuit model for silicon carbide (SiC) metal-oxide semiconductor field effect transistors (MOS- FETs) using hybrid modeling method based on artificial neural network (ANN) and improved artificial bee colony (ABC) algorithm is proposed in this paper. In order to improve the search ability of the ABC, particle swarm optimization (PSO) is introduced to the scout bees' search strategy. The improved ABC is employed to find suitable initial parameters for ANN model, which can improve the accuracy of modeling results. Based on hybrid modeling method, the normal working model of SiC MOSFETs is established first. The modeling results of I-V characteristics, C-V characteristics and small signal parameters (gm, gd, etc.) are in good agreement with datasheet, which fully demonstrates the validity of the normal working model. Then the short-circuit model of SiC MOSFETs is further obtained based on the relationship between short-circuit current and junction temperature and normal working model. Eventually, the proposed short-circuit model is verified by device- and circuit-level tests. With its precision and simplicity, the proposed short-circuit model can be used to analyze short-circuit faults in SiC MOSFET simulation circuits and provide assistance for the design of protection circuits.

Keywords: Artificial bee colony (ABC) algorithm, artificial neural network (ANN), silicon carbide (SiC) metal-oxide semiconductor field effect transistors (MOSFETs)

I. INTRODUCTION

With the rapid development of process technologies of silicon carbide (SiC), SiC metal-oxide semiconductor field effect transistors (MOSFETs) have been commercialized in mass production and are popular in the design of high-power electronics [1]. Compared with traditional Si MOSFETs, SiC MOSFETs have lots of outstanding advantages, such as higher switching speed, higher switching frequency, smaller ON-state resistance, and better high temperature stability [2]. Due to the excellent characteristics of SiC MOSFETs, they are often used in harsh circuit conditions. Hence, it is necessary to ensure its reliability and safety to guarantee that SiC MOSFETs can operate normally under harsh conditions. One of the key reliability issues is the short-circuit capability of the SiC MOSFETs [3]. Therefore, an accurate and simple SiC MOSFET short-circuit simulation model is urgently needed to predict the characteristics of the faults caused by the short-circuit and provide guidance for the design of protection circuits.

In the past few decades, many SiC MOSFET models [4–6] have been proposed, but most of them only consider normal working scenarios. Recently, several models [7–9] describing the short-circuit characteristics of SiC MOSFETs have been reported. Physics-based models [7] can describe the internal physical characteristics of SiC MOSFETs and are usually considered to be accurate, but they are too complex to be suitable for power electronic circuit simulation [10]. The PSpice short-circuit model of SiC MOSFETs [8, 9] is simpler than the physics-based model, but it still has many parameters. The extraction of parameters is time-consuming and may lead to inaccurate results. In addition, the PSpice model only considers the short-circuit situation when the case temperature is 25°C, but different case temperatures have an impact on the short-circuit current. Data-oriented modeling methods can be quickly applied for the newly generated device data. Artificial neural network (ANN) is considered as a data-oriented modeling method [11] and can achieve an accurate model in a short time, which has been employed in the modeling of semiconductor devices [12, 13]. In order to reduce the developing time and obtain an accurate model, a short-circuit model of SiC MOSFETs considering case temperatures based on ANN is proposed in this paper.

In this work, a Multi-layer perceptron (MLP) [14] based on the levenberg-marquardt (LM) algorithm [15] is adopted to establish a short-circuit model for SiC MOSFETs. Since the LM algorithm is quite sensitive to the initial values, for the sake of overcoming the sensitivity of the LM to the initial values and get better modeling results, an improved artificial bee colony (IABC) algorithm [16] combined with particle swarm optimization (PSO) [17] (IABCPSO) is proposed and introduced into the training of MLP to find the appropriate initial weights and biases for the LM. In this paper, we first build the SiC MOSFET model under normal working conditions, and then the short-circuit model is developed based on the normal working model and junction temperature. A SiC MOSFET of type C2M0080120D (1200V/36A) [18] is chosen as the modeling object in this paper. Furthermore, the accuracy of the short-circuit model based on this hybrid modeling method is verified by both the device and circuit-level tests.

1. Normal Working ANN Model

Since the drain-source current I_{ds} under normal operating conditions also contributes to the short-circuit current, it is first modeled based on ANN modeling method, which takes into account the temperature characteristics. The ANN model contains the drain-source current I_{ds} , body diode D_b , gate-drain capacitor C_{gd} , gate-source capacitor C_{gs} , drain-source capacitor C_{ds} and internal gate resistor R_g , as shown in Fig. 1.

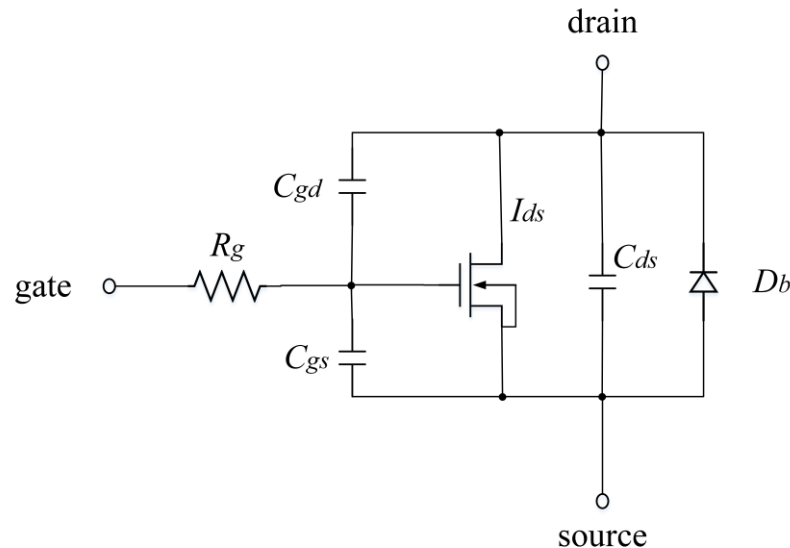


Fig. 1 The ANN model of SiC MOSFET

1.1 Improved artificial bee colony algorithm combined with particle swarm optimization

In our previous work [19], we used the MLP based on the LM algorithm for modeling SiC MOSFETs, which is also adopted as the basis of this paper. Different from [19], the ABC algorithm in this paper is improved by introducing PSO into the search strategy of the scout bees.

In PSO [17], each particle represents a possible solution, and the optimization process of the particle is related to two important factors: the individual optimal solution (pbest) and the swarm's optimal solution (gbest). And the fitness function of PSO will guide the particle swarm to find the optimal solution. In this paper, PSO is introduced into the optimization process of the scout bees of ABC. When the employed bees

and onlooker bees are converted to scout bees because their corresponding nectar sources aren't updated in

the limited times, they will restart the search for the best solution in the entire range set at the beginning, which is undoubtedly a waste of current information resources, such as the current best solution of the entire bee colony (Xbest) found by the employed bees and the onlooker bees. After introducing PSO into the optimization process of the scout bees, we can effectively use the Xbest information, and the optimization of the scout bees will be carried out in accordance with the idea of PSO, thereby improving the efficiency of the whole algorithm. The optimization process of the scout bees can be described as:

$$N_{ij} = w \cdot N_{ij} + r_{i1} \cdot c_1 (p_{best} - M_{ij}) + r_{i2} \cdot c_2 (g_{best} - M_{ij}) \quad (1)$$

$$M_{ij} = M_{ij} + N_{ij} \quad (2)$$

where N_{ij} and M_{ij} represent the velocity and position of the i th particle, respectively; w is an inertia factor describing the contribution rate of the particle's previous speed to its current speed, which helps particles to search a wider area in the previous direction. Moreover, r_{i1} and r_{i2} are random numbers in

the range of $[0,1]$; c_1 and c_2 are the acceleration factors. In order to use the X_{best} information, we set M_i as:

$$M_i = X_{best}. \quad (3)$$

Then, the particle swarm will use X_{best} as the initial position to help scout bees search for the best solution, which effectively enhances the search ability of the whole algorithm. After that, the mean square error of the I-V modeling results and the datasheet is set as the fitness function, and we compared modeling results of IABCPSO and IABC in [19] running 100 times respectively, the results of which are shown in Fig. 2. The conclusion can be drawn from Fig. 2 that, IABCPSO can get better results in a shorter time, which confirms the effectiveness of our proposed algorithm in this paper.

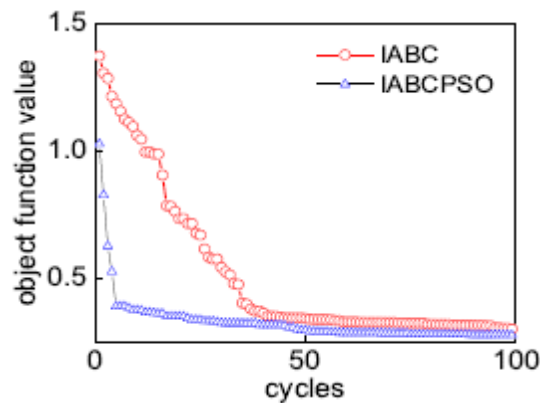


Fig. 2 Comparison results between IABCPSO and IABC

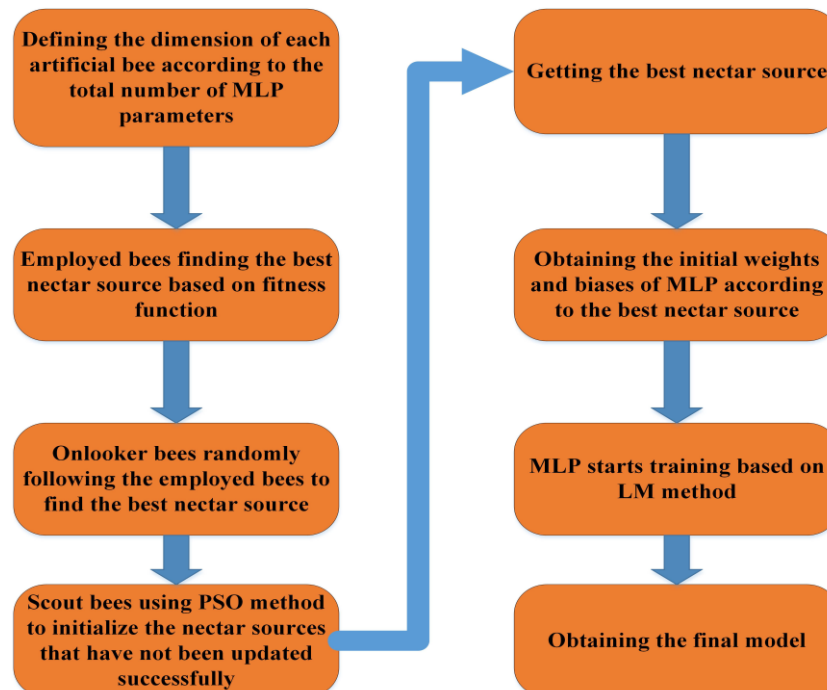


Fig. 3 The flow chart of a hybrid algorithm based on MLP and IABCPSO

2.3 Modeling of drain-source current I_{ds} , body diode I_{bd} and internal capacitors

In this paper, the drain-source current I_{ds} , body diode I_{bd} and internal capacitors are all modeled using our

proposed hybrid modeling method (IABCPSO-MLP). According to I-V curves provided by datasheet [18], the drain-source current I_{ds} can be modeled by an ANN with three inputs (drain-source voltage V_{ds} , gate-source voltage V_{gs} , and operating temperature T). In order to obtain a high-precision model, we use an ANN containing two hidden layers to model I_{ds} and each layer contains 8 neurons. The final modeling results can reach an accuracy of more than 99%.

From datasheet [18], we can find that the current of body diode I_{bd} , like I_{ds} , varies with V_{ds} , V_{gs} , and T . Therefore, the modeling of I_{bd} adopts the same ANN structure as that of I_{ds} and the accuracy of modeling

results of I_{bd} can also reach more than 99%.

According to the datasheet [18], both C_{ds} and C_{gs} vary nonlinearly with one variable, i.e., V_{ds} or V_{gs} . Hence, C_{ds} and C_{gs} can be modeled by same MLP structure with one input (V_{ds} or V_{gs}) and one output (C_{ds} or C_{gs}). Considering the simplicity and accuracy, the 1-5-5-1 MLP structure is finally selected among many tested structures, the accuracy of which can reach 98%.

3 Short-circuit model of SiC MOSFETs

When the short-circuit faults occur, the circuit power loop impedance will become extremely small, and the short-circuit current I_{sc} of the SiC MOSFETs will rise to a large amount. As the current of the circuit is very large, the power loss P_{loss} at this time will also become very large. Therefore, the junction temperature T_j begins to increase, leading to decrease of the channel carrier mobility and I_{sc} . However, T_j is still increasing, and the leakage current caused by thermal ionization is also gradually increasing. When the leakage current rate generated by thermal ionization is higher than the decrease rate of carrier mobility, I_{sc} starts to rise again. It can be concluded that the change of the short-circuit current of the SiC MOSFETs is mainly caused by the change of T_j . Therefore, to establish a short-circuit model, the change curve of T_j during the short-circuit process should be obtained first.

3.1 Thermal network model

In order to obtain the change curve of T_j during the short-circuit process, the thermal network of the SiC MOSFETs is established. The thermal network model based on the case-to-junction thermal impedance formed by a resistance-capacitance (RC) network [9] is the most commonly used, which is also used in this paper. As shown in Fig. 4, T_c and T_j are the case and junction temperatures of SiC MOSFETs, respectively. R_i and C_i are the thermal resistance and thermal capacitance, respectively.

After the development of the thermal network model, the transient thermal impedance Z_{th} can be obtained

by [9]:

$$Z_{th} = \sum_{i=1}^n R_i \cdot (1 - e^{-\frac{t}{R_i \cdot C_i}}). \quad (4)$$

The transient power loss P_{loss} is given by [9]:

$$P_{loss} = V_{ds} \cdot I_{ds} \quad (5)$$

After getting P_{loss} and Z_{th} , the junction temperature T_j of SiC MOSFETs can be obtained, which can be expressed as [9]:

$$T_j = P_{loss} \cdot Z_{th} + T_c \quad (6)$$

In this paper, the experimental data [20] is used as model reference. In [20], the DC bus voltage (V_{ds}) is set as 400V and the corresponding short-circuit current curves under different case temperatures are given.

In Fig. 5, the change of T_j is shown for $T_c=25^\circ\text{C}$ and $V_{ds}=400\text{V}$, which is obtained by Eq. (6) after substituting the transient power loss P_{loss} . When SiC MOSFETs work under normal conditions, the junction temperature is consistent with the case temperature, and when a short-circuit fault occurs, the junction temperature begins to rise.

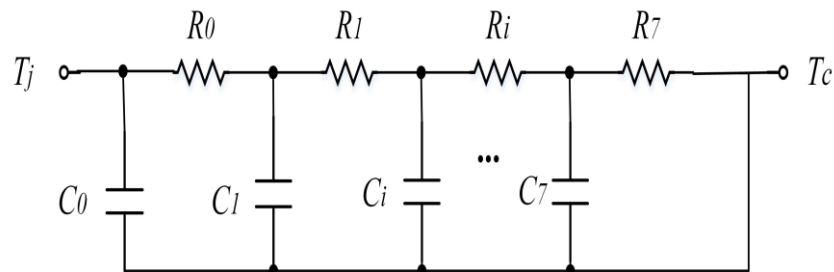


Fig. 4 Thermal network model between case and junction

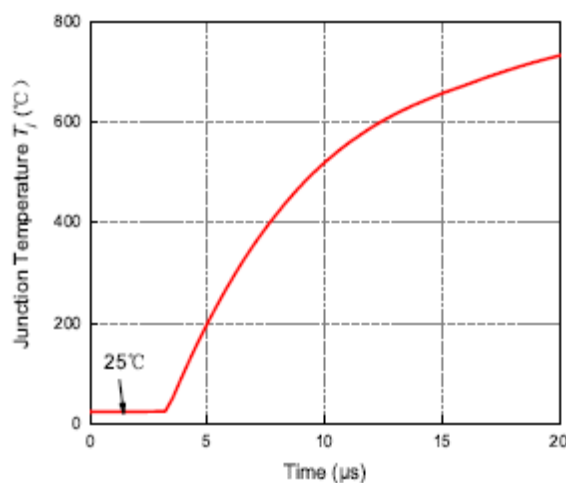


Fig. 5 The change curve of junction temperature T_j

3.2 Modeling of short-circuit current I_{sc}

After getting the instantaneous change curve of T_j , we can acquire the relationship between I_{sc} and T_j , as shown in Fig. 6, where the short-circuit current I_{sc} can be fitted based on T_j . Since when the short-circuit fault occurs, the current I_{ds} under normal working conditions also has output, I_{sc} needs to be fitted based on I_{ds} .

In this paper, the impact of different case temperatures on the short-circuit current is considered. Since the relationship between I_{sc} and T_j is various under different T_c , I_{sc} can be expressed as:

$$I_{sc} = I_{ds} \cdot f(T_j, T_c), \quad (7)$$

where $f(T_j, T_c)$ is a variable that changes with T_j and T_c . In this paper, $f(T_j, T_c)$ is fitted by a 2-5-5-1 ANN structure with hybrid modeling method, that is, ANN has two inputs (T_j and T_c), five neurons in two hidden layers and one output ($f(T_j, T_c)$). Hence, the final expression of I_{sc} can be rewritten as:

$$I_{sc} = \begin{cases} I_{ds_{ANN}} & T_j = T_c \\ I_{ds_{ANN}} \cdot f(T_j, T_c)_{ANN} & T_j > T_c. \end{cases} \quad (8)$$

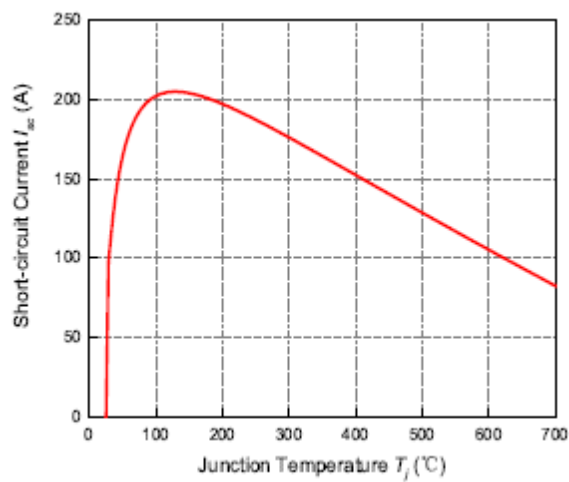


Fig. 6 The corresponding relationship between short-circuit current I_{sc} and junction temperature T_j

4. Conclusion

A short-circuit model based on IABCPSO-MLP modeling method for SiC MOSFETs is presented in this paper. In order to overcome the sensitivity of the basic algorithm (LM) of ANN to the initial values and enhance model accuracy, a scheme that uses IABCPSO to find the initial values for ANN is proposed and verified. The model under normal working conditions is verified by comparing the simulation results of the I-V characteristics, C-V characteristics and small signal parameters (g_d and g_m) that are not exposed in the training process with experimental data. And the short-circuit characteristics of the proposed model are proved by comparing short-circuit current waveforms predicted by our model and experimental data under different working conditions. Hence, our proposed SiC MOSFET short-circuit model can facilitate analysis of short-circuit faults and provide guidance for circuit design.

II. REFERENCES

- [1]. Mill'an, J., Godignon, P., Perpiñan, X., Tomas, A., Rebollo, J.: A survey of wide bandgap power semiconductor devices. IEEE Transactions on Power Electronics. 29(5), 2155-2163 (2014)
- [2]. Duan, Z., Fan, T., Wen, X., Zhang, D.: Improved SiC Power MOSFET model considering nonlinear junction capacitances. IEEE Transactions on Power Electronics. 33(3), 2509-2517 (2018)

- [3]. Sun, J., Xu, H., Wu, X., Sheng, K.: Comparison and analysis of short circuit capability of 1200V single-chip SiC MOSFET and Si IGBT. 2016 13th China International Forum on Solid State Lighting: International Forum on Wide Bandgap Semiconductors China (SSLChina: IFWS), 42-45 (2017)
- [4]. Fu, R., Grekov, A., Hudgins, J., Mantooth, A., Santi, E.: Power SiC DMOSFET model accounting for nonuniform current distribution in JFET region. *IEEE Transactions on Industry Applications*. 48(1), 181-190 (2011)
- [5]. Li, H., Zhao, X., Sun, K., Zhao, Z., Cao, G., Zheng, T.Q.: A Non-Segmented PSpice Model of SiC mosfet With Temperature-Dependent Parameters. *IEEE Transactions on Power Electronics*. 34(5), 4603-4612 (2019)
- [6]. Benedetto, D. L., Licciardo, D. G., Erlbacher, T., Bauer, A. J., Liguori, R., Rubino, A.: A model of electric field distribution in gate oxide and JFET-region of 4H-SiC DMOSFETs. *IEEE Transactions on Electron Devices*. 63(9), 3795-3799 (2016)
- [7]. Duong, T. H., Ortiz, J. M., Berning, D. W., Hefner, A. R., Ryu, S. H., Palmour, J. W.: Electro-thermal simulation of 1200V 4H-SiC MOSFET short-circuit SOA†. *IEEE 27th International Symposium on Power Semiconductor Devices & IC's (ISPSD)*. Hong Kong, 217-220 (2015)
- [8]. Zhao, X., Zhou, Z., Li, H., Sun, K., Zhao, Z.: A Temperature-dependent PSpice Short-circuit Model of SiC MOSFET. *IEEE Workshop on Wide Bandgap Power Devices and Applications in Asia (WiPDA Asia)*. (2019)
- [9]. Li, H., Wang, Y., Zhao, X., Sun, K., Zhou, Z., Xu, Y.: A Junction Temperature-based PSpice Short-circuit Model of SiC MOSFET Considering Leakage Current. *IECON 2019 - 45th Annual Conference of the IEEE Industrial Electronics Society*. (2019)
- [10]. Wang, Z., Shi, X., Leon, M., Fred, T., Wang, Z.: Temperature-Dependent Short-Circuit Capability of Silicon Carbide Power MOSFETs. *IEEE Transactions on Power Electronics*. 31(2), 1555-1566 (2016)

IOT based Contactless Temperature using Raspberry Pi

Anushree N R¹, Nilu Mishra², Kavitha L³, Dr. Nandini V L⁴

^{1,2,3}, Assistant Professor, Dept of ECE, East Point College of Engineering and Tecnology

ABSTRACT

In this paper we present the development of IOT based contactless body temperature monitoring using raspberry pi with camera and email alert. The proposed system offers the image of the person if the temperature of any particular person exceeds the set value. Experimental results of the suggested prototype show the measuring temperature and sending mail alert with PI.

Keywords : Raspberry pi3, pi camera, MLX90614-IR Temperature sensor, Temperature measurement, Electronic circuits.

I. INTRODUCTION

It has become truly challenging to recognize the individuals who are influenced by the infection or not. To tackle this issue, temperature gadgets are regularly used to gauge internal heat level. These gadgets have non-contact IR temperature sensors which can gauge the internal heat level with no actual contact. There are numerous temperature weapons accessible on the lookout, however none of them gives any ready or email warning to higher specialists to make fitting moves when the temperature surpasses a specific cut-off. In this undertaking, we will interface an IR temperature sensor and send the email alarms with the picture of the individual if the temperature of a specific individual surpasses the set is important. The Internet of Things is upsetting our life by fostering various frameworks which can be observed and controlled distantly. IoT can offer generous benefit across the whole life sciences esteem chain, from innovative work digitalization to upgrading the patient experience. This distant innovation dependent on IoT stage is particularly valid in Coronavirus-19 sickness, straightforwardly affecting general wellbeing measures on help clinical in friendly region. This exploration article proposes the contactless internal heat level checking of the in-patient division (IPD) utilizing the web of clinical advancement. IoT has begun to discover more extensive applications in the field of clinical material the executive's perception. Nodayway's, health monitoring is a global challenge in peoples life time solid condition which affected by natural and careful realities. The estimation of human body fundamental signs is an essential to recognize the wellbeing status. The exhibition of any work or exercise in hot conditions upsets the decent warm homeostasis condition of human body (HB). This equilibrium recognizes the HB about physiological and intellectual execution of body. The typical internal heat level reaches by 36.50C to 37.50C. The situation with wellbeing beneath this cut-off is expressed as hypothermia and the status above is alluded as fever and hyperthermia conditions. The hyperthermia likewise alluded as cancer contingent stage that ranges more than 38.5 0C. The singular body temperature estimation is reliant of various viewpoints for

example age, effort, contamination and spot of body at which estimation made. There are a few techniques to gauge the HBT for example oral, rental and axillary through inconsistent and contactless thermometers.

Literature Review

It utilizes high LM-35DZ temperature sensor for estimation of human internal heat level. It utilizes GSM innovation and its usefulness for versatile correspondence to communicate the physiological sign data to an approved individual's PDA. This framework has GPS innovation for area recognizable proof. By using this method, we can sense, send, display, and store the physiological parameter such as human body temperature.

Thermo-vision system is used to detect the overheated spots in electronic PCBs or integrated circuits in a non-destructive, contactless manner, in order to improve their thermal stability and reliability. It offers a low-cost solution for laboratory testing of electronic circuits that has good accuracy and flexibility.

3 IOT based health monitoring system using Raspberry Pi, it uses different sensors like Pulse/Heart beat sensor, Body temperature sensor, ECG sensor, Blood pressure sensor and Patient position sensor are attached to the patient and sensor output serially are sent to Raspberry Pi. It will be helpful for students, patients, athletes, gymnastics for their health analysis easily at any place.

4 The iRT incorporate a microcontroller with native Wi-Fi support, a Fire Beetle ESP8266 (DFRobot) and the sensor is connected using I2C interface. To make specialized upgrades, including the improvement of significant cautions and notices to inform the client when the temperature meets characterized setpoints. An embedded system using an infrared temperature sensor that works with an IoT-Wi fi controller on the NodeMCU ESP32 board and the detected data will be transferred to users via the internet network, and it will be stored on a cloud internet system. This method is helpful to reduce the contact, proximity between patients and healthcare professionals.

5 This system starts with initialization of temperature sensors for collection of real time temperature data in compare to environmental temperature values. The affectability of temperature sensors LM35 (S1) and MLX-90614 (S2) is customized in C++ language and access through Arduino CT-UNO regulator. The daily monitoring of body temperature can prevent the people from threaten of fever, hypothermia and hyperthermia illness.

6 A circuit consisting of a microcontroller, Bluetooth, LED, light-dependent resistor (LDR), and MLX 90615 IR temperature sensor has been designed. At the entrance of a building such as a university or a mall, the fever of the visitors can be detected safely, without contacting physically.

7 The temperature sensor type (MLX90614ESF) was used similarly as the usage of the beat sensor type (KY039), which related with Arduino Uno where the results were taken care of and sent by a nRF24L01 development to the far away end and ensuing to tolerating them in the far side are arranged using Arduino Uno. It will show the perusing of the heartbeat sensor and blood heat sensor in BPM (Beats Per Minute) and in Celsius or Fahrenheit.

8 To make a classifier that will differentiate between faces with masks and without masks. A Pre-prepared organization called mobileNetV2 which is prepared on the ImageNet dataset with our neural organization model. Various deep learning and computer vision frameworks are used for social distance finding with our proposed system on raspberry pi.

9 This system will help to identify people on image/ video stream wearing a facemask with the help of Deep Learning and Computer Vision algorithms by using various libraries such as OpenCV, Keras, TensorFlow etc. The images are downloaded from various open-source websites and are differentiated as “mask” and “no mask”. The pictures that we downloaded were of various sizes and various goals. Face Mask and internal heat level recognition can assist us with diminishing the enormous social affair of individuals in a single spot without veils, lessening the danger of getting contaminated.

Need of Temperature Monitoring System

The variation in human body temperature (HBT) can lead to different disease. It is essential to quantify the range of temperature as shown in body temperature measurement range (Fig1). As expressed by analysts that, while assessing and estimating the wellbeing status extraordinarily HBT, some crucial focuses are essential. Few measurement methods are shown in temperature measurements methods (Fig2), while some aspects are justified in sub-sections diurnal variations (2.1) and emotional status (2.2) respectively and linked are listed in variations in body temperature by age (Table 1).

2.1. Diurnal variations - This variety is reliant of human body digestion. During the sleep the metabolism is slower as decrement in contractions of muscles.

2.2. Emotional states- These variations frequently observed with young children during extreme anger and crying state which increase the body temperature.

MLX90614 IR Temperature Sensor: There are numerous sensors accessible in the market which can give us temperature and humidity. What makes this sensor unique in relation to any remaining sensors is that it can give us object temperature and different sensors give surrounding temperature. We have used DHT11 Sensor and LM35 extensively for many applications where atmospheric humidity or temperature has to be measured. But here for making a temperature gun which doesn't need physical contact and can measure the object temperature instead of ambient temperature, we use IR based MLX90614. MLX90614 sensor is made by Melexis Microelectronics Integrated frameworks, it chips away at the rule of InfraRed thermopile sensor for temperature estimation. These sensors comprise of two units inserted inside to give the temperature yield. The primary unit is the detecting unit which has an infrared identifier which is trailed constantly unit which plays out the calculation of the information with Digital sign preparing (DSP). This sensor deals with Stefan-Boltzmann law which clarifies power emanated by a dark body as far as its temperature. In straightforward terms, any item radiates IR energy and the power of that will be straightforwardly corresponding to the temperature of that article. MLX90614 sensor changes over the computational worth into 17-bit ADC and that can be gotten to utilizing the I2C correspondence convention. These sensors measure the ambient temperature as well as object temperature with the resolution calibration of 0.02°C. To find out about the elements of the MLX90614 sensor, allude to the MLX90614 Datasheet.

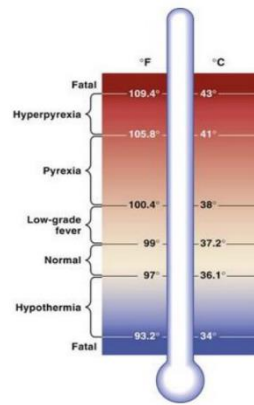


Figure 1. Body temperature measurement range

Features of MLX90614:

- Operating Voltage: 3.6V to 5V.
- Ambient Temperature Range: -40°C to 125°C.
- Object Temperature Range: -70°C to -382.2°C.
- Resolution/Calibration: 0.02°C.
- 17-bit ADC.
- I2C communication

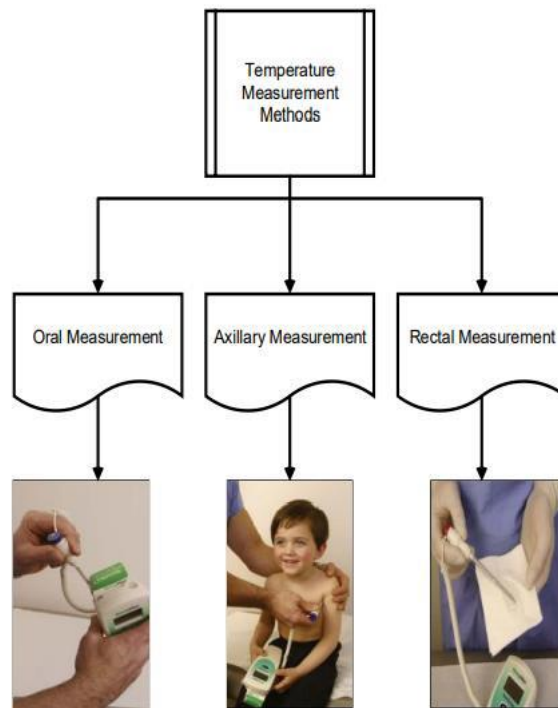
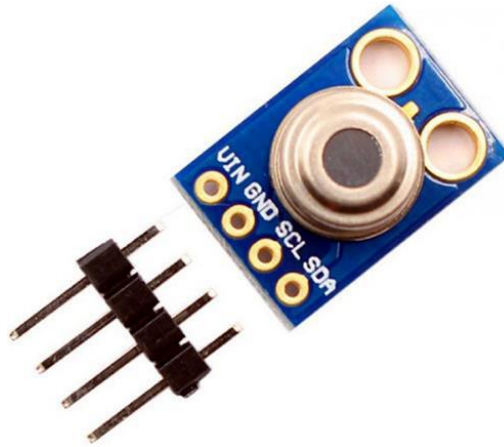


Figure 2. Temperature measurement methods



Methodology

Interfacing MLX90614 with raspberry pi

Step1: - Enabling the I2C from raspberry pi setting.

Step2: -Download the package/library of MLX90614 by going to [https://pypi.org/project/PyMLX90614/# files](https://pypi.org/project/PyMLX90614/#files) Pi camera interfacing with raspberry pi

Step1: -Enabling the camera from raspberry pi setting.

Step2: -To check if the camera to click a picture with the name image and store that on your desktop.

Setting up SMTP email with raspberry pi

Step1: -Go to the right corner and click on my manage your google account.

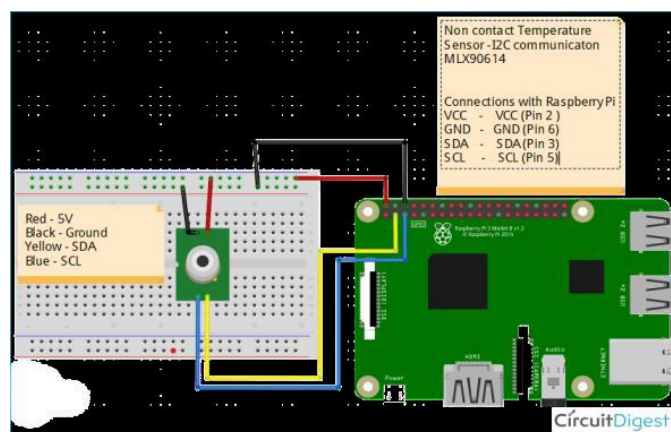
Step2: - Click on security and scroll down to “less secure app access”

Step3: - Enable the less secure app.

Step4: - Repeat with the other email id as well to send/receive the email from the python script.

Step5: -Download the required packages.

Step6: - After the establishment of the relative multitude of libraries is done, we need to make changes in the smtp.conf document where we need to enter the sender's email subtleties.



Steps to Send Mail with attachments using SMTP (smtp lib)

1. Create MIME.
2. Add sender, recipient address into the MIME.
3. Add the mail title into the MIME.
4. Attach the body into the MIME.
5. Start the SMTP meeting with legitimate port number with appropriate security highlights.
6. Login to the system.
7. Send mail and exit.

The Raspberry Pi Foundation explicitly chose Python as the fundamental language due to its force, flexibility, and convenience. Python comes preinstalled on Raspbian, so you'll be prepared to begin consistently. You have various choices for composing Python on the Raspberry Pi..

Raspberry Pi program is, without a doubt, an extremely insignificant beginning. A lot more impressive applications can be composed utilizing the Python programming language. Obviously, on the off chance that you simply need a modest \$35 Linux machine, the Raspberry Pi turns out extraordinary for that to.

Python is generally utilized for creating sites and programming, task computerization, information investigation, and information perception. Since it's moderately simple to learn, Python has been taken on by numerous non-developers like bookkeepers and researchers, for an assortment of ordinary undertakings, such as getting sorted out accounts.

Advantages and Disadvantages

Advantages

Smart sensors examine ailments, way of life decisions and the climate and suggest deterrent measures, which will diminish the event of sicknesses and intense states. Decrease of medical care costs: IoT lessens expensive visits to specialists and emergency clinic affirmations and makes testing more moderate.

1. Distant observing: Real-time far-off checking through associated IoT gadgets and savvy cautions can analyze ailments, treat infections and save lives in the event of a health-related crisis.
2. Prevention: Smart sensors dissect medical issue, way of life decisions and the climate and suggest protection measures, which will lessen the event of sicknesses and intense states.
3. Reduction of healthcare costs: IoT reduces costly visits to doctors and hospital admissions and makes testing more affordable.
4. Medical data accessibility: Accessibility of electronic medical records allow patients to receive quality care and help healthcare providers make the right medical decisions and prevent complications.
5. Improved treatment management: IoT devices help track the administration of drugs and the response to the treatment and reduce medical error.
6. Improved healthcare management: Utilizing IoT gadgets, medical services specialists can get significant data about hardware and staff adequacy and use it to recommend developments.

7. Research: Since IoT devices are able to collect and analyze a massive amount of data, they have a high potential for medical research purposes.

DISADVANTAGES

Security and privacy: Security and privacy remain a major concern deterring users from using IoT innovation for clinical purposes, as medical care checking arrangements can possibly be penetrated or hacked. The hole of touchy data about the patient's wellbeing and area and interfering with sensor information can have grave results, which would counter the advantages of IoT.

2. Risk of failure: Disappointment or bugs in the equipment or even force disappointment can affect the exhibition of sensors and associated gear putting medical services tasks in danger. Likewise, avoiding a planned programming update might be significantly more unsafe than skirting a specialist examination.

3. Integration: There's no agreement with respect to IoT conventions and norms, so gadgets delivered by various makers may not function admirably together. The absence of consistency forestalls full-scale coordination of IoT, thusly restricting its expected viability.

4. Cost: While IoT vows to lessen the expense of medical care in the long haul, the expense of its execution in clinics and staff preparing is very high.

CONCLUSION

When the hardware and software are ready, just run the python code on your pi. it will print the worth of temperature read from the sensor. If the object temperature, then our python program will take an image from the camera, save it on raspberry pi, and also share it via email.

REFERENCES

- [1] Sudhindra F 1, Annarao S.J2, Vani R.M3, Hunagund P.V4 “Development Of real time human body temperature [Hypothermia and Hyperthermia] monitoring and Alert Systems with GSM and GPS” 2016.
- [2] Miljana Milić and Miloš Ljubenović “Arduino-based non-contact system for thermal-imaging of electronic circuits” 2018.
- [3] Sunil Kumar Laxman Bhai Rohit and Bharat V. Tank “IOT Based health monitoring system using raspberry pi” 2018.
- [4] Gonçalo Marques* and Rui Pitarma “Non-contact Infrared temperature acquisition system based on IOT for laboratory activities monitoring” 2019.
- [5] Wasana Boonsong1, Narongrit Senajit2, Piya Prasongchan3 “Contactless body Temperature Monitoring of In-patient department (IPD) Using 2.4GHZ microwave frequency via the IOT network” 2020.
- [6] Asif A. Rahimoon1, Mohd Noor Abdullah2, Ishkrizat Taib3 “Design of a Contactless body temperature system measurement using arduino” 2020.
- [7] Ahmet Remzi Ozcan1, Ahmet Mert1* “Low-cost android based telemonitoring System for body temperature measurement” 2021.
- [8] Shantilal Sen1, Manali Patil2, Sejal Ravankar3, Janhavi Sangoi4 “Survey of a symptoms Monitoring system for covid-19” 2021.

- [9] Sheetal Mahadik¹, Namrata J. Ravat², Kunal Y. Singh³, Suvita K. Yadav⁴ “Contactless system with mask and temperature detection” 2021.
- [10] NaveenKumar K, ²Surya.S, ³Mohammed Nihaal. S. S, ⁴Suranthar. S, ⁵Manoj Kumar. A “Automatic covid-19 face mask and body temperature detection with deep learning and computer vision” 2021

Blackfin Processor Boom to Embedded System

Nilu Mishra¹, Anushree N R², Kavitha L³, Chaitali Darode⁴

^{1,2,3}Assistant Professor, Dept of ECE, East Point College of Engineering and Tecnology

⁴Assistant Professor, Dept of ECE, SBJain Institute of Technology, Nagpur

ABSTRACT

Digital signal processing (DSP) is a key requirement in a variety of industries and applications. It offer an assortment of digital signal processing solutions for applications including automotive, portable, motor/power control, security, test and measurement, and beyond it also meet design needs. Processor provides scalable low-latency audio performance, featuring large on-chip SRAM with many options including on-chip ASRCs and multi-channel IIR/FIR/FFT accelerators to facilitate real-time audio processing. System connectivity includes TDM/I2S, Ethernet, MLB, CAN, SPI, I2C, UART, and many others, making them a fit for a wide variety of embedded applications.

I. INTRODUCTION

Blackfin processor was designed, developed, & marketed through Analog Devices & Intel as Micro Signal Architecture (MSA). The architecture of this processor was announced in December 2000 & demonstrated first at the ESC (Embedded Systems Conference) in June 2001. This Blackfin processor was mainly designed to reach the power constraints & computational demands of present embedded audio, video & communications applications. This article discusses an overview of a Blackfin processor – architecture and its applications.

II. Architecture

The Blackfin processor provides both the functionalities of a micro-controller unit & digital signal processing within a single processor by allowing flexibility. So this processor includes a SIMD (single instruction multiple data) processor including some features like variable-length RISC instructions, watchdog timer, on-chip PLL, memory management unit, real-time clock, serial ports with 100 Mbps, UART controllers & SPI ports.

The MMU supports multiple DMA channels to transfer data between peripherals & FLASH, SDRAM, and SRAM memory subsystems. It also supports data caches & configurable on-chip instruction. The Blackfin processor is a simple hardware which supports 8, 16, and 32-bit arithmetic operations.

The Blackfin architecture is mainly based on the architecture of micro signal and this was jointly developed by ADI (Analog Devices) & Intel, which includes a 32-bit RISC instruction set and 8-bit video instruction set with dual 16-bit multiply-accumulate (MAC) units.

Analog devices are capable of achieving a balance between the DSP & MCU requirements through the instruction set architecture of Blackfin. Generally, the Blackfin processor is coupled with the powerful Visual DSP++ software development tools but now by using C or C++, it is possible to produce highly efficient code very easily than before. For real-time requirements, operating system support becomes critical, so the Blackfin supports a no. of operating systems & memory protection. Blackfin processor comes in both single-core like BF533, BF535 & BF537, and dual-core like BF561 models.

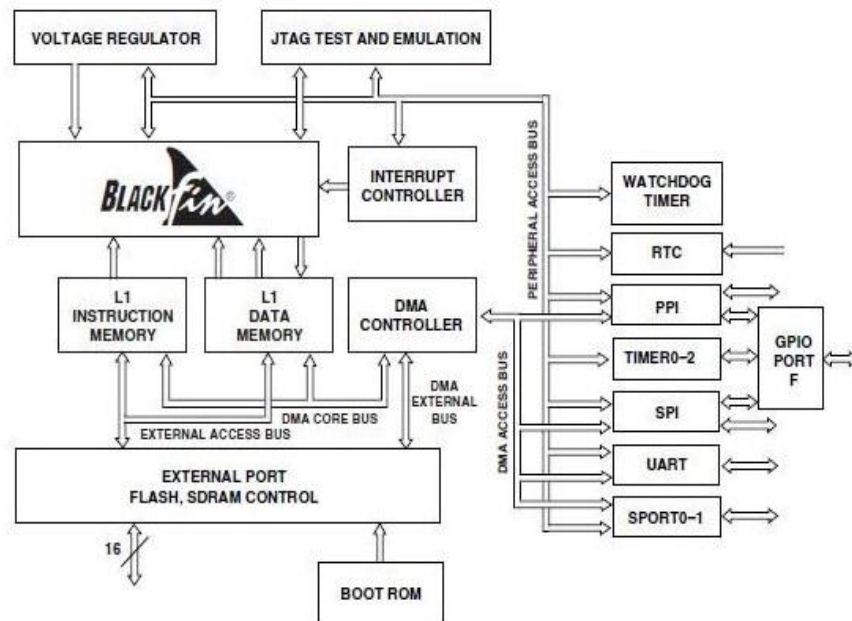


Figure 1.1 Blackfin Processor Architecture

The Blackfin processor architecture includes different on-chip peripherals like a PPI (Parallel Peripheral Interface), SPORTS (Serial Ports), SPI (Serial Peripheral Interface), UART (Universal Asynchronous Receiver Transmitter), General-purpose timers, RTC (Real-Time Clock), Watchdog timer, General-purpose I/O (programmable flags), Controller Area Network (CAN) Interface, Ethernet MAC, Peripheral DMAs -12, Memory to Memory DMAs -2 including Handshake DMA, TWI (Two-Wire Interface) Controller, a Debug or JTAG Interface & Event Handler 32 Interrupt Inputs. All these peripherals in the architecture are simply connected through different high-bandwidth buses to the core.

III. IMAGE PROCESSING APPLICATION OF BLACKFIN PROCESSORS

As high definition (HD) cameras and displays become commonplace, the need to quickly process large images increases. The embedded processors found in such devices have, for the most part, not followed the trend of increasingly faster clock speeds seen in general-purpose processors. High clock speeds translate to higher power usage, which in turn requires cooling systems to maintain reliable performance.

Such requirements are ill-suited to the constrained environments of embedded systems. For this reason, and because embedded processors tend to be geared more to specific classes of applications, embedded chips have specialized hardware resources to do more per cycle, rather than reducing the cycle time. Many image processing routines can be expressed as a set of instructions, called compute kernels, which transform raw image data into meaningful information. Vector processing units, special-purpose hardware such as video ALUs (vALUs), and convergent cores have extended some embedded architectures to allow multiple pixels to be transformed at once. But because of the vast amounts of data needing to be processed, memory performance is critical. Researchers have examined the memory hierarchy and proposed methods to minimize the latency associated with accessing high-capacity, slow off-chip SDRAM (called the Memory Wall effect). This need to feed the computational units which may otherwise be starved for data motivates our work and our examination of the stream model of computing.

The software modules are fully optimized for the Blackfin processor family and include image processing task level primitives to enable faster development cycles for video analytics applications. The free software modules, available in object code or a C source wrapper, provide advanced video design functionality such as video filtering, transforms, color operations and utilities suitable for a wide range of applications, including video surveillance, automotive vision systems and industrial vision.

A scheduling algorithm for image processing tasks which have two computations steps both of them depend of noise power. The scheduling algorithm trades off between the quality of the restored image and the constraint to meet the deadlines. The framework for real time implementation of such image processing algorithms that ensure a reasonable quality of the videoclips in systems prone to impulsive noise but meeting deadlines.[1]

Figure 1.2 proposed steps for Image processing

Video surveillance systems [VSS] are digital today due to advancement of processing capabilities of DSP compared to analog. Video surveillance technology is necessary and indispensable around the world for public safety and law enforcement control. The advantage of video surveillance is to monitor and provides the real-time protection for investigation and evidence preservation. Largely, it depends on the quality of the images transmitted by digital video surveillance cameras and networks. Image quality is paramount. Digital VSS provides various advantages such as viewing the video or images immediately as soon the incident captured by the VSS either near or remote locations. So, action for the captured incident will be address immediately to to apply intelligence and swift response [3-4].

VSS is a kind of any video surveillance technology which has features of enabling (videotapes, photographs or digital images) for continuous or periodic recording and viewing or monitoring of public areas. Monitoring and tracking will provide the safety for lives. A variety of applications are emerging to leverage the power of DSPs in products like video surveillance cameras and video servers. A surveillance is one of the major verticals that is witnessing exponential growth. The threat to security globally is the major driver for the growth in security surveillance market.[8-9]

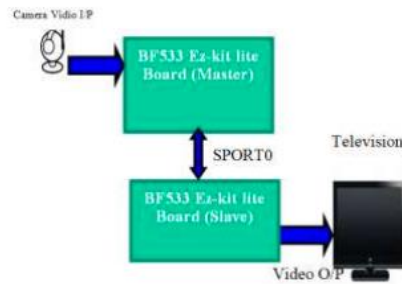


Figure 1. Block diagram of VSS

The various parameters for VSS are analyzed, how it will be implemented on the embedded processor. ADSP Blackfin processor BF533 is suitable for the video application. It can be developed on BF533 at low cost and low power consumption. The VSS is designed based on available ADSP BF533 Ez-kit lite. The concept is developed and verified on the Ez-kit lite. The application video signal processing is facilitating and achieved through the parallel peripheral interface (PPI) of the Blackfin processor which is connecting to both of video encoder and video decoder in the Ez-kit lite. Hence, two boards are used to prove the real time design as master and slave transfer mode. The VSS block diagram is shown in the below Figure. It gives the concept of system at the top level and interconnection. Two BF533 Ez-kit lite boards are interconnected through SPORT to transfer the data. The detailed technical design is described in the next section.

Video interfaces. The Video interfaces will be discussed in System on the BF533 Ez-kit lite board's features and how it is implemented. Also, it contains the block diagram, and flowchart representation for the design and implementation of the logic. The system architecture is discussed with the top-level block diagram. The board hardware configurations, setups and interfaces with respect to video processing are described though BF533 Ez-kit lite supports other features like Audio interface, UART. The basic configuration will be discussed for each section except detail as separate sections include memory and peripheral interfaces, power and clock signals, LED, pushbutton switch and video interfaces.

Audio compression (data), a type of lossy compression in which the amount of data in a recorded waveform is reduced for transmission with some loss of quality Dynamic range compression, also called audio level compression, in which the dynamic range, the difference between loud and quiet, of an audio waveform is reduced. Dynamic range compression, also called DRC (often seen in DVD and car CD player settings) or simply compression reduces the volume of loud sounds or amplifies quiet sounds by narrowing or "compressing" an audio signal's dynamic range.

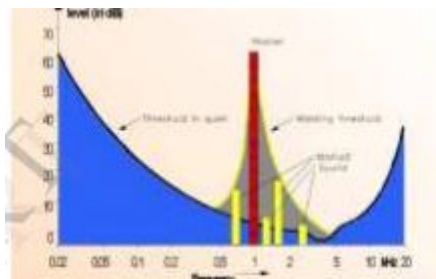


Figure shows the threshold of energy required in the 20Hz-20 KHz range for an average human to perceive sound in quiet, measured in deci-Bells (dBs)

Goals Of audio Compression:

Reduced bandwidth or storage make decoded signal as close as possible lowest implementation complexity reasonable arithmetic requirement. Application to as many signal type as possible robust, scalable extensible an `audio CODEC' is a system for the Needs of audio compression: Audio compression (data), a type of lossy compression in which the amount of data in a recorded waveform is reduced for transmission with some loss of quality Dynamic range compression, also called audio level compression, in which the dynamic range, the difference between loud and quiet, of an audio waveform is reduced. Dynamic range compression, also called DRC (often seen in DVD and car CD player settings) or simply compression reduces the volume of loud sounds or amplifies quiet sounds by narrowing or "compressing" an audio signal's dynamic range Goals Of audio Compression: Reduced bandwidth or storage make decoded signal as close as possible lowest implementation complexity reasonable arithmetic requirement. Application to as many signal type as possible robust, scalable extensible an `audio CODEC' i s a system for the encoding, and Decoding of audio data for use in digital systems The term `Lossy' refers to the fact that once audio data have gone through this process and been reconstructed, some information will be lost and the resulting signal will not be identical to that sampled. The key to successful CODEC is being able to identify where the redundant information in the signal is and being able to remove it, while at the same Time minimizing the perceived impact on the listener of the reconstructed signal. [10]

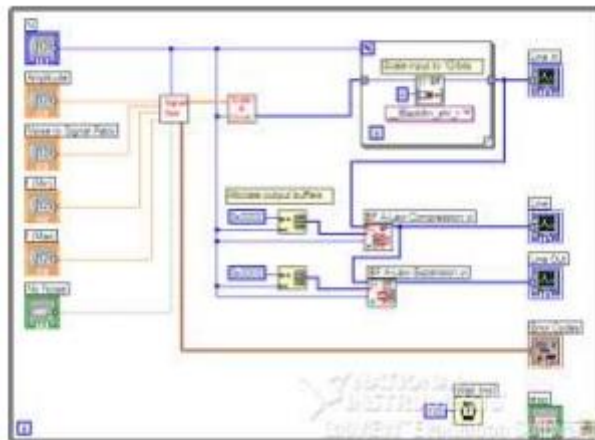


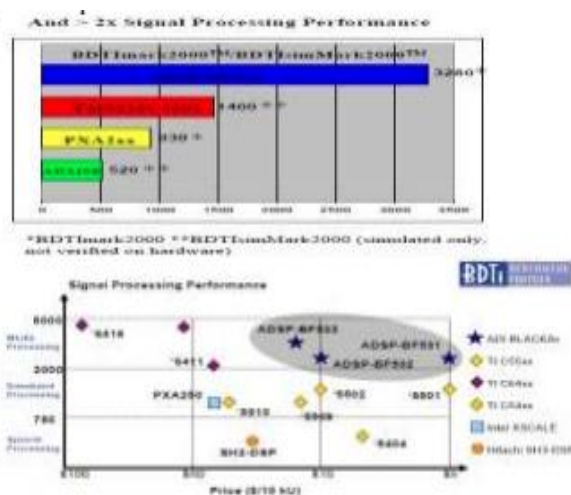
Figure Audio compression using Blackfin

Arbitrary bit and bit-field manipulation, insertion and extraction Integer operations on 8/16/32-bit data-types Memory protection and separate user and supervisor stack pointers Scratch SRAM for context switching Population and leading digit counting Byte addressing DAGs Compact Code Density.

Types of Audio Codec:

Non-compression formats: LPCM, generally only described as PCM is the format for uncompressed audio in media files and it is also the standard for CD DA note that in computers, LPCM is usually stored in Container Formats such as WAV FF mpeg Pulse Density Modulation (PDM) Pulse Amplitude Modulation (PAM) Lossless data compression: APPLE Lossless Audio Codec (ALAC) FF mpeg QuickTime ATRAC Advanced lossless (AAL) Direct Steam Transfer (DST) MPEG-4 DST reference software (ISO/IEC

14496-5:2001/Amd.10:2007) MLP but adds higher sample rates, bit rates, and more channels FF mpeg. (decoding only)



CONCLUSION

We have compared Video, Audio, Image and data coding using blackfin processors, only video and Audio reference we have taken in this paper. From above same it is clear that blackfin processor are very efficient, cost, effective and best suited for above applications.

IV. REFERENCES

- [1]. Use of an Embedded Configurable Memory for Stream Image Processing, Michael G. Benjamin and David Kaeli Northeastern University Computer Architecture Research Group Department of Electrical and Computer Engineering Northeastern University, Boston, MA 02115 {mbenjami, kaeli}@ece.neu.ed
- [2]. Blackfin processor based secure Audio, Video and image transmission, Ardina Aurthur, V Saravanan, Department of Embedded system technologies, Procedia Engineering 38(2012), 359-365.
- [3]. ADSP BF533 Ez-kit lite Specification, Analog Devices, 2010. [Online].
- [4]. A. Seema and M. Reisslein, "Towards efficient wireless video sensor networks: A HW/SW cross layer approach to enabling sensor node platforms," IEEE COMSOC MMTCE-Letter, vol. 7, no. 4, pp. 6-9, 2012. [5] Ahrenberg. L. Ihrke. I., Magnor. M, "A mobile system for multi-video recording," CVMP, 1st European Conference Visual Media Production, 2004, pp. 127-132.
- [5]. A. Bouyahya, Y. Manai and J. Haggege, "Application of new approach of design flow for hardware/software embedded systems with use of design patterns in fuzzy control system," International Journal of Reconfigurable and Embedded Systems, vol. 4, no. 2, pp. 142-160, 2015.
- [6]. S. Dessai and K. Ramakrishna, "Implementation of video capture and playback in mobile systems," International Journal of Reconfigurable and Embedded Systems, vol. 2, no. 3, pp. 106-115, 2013.
- [7]. S. Dessai and K. Ramakrishna, "Implementation of video capture and playback in mobile systems," International Journal of Reconfigurable and Embedded Systems, vol. 2, no. 3, pp. 106-115, 2013. [6] D. Fronczak and D. Seltz, "Motion JPEG and MPEG solutions for multimedia," IEEE transaction on Multimedia published in 2002, pp. 2-4.
- [8]. F. Gaarder, "Video streaming into virtual worlds" M.S. thesis, Department of Informatics, University of Oslo, Norway, 2009
- [9]. New Algorithms for Implementing Audio Compression Techniques Using Embedded System, Mr. A. V. Warhade, Prof A. D. Bijwe Prof. A. P. Deshpande, International Journal of Engineering Research & Technology (IJERT) Vol. 2 Issue 5, May - 2013

Selection of Suitable Filter Parameters for Denoising Breast Thermograms Using Anisotropic Diffusion Filter

Vijaya Madhavi M*, Vetrikani R, Malini V L

Department of Electronics and Communication Engineering, East Point College of Engineering and Technology, Bengaluru, India

ABSTRACT

The most common form of cancer among women is breast cancer. Breast thermography is the new technology employing infrared camera to detect heat emissions from the breast region. The acquired thermal images are of low contrast and are corrupted to a greater extent by quantum noise. The objective of the proposed work is to effectively denoise breast thermograms using anisotropic diffusion filter. In the proposed work, frontal breast thermograms are processed using anisotropic diffusion filter which preserves sharp edges and also effectively removes noise. The selection of optimum parameters to perform anisotropic diffusion determine the quality of denoised images. Two crucial parameters for filtering are gradient threshold parameter (k) and number of iterations (itr). The number of iterations is chosen based on subjective evaluation whereas the gradient threshold parameter is determined by selecting knee point from the plot of k versus Peak Signal to Noise Ratio (PSNR). The filtered output is evaluated using PSNR and Mean Structural Similarity Index (MSSIM). The values obtained are PSNR of 39.74 dB and MSSIM of 0.9859 indicating the usefulness of anisotropic diffusion filtering.

Keywords— Thermography, breast cancer, anisotropic diffusion filter, PSNR, MSSIM

Introduction

In all of the world's female population, breast cancer is the most prevalent cancer type. It effects women majorly from low- and middle-income countries. Five-year survival rate of high-income country is 90% whereas for middle-income country it is 66% and for low-income country it is 40%. World Health Organization (WHO) has taken initiative to save 2.5 million lives over a period of 20 years by means of health promotion, timely diagnosis and comprehensive breast cancer management [1].

Breast cancer is due to aberrant cell proliferation in the breast region. It occurs due to numerous factors such as family history of breast cancer, genetic mutation, obesity, smoking, alcohol consumption or due to higher levels of certain hormones. Various symptoms for breast cancer include development of lump, changes in breast shape, dimpling of the skin and so on [2]. By the time any one of the above-mentioned symptoms are identified by the patient, the cancer would have reached stage II or stage III. Nowadays the existence of breast cancer is more in young women especially from the age of 35 [3]. Thus, in order to increase the survival rate, early identification of breast cancer becomes crucial. Mammogram is a gold standard modality that helps to identify suspicious

findings in the breast but has limitation in imaging dense breast tissues. Thermography is a new technique proven to identify breast cancer in its initial stages. It has an advantage over mammogram by identifying abnormalities in dense breast tissues. Thus, breast cancer can be detected in initial stages using thermography. Several authors have asserted usage of pre-processing as an initial task before segmentation or classification of breast thermal images. Fractional-order derivative filter was used to improve the texture and denoise the image [4], median filter was used to remove noise [5], Gaussian filtering was used for denoising and Contrast Limited Adaptive Histogram Equalization (CLAHE) was used to enhance the image [6], combination of Gaussian and bilateral filter was employed for denoising thermograms [7]. The objective of image denoising is to remove noise and at the same time preserve the edge information of the objects in an image. Anisotropic diffusion filter is one of the popularly used filter for denoising of thermograms but authors failed to mention the procedure for selection of filter parameters [8-9]. The anisotropic diffusion filter was applied for denoising images of different modalities such as mammogram, brain MRI, ultrasound, microscopic and nature images [10-13]. Thus, in the proposed method procedure for selection of anisotropic diffusion filter parameters is explored.

Methodology

Image Database

In the proposed work, the frontal thermograms from Database of Mastology Research (DMR) recorded using FLIR SC-620 IR camera are taken into account for analysis. These images are recorded using static protocol and has a spatial resolution of 640x480 pixels. In static thermal image acquisition, the patient has to rest for 10 minutes in order to achieve thermal stability inside the temperature-controlled environment. After the patient has rested, 5 images (1 frontal, 2 lateral images of left breast at 45° and 90° and 2 lateral images of right breast at 45° and 90°) were acquired [14].

Thermogram Preprocessing

The acquired thermal images are color images, hence color to gray scale conversion is performed. These images contain undesired regions such as thoracic, arms, waist region along with the complete breast region as depicted in Figure 1. Hence, for the acquired image of size $M \times N$, the image was roughly cropped such that the coordinates of the cropped image were $x1 = 10$; $x2 = N - 40$; $y1 = 76 M/4$; $y2 = M - 0.3 * M$ resulting in removal of certain undesired regions.

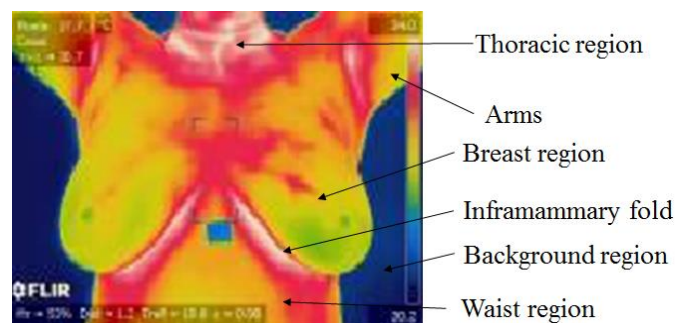


Figure 1. Breast thermogram with marked areas

Anisotropic Diffusion Filtering

The infrared cameras used in breast cancer detection are LWIR (Long Wave InfraRed) cameras with FPA (Focal Plane Array) uncooled microbolometers. The noise in IR images is not only determined by the detector but also by background and emissivity fluctuations of the object.

The major source of noise in infrared images is due to non-uniformity of FPA and read-out circuits of IR cameras [15].

The acquired breast thermal images are of low contrast and low Signal to Noise (S/N) ratio, hence denoising are carried out to enhance the image quality. Anisotropic Diffusion (AD) is a nonlinear filter utilizing diffusion approach that helps to reduce the noise and conserving the edges in an image. It reduces diffusion at strong image gradients (edges) and increases diffusion in other sections of the image. AD is represented by

$$f_t = \text{div}(c(x, y, t)\nabla f) = c(x, y, t)\Delta f + \nabla c \cdot \nabla f \quad (1)$$

where Δf is the gradient of an image f , div represents divergence, c is the conduction constant and ∇f is the Laplacian of an image f . The conduction constant is expressed as

$$c = \frac{1}{[1 + (\nabla f / \kappa)^2]} \quad (2)$$

where κ is a gradient threshold parameter that controls conduction as a function of gradient. Four nearest neighbour discretization of Laplacian operator is

$$f_{i,j}^{t+1} = f_{i,j}^t + \lambda [c_N \nabla_N f + c_S \nabla_S f + c_E \nabla_E f + c_W \nabla_W f]_{i,j}^t \quad (3)$$

Here, λ controls the speed of diffusion and takes value of 0.25; ∇ is the nearest neighbor difference in north (N), south (S), east (E) and west (W) direction [16].

AD filtering is implemented by computing the amount of differences ∇ in N, S, E and W directions, determining values of conduction in N, S, E and W directions using eq. 1, computing the diffused image using eq. 2 and repeating the above process for number of iterations (itr) times. The parameters κ and itr are important parameters that influence the quality of de-noised images. A low value of κ indicates that the diffusion process stops in early iterations yielding output image to be similar to input image whereas high values of κ over smoothens the image resulting in blurred image. Hence, optimum value of κ has to be selected. Initially, the set of images obtained by varying itr were subjected to subjective quality assessment followed by selection of optimum value of itr. For the obtained optimum number of iterations, κ value is varied from 5 to 100 in steps of 5 and the value of PSNR value was computed using the formulae

$$PSNR = 20 \log_{10} \left(\frac{255}{\sqrt{\frac{1}{M \times N} \sum_{i=1}^N \sum_{j=1}^M [f - f_t]^2}} \right) \quad (4)$$

Where f is the processed image and f_t is the filtered image. A graph has been plotted for κ versus PSNR and knee point is computed from the graph which determines the optimum value of κ . MSSIM is a quality measure that computes similarity between degraded and filtered image. MSSIM is computed to estimate the performance of the algorithm given by

$$MSSIM(f, f_t) = \frac{1}{MN} \sum_{i=1}^m \sum_{j=1}^n SSIM[f(i, j), f_t(i, j)] \quad (5)$$

$$SSIM = \frac{(2\mu_f\mu_{ft}+C_1)(2\sigma_f\sigma_{ft}+C_2)}{(\mu_f^2+\mu_{ft}^2+C_1)(\sigma_f^2+\sigma_{ft}^2+C_2)} \quad (6)$$

where, C_1 and C_2 are constants described as $C_1 = (M_1L)^2$ and $C_2 = (M_2L)^2$, M_1 and M_2 are constants taking value less than 1, L is the image's dynamic range, μ is the mean and σ is the SD [14]. In eq. 6, local statistics are calculated in 11x11 Gaussian window of standard deviation 1.5; with constants $M_1 = 0.01$, $M_2 = 0.03$ and dynamic range, $L = 255$ [17].

Results and Discussion

Figure 2(a) depicts the acquired frontal thermal breast image and Figure 2(b) depicts the corresponding gray scale converted image. It is perceived that various colors in the acquired image are represented in different shades of gray.

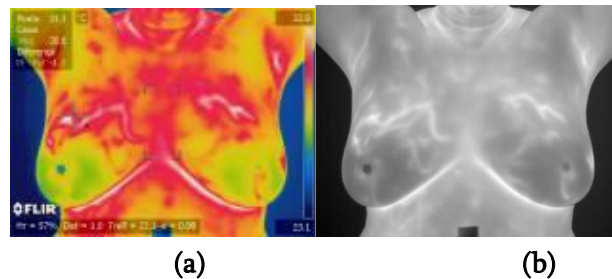


Figure 2. Breast thermogram (a) Color image (b) Gray scale image

To perform denoising of images, the parameters itr and κ have to be carefully selected. First the number of iterations is chosen by visualizing the results obtained for different values of itr . Figure 3(a) represents gray scale image, figure 3 (b)-(d) represents AD filtered images for $itr=5$, 15 and 100 respectively. We can perceive that for $itr=5$, the resultant filtered image is not completely free from noise, for $itr=100$ the filtered image is over smoothed and for $itr=15$, noise is removed and also edges are preserved. Hence $itr=15$ is employed in AD filter.

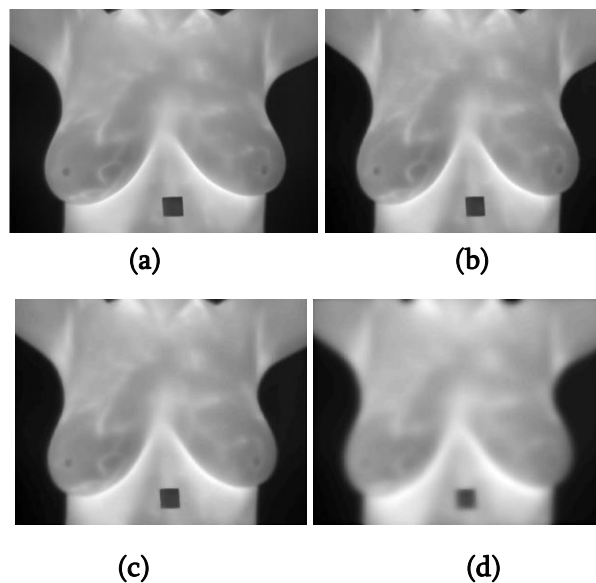


Figure 3. Selection of number of iterations (a) Gray scale image (b) AD filtered image ($itr=5$) (c) AD filtered image ($itr=15$) (d) AD filtered image ($itr=100$)

The value of parameter κ is determined by computing PSNR for κ varying from 5 to 100 in steps of 5 and the obtained results are represented as line plot in figure 4. Knee point is computed from the graph and the obtained knee point value is considered as the gradient threshold parameter. From the graph, the gradient threshold parameter obtained is $\kappa = 25$. Hence all the images considered in the dataset are filtered using *itr* as 15 and κ as 25.

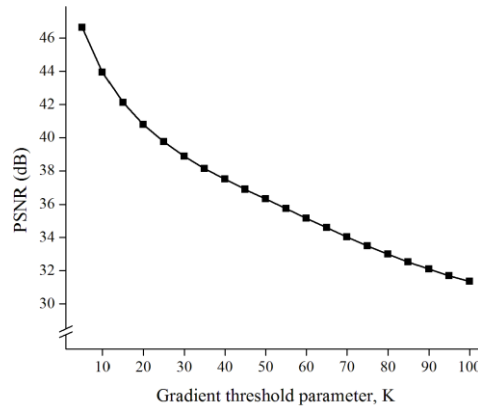


Figure 4. Line plot for determination of κ

Cropped image is shown in figure 5(a) wherein undesired regions are eliminated to some extent. AD filtered image employing the obtained optimal parameters is shown in figure 5(b) and from the obtained image we can observe that the image is smoothed as a result of noise removal and at the same time the edges are clearly visible.

The image quality assessment metrics obtained for de-noised thermograms are $PSNR_{avg}=39.74$ dB, $MSSIM_{avg}=0.9859$. The average value of PSNR above 30 dB represents good quality of de-noised image [18] and average MSSIM close to 1 indicates that the structural information is well retained [17].

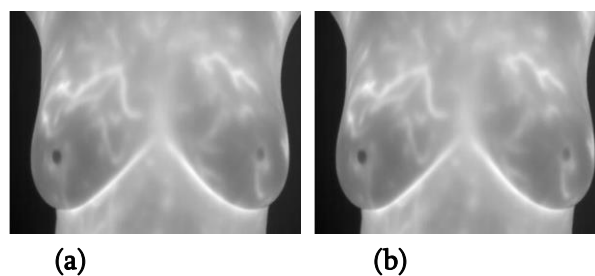


Figure 5. Breast thermogram (a) Cropped image (b) AD filtered image

Table 1 describes comparison of proposed work with other works employing images of different modalities. From the obtained results it is evident that the methodology employed for selection of filter parameters produced better results in terms of PSNR and comparable results in terms of MSSIM when compared to other methods applied on different categories of images.

TABLE 1. COMPARISON OF PROPOSED WORK WITH OTHER WORKS

Sl. No	Methodology	Category of images	Total number of images	PSNR (dB)	MSSIM
1	Enhanced anisotropic diffusion (EADF) based method for Unsharp masking and crispening of images [11]	MRI brain images	10	36.85	0.9921
2	Speckle reduction anisotropic diffusion filter [12]	Uterus ultrasound images	-	28.19	-
3	Anisotropic diffusion filtering [13]	Medical images (5), Satellite images (5), nature images (5) and microscopic images (5)	20	30.42	0.9079
4	Proposed work	Breast thermography images	70	39.74	0.9859

Conclusion

Breast cancer is a common cancer among women and when identified in early stages can save lives. Thermogram is a modality that aids in early detection of cancer. The acquired thermal images are corrupted by noise and are low contrast images. The images need to be processed prior to segmentation or classification. Anisotropic diffusion filter has capability of removing noise along with preserving edges and is hence the preferred type of filter. There are two key filter parameters, number of iterations, *itr* and global threshold parameter, κ that need to be optimally selected. *Itr* is determined by subjective evaluation whereas for κ , knee point is determined from the plot of κ vs PSNR. The above procedure is evaluated by calculating Mean Structural Similarity Index Measure (MSSIM) and the average value obtained is 0.9859 justifying the retainment of structural information in the image. Hence in order to diagnose breast cancer, Computer Aided Diagnosis (CAD) systems can employ the recommended method of parameter selection for an anisotropic diffusion filter.

References

- [1] <https://www.who.int/initiatives/global-breast-cancer-initiative>. [last accessed 5th July 2023]
- [2] <https://medicalnewstoday.com/articles/322832> [last accessed 5th July 2023]
- [3] C. A. Gabriel and S. M. Domchek, "Breast cancer in young women", *Breast Cancer Research*, vol. 12, no. 212, 2010. doi: 10.1186/bcr2647
- [4] R. Sharma, J. B. Sharma, R. Maheshwari and P. Agarwal, "Thermogram Adaptive Efficient Model for Breast Cancer Detection Using Fractional Derivative Mask and Hybrid Feature Set in the IoT Environment",

- Computer Modeling in Engineering & Sciences, Vol. 13, Issue 2, pp. 923-947, 2022. doi: 10.32604/cmcs.2022.016065
- [5] B. V. Solanki and N. Patel, "Thermographic imaging-based breast cancer diagnosis using deep learning", *International Journal of Current Science*, Vol. 13, No. 2, 2023, pp. 938-948. <https://www.ijcspub.org/download.php?file=IJCSP23B1115.pdf>
- [6] R. Gonzalez-Leal, M. Kurban, L.D. López-Sánchez, and F.J. Gonzalez, "Automatic breast cancer detection on breast thermograms", in *15th Quantitative InfraRed Thermography Conference*, Mexico, 2020. doi: 10.21611/qirt.2020.100
- [7] A. A. Edwin Raj, A. Sundaram and T. Jaya, "Advanced framework for effective denoising the enhanced thermal breast image", *IETE Journal of Research*, Vol. 69, No. 1, 2021, pp. 59-72. Doi: 10.1080/03772063.2021.1898481
- [8] Vijaya Madhavi and T. Christy Bobby, "Assessment of asymmetry in bilateral static frontal breast thermograms using difference image and radiomic features", *Biomedical Sciences Instrumentation*, Vol. 57, no. 2, pp. 256-263, 2021. doi: 10.34107/YHPN9422.04256
- [9] J. S. Jeyanathan and A. Shenbagavalli, "The Efficacy of Capturing Lateral View Breast Thermograms," *2019 IEEE International Conference on Clean Energy and Energy Efficient Electronics Circuit for Sustainable Development (INCCES)*, Krishnankoil, India, December 2019, pp. 1-4, doi: 10.1109/INCCES47820.2019.9167722.
- [10] Y. Gherghout, Y. Tlili and L. Souici, "Classification of breast mass in mammography using anisotropic diffusion filter by selecting and aggregating morphological and textural features", *Evolving systems*, Vol. 12, pp. 273-302, 2021. doi: 10.1007/s12530-019-09270-z
- [11] R. R. Kumar, A. Kumar and S. Srivastava, "Anisotropic diffusion based unsharp masking and crispening for denoising and enhancement of MRI images" in *2020 International Conference on Emerging Frontiers in Electrical and Electronic Technologies (ICEFEET)*, Patna, India, 10-11 July 2020, pp. 1-6, doi: 10.1109/ICEFEET49149.2020.9186966.
- [12] K. T. Dina and D. J. Hemanth, "Novel image enhancement approaches for despeckling in ultrasound images for fibroid detection in human uterus", *Open Computer science*, Vol. 11, pp.399-410, 2021. doi: 10.1515/comp-2020-0140.
- [13] S. S. Filwa and S. Nithya Selvakumari "Analysis and Comparison of Edge Preserving Filtering using Bilateral Filtering of Images with Gaussian Kernels and Anisotropic Diffusion Filtering", *European Chemical Bulletin*, Vol. 15, No. S1, pp. 3855-3867, 2023. <https://www.eurchembull.com/uploads/paper/01d5ccda8eb8f0008720818fc0c228ae.pdf>
- [14] L. F. Silva, D. C. M Saade, G. O. Sequeiros, A. C. Silva, A. C. Paiva, R. S. Bravo and A. Conci, "A New Database for Breast Research with Infrared Image", *J. Med. Imaging Health Inf.*, vol. 4, no. 1, pp. 92-100, 2014, doi:10.1166/jmihi.2014.1226.
- [15] [15] S. Budzan and R. Wyzgolik, "Remarks on noise removal in infrared images", *Measurement Automation Monitoring*, Vol. 61, No. 06, 2015. https://yadda.icm.edu.pl/baztech/element/bwmeta1.element.baztech-6a63485c-1dbe-4a00-83e2-4449e3e66210/c/Budzan_remarks_MAM_6_2015.pdf

- [16] P. Perona and J. Malik, "Scale-space and edge detection using anisotropic diffusion", *IEEE Trans. Pattern Anal. Mach. Intell.*, pp. 629- 639, July 1990. doi: 10.1109/34.56205
- [17] Z. Wang, A.C. Bovik, H.R. Sheikh and E.P. Simoncelli, "Image quality assessment: from error visibility to structural similarity", *IEEE Transactions on Image Processing*, vol. 13, no. 4, 2004, pp. 600-612. doi:10.1109/TIP.2003.819861.
- [18] M. Talha, G.B. Sulong and A. Jaffar, Preprocessing digital breast mammograms using adaptive weighted frost filter, *Biomedical Research*, vol. 27, no. 4, 2016, pp.1407-1412.

Sign Language Recognition System based on posture using Seer pipe

Radhamani R, Praveen Kumar K C

Department of ECE, East Point College of Engineering and Technology, Bangalore.

ABSTRACT

Sign language is a visual language that uses hand motions, changes in hand shape, and track information to convey meaning. It is the primary mode of communication for those with hearing and language impairments. The use of sign language for communication is limited, despite the fact that sign language recognition can help a large number of such persons deal with regular people. As a result, there is a need to create a more comfortable approach for people with hearing and language impairments to learn and work in order to improve their lives. Therefore, the basic idea behind this article is to make the communication between normal human beings and deaf people much easier. In order to recognize static postures associated with sign language alphabet and a few commonly used words, we conducted a comprehensive research study employing the hand tracking technique Seerpipe and a posture classification model based on Support Vector Machine (SVM). The results of the experiments are validated using Recall, F1 Score and Precision. Based on the validated results, we recommend the application of the discussed techniques for such communication. The suggested methods have high generalization qualities and deliver a classification accuracy of around 99 percent on 26 alphabet letters, numerical digits, and some regularly used words.

Keywords : Machine Learning, Seerpipe, SVM, Sign Language, Posture recognition, Assistive technology.

I. INTRODUCTION

Humans communicate with one another using natural language channels such as words and writing, or by body language (postures) such as hand motions, head postures, facial expression, lip motion, and so forth.

Comprehending sign language is equally as vital as understanding natural language [13]. People with hearing impairment use sign language as their preferred mode of communication. Without a translation, people with hearing impairments have difficulty speaking with other hearing people. As a result, implementing a system that understands sign language would have a substantial positive impact on the social lives of deaf people. According to the World Health Organization, 466 million individuals worldwide (more than 5 percent of the population) have impaired hearing, with 34 million of them being teens (WHO). According to studies, by 2050, these numbers will have surpassed 900 million. Furthermore, the majority of cases of profound hearing loss, which afflict millions of individuals, occur in low and middle-income nations [2]. Furthermore, the majority of cases of substantial hearing loss, which affects millions of individuals, occur in low- and middle-income nations.

There are more than 135 distinct sign languages spoken worldwide, including American Sign Language (ASL), British Sign Language (BSL), and Indian Sign Language (ISL) [15].

Machine learning enables the development of systems that accurately interpret sign language, which can greatly improve communication and social lives of deaf people. These technologies are particularly important for those living in low and middle-income nations where the majority of hearing impairments occur. The growing prevalence of hearing loss worldwide highlights the urgent need for technological solutions to help bridge the communication gap between hearing-impaired individuals and the rest of society. Machine learning is a branch of artificial intelligence that deals with the methods that let computers extract meaning from data and create AI applications. In the meanwhile, deep learning is a subset of machine learning that enables computers to resolve increasingly challenging issues [11]. As deep learning develops transferable answers, it is more powerful than traditional machine learning. Through neural networks, or layers of neurons/units, deep learning algorithms are able to produce transferable solutions [12]. Deep learning is a subset of machine learning where a computer program learns to carry out classification operations on complex input such as images, text, or sound. These algorithms are able to execute at a state-of-the-art (SOTA) level of accuracy and, in certain situations, even surpass humans. Numerous labeled data points and intricate neural network topologies are used to learn them. It is a vital part of modern innovations like self-driving cars, virtual assistants, and face recognition. In our research, we have thoroughly examined the existing literature on Sign language recognition. We will now focus on the most notable research papers and discuss their methods for feature extraction, image pre processing, and image classification, which employ a variety of algorithms including SVM, KNN, and CNN.

Additionally, we have examined several image- processing techniques, including Canny-edge detection, Convex-hull algorithm, and Gaussian blur filter, among others. A Microsoft Kinect camera was used to create a sign language recognition system in [6]. This was chosen to allow the whole programme to be independent of restrictions such as poor illumination, loud input, and so on. Depth and Motion were the two main feature capturing modules used in their methodology. In fact, a feature vector was calculated for each frame of the video series, and some pre processing was applied to each frame to eliminate undesired noise and provide a clean image of the depth map. They used the Gaussian blur filter 15 and the Erosion filter to do this and also presented the depth information using a 256-bin histogram for a depth image. They were able to create the feature matrix for that particular video sequence or posture using the combined array of feature vectors from all of the frames in the video sequence. Following this pre-processing, the feature matrix was given as an input to a multi-class SVM classifier to construct an appropriate Machine Learning model for classification of the test files using kernel functions, with the linear and RBF kernels being specifically employed. The total accuracy achieved was between 81.48 and 87.67 percent. However, this work was unable to investigate other high-level characteristics such as optical flow information, motion gradient information, and so on, which may have improved accuracy performance. A more precise real-time Hand Posture Recognition (HGR) system based on American Sign Language is the primary goal of [8], which is to illustrate (ASL). The combination of K-curvature and convex hull approaches is proposed as a novel feature extraction technique. This method, known as the "K Convex Hull" technique, can recognize fingers with extreme precision. An ANN is used in this system together with feed forward and reverse propagation techniques to train a network with 30 feature vectors to accurately identify 37 indications of American alphanumeric letters, which is beneficial for HCI applications. The entire posture recognition rate of this system in a real-time scenario is 94.32 percent. [19] reviews and compares

several algorithms and techniques for creating single hand posture detection systems utilizing various vision-based methodologies. The research uses the hand's fundamental structure as well as properties like centroid to identify the pattern the fingers and thumb generate and assign code bits, i.e., changing each posture into a set of 5 digits representation. Motion is recognized using centroid movement in each frame. The study uses techniques like K-means clustering or thresholding for background removal, Convex Hull or a custom peak identification algorithm, and text to voice API to translate posture-related words and phrases into speech. The Convex Hull algorithm is used to identify the smallest convex polygon that contains every point from the frame.

II. Dataset

In this work, we have utilized the ASL dataset [20] consisting of 51 classes, with approximately 4000 images per class. The classes comprise the alphabet, numbers, and commonly used words such as 'Hello', 'Help', and 'Stop'. The alphabet class enables the formation of new words through fingerspelling, where individual letters are used to represent words without a designated sign symbol. A Python script was employed to efficiently convert the image class folders into a .csv file, which stores the (x, y, z) coordinates of all landmark points of each sign with their respective outputs. An 80:20 train-test split was implemented to improve the model's feature extraction process.



Fig1: Various Sign symbols

III. Seerpipeline

Sign language recognition has the potential to improve the situation of a large number of disabled people while dealing with normal human beings but the use of sign language for communication is limited. As a result, there is a need to create a more convenient approach for persons with hearing impairments to learn and work in order to improve their lives. Posture recognition has been studied extensively utilizing traditional techniques such as body component tracking, different color glove-based tracking, Kinect depth sensor tracking, and skeleton tracking. Multiple methods have been used to solve this problem like modified CNN, image segmentation, SVM and deep

learning. Many machine learning algorithms have been developed for hand posture recognition so as to create AI-based applications. Out of them, Seerpipe can be used for hand posture recognition. Google supported Seerpipe framework can be used for solving several problems like face-recognition, face-map, eye, hand, poseestimator, holistic, hair, object-detection, box tracking and KIFT. With the help of the Seerpipe framework, we can develop an algorithm or model for the application, then help the application by providing results that can be cloned across different platforms. The Seerpipe framework is composed of three major components: (1) performance evaluation, (2) a mechanism for collecting data from the sensor (3) an assembly of reusable parts. A graph consisting of all the parts called the calculators is known as pipeline, wherein every calculator is interconnected by channels through which the data flows. Developers can create their required application by removing or delineating

user defined calculators anywhere in the graph. This result of calculators and channels creates a data-flow diagram.

Hand posture recognition with the Seerpipe framework is a dependable and high-fidelity hand and finger tracking system. Seerpipe hands uses an integrated ML pipe of several models working together [18]: (1) A palm recognizer processes the captured hand image, (2) A hand landmark model takes processed image as input and returns hand with 3D key points as output. (3) A posture recognition model which processes the 3D hand key-points and classifies them into a discrete set of postures.

The palm detection model outputs a precisely cropped picture of the palm that is then sent to the landmark model. This method does away with data augmentation, which is used in deep learning models [5] to rotate, flip, and scale images. The technique of detecting hands is time-consuming and difficult since it involves working with different hand sizes, thresholding, and image processing. Prior to identifying hands with connected fingers, a palm detector is trained, which estimates bounding boxes around hard objects like fists and the palm. The second method is to utilize an encoder-decoder as an extractor for a larger scene context [14].

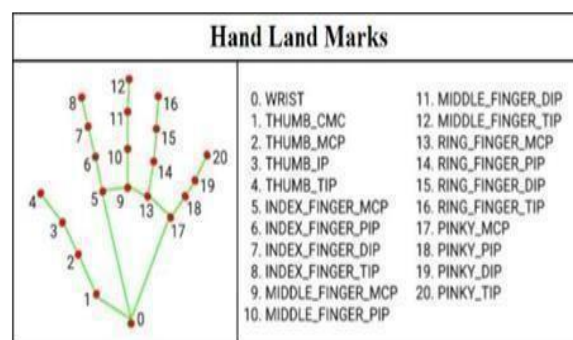


Fig2: Hand Landmark

Hand-knuckles of the landmark have x, y, and z coordinates where x and y are normalized to [0, 1] as width and height of the image, while z represents the depth of the landmark. The closer the landmark to the camera, the value of z becomes smaller.

IV. Experimentation

In order to achieve our desired objective, we have created an end-to-end web application that allows real-time communication between common people and deaf people without any use of hardware technologies like sensors, microcontrollers, etc. This website makes user interaction comfortable as it consists of combined

application of Sign to Text and Text to Sign conversion, along with other essential features. To create this application, we have made use of multiple technologies and frameworks. HTML, CSS and JavaScript tools are used for Frontend and Flask (a Python web framework) is used for Backend. In Backend, the machine learning model is loaded in the form of a pickle (.pkl) file. This .pkl file allows easy serialization and deserialization of any ML model.

The functionality of our website is that it takes the webcam video as the input which captures our hand image. Later, Seerpipe technique is applied to this extracted image and key points are marked accordingly which then stores the (x, y, z) coordinates of the landmarks. Last but not least, this data is sent into the Support Vector Machine classifier, a supervised machine learning classifier (SVM). Regression and classification studies both use the SVM model. Finding the most important dividing line is done using it. The primary objective of this approach is to identify the best hyperplane for dividing and separating training vectors. Using gamma as the RBF parameter, SVC is an SVM classifier (Radial basis function kernel). To determine if a model is overfitting, underfitting, or providing the optimum fit, one uses the gamma value. The pickle (.pkl) module was utilized to load the two files, X and y, which are data files used for training the SVM model. The X file contains a list of image pixels, while the Y file contains labels for the list of pixels. After loading the dataset, it is passed to the model for training purposes.

The SVM model is represented by the equation:

$$f(x) = \text{sign}(\text{sum}(\alpha_i * y_i * \exp(-\text{gamma} * \|x_i - x\|^2)) + b) \quad \dots\dots\dots (1)$$

where α_i are the Lagrange multipliers, y_i are the corresponding labels, $\exp(-\text{gamma} * \|x_i - x\|^2)$ is the RBF kernel function, x represents the input feature vector, and b is the bias term. The hyperparameters C and gamma are typically determined through a grid search or cross-validation process. Once the model is trained, the webcam images are passed to the model for testing. The model recognizes the corresponding letter/word and outputs it on the screen.

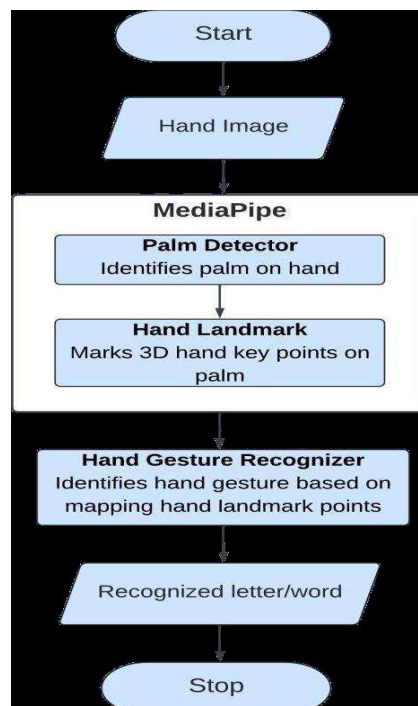


Fig3: Methodology

V. Results

Various machine learning models are used for sign detection. These models are evaluated based on parameters like accuracy, recall, F1 score, etc. Among the utilized models, it is observed that SVM outperformed other machine learning techniques such as Naive Bayes, KNN, Decision Tree, etc. by achieving an accuracy of 98.65% (training) and 98.35% (testing) as shown in table 0. The reason it outperformed is because of its effectiveness in high- dimensional spaces where it draws a hyperplane boundary in order to classify the labels. The below table shows the values of training and testing accuracy along with Recall, F1Score and Precision for different tried models:

The below confusion matrix for SVM algorithm prints the correct and incorrect values in number count which gives us a good data visualization.

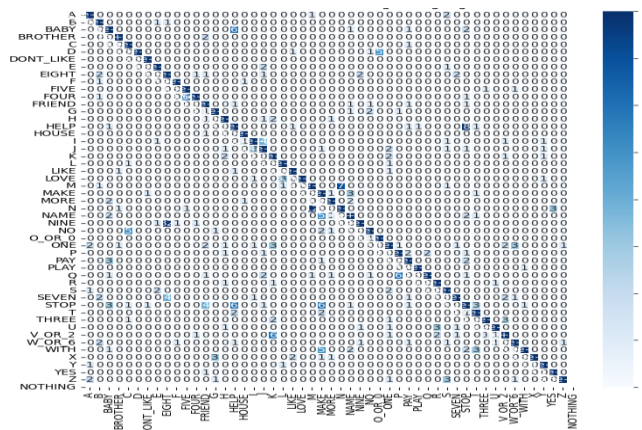


Fig4: Confusion Matrix for SVM Model

The output images captured for some of the real time inputs are shown below:



Fig5: Output 5 and L

Results obtained in [12] and [5] are less accurate due to the use of ineffective feature extraction approaches and inappropriate models. Despite using the same dataset, accuracy mentioned in [22] is around 94.88%. Additionally, some of the research papers have attained an accuracy of about 99%, however these articles employ a small dataset with a small number of classes. Our machine learning approach is suitable for use in mobile applications since the learned model is deliberately light. Our methodology’s real-time sign language identification makes it quick, reliable, and especially flexible for smart devices. Seerpipe makes feature extraction simple by deconstructing and analyzing challenging hand-tracking data. This strategy uses less computer resources and takes less time to train the model than other cutting-edge approaches.

This table compares the effectiveness of different preprocessing techniques and algorithms on our dataset and simpler datasets. It includes the preprocessing technique and algorithm used, along with the training accuracy and validation/test accuracy achieved by each technique. As shown in table 1, several preprocessing techniques were tested, including convex hull, Gaussian blur, and Canny edge detection. The algorithms used included CNN, VGG, ResNet, and EfficientNet. After analyzing the results from the experiments using the techniques and algorithms presented in the above table, we found that they did not yield satisfactory performance on our dataset. Therefore, we decided to discard these techniques and algorithms and explore other approaches to achieve better results.

Table 1 : Comparative Analysis of Accuracy for Various Models and Preprocessing Techniques with Simpler Datasets

Preprocessing & Algorithm	Training Accuracy	Validation/ Test Accuracy
Convex Hull + CNN	99.54%	91%
Gaussian Blur + CNN	89.8%	91%
Gaussian Blur + VGG	84.66%	84.92%
Canny Edge Detection + VGG	93.71%	93.69%
Convex Hull + ResNet	94.03%	91.98%
Convex Hull + EfficientNet	90.68%	90%

Table 2 : Performance Comparison with Similar Techniques

Type of Dataset	Our Accuracy	Existing/Others Accuracy
Alphabets only	99.43%	99.15% [7]
Alphabets, Numbers, and Words	98.975%	98.62% [7]

Based on our analysis, we could improve the accuracy of the model by adjusting the parameters. The improvement in accuracy was found to be around 0.28% to 0.35%. Our experiments also revealed that the model tends to overfit at higher values of C, and the choice boundary's curvature weight decreases with lower values of gamma. As a result, the areas separating different classes become more generic. After tuning the parameters, we were able to identify the optimal decision boundary for our dataset at C = 52 and gamma = 0.6.

VI. CONCLUSION

Individuals with hearing disabilities often face significant challenges in communicating with people who can hear. One of the most effective ways for them to communicate is through sign language. However, for people who do not know sign language, understanding what is being communicated can be a significant challenge.

This communication gap can have a detrimental impact on the social and emotional well-being of individuals with hearing disabilities, making it difficult for them to engage fully in society.

The proposed Sign Language Recognition system offers an innovative solution to the communication gap between individuals with hearing disabilities and those who can hear. The proposed system successfully recognizes sign language with high accuracy, with an SVM model achieving a classification accuracy of 98.975%. Moreover, the use of Google's Seerpipe palm detector method has made the system accessible to people without any special hardware, which is a significant advantage.

The proposed method's potential for practical applications is considerable, and it has the capacity to improve the quality of life for individuals with hearing disabilities, helping to bridge the communication gap between them and the rest of the world. Future work will expand the current system to add more indicators and create complete and reliable system for mobile platforms. Additionally, the proposed method can be adapted for use in other Indian regional languages, such as Hindi, Kannada, Malayalam, Telugu, and more.

Although there are still some research gaps that need to be addressed, such as improving the system's accuracy in recognizing signs for complex phrases and developing a portable and affordable device for practical use in daily life, the proposed Sign Language Recognition system offers a promising step towards creating a more inclusive society. With further development and refinement, this system can play a significant role in breaking down communication barriers and facilitating greater accessibility and understanding for individuals with hearing disabilities.

REFERENCES

- [1] Akoum, Alhussain, and Nour Al Mawla. "Hand gesture recognition approach for ASL language using hand extraction algorithm." *Journal of Software Engineering and Applications* 8.08 (2015): 419.
- [2] Bandgar, Bapurao. "Implementation of Image Processing Tools for Real-Time Applications." *International Journal of Engineering Research & Technology (IJERT)* 10.07 (2021).
- [3] Bazarevsky, Valentin, and G R Fan Zhang. "On-Device MediaPipe for Real-Time Hand Tracking." (2019).
- [4] Brahmankar, Vipul, et al. "Indian Sign Language Recognition Using Canny Edge Detection." *International Journal* 10.3 (2021).
- [5] Das, P., T. Ahmed, and M. F. Ali. "Static Hand Gesture Recognition for American Sign Language Using Deep Convolutional Neural Network." *2020 IEEE Region 10 Symposium (TENSYP)* (2020): 1762-1765.
- [6] Devineau, G., F. Moutarde, W. Xi, and J. Yang. "Deep Learning for Hand Gesture Recognition on Skeletal Data." *2018 13th IEEE International Conference on Automatic Face & Gesture Recognition (FG 2018)* (2018): 106-113.
- [7] Halder, Arpita, and Akshit Tayade. "Real-Time Vernacular Sign Language Recognition Using MediaPipe and Machine Learning." *International Journal of Recent Technology and Engineering (IJRTE)* 10.2 (2021): 7421.
- [8] Islam, M. M., S. Siddiqua, and J. Afnan. "Real-Time Hand Gesture Recognition Using Different Algorithms Based on American Sign Language." *2017 IEEE International Conference on Imaging, Vision & Pattern Recognition (icIVPR)* (2017): 1-6.
- [9] Jin, C. M., Z. Omar, and M. H. Jaward. "A Mobile Application of American Sign Language Translation via Image Processing Algorithms." *2016 IEEE Region 10 Symposium (TENSYP)* (2016): 104-109.
- [10] Khan, Rafiqul Zaman, and Noor Adnan Ibraheem. "Hand Gesture Recognition: A Literature Review." *International Journal of Artificial Intelligence & Applications* 3.4 (2012): 161.

- [11] Li, Y., X. Wang, W. Liu, and B. Feng. "Pose Anchor: A Single-Stage Hand Key Point Detection Network." *IEEE Transactions on Circuits and Systems for Video Technology* 30.7 (2020): 2104-2113.
- [12] Martinez-Martin, Ester, and Francisco Morillas-Espejo. "Deep Learning Techniques for Spanish Sign Language Interpretation." *Computational Intelligence and Neuroscience* 2021 (2021).
- [13] Pal, D. H., and S. M. Kakade. "Dynamic Hand Gesture Recognition Using Kinect Sensor." 2016 *International Conference on Global Trends in Signal Processing, Information Computing and Communication (ICGTSPICCC)* (2016): 448-453.
- [14] Raheja, J. L., Anand Mishra, and Ankit Chaudhary. "Indian Sign Language Recognition Using SVM." *Pattern Recognition and Image Analysis* 26.2 (2016): 434-441.
- [15]. Shriram, S., Nagaraj, B., Jaya, J., Shankar, S., & Ajay, P. (2021). Deep Learning Based Real-Time AI Virtual Mouse System Using Computer Vision to Avoid COVID-19 Spread. *Journal of Healthcare Engineering*, 2021, 8133076.
- [16]. Singha, J., & Das, K. (2013). Hand gesture recognition based on Karhunen-Loeve transform. *arXiv preprint arXiv:1306.2599*.
- [17]. Trigueiros, P., Ribeiro, F., & Reis, L. P. (2012). A comparison of machine learning algorithms applied to hand gesture recognition. In *7th Iberian Conference on Information Systems and Technologies (CISTI 2012)* (pp. 1-6).
- [18]. Zhang, F., Bazarevsky, V., Vakunov, A., Tkachenka, A., Sung, G., Chang, C. L., & Grundmann, M. (2020). *MediaPipe Hands: On-device Real-time Hand Tracking*. *arXiv preprint arXiv:2006.10214*.
- [19]. Zivkovic, Z., & Van Der Heijden, F. (2006). Efficient adaptive density estimation per image pixel for the task of background subtraction. *Pattern recognition letters*, 27(7), 773-780.
- [20]. <https://www.kaggle.com/datasets/belalelwikel/asl-and-some-words?select=ASL>.
- [21]. <https://google.github.io/mediapipe/solutions/hands.html>.
- [22]. <https://www.kaggle.com/code/vaishnaviasonawane/asl-recognition-model-training-revisited>.

Energy Conservation through Energy Audit in LT2 Consumers

Avinash B C, Kiran Kumar Kommu, Rajesh K

Assistant Professor, Department of Electronics & Communication Engineering, East Point College of Engineering and Technology Bengaluru

ABSTRACT

Electricity bill or consumption rate is growing at exponential rate in Low Tension i.e 230V ,1 phase consumers because of various reasons like modern life style, inductive loading, improper knowledge of consumption.

Energy audit in LT-2 consumers gives scope of setting benchmark of consuming around 100 units kwh energy or reduction of around 20 percent of kWH consumption, low cast and safe compensation of reactive power KVAR through pf capacitor at consumer premises without affecting comfort and security of the consumer and also we emphasis on right use of illumination as the standard level and maintenance factor.

Keywords— KWH, KVAR, energy audit, illumination, maintenance factor, pf capacitor.

I. INTRODUCTION

Energy Audit is an inspection, survey and analysis of energy flows for energy conservation in a building or system to reduce the amount of energy input to the system without negatively affecting the output..

As per the Energy Conservation Act, 2001, Energy Audit is defined as “the verification, monitoring and analysis of use of energy including submission of technical report containing recommendations for improving energy efficiency with cost benefit analysis and an action plan to reduce energy consumption”.

It is an effective and concrete method to achieve rapid improvement in energy efficiency in buildings and industrial process First step in identifying opportunities to reduce energy expense. Which is a Systematic procedu.re includes some steps. Energy auditing is also called as Energy assessment, Energy survey etc...

The objectives are production & quality

- To minimize energy costs / waste without affecting
- To minimize environmental effects.

The primary objective of Energy Audit is to determine ways to reduce energy consumption per unit of product output or to lower operating costs. Energy Audit provides a “bench-mark” for managing energy in the organization and also provides the basis for planning a more effective use of energy throughout the organization.

Statistical review of world energy

Focus/Methodology : Percentage increase in power consumption and carbon emission in India

Published : August 8,2020

Conclusion : Indian Power Consumption Growth rate per annum:

- From the year 2008-18 – 5.2%
- From the year 2019 - 2.3%
- Power share on year 2019 – 5.8%

Carbon dioxide emission in India , Growth rate per annum:

- From the year 2008-18 – 5.3%
- From the year 2019 - 1.1%
- Share on the year 2019 – 7.3%

The lighting hand book Focus/Methodology : lighting technology Published : August 8,2013

Conclusion : Basic parameters used in lighting:

Luminous flux- Luminous intensity – Illuminance –Luminance Quality Characteristics of Lighting: Glare – glare limitation

1. Direct glare 2. Reflected glare

I. cause

-Luminaries without glare control -Reflective surfaces

-Very bright surface -Incorrect luminaire arrangement

-Incorrect workstation position

II. Effect

-Loss of concentration-More frequent mistakes -Fatigue

III. Remedy

-Luminaires with limited -Matching luminaire to luminance level workstation (layout)

-Blinds on windows -Indirect lighting

-Matt surface

Preliminary Energy Audit Flowchart

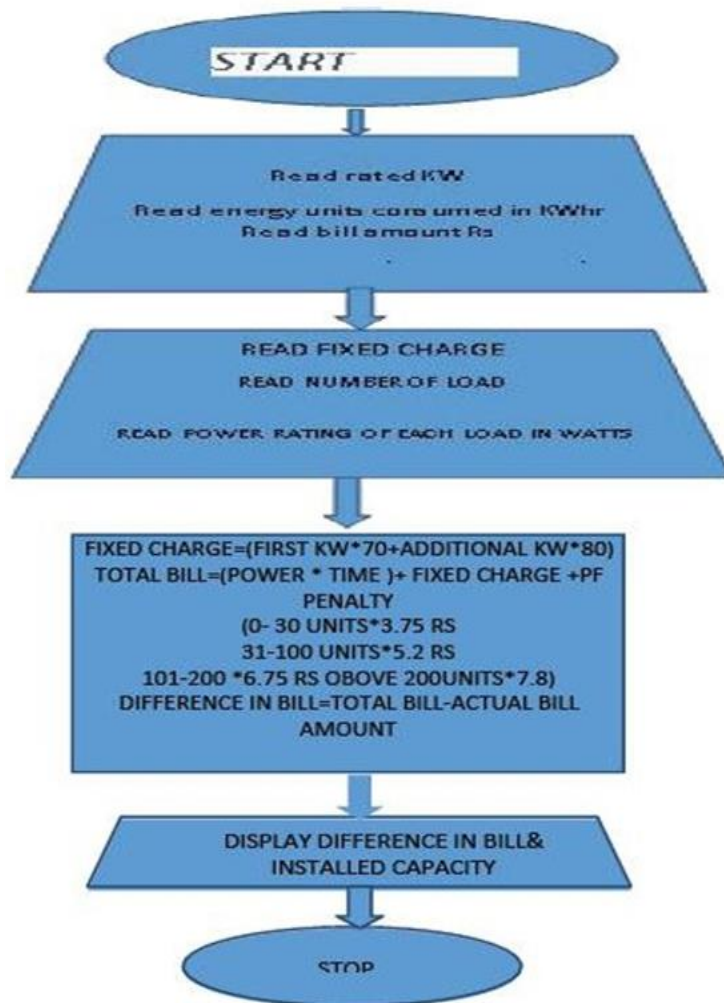
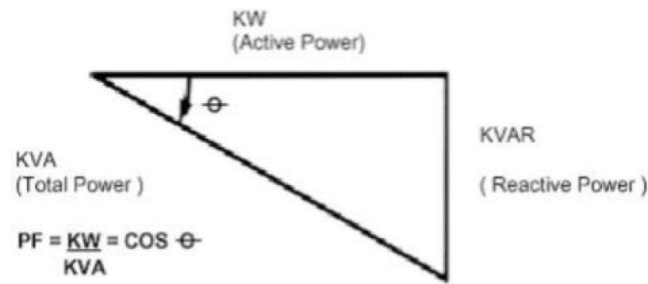


Fig 1: preliminary audit calculation

POWER FACTOR CALCULATION In all industrial electrical distribution systems, the major loads are resistive and inductive. Resistive loads are incandescent lighting and resistance heating. In case of pure resistive loads, the voltage (V), current (I), resistance (R) relations are linearly related, i.e. $V = I \times R$ and Power (kW) = $V \times I$

Typical inductive loads are A.C. Motors, induction furnaces, transformers and ballast type lighting. Inductive loads require two kinds of power: a) active (or working) power to perform the work a b) reactive power to create and maintain electromagnetic fields. Active power is measured in kW (Kilo Watts). Reactive power is measured in KVAR (Kilo Volt- Amperes Reactive). The vector sum of the active power and reactive power make up the total (or apparent) power used.

This is the power generated by the SEBs for the user to perform a given amount of work. Total Power is measured in KVA (Kilo Volts-Amperes) Managers and Energy Auditors conducted by Bureau of Energy Efficiency, Government of India.

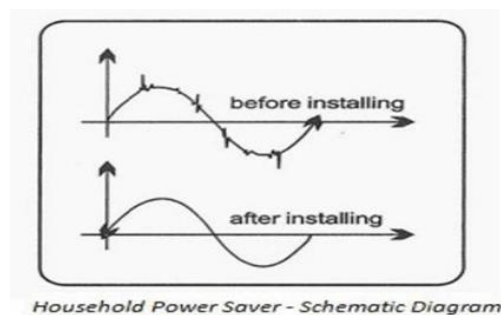


The active power (shaft power required or true power required) in kW and the reactive power required (KVAR) are 90° apart vertically in a pure inductive circuit i.e., reactive power KVAR lagging the active KW. The vector sum of the two is called the apparent power or KVA, as illustrated above and the KVA reflects the actual electrical load on distribution system.

SCOPE OF PROJECT

It is known that the electricity that comes to our homes is not stable in nature. There are many fluctuations, raise and falls, and surges/spikes in this current. This unstable current cannot be used by any of the household appliances. Moreover, the fluctuating current wastes the electric current from the circuit by converting electrical energy into heat energy. This heat energy not only gets wasted to the atmosphere, but also harms the appliances and wiring circuit.

Power Saver stores the electricity inside of it using a system of capacitors and they release it in a smoother way to normal without the spikes.



1) Cost Saving (Improve the P.F)

Reactive power control can regulate the voltage. But installation of reactive power equipment required investment.

Consider a simple two-part tariff given by,

$$T = x \cdot KVA + y \cdot kWh$$

here x is charge for KVA, y is charge for kwh.

Let us draw an active power P_1 at a power factor $\cos \phi_1$

the KVA is $P_1 / (\cos \phi_1)$

If now the power factor is improved to $\cos \phi_2$ the new KVA is $P_1 / (\cos \phi_2)$

The saving in cost is $x[(P_1 / \cos \phi_1) - (P_1 / \cos \phi_2)]$

The reactive power required to change the power factor is $[P_1 \tan \Phi_1 - P_1 \tan \Phi_2] (\text{KVAR})$

If the cost of installation is Rs C/(KVAR) Then total cost of installation is

$CP_1 [\tan \Phi_1 - \tan \Phi_2]$ hence the net saving is given by $\text{Saving} = x P_1 [(1/\cos \Phi_1) - (1/\cos \Phi_2)] - CP_1 [\tan \Phi_1 - \tan \Phi_2]$ Rs

Maximum saving is obtained when $d[\text{saving}]/(d\Phi_2) = 0$

or $\sin \Phi_2 = C/x$

2) INSTRUMENTS USED IN THE ENERGY AUDIT

- Lux Meters
- CLAMP on METER
- ENERGY METER 1 phase and 3

DETAILED ENERGY AUDIT ANALYSIS

3) Data collected from domestic load 1

CONCLUSION

From above analysis, energy conservation through energy audit has shown tremendous improved results. During lighting audit, the main objective is to improve the lighting efficiency without affecting the productivity and visual comfort. For improvement of lighting efficiency we have improve luminous efficiency and for greater luminous efficiency LED is the best option. For energy conservation we replace old luminaries with new efficient LED lamps and by replacing luminaries we can save the energy up to 3.536kW. By replacing old luminaries

we can reduce lighting load by 40.47%. For that we have invest Rs.2,30,740 and from that we can save Rs.12237.39 per month. Payback period for this investment is 18 months

i.e. 1 year 6 months. Also during load management audit, we calculated that how much and what type of load is available in industry, and duration of working hours for one day and one month. Also calculate load curve of one day which defines how energy is used in industry. Load curve

also shows peak load hours are at 9am to 1pm and non-peak load hours is at 11pm to 6am.

Electric load management helps to reduce unnecessary load, also separate metering helps to evaluate production cost.

DATA COLLECTION

Consumer Type	Sl.No	Light Load	Power Rating	Actual Power Consumption	Time of Consumption in hr	Illuminance in Lux (without msc)	Illuminance in Lux (with msc)	Power Factor	HVAC Load	Power Rating	Time of Consumption in hr	Power Factor
LT2(1)	1	LED Lamp	40	38.9	4	98	105	0.7	1	Ceiling fan	4	0.9
Allotted KW	2	Incandescent	60	62	1	49	53	0.94	2	Ceiling fan	6	0.91
0.48kw	3	LED	40	39	1	96	103	0.7	3	Ceiling fan	7	0.9
Unit Consumed	4	Incandescent	60	61	1	46	51	0.93	4	Water Heater	1/2	0.95
108	5	LED	9	7	0	42	51	0.7	5	Television	9	0.7
	6	LED	40	39	2	99	105	0.71	6	Refrigerator	24	0.6
	7	LED	9	14	1	47	54	0.71	7	Sump pump	5	0.86
	8	LED	18	21	2	72	79	0.68				
	9	CFL	12	16	2	43	47	0.84				



Fig.-2. Audit data collection

Billing Before and After Implementation

Fig: Glimpse of electricity bill before and after energy audit

Result

Load curve

also shows peak load hours are at 9am to 1pm and non-peak load hours is at 11pm to 6am.

Electric load management helps to reduce unnecessary load, also separate metering helps to evaluate production cost.



Illumination level before and after maintenance



Reference

- [1] Bureau of energy efficiency guide books, book 1, chapter 03 "Energy Management and Audit", page no. 54-78.
- [2] Sandip Ballal, "Energy Performance Important and Energy Cost Reductions at Baltic Place Commercial Office Complex", thesis published in STAFFORDSHIRE University, February 2016, page no.1- 64.
- [3] Rakiba Rayhana, "Electric and Lighting Energy Audit: A Case Study of Selective Commercial Buildings in Dhaka", 2015 IEEE international WIE conference on 20 December 2015, page no 1-4.

- [4] Barney L. Capehart, "Guide to Energy Management", Book published by The Fairmont Press, Inc 2003, Chapter no 5.
- [5] Rajesh Tilwani, "Energy saving potentials in building through energy audit – A case study in an Indian building", published in 2015 IEEE International Conference on Technological Advancement in Power & Energy, June 2015 page no 289-293.
- [6] Sonal Desai, "Handbook of Energy Audit", Book published by McGraw Hill (India) Private Limited, 2015, chapter 1 & 2.
- [7] Shailesh K. R., "Energy consumption optimization in classrooms using lighting energy audit", Research and technology in coming decades (CRT 2013), IEEE National Conference, 27-28 Sept. 2013, page no.1-5.
- [8] Muhammad Usman Khalid, "Energy Conservation through Lighting Audit", 2012 IEEE International Conference on Power and Energy, 2-5 December 2012, page no.840-845.
- [9] G. Paris, "Combined electric light and day light systems Ecodesign", IEEE Industry Applications Society Annual Meeting (IAS), 2011, page no. 1-5.
- [10] Jian Zhang, "How to Reduce Energy Consumption by Energy Audits and Energy Management: The Case of Province Jilin in China", Technology Management in the Energy Smart World (PICMET), 2011 Proceedings of PICMET '11, September 2011, page no. 1-5.
- [11] J. A. Qureshi, et al., "Demand Side Management through innovative load control" in TENCON 2010 - 2010 IEEE Region 10 Conference, 2010, page no. 580-585.

Machine Learning based Agriculture Bot

Dr. Pradeep Kumar N S¹, Mr Suhas S K², Dr. Girish H³, Mr B C Divakara³, Mrs.K Revathi³, Mrs. Swetha C S³

¹Professor, Department of ECE, SEACET, Bengaluru, India

²Associate Professor, Department of ECE, Cambridge Institute of Technology, Bengaluru, India

³Assistant Professor, Department of ECE, SEACET, Bengaluru, India

ABSTRACT

Diseases on plants cause significant damage and economic losses in crops. Subsequently, reduces the diseases on plant by early diagnosis results in substantial improvement in quality of the product. Incorrect diagnosis of disease and its severity leads to inappropriate use of pesticides. The goal of proposed system is to diagnose the disease by using image processing and artificial intelligence techniques on images of plant leaf. This system is divided into two phases, in first phase the plant is recognized on the basis of the features of leaf, it includes preprocessing of leaf images, and feature extraction followed by ANN based training and also classification for recognition of leaf. In second phase the classification of disease which is present in the leaf is done, this process includes K- Means based segmentation of defected area, feature removal of defected portion and the ANN based classification of disease.

Keywords : Artificial Neural Networks (ANN), Conventional Neural Networks (CNN), Artificial Intelligence (AI).

I. INTRODUCTION

In Agriculture sector plants or crop cultivation have seen fast development in both the quality and quantity of food production, however, the presence of destructive insects and diseases on crops especially on leaves has hindered the quality of agricultural goods. If the presence of pests on crops and leaves is not checked properly and the timely solution is not provided then the quality and quantity of food production will be reduced, which results in upsurge in poverty, food insecurity and the mortality rate . This severe effect can disturb any nation's economy especially of those where 70% of the inhabitants rely on the products from the agricultural sector for their livelihood and endurance. One of the major problems for agriculturists is to lessen or eradicate the growth of pests affecting crop yields. A pest is an organism that spreads disease, causes damage or is a nuisance.

The most frequent pests that affect plants are aphids, fungus, gnats, flies, trips, slugs, snails, mites and Caterpillars. Pests lead to sporadic outbreaks of diseases, which lead to famine and food shortage. According to H. Al-Hiary et al in most of the countries farmers are used to detect pests manually through their observation of naked eyes, which requires continuous monitoring of the crop stem and leaves, which is a difficult labor intensive, inaccurate and expensive task for large farms. Further the early detection of diseases

on plants is really required as a very small number of diseased leaves can spread the infection to the whole batch of fruits and vegetables and thus affects further storage and sales of agriculture products. This effect of plant diseases are very destructive as a lot of farmers were discouraged to the point where some decided to give up the work of crop cultivation. There is therefore a need to identify these diseases at an early or superior stage and suggest solutions so that maximum harms can be avoided to increase crop yields. The applications like plant recognition, crop yield estimation, soil quality estimation etc. With the existence of massive volume of plant species and their use in various fields, the quality of agricultural products has become a major issue in agriculture sector.

Image processing technique such as machine vision system has been proven to be an effective automated technique. Image processing based artificially intelligent computer vision techniques can reduce the computational time and as a result, the automated leaf disease detection can be made much faster.

In future, the farmer can obtain a consolidated view of the farm along with decision support statistics for planning purposes. In the field of agriculture digital image processing techniques have been established as an effective means for analyzing purposes in various agricultural applications like plant recognition, crop yield estimation, soil quality estimation etc.

The problem of efficient plant disease protection is closely related to the problems of sustainable agriculture and climate change In India, Farmers have a great diversity of crops. Various pathogens are present in the environment which severely affects the crops and the soil in which the plant is planted, thereby affecting the production of crops .Various disease are observed on the plants and crops .The main identification of the affected plant or crop are its leaves. The various colored spots and patterns on the leaf are very useful in detecting the disease. The past scenario for plant disease detection involved direct eye observation, remembering the particular set of disease as per the climate, season etc. These methods were indeed inaccurate and very time consuming.



Fig 1: AGROBOT

II. LITERATURE SURVEY

The Design of General Purpose Autonomous Agricultural Mobile-Robot:

“AGROBOT” Halil Durmuş Burak Berk Üstündağ in 2015, Purpose of this work is to increase the production efficiency in agricultural field by developing a mobile autonomous robot which has the capability of processing and monitoring field operations like spraying remedies for precision farming, fertilization, disease diagnosis, yield analysis, soil analysis and other agricultural activities.

A Low Power IoT Network for Smart irrigation:

Soumil Heble, Ajay Kumar, et al. in 2018, `proposed a low- power, low-cost IoT network for smart agriculture. For monitoring of the soil moisture content, they have used an in- house developed sensor.

Performance Analysis of Multipurpose AGROBOT:

Sharif Ullah Al- Mamun, Md. Rabiul Islam, Arpita Hoque in2019, The goal of the AGROBOT projectis the implementation of a robotic system for agricultural operations such as plowing the field, sowing seeds, spraying fertilizers, nutrition deficiency and controlled use of fertilizers and pesticides. The agricultural scientists are experimenting to replace tractor driven mechanization with robotic agriculture by introducing “AGROBOT”.

Machine Vision and Machine Learning for Intelligent Agrobots:

A review Bini D, Pamela D, Shajin Prince in2020, A machine vision-based Agrobots along with artificial intelligence provides unmanned ground vehicle and unmanned aerial vehicle to navigate the path and to implement the agricultural task for minimizing labour and increasing quality food production.



Fig 2: Demo model of AGROBOT

Components Required

Hardware Requirements

- Raspberry Pi
- Motor Driver
- Raspberry Pi Camera
- Johnson's motors
- Nodemcu
- Lead acid battery

Software Requirements

- Anaconda
- Arduino IDE
- Raspberry Pi OS

Machine Learning Approach

A Convolutional Neural Network (ConvNet/CNN) is a Deep Learning algorithm which can take in an input image, assign importance (learnable weights and biases) to various aspects/objects in the image and be able to differentiate one from the other. The pre-processing required in a ConvNet is much lower as compared to other classification algorithms. While in primitive methods filters are hand-engineered, with enough training, ConvNets have the ability to learn these filters/characteristics.

The architecture of a ConvNet is analogous to that of the connectivity pattern of Neurons in the Human Brain and was inspired by the organization of the Visual Cortex. Individual neurons respond to stimuli only in a restricted region of the visual field known as the Receptive Field. A collection of such fields overlap to cover the entire visual area.

The objective of the Convolution Operation is to extract the high-level features such as edges, from the input image. ConvNets need not be limited to only one Convolutional Layer. Conventionally, the first ConvLayer is responsible for capturing the Low-Level features such as edges, color, gradient orientation, etc [2]. With added layers, the architecture adapts to the High-Level features as well, giving us a network which has the wholesome understanding of images in the dataset, similar to how we would. Image recognition also known as classification is the first step done here. It is the process where an image is given to the neural network as an input and an output with a label for that image is expected. This is called as "feature extraction", which is a vital ability of any neural network to extract minute details from an object.

Working Module

The working module is shown in the below fig 3. The plant is first captured by the camera which is connected to the raspberry pi. The captured image is processed in the raspberry pi4 model. The raspberry pi can be considered as minicomputer[1]. The raspberry pi is programmed to detect whether the plant is healthy or it is infected by a disease. If the plant is said to be infected, then which type of disease the plant is suffering from is also checked, using different machine learning algorithms and the datasets. The raspberry pi compares the input data with the standard data provided in the dataset and hence the disease is detected from which the plant is suffering. The raspberry pi camera takes the image as the input. The raw input is

then sent to the raspberry pi for processing the image. An image is made up of pixels arranged in a form of square matrix, a two-dimensional view having coordinates as x and y.

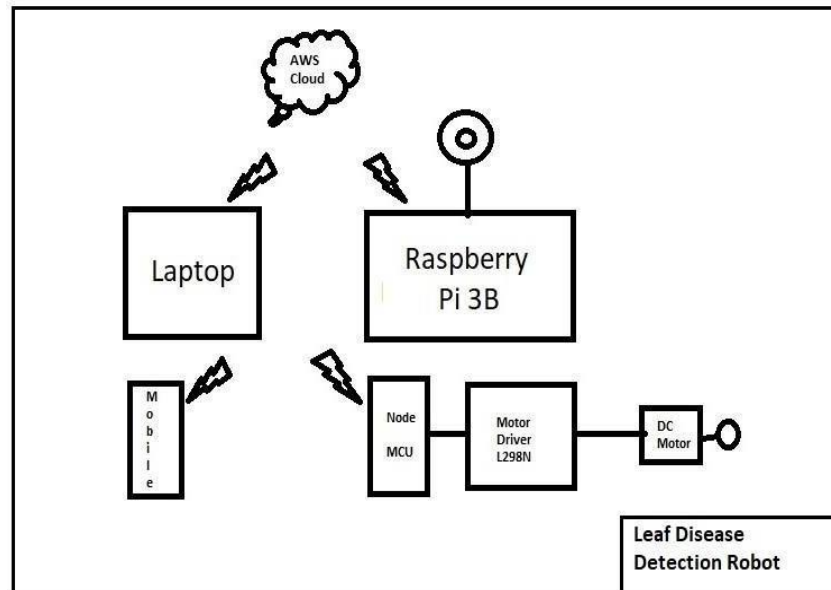


Fig 3: Block Diagram of working Module

The agrobot will survey the crop by scanning the image of the crop through the raspberry pi camera. The camera takes the image as input for raspberry pi and starts with the pre- processing which include the elimination of the undesirable distortions from the image. The raspberry pi then extracts the features of the image and proceed with the classification of the image as a normal or abnormal one [4].

If the image is classified to be normal then the crop is not infected whereas if the image is classified as abnormal then it detects the disease with which the plant is suffering. The classification is done by using the machine learning algorithms which checks the feature extracted image with the training dataset whose prediction accuracy is checked by the test dataset [3] as soon as the disease is detected.

Image Aquisition

The images are obtained using the digital camera that is connected to the Latte panda as shown in fig 4. The images captured are subjected to further preprocessing. For each observation of an individual leaf, we systematically varied the following image factors: perspective, illumination, and background. We captured two perspectives per leaf in-situ and in a non- destructive way: the top side and the back side, since leaf structure and texture typically substantially differ between these perspectives. If necessary, we used a thin black wire to arrange the leaf accordingly [5].



Fig 4: Image Acquisition

Image Preprocessing

The images obtained from the camera are subjected to preprocessing for increasing the quality of the images. The preprocessing steps may include color transformation, noise removal, histogram equalization, green masking etc as shown in fig 5. Here we use the technique of color transformation for increasing the quality of the image .Conversion of RGB image into Grey and also HSI to increase the quality .

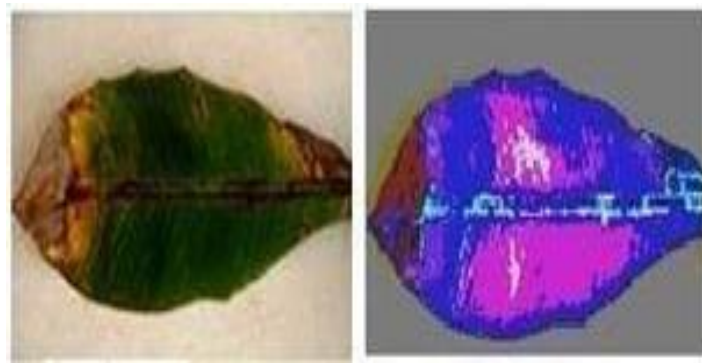


Fig 5 : Image preprocessing

Image Segmentation

Image segmentation are of many types such as clustering, threshold, neural network based and edge based. In this implementation we are using the clustering algorithm called mean shift clustering for image segmentation. This algorithm uses the sliding window method for converging to the center of maximum dense area. This algorithm makes use of many sliding windows to converge the maximum dense region.



Fig 6: Image segmentation

Applications

Some of the applications includes

- Weed control, Planting and Seeding and soil analysis
- Used in Horticulture: to transport potted plants in a greenhouse or outdoor setting.
- Fruit plucking robots
- Bug Vacuum

Conclusion

India is a global agricultural power house where the most of the farmers are failed to implement new strategies from the containment of the leaf disease. Leaf disease is a wide spread infectious disease which affects the whole crop on the fields by spreading. To overcome this problem faced by farmers in leaf disease recognition. We are using robotics that is agricultural surveillance robot which will help farmers to clear out their problems regarding the leaf disease by the working process as discussed in this paper which will ever reduce the man power and also time and helps the farmers to spray the pesticides on time so that they can overcome the loss faced by them due to leaf disease. Also these robots go way ahead for the future use. The robot is controlled by using android application.

In the proposed system, the leaf disease detection was only constricted to a specific disease in the proposed system. The number of diseases to be identified can be extended for more diseases in future with the development of the robot. In future the robot can be integrated with another machine learning . It can also be fixed with another camera that can be used for navigational purpose and later robot will be trained to navigate through the entire field and later it is allowed to move independently and take actions.

References

- [1] G. Eason, B. Noble, and I. N. Sneddon, "On certain integrals of Lipschitz-Hankel type involving products of Bessel functions," *Phil. Trans. Roy. Soc. London*, vol. A247, pp. 529–551, April 1955. (references) M. Sardogan, A. Tuncer and Y. Ozen, "Plant Leaf Disease Detection and Classification Based on CNN with

- LVQ Algorithm," 2018 3rd International Conference on Computer Science and Engineering (UBMK), 2018, pp. 382-385.
- [2] D. Bini, D. Pamela and S. Prince, "Machine Vision and Machine Learning for Intelligent Agrobots: A review" 2020 5th International Conference on Devices, Circuits and Systems (ICDCS), 2020, pp. 12- 16.
- [3] G. M. Sharif Ullah Al- Mamun et al., "Performance Analysis of Multipurpose AGROBOT," 2019 IEEE International WIE Conference on Electrical and Computer Engineering (WIECON-ECE), 2019, pp. 1-4.
- [4] H Durmuş, E. O. Güneş, M. Kırıcı and B. B. Üstündağ, "The design of general purpose autonomous agricultural mobile-robot: "AGROBOT"," 2015 Fourth International Conference on Agro- Geoinformatics (Agro- geoinformatics),2015,pp.49-53.
- [5] N G. Kurale and M. V. Vaidya, "Classification of Leaf Disease Using Texture Feature and Neural Network Classifier," 2018 International Conference on Inventive Research in Computing Applications (ICIRCA),2018,pp. 1-6.

Deep Learning Techniques for Detection of Deepfakes

Deshagouni Manasa*, Vasudev Dehalwar

Computer Science Engineering Department, Maulana Azad National Institute of Technology
Bhopal, India

ABSTRACT

There have been ground-breaking developments in machine learning and artificial intelligence thanks to science and information technology development. With the widespread use of social media comes the issue of Deepfakes, which has led to a rise in digital media content that has been altered or fabricated. The manipulated videos and photographs pose a severe risk to people's safety and privacy, which may also have catastrophic ramifications for a country's politics, religion, and social cohesion. Humans can spot image forgeries like face swapping, but Generative Adversarial Networks (GAN) can create images that are tough to detect even by humans; identifying such pictures and videos is a real challenge. Deep learning techniques are gaining popularity for detecting face swaps. Thus for stopping political unrest, blackmail we need smart algorithms to combat fake videos. In this paper, we suggest some deep learning models for detecting deepfakes videos to classify them accurately as real or fake.

Index Terms : Deepfakes, Classification, Deep Learning, Convolution Neural Networks, ResNet50, InceptionResnetV2 , M2model.

I. INTRODUCTION

The use of cell phones has multiplied with the emergence of technology. The use of videos and photographs on social media has increased due to social networks' growth. A survey found that every day, around a million images are shared online. The excessive usage of images on online platforms has given rise to various techniques for altering digital information utilizing Photoshop, among others.

In a narrow definition, deepfakes (stemming from "deep learning" and "fake") are created by techniques that can superimpose face images of a target person onto a video of a source person to make a video of the target person doing or saying things the source person does. This constitutes a category of deepfakes, namely face-swap. In a broader definition, deepfakes are artificial intelligence-synthesized content that can also fall into two other categories, i.e., lip-sync and puppet-master. Lip-sync deepfakes refer to videos that are modified to make the mouth movements consistent with an audio recording. Puppet-master deepfakes include videos of a target person (puppet) who is animated following the facial expressions, eye and head movements of another person (master) sitting in front of a camera (Agarwal et al., 2019) While some deepfakes can be created by traditional visual effects or computer-graphics approaches, the recent common underlying mechanism for deepfake creation is deep learning models such as autoen coders and generative adversarial networks (GANs), which have been applied widely in the computer vision domain. These models are used to examine facial expressions and movements of a person and

synthesize facial images of another person making analogous expressions and movements. Deepfake methods normally require a large amount of image and video data to train models to create photo-realistic images and videos. Deep learning methods called generative adversarial networks (GANs) [1] can create fake photos and videos that are difficult for a person to distinguish from the real ones. These models produce faked images and videos after training on a data set. For those deepfake media, this form of deepfake model needs a sizable amount of training data. The model may produce more credible and realistic photos and movies with an enormous data collection. In reality, the widespread availability of films featuring presidents and Hollywood celebrities on social media might aid people in creating plausible rumours and false information that could have a significant negative impact on our society.

Fake images and videos including facial information generated by digital manipulation, in particular with DeepFake methods, have become a great public concern recently. The very popular term “DeepFake” is referred to a deep learning based technique able to create fake videos by swapping the face of a person by the face of another person. This term was originated after a Reddit user named “deepfakes” claimed in late 2017 to have developed a machine learning algorithm that helped him to transpose celebrity faces into porn videos. In addition to fake pornography, some of the more harmful usages of such fake content include fake news, hoaxes, and financial fraud. As a result, the area of research traditionally dedicated to general media forensics, is being invigorated and is now dedicating growing efforts for detecting facial manipulation in image and video part of these renewed efforts in fake face detection are built around past research in biometric anti-spoofing and modern data-driven deep learning.

Fake news has been spreading at an alarming rate recently, and videos of a million hours or more in length are being shared widely on social media, endangering civilization. Although there has been an impressive development in identifying image forgeries, finding faked films is still tricky. Many imagebased algorithms can't be used directly on videos because of compression. The majority of current video research is concentrated on re-encoding [2] and re-capturing [3] [4], although video detection is still challenging.

Face-swapping videos have been created using deep learning algorithms. A robust method for capturing and recreating facial expressions is deepfake. The creation of adult content was the main application of this technique.



Fig. 1. Deepfake manipulation [5]

Technologies based on artificial intelligence have been developed to find tampering [6] [7]. Convolution Neural Networks are being used to address the problem because they perform remarkably well in photos. Generative Adversarial Networks (GAN) have been used to create imitations of real videos and other content. Thus, a new category of movies known as “DeepFake” videos has been created as a result of the usage of Variational Autoencoder and Generative Adversarial Networks (GANs) [1].

Deepfake videos, which are produced using the image modification program Abode, are simpler to make and have a more realistic appearance than traditional Hollywood movies. Face swapping is made possible in film by using deep learning techniques on various video samples. The results are more realistically represented the more significant the sample sizes. The general public, particularly women, are now victims of deepfakes, and the bulk of these victims are portrayed in porn. In a post, Washington claimed that face photos and pornographic images were expertly combined and shared on social media without the consent of any outside parties. Deep learning techniques have proved to be quite successful in image forensics in recent years. Many researchers in the field of image forensics, eg. Barni et al. used deep learning algorithms for detection of changes in images due to JPEG compression. For the identification of deepfake movies, various techniques are used because identification of deepfakes necessitates the extraction of complex features; therefore, a good number of fake and real videos are required for training purposes. FaceForensics++ [8], Deepfake Detection Challenge (DFDC) [9] and Celeb-DF [5] are a few of the data.

II. RELATED WORKS

Li and Lyu et al. [10], suggested machine learning method for detection of deepfake videos. They offer an approach that pits one machine learning methodology against another. Convolutional neural networks (CNN) were trained with real and fake images. CNN networks were utilised in the experiment, with result accuracies ranging from 84 to 99%. The precision of the results acquired by their method was excellent. Ricard Durall et al. [11] proposed a technique for identifying deepfakes. Their method relied on frequency response and then used a simple classifier. The technique produced excellent results with only a few training samples and high accuracy compared to prior methods. The author generated their datasets by integrating available datasets such as Faces-HQ to obtain high-face-resolution photos. After only ten high-resolution photos, the approach obtained a classification accuracy of about 100%. The videos demonstrate how their technique yields excellent outcomes.

Tackhyun Jung et al. [12] proposed an architecture using the DeepVision algorithm to detect blinking pattern changes, a spontaneous movement, to identify Generative Adversarial Networks (GAN) generated deepfakes. The human eye pattern is thought to differ from one person to the other based on the person's biology and physical state. The pattern is determined by factors such as sex. Deepfakes can be recognised using algorithms that track significant difference in the blinking patterns of human eyes.

Xin Yang et al. [13] introduced a novel technique for detecting altered or fraudulent photos or videos. Deepfakes are generated by splicing the region of interest in the face of the source image, that creates inconsistencies that can be identified when 3D postures of heads are acquired from face photographs, according to the method. Experiments were carried out to demonstrate the approach, and a classification system based on the concept was developed. An SVM classifier that incorporates features found on this cue is used for evaluation.

Haya R Hashan and Khaled Salah et al. [14] presented a technique and broad framework for tracking the computerised items back to their source using Ethereum smart contracts. In the keen agreement, hashes from the interplanetary document framework (IPFS) are used to store advanced data and metadata. Their method is based on the fact that if the digital content to be tracked down to a reliable origin, the chances are that it is authentic.

David Guera et al. [15] demonstrated a method for automatically detecting fake films. The technique utilized a Convolutional Neural Network for extracting features. The features or aspects gathered are used for training a recurrent neural network. The method showed a good classification accuracy. Hany Farid et al and Shruti Agarwal [16] suggested a technique for detecting tampered films based on the motion of the mouth(visemes) is most

consistent with spoken phenome. Mismatches of a phoneme can thus be used to identify changes in time and location. The proposed approach proved reliable and effective in detecting deepfakes.

Darius Afchar et al. [17] proposed a method for effectively detecting face alteration in films, focusing on the Face2Face and Deepfake techniques for creating believable forged videos. The researchers utilised a deep learning method to develop two networks concentrating on the image's mesoscopic properties. They put rapid networks to the test on a dataset produced from films. Deepfake detects more than 98% of the time, according to the tests.

Yuezun Li, Siwei Lyu and Ming-Ching Chang et al . [18] suggested a model which focuses on identifying the blinking pattern of eyes in video films, which is an involuntary response of human beings that is not well addressed in the generated fake videos. The algorithm was tested on eye-blinking dataset and has shown great results in detection of DeepFake movies.

Mohit Patel, Aaryan Gupta et al. [19] discussed various transfer learning methods for detecting deep fake videos. In the study, they forwarded a technique for extracting and detecting a person's face from videos and then utilising them to extract features. Based on the extracted features, the model classifies them as fake or real. The features were extracted using pretrained models like VGG, MobileNet, ResNet etc. For the classification task, they used a random forest classifier. The accuracy achieved by the model was around 90% in classifying deepfakes.

A. Dataset used in our study

The dataset used in our study has been taken up from Kaggle deepfake detection challenge. The Facebook Deepfake detection challenge initially released the dataset.

For the study, we have taken 800 videos of training data. The JSON file contain real and fake videos labels. The frames were extracted from the videos, and they were used for training the model. The dataset is in the form of videos, with over one lakh clips taken from various paid actors and generated using a variety of GAN-based methods.

Deepfakes are a recent off-the-shelf manipulation technique that allows anyone to swap two identities in a single video. In addition to Deepfakes, a variety of GAN-based face swapping methods have also been published with accompanying code. To counter this emerging threat, we have constructed an extremely large face swap video dataset to enable the training of detection models, and organized the accompanying DeepFake Detection Challenge (DFDC) Kaggle competition. Importantly, all recorded subjects agreed to participate in and have their likenesses modified during the construction of the face-swapped dataset. The DFDC dataset is by far the largest currently and publicly available face swap video dataset, with over 100,000 total clips sourced from 3,426 paid actors, produced with several Deepfake, GAN-based, and non-learned methods. In addition to describing the methods used to construct the dataset, we provide a detailed analysis of the top submissions from the Kaggle contest. We show although Deepfake detection is extremely difficult and still an unsolved problem, a Deepfake detection model trained only on the DFDC can generalize to real "in-the-wild" Deepfake videos, and such a model can be a valuable analysis tool when analyzing potentially Deepfaked videos.

III. PROPOSED METHODOLOGY

In our proposed methodology we took the dataset from Kaggle deepfake detection challenge, the videos are labelled as fake and real. The region of interest in identifying deepfake images



Fig. 2. Frames of videos

is the face so we have used Dlib face detector. The frames from the input videos are taken at various instances and then they are saved as images. The frames are captured at different instances of time. The images are labelled as real and fake. The labelled images are fed into the training model and the model is trained for certain number of epochs. The model have different layers in which the input data is fed like different convolution, pooling layers and the final layers are dense layers in the models. The features from the input images are extracted and are used for training the model. The dataset is divided for 70% training data and 30% testing data. We have used M2, Modified InceptionResnetV2, Modified Resnet50 model. The model trained is now used on the testing data.

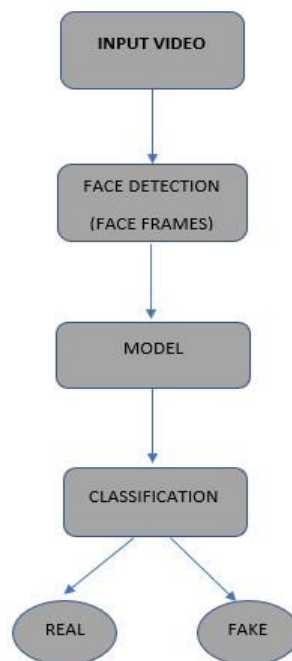


Fig. 3. Proposed Methodology

IV. DEEP LEARNING MODELS

A. Convolution Neural Networks

In neural networks, Convolutional neural network [20] is a neural networks to do the image recognition and image classifications, Object detections, etc.

There are majorly three types of layers:

- Convolutional Layer: the input neurons are connected to hidden neurons in the hidden layers; certain neurons can be left without being connected to the next layer's hidden layer(dropout).
- Pooling Layer: is used for reducing the dimensions of the features extracted either by using min, max, or average Pooling. In a neural network, there can be several pooling layers
- Fully Connected layer: these are the final layers of the neural network. Output from the previous layers or the pooling layers are flattened and then fed into these layers. The proposed architecture is given below, and there are several convolution layers, max-pooling layers and some dense layers are added at the end of the model consisting of one twenty eight neurons in the first and one neuron at the last layer of the model.

Layer	Parameters	Activation
Input		
Rescaling		
Conv2D	16x3x3	ReLU
Max Pool	2x2	
Conv2D	32 x 3 x 3	ReLU
Max Pool	2 x 2	
Conv2D	64x3x3	ReLU
Max Pool	2x2	
Conv2D	32x3x3	ReLU
Max Pool	2x2	
Flatten		
Dense		ReLU
Dense		Sigmoid

Fig. 4. M2 model

B. RESNET50

ResNet-50 [21] is a convolutional neural network with fifty layers.

It is a variation of Resnet with forty-eight Convolutional layers, one max pool layer and one average pool layer. Architecture of resnet50: The first layer is produced using a convolution using 64 distinct kernels, each having a size of 7x7, and a stride of 2. There is a max pooling layer of stride 2 in the next step. This is followed by a convolutional layer using a 1x1,64 kernel, a 3x3,64 kernel, and finally a 1x1,256 kernel. These layers are repeated three times to create a total of nine layers. Following a layer of 3 x 3,128 and a layer of 1 x 1,512 kernel, we see a convolution of 1 x 1,128 once more. These layers are repeated four times for a total of twelve layers.

This is followed by a convolution with a 1 x 1,256 kernel, two further convolutions with 3 x 3,256 kernel, and finally a third convolution with a 1 x 1,1024 kernel. These three layers are then repeated six times in total to give us eighteen layers. These layers were repeated three times, giving us a total of nine layers. Then, there is a convolution of kernel 1 x 1,512, followed by two further convolutions of 3 x 3,512 and 1 x 1,2048. Following this, there is average pooling, followed by a layer with 1,000 nodes that is fully connected, and finally, a softmax function that yields one layer.

In the proposed model, we modified the Resnet50. We have added a global average pooling layer, and we have added three dense layers. In the first dense layer of one twenty eight neurons have relu activation function. In the

second dense layer of sixty-four neurons have relu activation function, and in the last dense layer of one neuron we have used the sigmoid activation function.

Layers of the model
Resnet50
GolbalAveragePooling2D
Dense layer
Dense layer
Dense layer

Fig. 5. Modified Resnet50 architecture

InceptionResnet V2

The Inception-ResNet-v2 [22] architecture is a convolutional neural architecture that expands on the Inception family of architectures while also including residual connections. It is a variant of Inception and ResnetV2 architectures. The 164-layer network can recognise images into one thousand object categories including animals, mice, pencils .

A hybrid inception module was proposed, inspired by ResNet's performance. Inception ResNet is divided into two versions: v1 and v2.

The cost of Inception-ResNet v1 is comparable to that of Inception v3 in terms of computing. The cost of InceptionResNet v2 is comparable to that of Inception v4 in terms of computing. They have various stems.

In the proposed model, we modified the InceptionResnetV2. We have added a global average pooling layer and one Dropout layer of 20 % and three dense layers. In the first layer, we used dense layer of two fifty six neurons having relu activation function, in the second layer, we used dense layer one of twenty eight neurons having relu activation function and in the last dense layer we used a sigmoid activation layer.

V. ANALYSIS OF RESULTS

The models were trained for 25 epochs and the batchsize was taken as 32, thus the testing accuracies that we achieved are given in the table 1 below.

The models were able to achieve good accuracy. The classification accuracy for M2model, InceptionResnetV2, ResNet50 is

Layers of the model
InceptionResnetV2
GolbalAveragePooling2D
Dropout
Dense layer
Dense layer
Dense layer

Fig. 6. Modified InceptionResnetV2 architecture

TABLE I. COMPARATIVE ANALYSIS

MODEL	Accuracy
M2 model	92%
InceptionResnetV2	96%
Resnet50	96.5%

92%, 96%, 96.5%, The best classification accuracy obtained is for modified Resnet50. The confusion matrix was obtained for M2 model, Modified InceptionResnetV2, Modified Resnet50 where df label represents deepfake image and real label represents real image. The Modified model has InceptionResnetV2, Resnet50 as it's first layers and the new model was made adding global average pooling layer and few dense layers, it can be seen that M2 model which has few convolutional and pooling layers also achieves good accuracy.

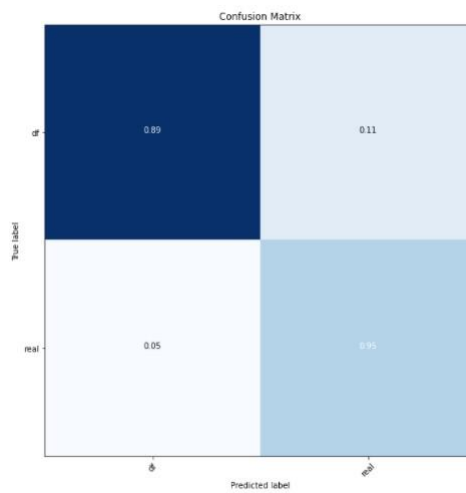


Fig. 7. Confusion matrix of M2 implementation

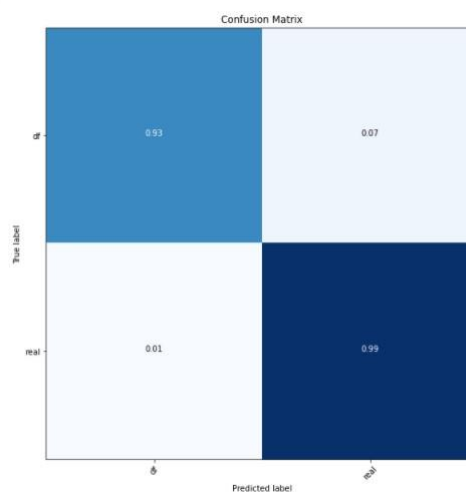


Fig. 8. Confusion matrix of InceptionResnetv2 implementation

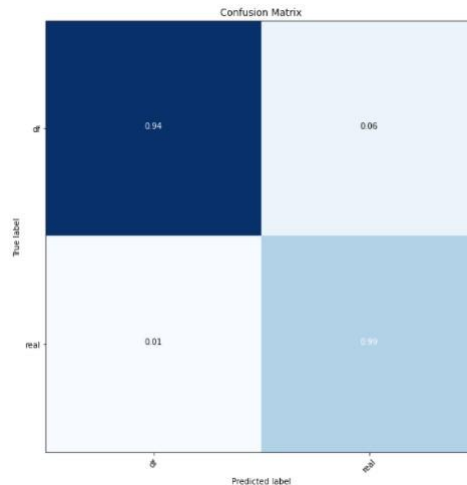


Fig. 9. Confusion matrix of Resnet50 implementation

VI. CONCLUSION

The proposed method above uses various models. The different architecture used helped us in detection of deepfakes. The use of models like modified InceptionResnetV2, modified Resnet50 helped us in achieving good accuracy of detection. It can be seen that the M2 model also accomplishes a good classification accuracy of 92% whereas by using modified models we can achieve best accuracy of 96.5%. In future we would be gathering more data from various sources including compressed ones for making our model more efficient.

REFERENCES

- [1] I. Goodfellow, J. Pouget-Abadie, M. Mirza, B. Xu, D. Warde-Farley, S. Ozair, A. Courville, and Y. Bengio, "Generative adversarial nets," *Advances in neural information processing systems*, vol. 27, 2014.
- [2] W. Wang and H. Farid, "Exposing digital forgeries in video by detecting double mpeg compression," in *Proceedings of the 8th workshop on Multimedia and security*, pp. 37–47, 2006.
- [3] W. Wang and H. Farid, "Detecting re-projected video," in *International Workshop on Information Hiding*, pp. 72–86, Springer, 2008.
- [4] J.-W. Lee, M.-J. Lee, T.-W. Oh, S.-J. Ryu, and H.-K. Lee, "Screenshot identification using combing artifact from interlaced video," in *Proceedings of the 12th ACM workshop on Multimedia and security*, pp. 49–54, 2010.
- [5] Y. Li, X. Yang, P. Sun, H. Qi, and S. Lyu, "Celeb-df: A largescale challenging dataset for deepfake forensics," in *Proceedings of the IEEE/CVF Conference on Computer Vision and Pattern Recognition*, pp. 3207–3216, 2020.
- [6] H. Farid, "Image forgery detection," *IEEE Signal processing magazine*, vol. 26, no. 2, pp. 16–25, 2009.
- [7] J. A. Redi, W. Taktak, and J.-L. Dugelay, "Digital image forensics: a booklet for beginners," *Multimedia Tools and Applications*, vol. 51, no. 1, pp. 133–162, 2011.
- [8] A. Rossler, D. Cozzolino, L. Verdoliva, C. Riess, J. Thies, and M. Nießner, "Faceforensics++: Learning to detect manipulated facial images," in *Proceedings of the IEEE/CVF International Conference on Computer Vision*, pp. 1–11, 2019.
- [9] B. Dolhansky, J. Bitton, B. Pflaum, J. Lu, R. Howes, M. Wang, and C. C. Ferrer, "The deepfake detection challenge (dfdc) dataset," *arXiv preprint arXiv:2006.07397*, 2020.

- [10] Y. Li and S. Lyu, "Exposing deepfake videos by detecting face warping artifacts," *arXiv preprint arXiv:1811.00656*, 2018.
- [11] R. Durall, M. Keuper, F.-J. Pfrendt, and J. Keuper, "Unmasking deepfakes with simple features," *arXiv preprint arXiv:1911.00686*, 2019.
- [12] T. Jung, S. Kim, and K. Kim, "Deepvision: deepfakes detection using human eye blinking pattern," *IEEE Access*, vol. 8, pp. 83144–83154, 2020.
- [13] X. Yang, Y. Li, and S. Lyu, "Exposing deep fakes using inconsistent head poses," in *ICASSP 2019-2019 IEEE International Conference on Acoustics, Speech and Signal Processing (ICASSP)*, pp. 8261–8265, IEEE, 2019.
- [14] H. R. Hasan and K. Salah, "Combating deepfake videos using blockchain and smart contracts," *Ieee Access*, vol. 7, pp. 41596–41606, 2019.
- [15] D. Guera and E. J. Delp, "Deepfake video detection using recurrent neural networks," in *2018 15th IEEE international conference on advanced video and signal based surveillance (AVSS)*, pp. 1–6, IEEE, 2018.
- [16] S. Agarwal, H. Farid, O. Fried, and M. Agrawala, "Detecting deepfake videos from phoneme-viseme mismatches," in *Proceedings of the IEEE/CVF Conference on Computer Vision and Pattern Recognition Workshops*, pp. 660–661, 2020.
- [17] D. Afchar, V. Nozick, J. Yamagishi, and I. Echizen, "Mesonet: a compact facial video forgery detection network," in *2018 IEEE International Workshop on Information Forensics and Security (WIFS)*, pp. 1–7, IEEE, 2018.
- [18] Y. Li, M.-C. Chang, and S. Lyu, "In ictu oculi: Exposing ai created fake videos by detecting eye blinking," in *2018 IEEE International Workshop on Information Forensics and Security (WIFS)*, pp. 1–7, IEEE, 2018.
- [19] M. Patel, A. Gupta, S. Tanwar, and M. Obaidat, "Trans-df: a transfer learning-based end-to-end deepfake detector," in *2020 IEEE 5th international conference on computing communication and automation (ICCCA)*, pp. 796–801, IEEE, 2020.
- [20] L. Alzubaidi, J. Zhang, A. J. Humaidi, A. Al-Dujaili, Y. Duan, O. AlShamma, J. Santamaría, M. A. Fadhel, M. Al-Amidie, and L. Farhan, "Review of deep learning: Concepts, cnn architectures, challenges, applications, future directions," *Journal of big Data*, vol. 8, no. 1, pp. 1–74, 2021.
- [21] S. Targ, D. Almeida, and K. Lyman, "Resnet in resnet: Generalizing residual architectures," *arXiv preprint arXiv:1603.08029*, 2016.
- [22] C. Szegedy, S. Ioffe, V. Vanhoucke, and A. A. Alemi, "Inception-v4, inception-resnet and the impact of residual connections on learning," in *Thirty-first AAAI conference on artificial intelligence*, 2017.

IOT Based Vehicle Accident Prevention and Detection System Using Raspberry-Pi

Rahul Devnath Tiwari¹, P. P. Tasgaonkar²

¹Department of E&TC College of Engineering, Pune, India

²Professor, Department of E&TC College of Engineering, Pune, India

ABSTRACT

The pace of our life has accelerated due to the transit system thanks to continual technological advances. Accidents are still a major problem, especially on the highways where they often result in fatalities and have catastrophic consequences for the victims. Innovative smart city systems are highly desired to avert such accidents. A self-driving autonomous car is created in this study to be used in accident prevention applications. The working prototype is totally managed by a Raspberry Pi that integrates smart sensors for automation and ADXL345 for accident detection. The Raspberry Pi is used because it has a faster processing speed than other microcontrollers and is excellent for creating software applications. Accident Utilizing a Pi-camera and an IR sensor, prevention is carried out by alerting the driver about nearby cars when their distance from one another exceeds a threshold value, and if it violates a limit, the vehicle will stop automatically. Additionally, a Wi-Fi connection is successfully established using the Thing Speak platform for real-time monitoring of the system online.

Index Terms : Raspberry-Pi, IR Sensor, Thingspeak Cloud, ADXL345, Smart City ,API, IOT.

I. INTRODUCTION

As number of vehicles are rising day by day, with increase in population, so are the road accidents. About 80 percent of the accidents occurrence end up in losing lives. According to the survey which was conducted by the research agency [1], about 1.25million people die every year whereas 3,287 deaths happen every day. National expressways or highways have been made to cut down the travelling cost between the cities. But, the major thing which misses out is to manage the traffic which eventually causes deadly accidents. A total of [8] 280 accidents happened between 1st January-2016 to 31st December-2017 on expressways as per the accident researchers which was published on July-2018. These involved 218 road users (193 vehicles and 25 pedestrians) and 443 victims out of which 65 were lethal, 105 were serious and 129 suffered minor injuries, which invoked a thought of doing something in order to decrease the accidents and also monitor it 24x7, throughout the year. This system described will monitor the accidents continuously by the help of internet of things using various protocols. So, if in case accident happens, it will be immediately informed to nearby authorities and accordingly necessary actions can be taken. We can see that with each passing year, the number of accidents keep on rising.

Year	Total Accidents	Fatal	Fatal (In %)	Killed
2015	5,01,423	1,46,133	26.3	1,46,133
2016	4,80,652	1,50,785	28.3	1,50,788
2017	4,64,210	1,47,913	29	1,47,913
2018	4,67,044	1,51,417	29.5	1,51,417
2019	4,49,002	1,51,113	30.7	1,51,113
2020	3,66,128	1,31,714	33	1,31,714

Fig. 1. Major parameters Contributes to road accidents.

As we can see that with each coming years the number of accidents is keep on rising. Also number of people killed in the accidents are going up so, we need some system or technology which can help in decreasing the number of accidents. The concept of “Smart city” is introduced for development of urban cities. Smart means something which is more technology oriented makes life easier and more efficient. The major contribution of “smart city” is to make the life of people more comfortable, easy and sustainable. There are so many smart technologies which can be used at wide range of areas such as transportation, healthcare, aviation etc. With the IoT this idea is more achievable. Transportation plays an essential role for any city to be smart. In this paper the main focus would be to eradicate the amount of accidents happening in a city for safety of the citizens. Smart transportation mainly consists of infrastructures, AI based (artificial intelligence) based traffic control and management systems aiming to transform sustainable and green system. Major areas on which smart transportation supports are:

- a. Smart Automobile.
- b. Smart Infrastructure.
- c. Intelligent Transport System.
- d. Sustainable fuels.

The paper starts by describing the standalone, lightweight and smart detection system in the current scenario which can be implemented in a Smart City. A brief discussion on the Past approaches is present in Section II. A brief methodology and block diagram is described in Section-III. Hardware requirements has been also discussed in Section- IV. Finally results are present in Section-V. At the end final conclusion has been given in Section-VI.

II. LITERATURE REVIEW

A lot of research has been done till date to detect the accident and later on notification is sent to emergency medical services.

In [2] this author has present eye blink monitor technique for accident detection which alerts during drowsiness states. A system which depends on psychological state of focus and eye movement are helpful in alerting driver during drowsiness state. There will be no effect during an ordinary movement of the eyes. In [3]

this author has designed a speed automatic detection system which detects the speed of a vehicle. In case over speed happens a mail will be send to toll plaza and fine will be imposed. Here Doppler effect has been employed for ensuring the speed of a vehicle. And if over speed happens the image of a vehicle is taken and license will be removed using DIP method. In [4] this author proposed a system that notifies emergency contacts like police, ambulance when accident happens. The system uses mamdani fuzzy logic based on a support taken from programmed smartphone and the information will be stored to data centre. Data is taken with the help of accelerometer, gyroscope sensors that is attached to different side of the vehicle. However, the hardware system has excessive sensors which was not compact enough. In [11] author has used a function which is programmable oriented and developed a Software Network(SDN) in order to improve the quality of services in IOV network which is very important while vehicle reports the accident to each other. In [12] have discussed about VCA (vehicle cloud access) problem that has been modelled with the help of evolutionary gaming and have given two important algorithms based on the EG-VCA and QL-VCA.

In [13] author has used detection based system which is due to collision by using a smart phone and different sensors like accelerometer, gyroscope, magnetometer in order to reduce the false alarms occurs in the system. In [5] author has employed a shock sensor and geographical location is sent when the accident occurs. Additional information such as full name, email, phone number etc. are being send to the public safety organization. Main drawback of this system is passenger need to pre-register its vehicle information which is currently not possible. In [6] on-board diagnostic system has been implemented and acceleration data is used for accident detection. But implementation of OBD in each vehicle is not possible. An alert is generated along with email notification with the help of Message queuing telemetry transport(MQTT). With the help of ultrasonic and accelerometer sensor data will be received and stored on Iot platform Losant [7]. Real time accident detection algorithm is used with the help of RFID is shown in [9] which collects a lot of information such as speed, number of passengers inside the vehicle etc. Also multiple sensors have been used at different corner of the vehicle which make this method less compact. In [14] author has mentioned about IR sensor which is interfaced with Arduino board also 16*2 counter is used to count the vehicles at the turning point to improve the accuracy of the road.

III. PROPOSED METHODOLOGY

1. Hardware arrangement

Fig demonstrates the electronic components necessary to create a smart, autonomous automobile. The Raspberry Pi Microcontroller is used in the model to provide control and offer interface between several sensors, including ADXL-345, IR, alcohol, gas, and alcohol sensors. To enable viewing of data on the cloud, a Wi-Fi module is interfaced with the board. Additionally, Pi-Camera is employed to record high definition images and videos for real-time monitoring. Hardware setup is shown in Figure 2. The Raspberry Pi, Motor Driver (L293d), and 9V battery are included. Battery is utilised to power the circuit, and L293D is interfaced with the board. The motor driver is essential for managing the speed of a DC motor. It is an integrated circuit (IC) or circuit that supplies energy to the car's motor. The speed of a motor is directly correlated with the voltage applied to its terminals. As a result, when the voltage of the motor varies, the vehicle's speed also does. The motor driver receives a pulse width modulation (PWM) signal from the Raspberry-Pi board. The reference signal is used to control the motor's speed. The used DC motor spins at a speed of 1000RPM.

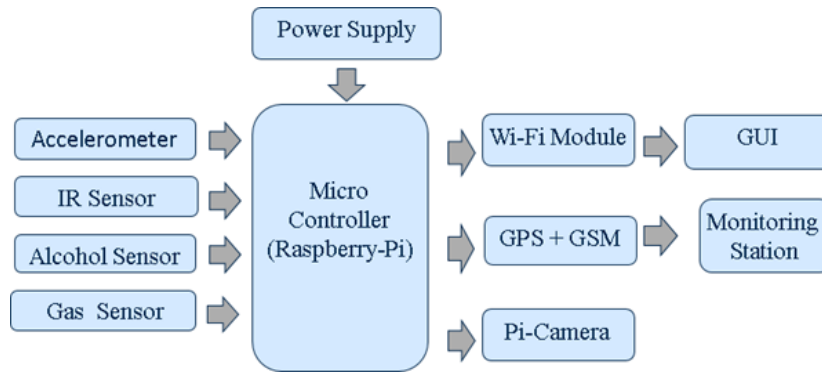


Fig. 2. Architecture of proposed model.

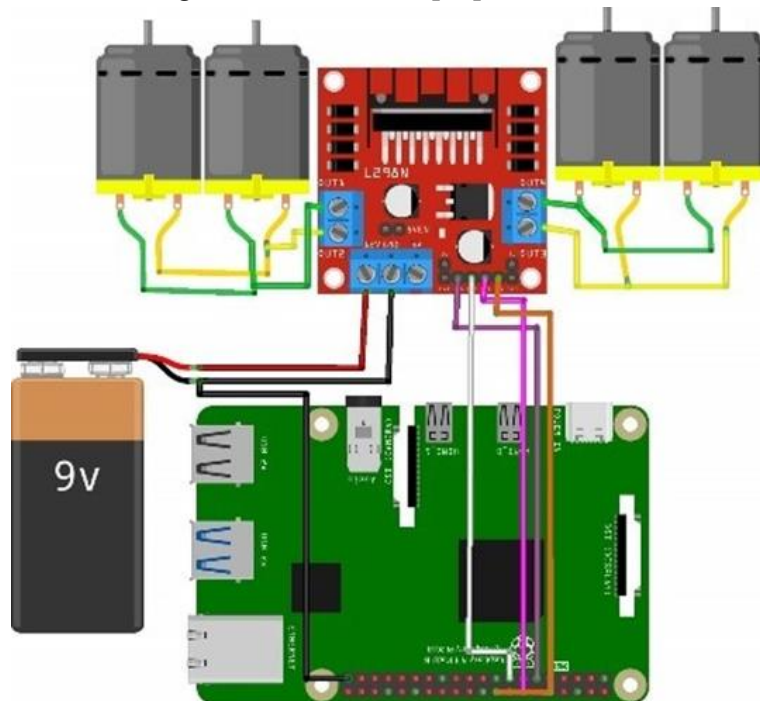


Fig. 3. hardware setup.

2.Sensors

A. Accelerometer

A sensor which measures acceleration of an object or body when it is in rest state that helps in accident detection. It acquires data from the 3 axial components along with three different orthogonal axis. The acceleration can be calculated from three equations given below:

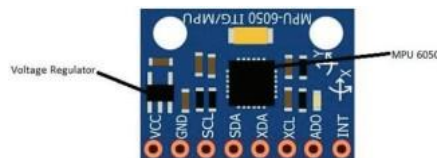


Fig. 4. Accelerometer

$$A = (V_i - V_f)/T \quad (1)$$

$$A = (2(D - V_i T))/T^2 \quad (2)$$

Where V_i = Initial velocity.

V_f = Final velocity

T = Time taken during acceleration.

D = Distance travelled.

Suppose 3-axis accelerometer is mounted on a device in the gravitational field, and undergoing acceleration a . It will generate output G which is given by:

$$G = R(F - a) \quad (3)$$

Where R is the rotational matrix defines the orientation of the device with respect to the earth. F is a gravitational force and a is acceleration. Whenever a running vehicle is dropped from a certain height the orientation of the vehicle changes. In such case gravitation of a vehicle changes with respect to X, Y and Z axis. And declaration due to the impact will be distributed to more than one axis. Therefore, it is very difficult to detect the precision of the declaration. To address this problem absolute linear acceleration is calculated with the help of X, Y and Z axis. ALA is calculated by:

$$ALA = \sqrt{(x^2 + y^2 + z^2)} \quad (4)$$

Where X, Y, Z are the deceleration at x-axis, y-axis, and z-axis. When a vehicle is collided with an object or any other solid object at the speed of 30km/h, the intensity of declaration always crosses 5g.

B. Alcohol sensor

The presence and quantity of alcohol vapours in the air are detected by an alcohol sensor, also referred to as an alcohol gas sensor or alcohol detector. It is frequently employed in alcohol detection systems, industrial safety applications, and breathalyser equipment. If a drunk person take air near the sensor, then it detects the ethanol in his breathe and output is generated passed on the alcohol concentration. In case the driver is in dunked state notification will be send to the owner's number and buzzer will lit up The analog output pin of alcohol sensor is connected to pin number 37 i.e. GPIO 26.

C. Pi-Camera

The camera module created especially for use with the well- known single-board computer Raspberry Pi is referred to as the "Pi Camera". A special CSI (Camera Serial Interface) connector is used to link the Pi Camera modules to the Raspberry Pi board. For the direct connection of camera module to raspberry-pi CSI port is use. Raspbian, the official operating system for the Raspberry Pi, often comes with the essential software drivers and libraries pre-installed or is readily installable.



Fig. 5. Pi-camera.

D. IR sensor

A sensor that detects and measures infrared radiation that is emitted by things or substances in its range of vision is known as an infrared (IR) sensor. In the model we have used this device to detect any obstacle present, according to the location of the obstacle the car will move in a particular direction. Based on each gas's distinct infrared absorption properties, IR sensors are used to identify, quantify, and measure its existence and quantity. IR sensor can be interfaced with Raspberry-Pi by using software drivers and libraries. The analog output pin of IR sensor is connected to pin number 16 i.e. GPIO 23.

E. Motor Driver(L293D)

The L293D device is a quadruple which produces high current Half-H. It is designed to produce bidirectional drive currents up to 600mA at a voltage from 4.5v to 36v. four Dc motor with 1000rpm is attached to 4 wheel of the car. The motor driver is essential for managing the speed of a DC motor. It is an integrated circuit (IC) or circuit that supplies energy to the car's motor. The speed of a motor is directly correlated with the voltage applied to its terminals. As a result, when the voltage of the motor varies, the vehicle's speed also does. The motor driver receives a pulse width modulation (PWM) signal from the Raspberry-Pi board. The reference signal is used to control the motor's speed.

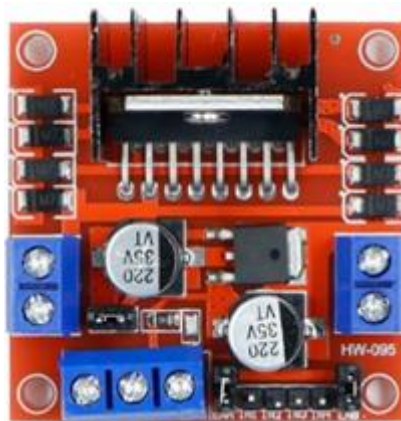


Fig. 6. Motor-driver IC(293d).

F. GPS/GSM

GSM/GPS is also installed on the device. GPS helps in track the location of vehicle. In our proposed methodology we used to find the current location of the device if accident occurs. When the microcontroller receives the signal from accident location it will request the current location to the GPS. GSM is a device helps in mobile communication. The notification will be sent via GSM to nearby hospitals and nearby police station whenever any mishap take place. There is a SIM installed inside the GSM that is used for communicating purpose with the date and time. Whereas GPS helps to trace the location of particular vehicle if in case something happens. Both GSM/GPS is interfaced with Raspberry-Pi.

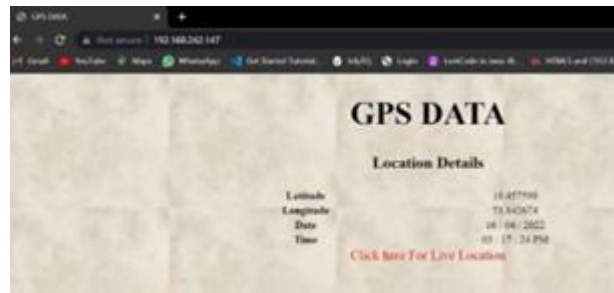


Fig. 7. Shows the location with Date and Time.

G. Raspberry Pi (3A)

It is equipped with a quad-core, 1.2GHz Broadcom BCM2837 processor, which has enough processing capacity for a variety of applications. The board's 512MB of LPDDR2 SDRAM enables multitasking and the use of numerous software programmes. With built-in Wi-Fi (802.11n) and Bluetooth 4.2 connectivity, the Raspberry Pi 3 Model A enables wireless communication and IoT projects without the need for extra adapters. It contains a 40-pin GPIO header that enables the board to be expanded by connecting different sensors, modules, and peripherals. A 5V power supply can be used to power the board using a micro USB port.

IV. CLOUD (THING SPEAK)

The IoT is a system that connects things together. The things generally consist of operating systems and ability to connect with internet or any other neighbouring things. It is a platform which provides various exclusively services build for IoT applications. It has the capabilities to collect various data in real-time, visualized in the forms of charts has the ability to create apps and plugins for collaborating with social networks, web services, APIs. The main elements of thing speak is 'channel'. It stores the data that we send to thing speak. It comprises of Multiple fields in that any kind of data can be stored. Multiple location field for storing latitude, longitude and various types of elevation. This are very important while tracking a device which is in moving condition. Status field is used to describe the short message in the channel. Thing speak has a unique key through which data is secured that is a API. Every user id that is created has a different API key.

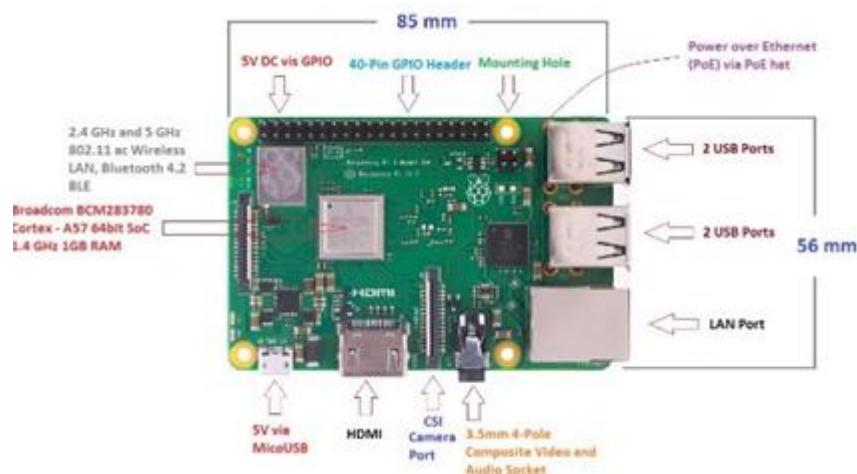


Fig. 8. Raspberry-Pi(3A).



Fig. 9. Axis-wise real time Accelerometer records on Thing speak.

Fig.3. shows the accelerometer readings on Cloud (Think speak) We can set up thresholds in Think Speak to set off alerts or notifications based on specific circumstances. For instance, we may enable Think Speak to send an email or push notice whenever the acceleration exceeds a predefined threshold in any axis. This function is helpful for identifying noteworthy events or unusual behaviour recorded by the ADXL345. The angle will start off at zero degrees and can increase all the way to 360 degrees in any direction. If the vehicle crosses the accelerometer threshold value in either direction, an accident is deemed to have occurred. The X-axis and Y-axis threshold values are 250 and 300, respectively. Depending on the vehicle's orientation, we can see various values on the display. As can be seen in Figure 3, if X is initially set to 255 but Y and Z are practically negligibly 0, then the car has been raised from the back. In contrast, if Y increases and X and Z are almost zero, the vehicle is lifted from the front. An alert will be produced and essential steps can be done if it lifts over a certain threshold. We can conclude an accident has happened if the variance at the various axes is quite large within a short period of time.

'Thing Speak' will be used to continuously monitor this system. All the real time data will be stored on the cloud and if the accident occurs, the spike will be seen on the terminal depending on the threshold value. The data could be monitored from anywhere around the world and can be accessed by anyone. Using this technique, emergency services can be easily alerted when the accident occurs.

V. EXPERIMENTS AND RESULTS

A. Device Prototype



Fig. 10. Prototype of Smart accident detection and prevention system.

B. Result Discussion:



Fig. 11. LCD Display for Obstacle Detection.

Fig.10. Shows the response of system when the obstacle is detected. The obstacle detection is carried out with the use of IR sensor Module. The Pi-Camera simultaneously captures the real time images of the obstacle detected. The image which is captured by the P-camera is processed with the help of image processing techniques.



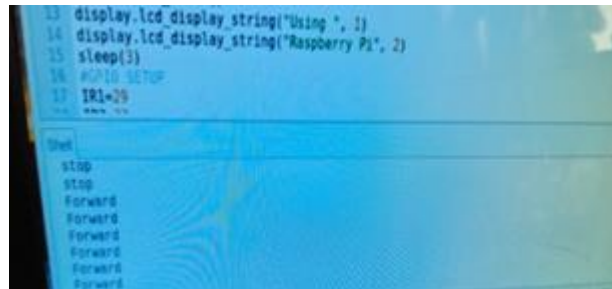
Fig. 12. LCD Display to stop vehicle .



Fig. 13. LCD display for obstacle location.

On similar lines, Fig.11. and Fig.12. depicts the stopping of vehicle on detection of obstacle. The IR sensor detects the precise location of obstacle and displays a message "Left side obstacle on road" on LCD.

Fig.14. Shows the code output generated in shell script. The code tells about the status of the vehicle whether moving forward, stop ,left, or right.



```

13 display.lcd_display_string('Using ', 1)
14 display.lcd_display_string('Raspberry Pi', 2)
15 sleep(3)
16 #GPIO SETUP
17 IR1=20
18
Shell
stop
stop
forward
forward
forward
forward
forward

```

Fig. 14. Automatic Moving code snapshot.

IV.CONCLUSION

Road deaths in India are among the highest in the world, and they are steadily increasing over time. Therefore, a mechanism that can lower fatalities across the nation is required. To prevent such accidents, innovative smart city solutions are widely desired. In this project, a self-driving autonomous car is built with the help of a Raspberry Pi and various sensors are interfaced for use in accident prevention applications. The paper includes results and a prototype. Additionally, sensor data is uploaded to think speak and is accessible for real-time monitoring.

V. REFERENCES

- [1]. S. Sarker, M. S. Rahman and M. N. Sakib, "An Approach Towards Intel- ligent Accident Detection, Location Tracking and Notification System," 2019 IEEE International Conference on Telecommunications and Pho- tonics (ICTP), 2019, pp. 1-4, doi: 10.1109/ICTP48844.2019.9041759.
- [2]. Arjun K., Prithviraj and Ashwitha A. (2017), "Sensor Based Application for Smart Vehicles", International Journal of Latest Trends in Engineer- ing and Technology, 8 (1), pp. 526-532.
- [3]. Rangan P. R. (2017), "Vehicle Speed Sensing and Smoke Detecting System", International Journal of Computer Science and Engineering, pp. 27-33
- [4]. A. Ali and M. Eid, "An automated system for accident detection," in I2MTC'15, 2015, IEEE, pp 1608-1612
- [5]. P. Nath and A. Malepati, "IMU based Accident Detection and Intimation System," in Proc. IEMENTech'18, 2018, IEEE, pp 1-4.
- [5]. P. Nath and A. Malepati, "IMU based Accident Detection and Intimation System," in Proc. IEMENTech'18, 2018, IEEE, pp 1-4.
- [6]. Prasanth P. and Karthikeyan U. (2016), "Effective Trackingof Misbe- haviorial Driver Over Speed Monitoring With Emergency Support", International Journal of Advanced ResearcCompuetechnology, 5 (10), pp. 2527-2529

- [7]. H. M. Sherif, M. A. Shedid, and S. A. Senbel, "Real Time Traffic Accident Detection System using Wireless Sensor Network," in Proc. SoCPaR'14, 2014, IEEE, pp 59-64.
- [8]. Report by J.P. Research India Pvt Ltd, Mumbai-Pune expressway Road accident study.
- [9]. P. Fabian, A. Rachedi, and C. Gue'guen, "Programmable objective function for data transportation in the Internet of Vehicles," Trans. Emerg. Telecommun. Technol., vol. 31, no. 5, 2020, Art. no. e3882, doi.
- [10]. T. Mekki, I. Jabri, A. Rachedi, and M. Ben Jemaa, "Vehicular cloud networking: Evolutionary game with reinforcement learning-based access approach," Int. J. Bio Inspired Comput., vol. 13, no. 1, pp. 45-58, 2019, doi.
- [11]. J. Smolka and M. Skublewska-Paszowska, "A method for collision detection using mobile devices," in Proc. 9th Int. Conf. Human Syst. Interact. (HSI), 2016, pp. 126-132, doi.
- [12]. R. K. Kodali and S. Sahu, "MQTT Based Vehicle Accident Detection and Alert System," in ProiCATccT'17, 2017, IEEE, pp 186-189.
- [13]. N. T. S. A. Wadhahi, S. M. Hussain, K. M. Yosof, S. A. Hussain and
- [14]. V. Singh, "Accidents Detection and Prevention System to reduce Traffic Hazards using IR Sensors," 2018 7th International Conference on Reliability, Infocom Technologies and Optimization (Trends and Future Directions) (ICRITO), Noida, India, 2018, pp. 737-741, doi: 10.1109/ICRITO.2018.8748458.
- [15]. J. Singh et al., "IR Sensor Based Accident Prevention System for Hilly Areas," 2023 International Conference on Disruptive Technologies (ICDT), Greater Noida, India, 2023, pp. 786-789, doi: 10.1109/ICDT57929.2023.10150715.
- [16]. M. Kumar, A. Kant, P. Kaktan, R. Bishnoi and K. Upadhyay, "Arduino Based System to Prevent Vehicle Accidents," 2021 International Conference on Design Innovations for 3Cs Compute Communicate Control (ICDI3C), Bangalore, India, 2021, pp. 140-144, doi: 10.1109/ICDI3C53598.2021.00037.
- [17]. V. Kinage and P. Patil, "IoT Based Intelligent System For Vehicle Accident Prevention And Detection At Real Time," 2019 Third International conference on I-SMAC (IoT in Social, Mobile, Analytics and Cloud) (I-SMAC), Palladam, India, 2019, pp. 409-413, doi: 10.1109/I-SMAC47947.2019.9032662.
- [18]. P. D. R. Dewmin, P. S. H. Yapa, S. D. Lokuge, M. G. N. M. Pemadasa and N. Amarasena, "License Detection and Accident Prevention System," 2022 4th International Conference on Advancements in Computing (ICAC), Colombo, Sri Lanka, 2022, pp. 381-386, doi: 10.1109/ICAC57685.2022.10025352.
- [19]. G. Ravindra, M. V. Rao and V. S., "Sensor Assisted Ghat Road Navigation and Accident Prevention," 2022 International Conference on Automation, Computing and Renewable Systems (ICACRS), Pudukkottai, India, 2022, pp. 1402-1407, doi: 10.1109/ICACRS55517.2022.10029037.
- [20]. R. Mounika, S. Hussian. Sk and L. Venkateshwara Kiran, "A Novel Approach for Accident Prevention Using IOT," 2019 International Conference on Vision Towards Emerging Trends in Communication and Networking (ViTECoN), Vellore, India, 2019, pp. 1-5, doi: 10.1109/ViTECoN.2019.8899717.
- [21]. L. Rupesh, A. Jain, S. Sarada, S. Gupta, S. I. Sajeesh and D. Palanisamy, "IoT and Cloud Based Integrated System for Accident Reporting and Vehicular Health Monitoring," 2018 Fourth International Conference on Research in Computational Intelligence and Communication Networks (ICRCICN), Kolkata, India, 2018, pp. 23-26, doi: 10.1109/ICRCICN.2018.8718699.

Scalable Design and Implementation IP for Advanced Extensible Interface (AXI) Protocol

Kaveri A. Sangamnerkar, Yogita D. Kapse, Nilima R. Kolhare

Department of E&TC, COEP Technological University, Pune, Maharashtra, India

ABSTRACT

The VLSI industry for semiconductors has undergone a transformation thanks to System-on-Chip technology. Recently, semiconductor hobbyists have been using a revolutionary approach, primarily over the past ten years, to integrate millions of ICs onto a silicon wafer. The on-chip communication is made possible by the communication protocols, which are crucial. AXI is a high-performance and efficient protocol that facilitates point-to-point transfers and interconnections. AXI is the most used AMBA protocol because of its distinct channel-wise distribution and hand-shaking. A scalable design for the Advanced Extensible Interface (AXI4.0Lite) protocol, a part of AMBA architecture, that provides control between the channel signals of protocol is presented in this work for master and slave configuration. It facilitates a simple and practical way to connect multiple IP cores in a system-on-chip or FPGA architecture, particularly for peripheral or control register access. The design is represented on the Intel Quartus Prime Lite 20.0 using Verilog for hardware description.

Keywords—VLSI, AXI, AMBA, System-on-Chip, communication, protocol, scalable

I. INTRODUCTION

The AXI is a part of Advance Microcontroller Bus Architecture (AMBA) developed by ARM. The AMBA makes it possible to design with a wide range of integrated and directly usable processing units and peripherals on the System on Chip. As opposed to other AMBA protocols like APB and AHB, the AXI provides substantially greater performance and throughput, making it a commonly used and acknowledged standard for constructing on-chip communication IPs. A subset of the AXI4 protocol called AXI4.0 Lite is frequently used in applications with defined burst lengths. AXI4-Lite's simplicity aids in lowering the interface's overall latency. Time-sensitive applications can benefit from its ability to communicate quickly and effectively between the master and slave modules. In this version of AXI, the data length is likewise expected to be fixed at 32 or 64 bits. The protocol, as depicted in Fig. 1, essentially establishes communication between its Masters and Slaves/Memory by using the Handshaking mechanism. The construction of a scalable architectural design for the AXI4.0 Lite Protocol employing sophisticated Verilog as a Hardware Description Language is the main emphasis of this work. State Machine (FSM) concepts are used to create an easy-to-understand and implement design that facilitates control between different protocol signals. For each of the master and slave's channels, a design is

created. Additionally, FPGA implementation of the synthesizable design is also carried out for hardware verification of the design functionality.

A. The AXI4.0 Basic Structure.

The protocol establishes communication between the master and slave using a handshaking approach. To execute the read/write transactions, the AXI protocol primarily consists of five communication channels, as depicted in fig. 1. They are listed as follows:

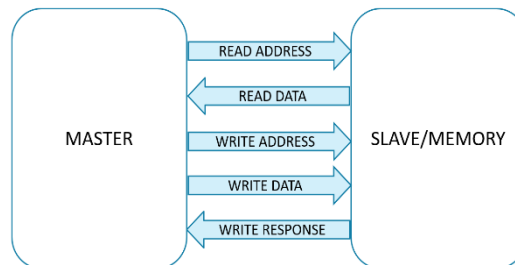


Fig. 1. Basic Structure of AXI.

Write Address Channel is specifically used by Master to know the address in slave on which the data is to be written. This channel includes the valid (AWVALID), ready (AWREADY), address (AWADDR) and protect (AWPROT). Write Data Channel enables the Master to write into the memory/slave. The signals that function within this communication channel are valid (WVALID), ready (WREADY), data (WDATA) and strobe (WSTRB). Write Response Channel helps the slave to send a response to the master after the data write operation has taken place. The signals that are directed within this channel are valid (BVALID), ready (BREADY) and response (BRESP). Read Address Channel employs its signals to read address from slave from which the data is to be read. The signals in this channel are valid (ARVALID), ready (ARREADY), address (ARADDR) and protect (ARPROT). Read Data Channel is utilised by the slave to read from the master with signals valid (RVALID), ready (RREADY), data (RDATA) and response (RRESP).

B. Signals in AXI4.0 Lite

a) The AXI is operational based on signals and controls between them. The protocol has two global signals clock (ACLK) and negedge reset (ARESETn). These signals are globally provided to all the channels for synchronisation and orderly operations. Valid signal is initiated by the master or slave depending on who is initiating the transaction. When the receiving segment is ready for the transaction, it sends back the ready signal. This enables reduction of power consumption. In order to read address from the slave or to write address, separate address signals are enabled. To read and write specific data within the master and slave channels, data signals are employed. If the channel wants to ensure if the read transaction is successful or a failure after the exchange of ready and valid signals, a response signal is generated. The responses are OKAY, EXOKAY, SLVERR and DECERR. 'Protect' is a special feature of AXI4.0 Lite. Due to this signal, secured reads and writes are carried out. Various values denote different access permissions such as unprivileged access, secure access, data access etc. 'Strobe' is also an exclusive feature of AXI4.0 Lite. It is used to mask particular bits of the write data channel and is used to enable the write action for specific desired bits.

TABLE I. SIGNALS OF AXI4.0 LITE PROTOCOL

Global Inputs	Write Address Channel	Write Data Channel	Write Response Channel	Read Address Channel	Read Data Channel

ACLK	AWVALID	WVALID	BVALID	ARVALID	RVALID
ARESETn	AWREADY	WREADY	BREADY	ARREADY	RREADY
	AWADDR	WDATA	BRESP	ARADDR	RDATA
	AWPROT	WSTRB		ARPROT	RRESP

II. RELATED WORK

A novel approach of the design for real time micro-architecture for interconnects has been devised by Zhe Jiang [1]. This design finds applications in highly integrated SOCs for higher throughputs. A performance-based comparison of various AMBA on chip communication protocols is presented by Anurag Shrivastava[2]. The protocols AMBA 2.0, AMBA3.0, AMBA4.0 AHB and AXI were compared based on performance, power consumption, speed and other design parameters in this work. Arun C G has proposed an Interface for Single Master and Singular slave has been designed for various burst operations[3]. The design is verified for functionality using the Universal Verification Methodology (UVM). Verification of all important features of five channels of AXI has been carried out by M Prasanna Deepu[4]. System Verilog has been used as a verification language for a coverage driven report. AXI protocol specifications were studied with the help of specification guide provided by ARM Limited[6]. Neethika[7], has designed a network on chip interface for AXI protocol with further PLD prototype.

III. PROPOSED METHODOLOGY

A design establishing control between the master and slave is proposed in this work that essentially uses the state machine algorithms as a basis of control and communication. The channels of AXI for the master and slave have been designed, each as a controlling unit state machine with various states through which the transfer mechanism takes place. These states are controlled by the signals of AXI included in that particular channel. The master and slave are further integrated together in the AXI top level entity.

A. Handshaking Mechanism.

The protocol obeys a handshaking mechanism that ensures a secure communication with reduction of power loss. A signal is passed from the master to slave and the slave returns back an acknowledgement to master so as to notify the receipt of signal from the master and vice versa. This process ensures that the data bits are transmitted and there's no loss of bits in between the channel.

B. Control Unit

The channels are designed as state machines whose states are controlled and determined by various signals of the protocol. The state table and state diagrams for each channel fsm is formed based on the signal enabling conditions and the design is developed accordingly.

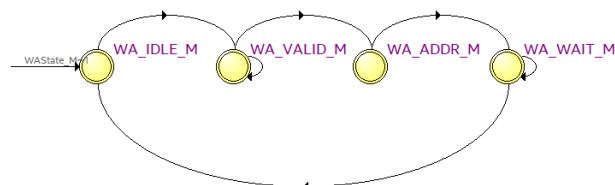


Fig. 2. State Diagram for Write Address Channel of Master.

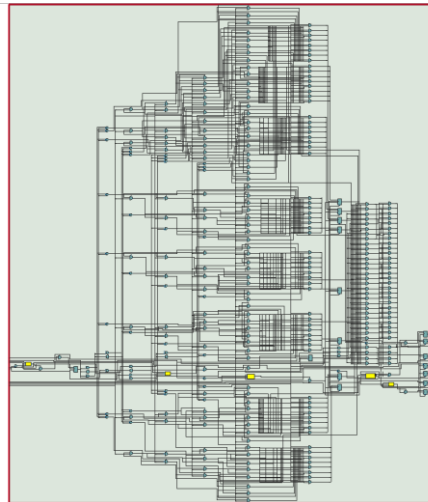


Fig. 5. RTL Design for AXI slave.

Fig. 4 shows the transcript snapshot that is taken once the simulation is stopped after the data transfer of Master is completed.

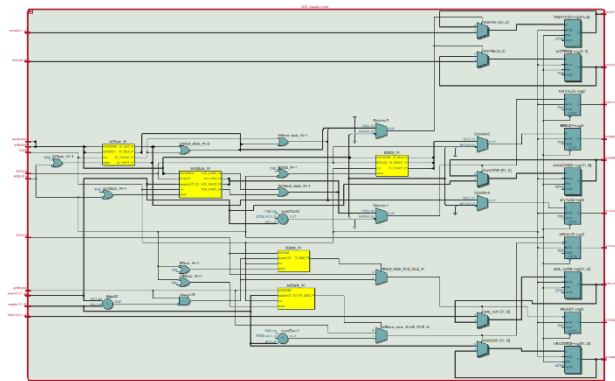


Fig. 6. RTL Design for AXI master.

Fig. 5 and 6. shows the RTL generated for master and slave of AXI. We can see that both the RTL consists of five FSMs, one for controlling each channel transactions, further interconnected by input and output decoders, integrated together to form a synthesizable RTL design for Master and Slave.

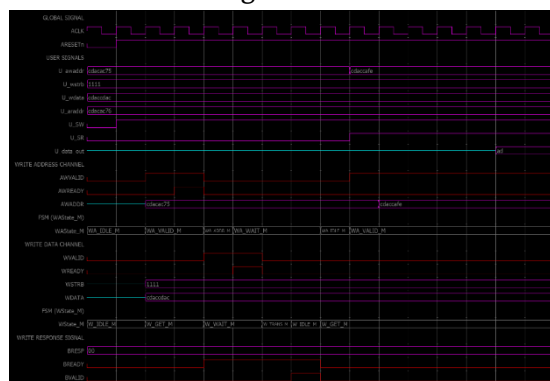


Fig. 7. Simulation result for AXI master.

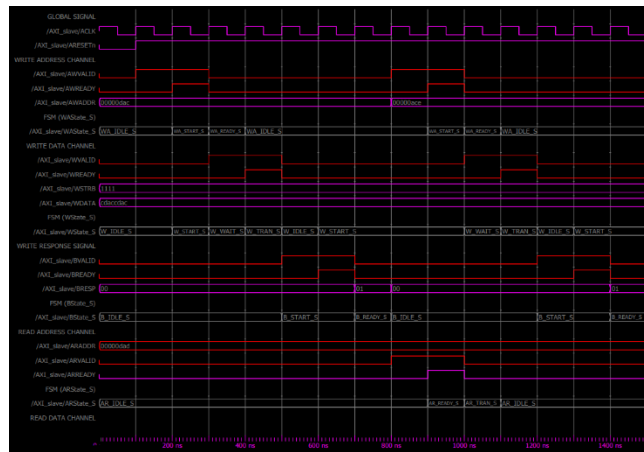


Fig. 8. Simulation result for AXI slave.

As seen in Fig. 8 and Fig. 9, the simulation for master and slave channels is generated, one can see that the ready signals are turned high on the next cycle of valid signals and the FSMs vary in the various states according to the signals.

V. CONCLUSION AND FUTURE SCOPE

The design for AXI4 Lite is thus developed for all its channels and the functionality is checked from the simulation results. The scalable design for AXI4.0 Lite can be utilized for the on-chip communication for establishment of on chip communication. The parameterized design makes it scalable for all existing and further AXI versions. The functionality can further be implemented and verified using the Field Programmable Gate Arrays (FPGA) for all existing and further AXI versions. The functionality can further be implemented and verified using the Field Programmable Gate Arrays (FPGA).

REFERENCES

- [1]. Zhe Jiang, Kechen Yang, Nathan Fisher, Ian Gray, "AXI-IC RT : towards a real-time AXI-interconnect for highly integrated SOCs," IEEE Transaction in Computers, 2023.
- [2]. Anurag Shrivastava, G.S. Tomar, Ashutosh Kumar Singh, "Performance Comparison of AMBA bus-based system-on-chip communication protocol," International Conference on Communication Systems and Network Technologies, 2011.
- [3]. Arun C G, Suganya .S, "Constrained random verification of burst operation in AXI-4," International Interdisciplinary Humanitarian Conference for Sustainability (IIHC), 2022.
- [4]. M. Prasanna Deepu, R. Dhanabal, "Validation of transactions in AXI Protocol using System Verilog," International conference on microelectronic devices, circuits and systems, 2017.
- [5]. Vazgen Melikyan, Stepan Harutyunyan, "UVM verification IP for AXI," IEEE East-West Design & Test Symposium (EWDTS), 2021.
- [6]. "AMBA AXI and ACE Protocol Specification," ARM IHI 0022H.
- [7]. Neethika Tidala, "High Performance Network On Chip using AXI4 protocol interface on an FPGA", Proceedings of the 2nd International conference on Electronics, Communication and Aerospace Technology (ICECA 2018).

A GSM-Based System for Vehicle Collision Detection and Alert

Dr. Pradeep Kumar N S¹, Suhas S K², Dr. Girish H², Mrs. Dhivya Karunya S³, Mrs. K Revathi³, Mrs. K Gayathiri³

¹Professor, Department of ECE, SEACET, Bengaluru, India

²Associate Professor, Department of ECE, Cambridge Institute of Technology, Bengaluru, India

³Assistant Professor, Department of ECE, SEACET, Bengaluru, India

ABSTRACT

Road accidents is one of the severe problems that leads the deaths of innocent pupil surrounding the world. India is currently at the highest of the list of road fatalities. This is a very severe problem that needs to be resolved to save the lives of many injured in the accident. With regards to WHO surveys and findings, more than 50% of people die each year from road accidents. Most of them suffer from cyclists due to head injuries. In the event of an accident, rescue of a person is delayed, so the proposed study aims to address this issue by building an automated system that alerts family members and nearby hospitals in the event of an accidents increase. In this work, we will introduce an accident prevention system with a vehicle accident detection function. This increases the chances of reducing the number of daily accidents on the road. At the same time, in the event of an accident, the system will locate it and automatically notify those who can respond immediately. Global Positioning System & # 40; GPS & # 41; and Global System for Mobile Communication (GSM) technology have built an Arduino-based system. Accelerometers are also used to measure the amount of vehicle speed and pitch when the vehicle collides with something. If the speed of the car exceeds the speed limit or falls.

Keywords— GPS, GSM, Accelerometer, Arduino

I. INTRODUCTION

The automobile industry's production has risen steadily over the world in recent years. Annually, millions of automobiles are manufactured. As a result of the increased traffic, the number of accidents is also rising. Because of a lack of competent treatment, many people have died in traffic accidents.[1] This accident on the highways and in a distant location has resulted in a large number of deaths and is a danger to society. The number of automobiles on the road is increasing faster than the economy and population. Road accidents and deaths, particularly among two-wheelers, are on the rise at an alarming rate.

Most crash fatalities are due to lack of prompt medical attention on highways and other roads. Accident site emergency medical facilities can further reduce fatalities. Hence the idea of an alarm system that recognizes the accident and its severity, alerts a nearby medical center, and brings an ambulance or medical assistance to the scene of the accident.

The proposed system will check if an accident has occurred and determine the extent of injury to the victim/driver. If the accident is determined to be serious, locate the nearest medical center and report the

accident. The exact location is transmitted via the victim's mobile phone so emergency services can reach the scene without delay. The system also sends messages to friends and relatives to inform them of the incident.

In recent years, studies on accident detection/alarm systems have been actively conducted. [2] In this topic, research presented a model with two main modules. The purpose of this system is to track the location of the vehicle using a GPS receiver and send that information to the owner's mobile phone via his SMS. Another prototype proposes a method to identify traffic accident victims and provide assistance more quickly. Here, a low-cost alert system is proposed to provide immediate medical assistance to accident victims by alerting the local medical assistance center with the exact location of the accident and patient details via SMS.

However, many if paramedics receive timely crash information, despite numerous attempts by different government and non-governmental groups around the world through various initiatives to raise awareness of the problem. Life should have been saved. A study by Virtanen et al. Shows that 4.6% of accident fatalities could be prevented only if rescue services were available at the time of the accident. Therefore, efficient automated accident detection with automatic notification of rescue services, including information about the location of the accident, is a fundamental requirement for saving valuable lives.

II. LITERATURE REVIEW

A This paper proposes to use a GPS receiver's capabilities to monitor a vehicle's speed, detect an accident based on the monitored speed, and broadcast the location and time of the accident using GPS data processed by a micro-Controller to the Alert Service Centre through the GSM network [1]. The interval between starting to brake and coming to a complete stop is greater at high speeds. [3] The square of speed determines braking distance. As a result, the chances of avoiding a collision decrease. A speedometer can also be used to detect speed reductions in automobiles, but it requires an analogue to digital converter to do so. As a result, a GPS is utilized to track the vehicle's speed at all times.

The vehicle speed is calculated at every instance by GPS. If there is decrease in new speed values then it raises an ALARM for accident detection. Then 10 secs will be given to abort the emergency Else the emergency is sent to Alert Service Centre and plot the location of accident by the GSM number received. There after rescuing the individual. This study proposes to use the features of accelerometers to collect data and identify accidents. It then sends the location of the accident, determined by the GPS data processed by the microcontroller, over the GSM network to the nearest hospital available on the network to alert the family. [4] If the angle is greater than 46 degrees and less than -46 degrees, the car will roll over. The weight and center of gravity of the vehicle, in addition to the rolling and pitching limit frequency values, have a decisive effect on rollover. When the threshold is reached, the notification mechanism is activated to alert the family and the nearest hospital to the rollover.

In addition, a GPS tracker is used to record false assumptions from the captured GPS data. The notification system shares information with family emergency contacts and the nearest hospital. When the detection threshold is reached, the notification system becomes active. The location is identified by GPS.

In this study, the function of the piezoelectric sensor is used to identify the accident based on the voltage generated by the collision, and the GPS data processed by the microcontroller is used to alert the location and time of the accident on the GSM network.

We suggest reporting to the service centre. Piezoelectric sensors generate a DC voltage that is proportional to the impact of the vehicle. When the voltage exceeds a certain value, the sensor is triggered.

The GPS module determines the latitude and longitude and is forwarded as a message to the rescue service via the GSM module. Another GSM module receives the message. Map created by Google. [5] Receive detailed SMS from the accident site. As a result, the coordinates change slightly. An OFF switch is also available if necessary to avoid false alarms.

Table 1: Comparison between Research Paper

	Research/Technical Paper	process	Advantage
Approach1	Accident Detection using GPS and GSM Technology.	Detects Accident and location is sent over GPS to mobile through GPS.	Just detects the location of accidents and alerts to the mobile.
Approach2	Accident Detection through GPS, GSM and Accelerometer.	Detects the location of accident by detecting the changes in the orientation levels of accelerometer	Detects the collision by the accelerometers.
Approach3	Read time detection using vibration sensor	Detects the accident by collision by voltage generated through sensors by collision	Sending of location To near-by hospitals through network.

III. METHODOLOGY

We presented this accident detection and alarm system project in order to protect the driver's life in all types of accident situations. We utilized an Arduino UNO to connect a GPS GY6MV2 receiver and a GSM module SIM 800L in our model. The X and Y axis co-ordinates of the car will be captured by the MEMS Accelerometer, and the GSM SIM 800L will send a notification message to the family members' registered contact numbers. [6] The GPS module continuously records the vehicle's latitude and longitude. If the mishap is minimal and does not necessitate notifying family members and requesting an emergency, we will use a reset button to stop the message from being sent.

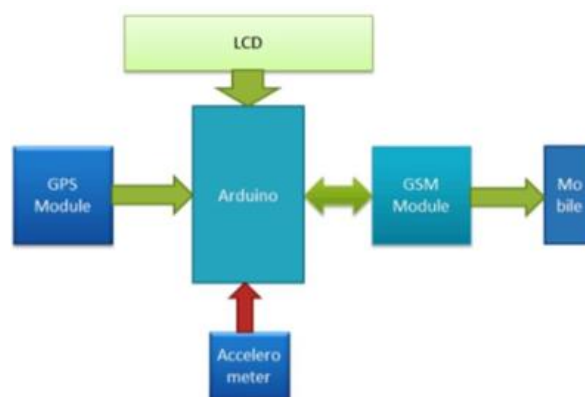


Fig 1. Block Diagram of the Accident Alert system

In Figure 1 shows an accident warning system from GPS modules, GSM modems, accelerometers to Arduino miniature controllers. The GPS module endlessly identifies the location of an accident as its perimeter and longitude. The accelerometer gets the X and Y coordinates of the vehicle, and when the coordinates exceed the

limit, the miniature controller sends a signal. The miniature controller activates the SIM 800L GSM module and sends notifications to family members.

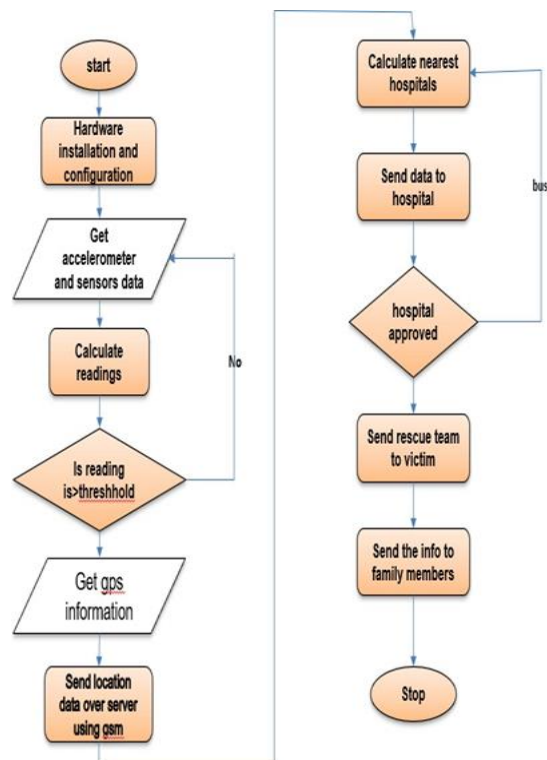


Fig 2. Flow chart

Monitors vehicle speed and detects sudden drops in vehicle speed. An Arduino UNO is used as the controller and reads the values from the accelerometer. An accelerometer detects if the axis is falling. When the Arduino observes a sudden change in vehicle speed. Read your current location from GPS module and send it to your mobile number via SMS via GSM module. [7] The Arduino will buzz before sending his SMS, and after 30 seconds it will buzz and he will send the SMS. However, if the passenger is not in danger, they can press the "I'm fine" button. This is done to avoid situations that lead to erroneous and accidental rescues.

System Implementation

The proposed system can be extremely useful in detecting automobile crashes, and when one occurs,[8] it will send a text message to family, hospitals, and police stations, among other places, in order to provide medical assistance to passengers as promptly as possible. The system is built on a microcontroller and interacts with a variety of sensors and modules, including an accelerometer, limit switch, GPS system, and GSM module. The accelerometer and limit switch are crucial components in this system for detecting the accident. The Arduino UNO board is chosen as a microcontroller device in this system since it is readily available and simple to implement. The next section goes through the many aspects of the proposed plan.

Arduino

The Arduino UNO board is used as a microcontroller device in this setup. The Arduino board is currently being used in a variety of IoT-based applications due to its ease of integration with a variety of devices (such as

sensors, different modules, etc.). The Arduino platform was used for the programming portion. [9] It comes with an Integrated Development Environment that allows it to communicate with a variety of devices. A programming language, such as C, is an open-source software that can be used to interface with the Arduino hardware and upload any program over USB.

Accelerometer

The acceleration is measured using an accelerometer, which is an electromechanical device. It can be dynamic (moving or vibrating) or static (still) (such as the constant force of gravity). The accelerometer is a transducer that detects the movement of an item by measuring the acceleration imparted. The ADXL335 Accelerometer, a three-axis accelerometer, is employed in this system. [10] It's a low-profile MEMS sensor that's made up of micro-machined structures on a silicon wafer suspended by a poly-silicon spring. It calculates the object's coordinates in relation to the earth using gravitational pull. It has two supply pins and three analogue pins for the three axes. It is mostly used for car-crash detection, scrolling, and other similar tasks.

GPS System

This module is extremely useful for tracking the location of an accident using the GPS system. This information can also be utilized to track the vehicle's speed, which is very useful in predicting the likelihood of an accident. The NEO 6M GPS module was utilized to track the vehicle's location in this system. The main advantage of this module is that it can easily be combined with the Arduino module, that it is simple to operate, and that it responds quickly, which is very helpful for sending the location to a specified number in order to receive assistance as soon as possible. There are 27 satellites orbiting the earth, and three of them are used to track the location.

GSM Module

A GSM module is a type of circuit that allows a mobile device to communicate with a GSM system. The most significant portion of this module is the modem, which is powered by the power supply circuit and used to connect to the network and send messages.[11] GSM-based communication systems are extremely useful for transmitting information to the police station, family members, hospitals, and other locations. The information on the Arduino board has been relayed in this system. To send/receive texts and make/receive phone calls to the predefined person, we utilize the GSM module SIM900A, which is attached to the Arduino board. The module operates at 3A power supply and uses Dual-Band 900 MHz and 1800 Mhz. Both limit switches are used in this system.

IV. RESULTS AND DISCUSSIONS

An experimental arrangement for vehicles has been devised in this work to continually relay the location when an accident happens. The experiment is carried out here different angles, and to double-check the correctness of the measurements. It is tried numerous times at the place with the time delay. From the data and observations gathered from the projected some findings are obtained using the model. The system keeps track of everything. The longitude and latitude of the locations where the car is parked Creating a virtual

environment necessitates unintentional observation. Environment. We have taken the following steps in this experiment.

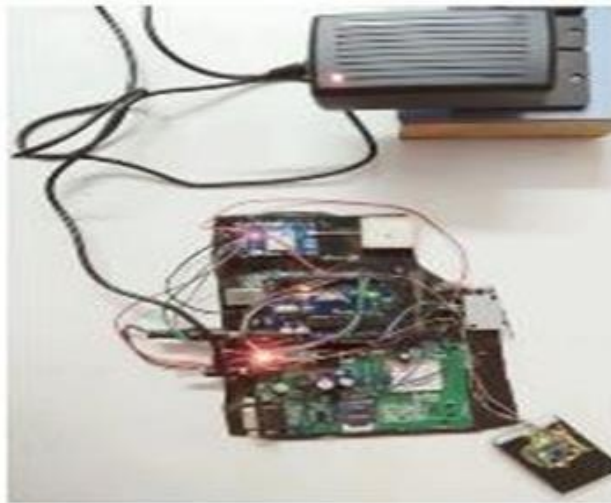


Fig 3: Experimental setup

We must ensure that the connection between Arduino and GSM is formed. There are two ways to achieve it: one is to link the TX pin of the GSM module to the RX pin of the Arduino, and the other is to connect the RX pin of the GSM module to the TX pin of the Arduino

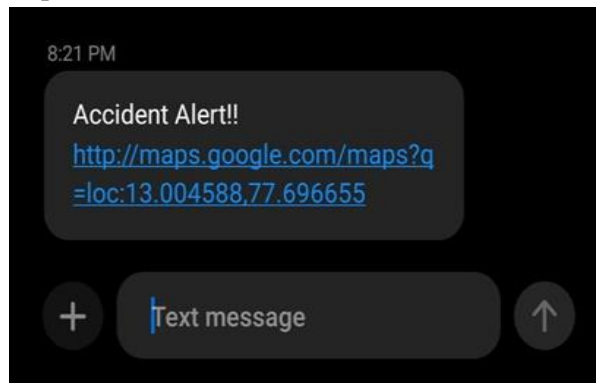


Fig 4: Output of GSM Module When Accident Occurs Receiving accident location message



Fig 5: Hardware Model of Accident Alert System

When our vehicle is struck from the front by another vehicle, we are said to be involved in a front accident. When our vehicle is struck from the left side by another vehicle, it is considered a left accident. The X and Y coordinates of our car will be detected by the MEMS Accelerometer.

When our vehicle is struck from the right side by another vehicle, it is considered a right accident. Our vehicle's X and Y coordinates will be detected by the MEMS Accelerometer. When our vehicle is hit from behind by another vehicle, it is considered a back accident. Our vehicle's X and Y coordinates will be detected by the MEMS Accelerometer.

The second method is to choose two Arduino pins that are PWM enabled (Pin 9, 10). It makes use of Arduino's software serial library, and once connected, data may be sent immediately to GSM.

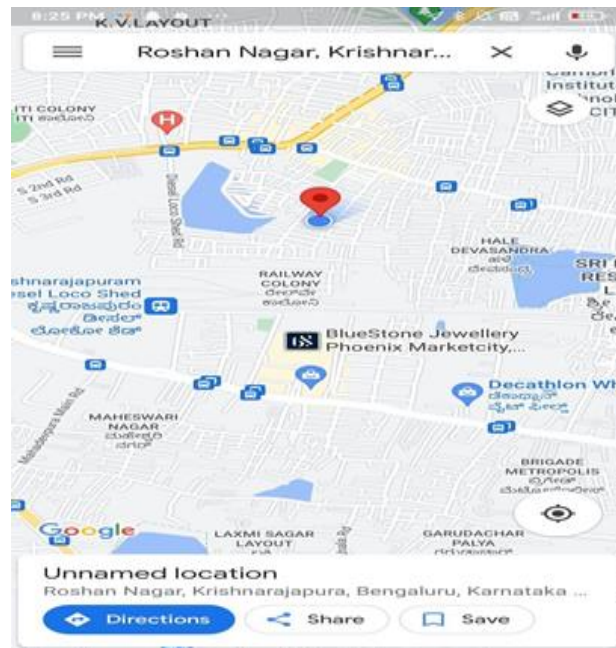


Fig 6: Receiving accident location message with google map link

In order to reduce accidents, we proposed this system that uses a GSM module to send warning messages to accident families and a GPS modem to continuously record the location of the accident site. Send the latitude and longitude of the accident site. When a vehicle collides with another vehicle, an ADXL335 MEMS accelerometer is used to detect the axis change. The MEMS accelerometer gets the X&Y axis values.

The proposed technique helps to reduce the number of people killed in car accidents. With the help of the proposed methodology, it detects the accidents that have occurred using the GPS module, determines the location of the accident and sends an alarm message using a GSM module to travel to the location of a medical emergency accidents happen all the time, and they can save people's lives. The death rate is reduced as a result of this feature accident- related deaths and injuries can be reduced.

V. CONCLUSION

We have created a mechanism to detect accidents. The proposed system handles accident detection and warning. It identifies the exact latitude and longitude of the accident vehicle and sends this information to the nearest emergency service. Arduino helps send messages to various components in the system. The direction of the accident is monitored by an accelerometer and the vehicle rollover is determined by the gyroscope. The data will be sent to the registered phone number via the GSM module. Locations are provided via a GPS

tracking system and cover the geographic coordinates of the entire area. Due to the popularity of vehicles, traffic accidents and road breakdowns are also increasing. People's lives are at stake. This is a direct result of our country's inability to access major issues.

II. REFERENCES

- [1] T Kalyani, S Monika, B Naresh, Mahendra Vucha, Accident Detection and Alert System, IJITEE, March 2019.
- [2] Parag Parmar, Ashok M. Sapkal, Real time detection and reporting of vehicle collision, IEEE, 2020.
- [3] Md. Syedul Amin, Jubayer Jalil, M.B.I. Reaz, Accident Detection and Reporting System using GPS, GPRS and GSM Technology, IEEE, 2019
- [4] Gowshika B, MadhuMitha, G, Jayashree, Vehicle accident detection system using GPS, GSM modem, IRJET
- [5] Sayanee Nanda, Harshada Joshi, Smitha Khairnar, An IOT Based Smart System for Accident Prevention and Detection, IEEE, 2018.
- [6] Norsuzila Yaacob, Ainnur Eiza Azhar, Azita Laily Yusofl, Suzi Seroja Sarnin, Darmawaty Mohd Ali and Ammar Anuar, Real Time Wireless Accident Tracker using Mobile Phone, IEEE
- [7] S. Sonika, Dr. K. Sathyasekhar, S. Jaishree, Intelligent accident identification system using GPS, GSM modem, DARCCE,
- [8] Girish H, Iot operated wheel chair, IJER, Vol-5, ISSN: 2347-5013, may 2016.
- [9] Girish H, Sridhar S, Bharath H, Vishvesh V, Gowtham K V, "IOT based transformer power theft detection and protection", IJER, Vol-5, ISSN: 2347-5013, may 2016
- [10] Girish H. "Intelligent Traffic Tracking System Using Wi-Fi." International Journal for Scientific Research and Development 8.12 (2021): 86-90.
- [11] GIRISH H , "Internet of Things Based Heart Beat Rate Monitoring System", © September 2022 | IJIRT | Volume 6 Issue 4 | ISSN: 2349-6002 IJIRT 156592 INTERNATIONAL JOURNAL OF INNOVATIVE RESEARCH IN TECHNOLOGY 227
- [12] A. Devipriya, H. Girish, V. Srinivas, N. Adi Reddy and D. Rajkiran, "RTL Design and Logic Synthesis of Traffic Light Controller for 45nm Technology," 2022 3rd International Conference for Emerging Technology (INCET), 2022, pp. 1-5, doi: 10.1109/INCET54531.2022.9824833.
- [13] Girish H, Shashikumar D R, "A Novel Optimization Framework for Controlling Stabilization Issue in Design Principle of FinFET based SRAM", International Journal of Electrical and Computer Engineering (IJECE) Vol. 9, No. 5 October 2019, pp. 4027~4034. ISSN: 2088-8708, DOI: 10.11591/ijece.v9i5.pp.4027-4034
- [14] Girish H, Shashikumar D R, "PAOD: a predictive approach for optimization of design in FinFET/SRAM", International Journal of Electrical and Computer Engineering (IJECE) Vol. 9, No. 2, April 2019, pp. 960~966. ISSN: 2088-8708, DOI: 10.11591/ijece.v9i2.pp.960-966
- [15] Girish H, Shashikumar D R, "SOPA: Search Optimization Based Predictive Approach for Design Optimization in FinFET/SRAM", © Springer International Publishing AG, part of Springer Nature 2019 Silhavy (Ed.): CSOC 2018, AISC 764, pp. 21–29, 2019. https://doi.org/10.1007/978-3-319-91189-2_3.

- [16] Girish H, Shashikumar D R, “Cost-Effective Computational Modelling of Fault Tolerant Optimization of FinFET-based SRAM Cells”, © Springer International Publishing AG 2017 R. Silhavy et al. (eds.), Cybernetics and Mathematics Applications in Intelligent Systems, Advances in Intelligent Systems and Computing 574, DOI 10.1007/978-3-319-57264-2_1.
- [17] Girish H, Shashikumar D R, “A Survey on the Performance Analysis of FinFET SRAM Cells for Different Technologies”, International Journal of Engineering and Advanced Technology (IJEAT) ISSN: 2249 – 8958, Volume-4 Issue-6, 2016.
- [18] Girish H, Shashikumar D R, “Insights of Performance Enhancement Techniques on FinFET-based SRAM Cells”, Communications on Applied Electronics (CAE) – ISSN: 2394-4714, Foundation of Computer Science FCS, New York, USA .Volume 5 – No.6, July 2016 – www.caeaccess.org
- [19] Girish H, Shashikumar D R, “DESIGN OF FINFET”, International Journal of Engineering Research ISSN: 2319-6890) (online), 2347-5013(print) Volume No.5 Issue: Special 5, pp: 992-1128, doi: 10.17950/ijer/v5i5/013 2016.

Design and Analysis of Parallel Slotted Multiband Microstrip Patch Antenna for Wireless Applications

Sreenvas Naik¹, Kiran Kumar K², Arun Kumar G³, Chandrappa D N⁴

¹Faculty, Department of Engineering, University of Technology and Applied Sciences, IBRI, OMAN.

²Assistant Professor, Dept. of ECE, East Point College of Engineering & Technology, Bangalore, Karnataka, India.

³Professor & HOD, Dept. of ECE, JSS Academy of Technical Education, NOIDA, Uttar Pradesh, INDIA.

⁴Associate Professor, Dept. of ECE, East Point College of Engineering & Technology, Bangalore, Karnataka, India

ABSTRACT

In this research article, we introduce a multiband- microstrip slotted antenna specifically designed for wireless communication applications. Microstrip patch antennas are extensively engaged due to their advantageous characteristics, including flexibility, robustness, compact size, lightweight nature, narrow radiation beam, and ease of installation and fabrication. Our proposed antenna is developed using a lossy FR-4 substrate with a permittivity of 4.3. It comprises a patch with four narrow slits and a ground plane, designed to generate a range of frequencies centered at 5.2 GHz, 9.33 GHz, and 12.038 GHz. To validate our design, we conducted simulations utilizing the CST MICROWAVE STUDIO software. These simulations enable us to analyze the performance behavior of the antenna across the desired frequency bands.

Keywords - microstrip, Multiband, Patch.

I. INTRODUCTION

Microstrip patch antennas are comprehensively utilized in various applications due to their appealing characteristics, such as a low profile, lightweight design, cost-effectiveness, compatibility with modern printed circuit technology, and integration capabilities with MMIC (Monolithic Microwave Integrated Circuit) design [1-3]. These features have made microstrip patch antennas popular in radar systems, microwave communication, and space communication. The construction of microstrip antennas involves a thin metallic strip, known as a patch, positioned above a ground plane. A dielectric sheet, referred to as the substrate, separates the strip patch and the ground plane. The resonating patch can be designed in various shapes, such as circular, square, elliptical, rectangular, or any other desired configuration [5- 7].

To achieve a smaller antenna size, we employ substrate materials with high dielectric constants [4]. Our primary objective is to enhance the operating bandwidth while simultaneously reducing the overall size of the antenna. The proposed antenna consists of a substrate with a height of 1.67mm and a dielectric constant of 4.3. To evaluate its performance, simulations are conducted using the CST MICROWAVE STUDIO software.

Wireless communication applications often necessitate antennas that can operate at multiple frequencies. Given its compact size, affordability, and lightweight nature, this antenna proves suitable for various applications such as radar communication, satellite TV communication, and K-band microwave communication. Simplicity is the major advantages of the proposed antenna. Its straightforward design allows for easy implementation and fabrication, thereby reducing manufacturing costs and time.

THE ANTENNA DESIGN

The antenna is structured using three layers, namely the patch, substrate, and ground. All dimensions are quantified in millimeters to ensure precise measurements. The planned antenna is integrated onto a FR-4 lossy dielectric sheet, which forms an essential part of its composition.

A. Wideband Microstrip Antenna

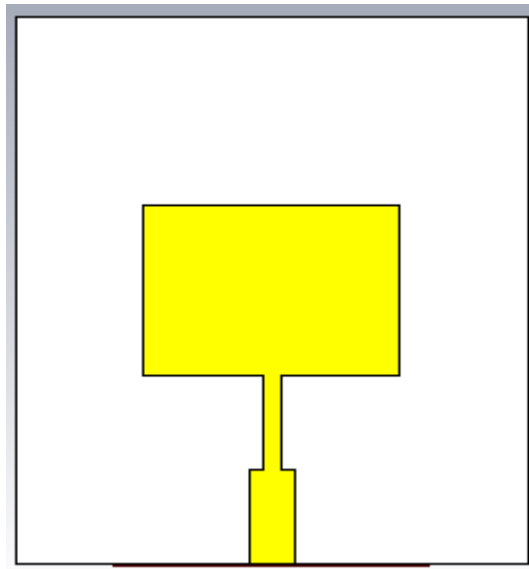


Fig.1: Basic patch antenna

The figure 1 illustrates a basic patch antenna designed to generate a single frequency. The essential formulas for calculating the width and length of such antennas are detailed below [1].

$$w = \frac{1}{2f_r \sqrt{\mu_0 \epsilon_0}} \sqrt{\frac{2}{\epsilon_r + 1}} = \frac{c}{2f_r} \sqrt{\frac{2}{\epsilon_r + 1}} \quad \dots\dots\dots(1)$$

$$L = \frac{c_0}{2f_r \sqrt{\epsilon_{reff}}} \quad \dots\dots\dots(2)$$

$$\epsilon_{reff} = \frac{\epsilon_r + 1}{2} + \frac{\epsilon_r - 1}{2} \left[1 + \frac{12h}{w} \right]^{-\frac{1}{2}} \quad \dots\dots\dots(3)$$

Patch	17.88X 13.51
Height of the substrate	1.60
QWT line width	1.27
QWT line length	7.45
Feed line width	3.16
Feed line length	7.41

I. The antenna results

$$\frac{\Delta L}{h} = \frac{0.412(\epsilon_{reff} + 0.3) \left(\frac{w}{h} + 0.264 \right)}{(\epsilon_{reff} - 0.258) \left(\frac{w}{h} + 0.8 \right)} \dots\dots\dots(4)$$

Where

L_{eff} = Effective patch length

c = Free space Velocity of light

f_r = Operating resonating frequency ϵ_r = Dielectric constant

h = Substrate thickness

The projected antenna underwent analysis and optimization using CST MWS software, resulting in the achievement of a tri-band patch slot antenna design. In this design, the first- band resonates at 5.10 GHz, with a reflection coefficient of -17.20 dB and a -10 dB bandwidth of 0.32 GHz. The second- band operates at 9.33 GHz, with a reflection coefficient of -21.90 dB and a -10 dB bandwidth of 1.002 GHz. Lastly, the third-band resonates at 12.03 GHz, with reflection coefficient of -23.053 dB and a bandwidth of 1.2942 GHz. The figure 3 showcases plot of reflection coefficient against frequency, providing a visual representation of the antenna's performance. The antenna basic parameters include a dielectric constant of $\epsilon_r=4.3$, a substrate height of $h=1.6\text{mm}$, and a resonating frequency of $f_r=5.2\text{GHz}$. The employed substrate material is FR-4 lossy.'

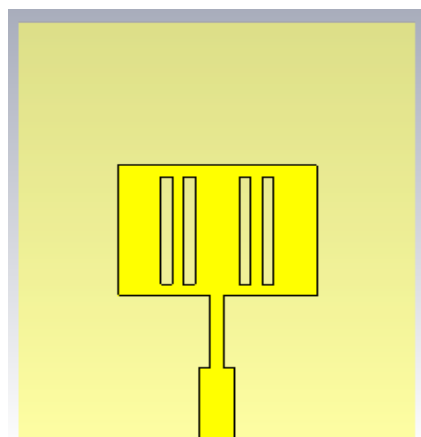


Fig.2: Geometry of the antenna with slots

Slots are introduced on the patch, where each slot is having length of 10.0 mm and width of 1.0 mm as shown in figure2.

Table 1: Dimension of antenna structure

Parameters	Dimensions
Ground	35.7X 27.02
Substrate material	35.7X 27.02

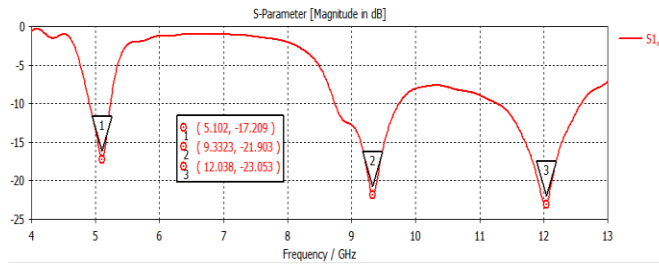


Fig.3: The return loss graph

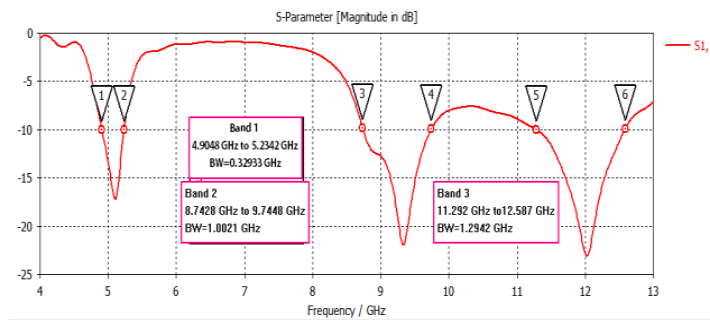


Fig.4: The bandwidth graph

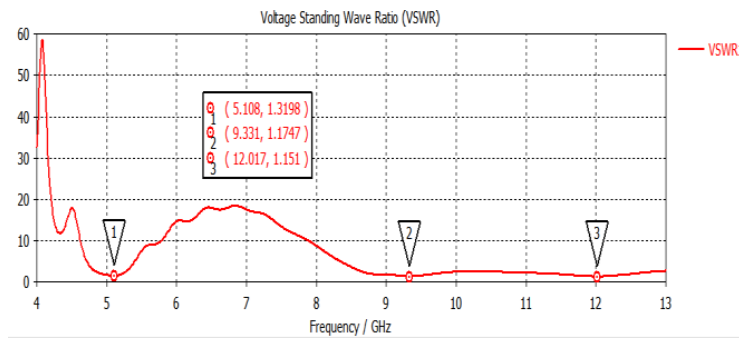


Fig.5: The VSWR graph

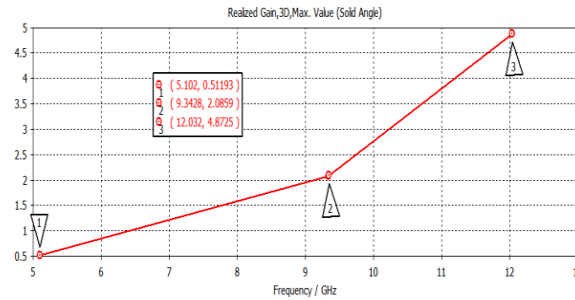


Figure 6: The gain plot

The projected antenna patterns have been thoroughly investigated. Figures 7, 8, and 9 depict the 2D patterns at 5.10 GHz, 9.33GHz, and 12.03 GHz. These patterns demonstrate the simulated total-field patterns, illustrating excellent wideband radiation characteristics at these radiating frequencies. To provide a more comprehensive view, figure 10, 11, and 12 showcase the 3D patterns specifically for the resonant frequencies of 5.10 GHz, 9.33GHz, and 12.03 GHz, respectively. These visual representations further highlight the antenna's radiation behavior at different frequencies.

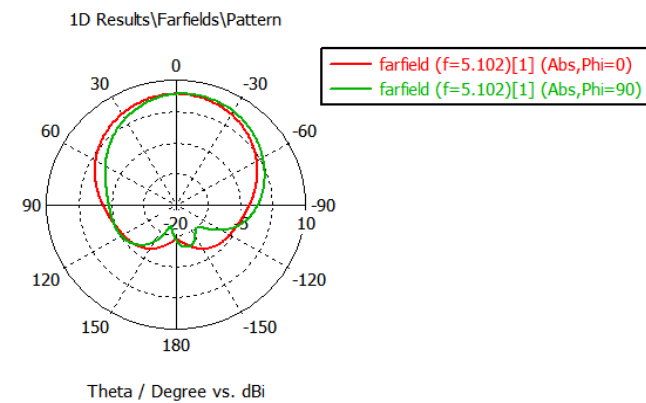


Fig.7: E and H-Planes at 5.10 GHz

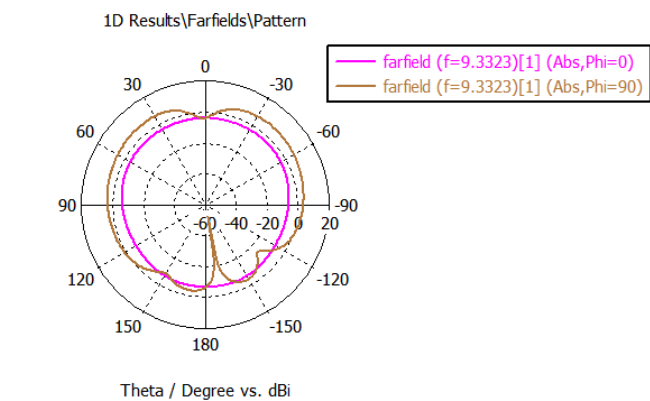


Fig.8: E and H-Planes at 9.33 GHz

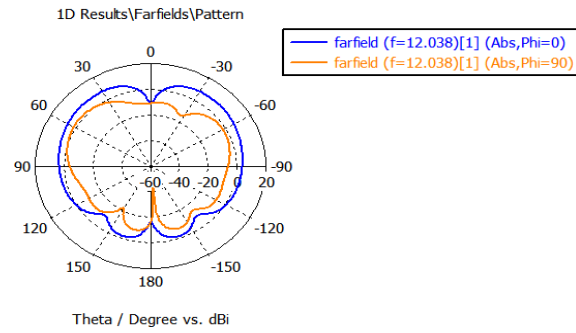


Fig.9 : E and H-Planes at 12.03 GH

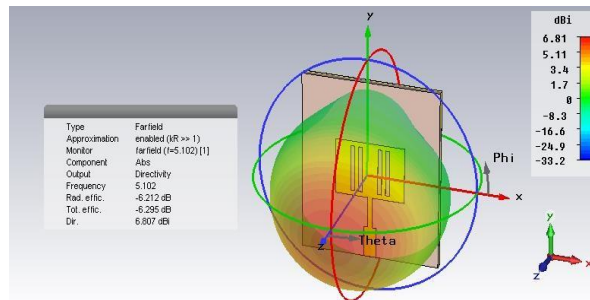


Figure 10: 3D pattern at 5.10 GHz

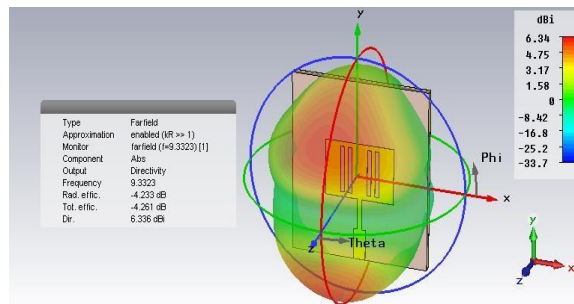


Fig.11: 3D pattern at 9.33 GHz

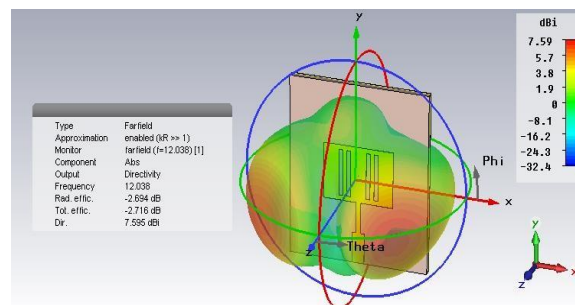


Fig. 12: 3D pattern at 12.03 GHz

The antenna gain provides an indication of its efficiency and directional capabilities. For the projected antenna, gains of 0.51193 dB, 2.0859 dB, and 4.8725 dB have been obtained at frequencies of 5.10 GHz, 9.33 GHz, and 12.038

GHz, respectively. These gain values illustrate the antenna's ability to focus and direct radiation in specific directions, thereby enhancing its overall performance.

TABLE II:
The antenna Performance

Parameters	Simulated results		
	5.108GHz	9.3323GHz	12.038GHz
Return Loss (dB)	-17.209dB	- 21.903dB	-23.053dB
Gain (dB)	0.51193	2.0859	4.8725
Directivity(dB)	6.807	6.33	7.59
Radiationefficiency	-6.21dB	-4.23dB	-2.29dB

II. CONCLUSION

The objective is to design, construct and simulate multi-band patch slotted antenna which operates in three distinct bands. The antenna design incorporates the microstrip feeding technique, and to achieve its functionality, the patch includes the insertion of four narrow slits. The antenna yields the following outcomes: The first-band resonates at 5.10 GHz, with a reflection coefficient of -17.20 dB and -10 dB bandwidth of 0.32 GHz. This band is appropriate for many applications, comprising mobile communication, wireless LAN, and radar communication. The second-band operates at 9.33 GHz, with a reflection coefficient of -21.90 dB and -10dB bandwidth of 1.002 GHz. This band is appropriate for satellite communication. The third-band operates at 12.03 GHz, with a reflection coefficient of -23.05 dB and -10dB bandwidth of 1.29 GHz. This band is appropriate for satellite and radar communications. The projected antenna displays minimum reflection loss and better gain at the frequencies of

5.10 GHz, 9.33 GHz, and 12.03 GHz, enabling its effectiveness in the desired frequency ranges.

II. REFERENCES

1. Rajendra Soloni, Rajappa H S and Chandrappa D N "Design and analysis of multiband reconfigurable microstrip patch antenna with switchable element" in Advances in Computing, Communications and Informatics (ICACCI), IEEE, 13-16 Sept. 2017, DOI: 10.1109/ICACCI.2017.
2. Chandrappa D.N., Mrs.Vani R.M. and P.V. Hunagund "Design and Implementation of Slotted Reconfigurable Microstrip Antenna for Wireless Application", International Journal of Electronics and Communication Engineering. ISSN 0974-2166 Volume 6, Number 3 (2013), pp. 233-239

3. Chandrappa D.N, P.A.Ambresh, P.V.Hunagund., "Design of compact reconfigurable multy frequency microstrip antennas for wireless applications" International Journal of Advanced Research in Computer and Communication Engineering (IJARCCE), Vol. 2, Issue 9, September 2013.
4. Chandrappa D N, Ambresh P A, Vani R M, P V Hunagund., "Multi-slots Reconfigurable MicrostripAntenna with Capacitive Loading Technique"., International Journal of Innovative Research in Computer and Communication Engineering, Vol. 2, Issue 1, Jan. 2014
6. Rekha D C, Rajappa.H.S, RajendraSoloni and Chandrappa.D.N "Design of dual band microstrip patch antenna for RFID" International Journal for Research Trends and Innovation, Volume 2, Issue 5, pp 253-257, 2017.
7. Jobins George and Shehana Pareeth "Multiband Microstrip patch Antenna using parallel slots for wireless applications" International Conference on Electrical, Electronics, and Optimization Techniques(ICEEOT) – 2016, pp 3614-3619, 2016.
8. J. H. Kim and C. G. Christodoulou, "A simple reconfigurable microstrip antenna for wideband applications," *2010 IEEE Antennas and Propagation Society International Symposium*, Toronto, ON, 2010, pp. 1-4

Performance Analysis of Fiber Optic Link Using Hybrid Dispersion Compensation Technique

Balgopal Raju¹, Tusharkant Panda^{2*}

¹PG Scholar, Dept. of ECE, GIET University, Gunupur

²Assistant Professor, Dept. of ECE, GIET University, Gunupur

ABSTRACT

Optical fibers are widely used for data transmission over longer distances with higher data rates. Fiber optic system suffers from various distinctive losses, non-linear effects and dispersion which degrades the signal quality. Among them, dispersion is the most significant signal deteriorating factor. There are many ways through which one can reduce dispersion but some of the most efficient techniques are using a Dispersion compensating fiber (DCF), Fiber Bragg grating (FBG) or Electronic dispersion compensation (EDC) techniques etc. In this project we have used both DCF and FBG together for reducing dispersion for long distance transmission with high data rate with suitable components. This hybrid model transmits signal over a distance of 360km with data rate 20Gbps. This paper also shows comparison between different techniques used for compensating dispersion which are mentioned above. The results obtained are analysed by considering Q-factor and BER as determining parameter.

I. INTRODUCTION

There is a significant development in Optical fiber communication technologies on invention of glass fibers and lasers in 1960s. Earlier, the attenuation in fiber communication was too high and in the range of > 1000 dB/km but in 1970, there was drastic improvement in the attenuation (to 20 dB/km). The fiber loss went below 1 dB/km on development of GaAsP lasers for data transmission in early 1980's. The transmission speed in graded index multimode fibers went up to 44.7 Mb/s over a distance of 23.3km and up to 274 Mb/s up to distance of 7.5 km without using repeaters [1,2].

Dispersion is the primary barrier to long-distance transmission in multi-mode fibers. To address this issue, single mode fibers were developed in 1981. Later, single mode in GaAsP semiconductor lasers were developed. These lasers have a wavelength of 1550 nm and can operate at 2 Gb/s, allowing repeater spacing to be increased to 130 km. The systems can currently transmit data at a 100 Gb/s bit rate up to a distance of more than 1000 km. The scientific and technological development in this field has been so fast and advanced that optical fiber communication system is already in the fifth generation within a period of about 25 years [3].

Attenuation loss in optical fiber is minimum and optimum at the wave length of 1550 nm [4,5]. Hence, the main limiting factor is the dispersion loss and this factor can be compensated or minimized using different techniques like use of DCF and FBG [6]. Each of these methods have their own limiting factors, hence we

propose a hybrid model which includes the advantageous features of DCF and FBG techniques. Through this hybrid model we can be able to send signals with high data rate over a long distance.

DISPERSION COMPENSATION

Dispersion compensation means canceling the effect of dispersion in fiber optic communications. The purpose is to avoid the widening of input pulses and/or the signal distortion in optical fiber communications. In optical communication, the broadening of the signals can occur. If each symbol would be broadened, there might be the case of overlapping between the symbols/signal [7].

By using fibre segments with various designs or other optical components, the effect of dispersion in fibre communication can be reduced [8]. Long dispersion-shifted fibre pieces or chirped fibre Bragg gratings are both possible components of dispersion compensation modules (DCMs). When compared to other dispersion compensation strategies, the fibre gratings are extremely compact and have low insertion losses [9,10].

A typical single mode fibre has a dispersion value of approximately +16–17 ps/nm/km at 1550 nm. To handle or control this quantity of dispersion coefficient, a particular kind of DCF with a negative value of dispersion coefficient is utilized inside the module. Such compensating fibers have a dispersion coefficient that ranges from -30 to -300 ps/nm/km.[11]

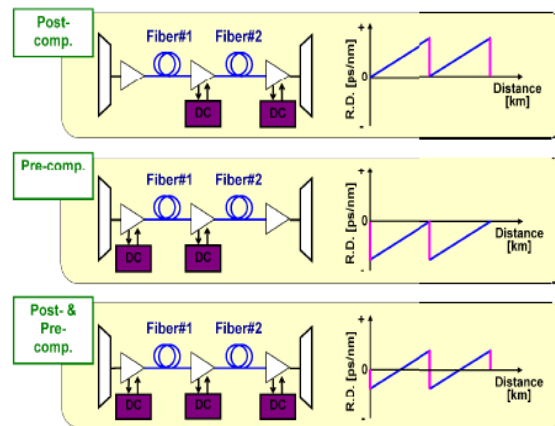


Fig 1: Different types Dispersion Compensating Fiber (DCF)

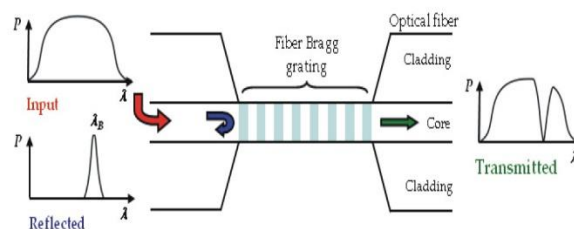


Fig 2: Systematic diagram of FBG

SIMULATION SETUP

Optisystem software is an ingenious and developing tool which helps us to simulate and test almost all kind of optical links. Here all the simulation setup was designed using Optisystem 19.0 simulation software. For the simulation setup we have used the following components-

The PRBS Generator: A Pseudo Random Sequence of binary data is generated by this single port device in accordance with various operating modes. The bit order is intended to mimic the properties of random data.

NRZ Pulse Generator:

It is a two-port device, with binary input delivered to the input port and electrical output provided by the output port. This model can generate pulses with various edge shapes depending on the parameter Rectangle shape.

CW Laser:

CW Laser is a single port device which provide continuous wave optical signal.

M-Z Modulator:

The Mach-Zehnder modulator is an interferometric-based intensity modulator. It is made up of two 3 dB couplers coupled by two equal-length waveguides. Depending on the voltage used, the various routes can result in both positive and negative interference at the output. The output intensity can then be modulated in accordance with voltage at that point [12].

Optical Fiber:

The optical signal is sent through optical fibre. It is a clear, malleable fibre made of plastic or glass. The three layers are core, cladding, and jacket, with jacket serving as the optical fiber's protective outer layer and core serving as the innermost layer in which the signal is conveyed [13,14].

EDFA:

An optical repeater with two ports uses an erbium-doped fibre amplifier to boost optical signal power.

Photodetector PIN:

Photodetector is a two-port device used to reciprocate the received optical signal into electrical.

Optical Filter:

It is a two-port device which only allows a particular wavelength of light signal to pass through it. Here we have used two optical filter i.e., Band pass Gaussian Filter and Low pass Gaussian Filter.

BER analyzer:

BER analyzer provides the result for the whole simulation setup.

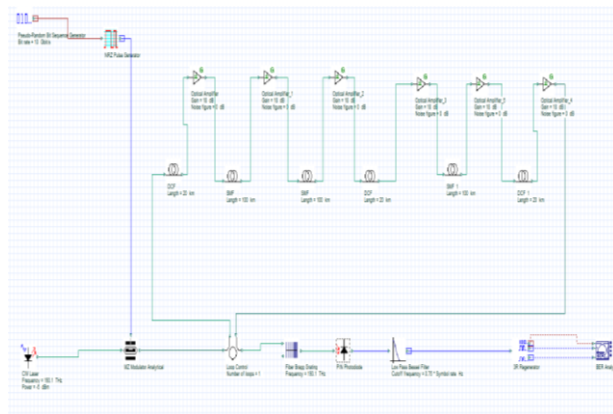


Fig 3: Simulation setup for hybrid model

SIMULATION PARAMETERS:

Parameters	SMF	DCF
Reference Wavelength	1550nm	1550nm
Distance	100 Km	20 Km
Dispersion	16.75ps/nm/km	85ps/nm/km
Attenuation	0.2 dB/km	0.5 dB/km

SYSTEM DESCRIPTION

To examine the effects of dispersion, an SMF of length 100 km in three stage is used in this simulation. In order to create a system with great performance, there are three stages where DCFs of 20 km each are employed in between the link for research while trying to recover the dispersed signal. Over various permutations and combinations, the DCF and SMF are used in various ways [15].

The following list includes the component parameters utilized in the simulation process:

The transmitter part of this simulation setup includes a Mach-Zehnder modulator. One of the input ports is connected to a CW laser, while another input port is connected via a band pass Gaussian filter, NRZ pulse modulator, and a series of pseudo random bit sequence generators.

The transmitter section's output port is linked to a channel that has optical fibre, EDFA, and DCF.

The receiver part, which includes a photodetector PIN, low pass Gaussian filter, electrical attenuator (which attenuates the electrical signal), and electrical equalizer, is then linked to the channel. Utilizing the BER Analyzer and eye diagram analyzer, the setup's outcome can be discovered.

RESULTS AND ANALYSIS

Here simulation is carried out in 4 stages. First simulation is carried out for the simulation setup described in the simulation setup section without using any dispersion compensation technique. The result is noted down for the same. Simulations are carried out then for the same simulation setup using DCF and FBG as compensator separately. Here the length of the fiber and data rate are kept constant to have a fare comparison. Finally the system is designed with both DCF and FBG together as dispersion compensator. The corresponding output is recorded through BER analyzer.

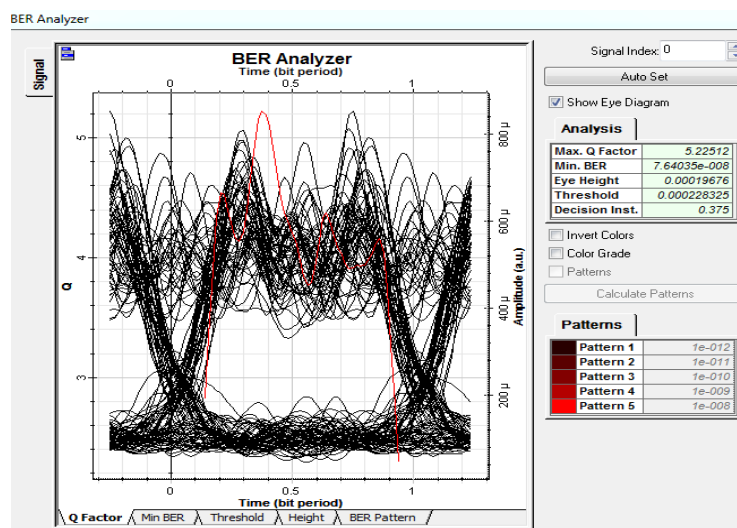


Figure 4: Eye Diagram without using any dispersion compensator

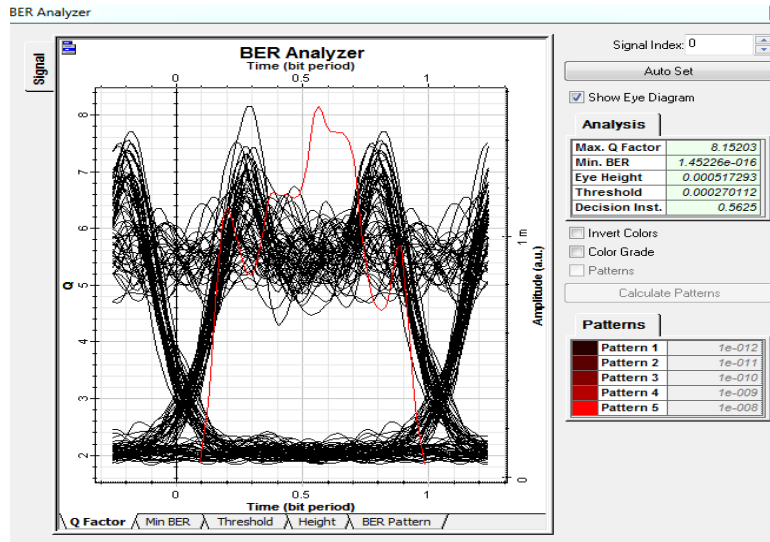


Figure 5: Eye Diagram with FBG as dispersion compensator

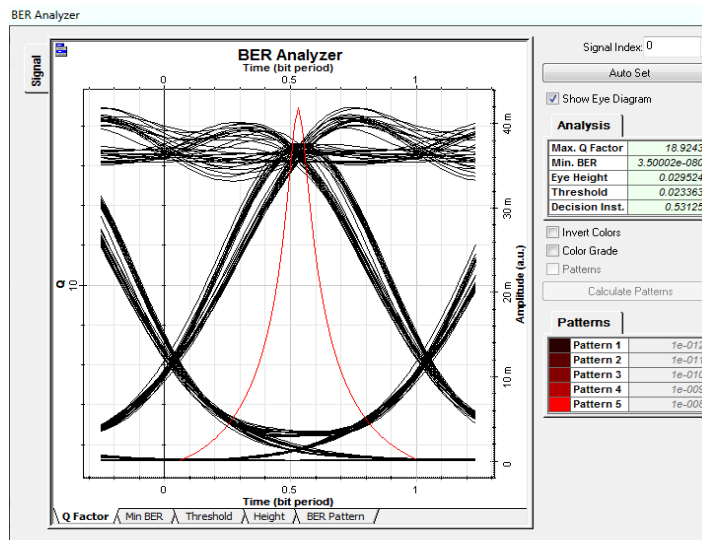


Figure 6: Eye Diagram with DCF as dispersion compensator

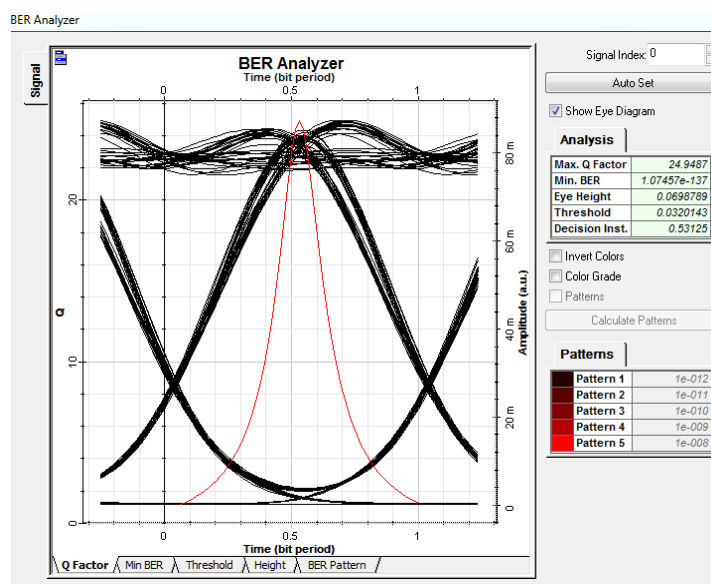


Figure 7: Eye Diagram with Hybrid Dispersion compensator

It can be observed that the system performance varies significantly with use of dispersion compensators. Figure 4 shows the eye diagram for the case when no dispersion compensator is used. Here the Q factor obtained is merely 5.2. This suggests that transmission of data for the specified length of the fiber isn't possible as the Q factor is well below the cutoff mark. Similarly figure 5 shows the eye diagram when only FBG is used in post configuration as dispersion compensator. It can be observed that the Q Factor is just above the cutoff mark and the BER is satisfactory. Similarly figure 6 shows the eye diagram when DCF is used in symmetrical configuration as dispersion compensator. This also shows satisfactory result with Q-Factor of 18.92 and a small bit error rate. Figure 7 shows the eye diagram of the proposed hybrid dispersion compensation technique that contains both FBG and DCF as dispersion compensator. Here DCF is used in symmetrical configuration and FBG is used in post configuration. The Q Factor here is maximum and the bit error rate is minimum among all configurations.

CONCLUSION

Performance of any fiber optic link transmitting optical signal at greater data rate is bound to be affected by attenuation and dispersion. The effect of attenuation is minimized to a large extent with advancement in the field of optical amplifier, optical modulator and availability of advanced Lasers operating at 1550 nm. Compensating the effect of dispersion still remains a critical task. In this thesis we have tried to design a hybrid dispersion compensating module comprising of both DCF and FBG as dispersion compensator. The results shows this module performs way better than using DCF and FBG alone as dispersion compensator. The design of this module is quite simpler and can be used at any length with appropriate calculation of the length of DCF.

II. REFERENCES

- [1]. A.J. Antos and D.K. Smith, Design and Characterization of Dispersion Compensating Fiber based on the LP-01 mode, *Journal of Lightwave Technology*, vol. 12, issue no.10pp. 1739-1745, October, 1994.
- [2]. J. M. Tang and K.A. Shore, 30-Gb/s Signal Transmission Over 40-km Directly Modulated DFB-Laser-Based Single-Mode-Fiber Links Without Optical Amplification And Dispersion Compensation, *Journal of Lightwave Technology*, IEEE, vol. 24, issue no. 6,pp. 2318-2327, June, 2006.
- [3]. Elham Jasim Mohammad, Gaillan H. Abdullah, Soliton Optical Fibers Super continuum Generation Near the Zero Dispersion, *International Journal of Industrial Engineering Research and Development (IJIERD)*, Volume 4, Issue 1, January - April (2013), pp. 52-58
- [4]. N.K. Kahlon and G.Kaur Various Dispersion Compensation Techniques for optical system: A Survey, *Open Journal of Communications and Software*, vol.1, issue no. 1, pp. 64-73, May, 2014.
- [5]. Ashwini Sharma, Shalini Sharma, Inder singh, Suman Bhattacharya, "Simulation and analysis of dispersion compensation using proposed hybrid model at 100 Gbps over 120km using SMF" *International Journal of Mechanical Engineering and technology (IJMET)* vol 8, issue 12Dec2017.
- [6]. A.B. Dar and R.K. Jha, *Chromatic dispersion compensation techniques and Characterization of Fiber Bragg Grating for Dispersion Compensation*, Springer, February, 2017
- [7]. Mishra, P., Panda, T., Rout, S.S., & Palai, G. (2020). Investigation of a 16 channel 40 Gbps varied GVD DWDM system using dispersion compensating fiber. 2020 International Conference on Computer Science, Engineering and Applications (ICCSEA), 1-5.

- [8]. S. Kumar, A. K. Jaiswal, Er. M. Kumar, and Er. R. Saxena, "Performance Analysis of Dispersion Compensation in Long Haul Optical Fiber with DCF," IOSR Journal of Electronics and Communication Engineering (IOSR-JECE), Vol. 6, No. 6, pp. 19-23, Jul.-Aug. 2013.
- [9]. T. K. Panda, P. Mishra, K. C. Patra and N. K. Barapanda, "Investigation and performance analysis of WDM system implementing FBG at different grating length and data rate for long haul optical communication," 2017 IEEE International Conference on Power, Control, Signals and Instrumentation Engineering (ICPCSI), Chennai, India, 2017, pp. 483-488, doi: 10.1109/ICPCSI.2017.8392343.
- [10]. Y.W. Song, Z. Pan, S.M.R.Motaghian Nezam et.al, Tunable Dispersion Slope Compensation for 40-Gb/s WDM Systems Using Broadband Non channelized Third Order Chirped Fiber Bragg Gratings, Journal of Lightwave Technology, IEEE, vol. 20, issue no. 12, December, 2002.
- [11]. Deepika Prajapati, Dhyanendra Parashar, Study of Dispersion Curves in M-Type Triple Clad Single Mode Optical Fiber, International Journal of Electronics and Communication Engineering & Technology (IJECET), Volume 6, Issue 4, April (2015), pp. 28-33
- [12]. Mir Zayed Shames, Md. Surat-E-Mostafa, Imtiaz Ahmed, Signal Quality of Dispersion Managed Quasi-Linear High Bit Rate Optical Transmission System, International Journal of Electronics and Communication Engineering & Technology (IJECET), Volume 4, Issue 3, May – June, 2013, pp. 108-114
- [13]. A. S. Verma, A. K. Jaiswal, and M. Kumar, "An Improved Methodology for Dispersion Compensation and Synchronization in Optical Fiber Communication Networks," International Journal of Emerging Technology and Advanced Engineering, Vol. 3, No. 5, pp. 769- 775, May 2013.
- [14]. Y. Zhou, Y. Shao, Z. Wang, C. Li, J. Zhou, and W. Ma, "Research on Dispersion Compensation of 40 Gb/s Optical Duo-Binary Coded Transmission System," Optics and Photonics Journal, 2016, Vol. 6, pp. 190-195, Aug. 2016.
- [15]. S. S. Muduli, L. Padhy, S. Polei, and T. Panda, "Performance Analysis of a High-Speed Optical Transmission System Using Various Pulse Generator", SPAST Abs, vol. 1, no. 01, Oct. 2021.

Effect of the Slot and Dielectric Materials on ThePerformance of Rectangular Microstrip Antenna

Anita R¹, Jayanthi Kumari T. R², Yogesh G.S³

¹Associate Professor, Dept of ECE, EPCET, Bangalore

²Professor, Dept of ECE, EPCET, Bangalore

³Principal, Dept of ECE, EPCET, Bangalore

ABSTRACT

This paper discusses the analysis of a rectangular microstrip antenna for different dielectric materials. The rectangular microstrip antenna is designed to operate at 2.4GHz. The rectangular microstrip antenna is designed and simulated using HFSS. The rectangular microstrip antenna is designed with FR4 substrate in which the different dielectric materials such as Mica, Teflon, rubber, paper, solid polymer material are integrated into an FR4 substrate. The rectangular microstrip antenna with different dielectric materials are fabricated and the results are experimentally verified. The results have shown that the performance of the antenna is improved in terms of return loss by -36.79 dB for the paper dielectric material and the gain is improved by 4.51 dB for the Teflon dielectric material.

Keywords—Rectangular Microstrip, Dielectric Materials, FR4 Substrate

I. INTRODUCTION

Due to the demand of wireless communication technology the demand has increased significantly for low profile and broad band antennas. Hence microstrip antennas have been used widely in wireless communication due to their light weight, low profile, low cost and ease of fabrication and excellent compatibility with planar integrated circuits and even non planar surfaces. In recent years, as the demand of the small systems have increased, small size antennas at low frequency have drawn much interest from researchers [1], [2]. Nowadays, microstrip patch antenna has become very popular and is widely used in many areas like in mobile communication, Wi-Fi and WiMAX applications.

The main disadvantage of the microstrip antenna is its narrow bandwidth. To increase the performance of a microstrip patch antenna there are several methods like increasing the thickness of substrate, using low dielectric substrate, using of various impedance matching and feeding techniques [3].

The selection of dielectric material is based on the following parameters: relative Dielectric Constant or permittivity, Height of the substrate material, Loss Tangent. Selection of dielectric material with appropriate dielectric constant is important as it has a major role in antenna performance. It directly affects gain, bandwidth, shift in operating frequency, radiation loss [4]. Also dielectric constant controls the fringing field

which is the main cause of radiation in microstrip patch antenna. The lower will be ϵ_r , the wider will be the fringes which in turns results into the better radiation and also increased bandwidth and efficiency[5].

In this paper, the rectangular microstrip antenna is designed with different dielectric materials. The substrate is considered as FR4 and a slot is made on the FR4 substrate into which the different dielectric materials are integrated inside into the substrate. The effect of the dielectric materials on the performance of antenna is analysed in terms of return loss, bandwidth, gain.

II. DESIGN OF RECTANGULAR MICROSTRIP PATCH ANTENNA

A. Design parameters:

The proposed rectangular microstrip patch antenna is designed with FR4 substrate. The patch has the dimensions of 28.33 mm x 37.26 mm. The ground plane has the dimensions of 67.5 mm x 65.5 mm. The substrate height is taken as 1.6 mm. A slot of 28.33 mm x 37.26 mm is made on the FR4 substrate and different dielectric materials such as Mica, Teflon, rubber, paper, solid polymer material with permittivity of 5.7, 2.1, 3, 3.1, 3.2 are integrated into FR4 substrate. The feed used for the rectangular microstrip antenna is microstrip line feed with a length of 22.65 mm and a width of 1.2 mm. Fig 1 shows the designed rectangular microstrip patch antenna.

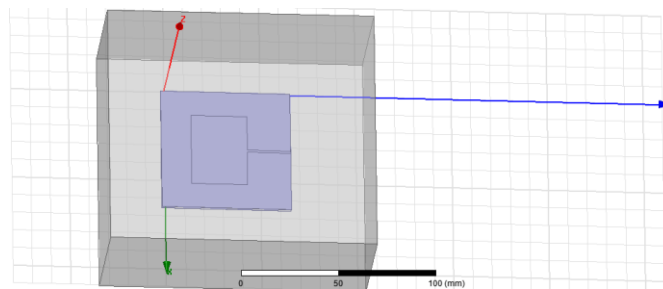


Fig 1. Rectangular microstrip antenna

B. Design of Length and Width of patch:

Depending on the relative permittivity, operating frequency the width and length of the patch are determined. the desired length and width can be found out by using following equations:

The effective dielectric constant of the microstrip patch antenna is calculated from,

$$\epsilon_{eff} = \frac{\epsilon_r + 1}{2} + \frac{\epsilon_r - 1}{2} \left(\frac{1 + \frac{12h}{w}}{\sqrt{1 + \frac{12h}{w}}} \right) \quad (1)$$

The actual Width (W) of patch:

$$W = \frac{C}{2f_r} \sqrt{\frac{2}{\epsilon_r + 1}} \quad (2)$$

$$C = \frac{1}{\mu_0 \epsilon_0} \quad (3)$$

Where,

μ_0 is the Permeability

ϵ_0 is the Permittivity

C is the Velocity

ϵ_r is the Dielectric constant

f is the resonant frequency

The actual length of the patch (L):

$$L = \frac{c}{2f_r \sqrt{\epsilon_{eff}}} - 2\Delta L \quad (4)$$

$$L_{eff} = \frac{c}{2f_r \sqrt{\epsilon_{eff}}} \quad (5)$$

$$L = L_{eff} - 2\Delta L \quad (6)$$

Where,

ΔL is the Line extension

II. RESULTS AND DISCUSSION

The rectangular microstrip patch antenna is designed to operate at 2.4 GHz. The parametric analysis of the rectangular microstrip antenna is carried out by considering different dielectric materials such as mica, Teflon, rubber, paper, solid polymer which are integrated on to the FR4 substrate. A slot is made on the FR4 substrate and the dielectric materials are integrated on to it one by one and the performance of the antenna in terms of return loss, gain, bandwidth, VSWR is measured.

I. Effect of mica on the performance of antenna:

The rectangular microstrip patch antenna is designed with FR4 substrate of permittivity 4.4. A slot of 28.33 x 37.26 mm are made on the FR4 substrate and the slot is filled with mica which has a dielectric constant of 5.7. The dimension of mica is taken as 28.3mm x 37.26mm. The ground plane has the dimension of 67.5mm x 65.5mm. The rectangular microstrip patch antenna is designed and simulated using HFSS. The fabricated rectangular microstrip antenna with slot on the FR4 substrate is shown in fig2. The performance of the antenna is measured in terms of return loss, bandwidth, gain and VSWR.

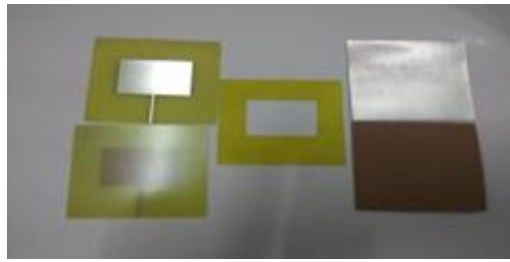


Fig2.Fabricated rectangular microstrip with slot on FR4 substrate

Fig2(a) shows the return loss plot of the rectangular microstrip antenna with mica as the dielectric material.

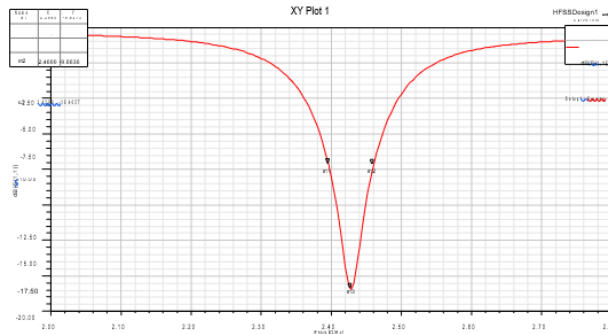


Fig2(a).Return loss plot of rectangular microstrip antenna with mica as dielectric material

From fig2(a), we can observe that the return loss of rectangular microstrip antenna with mica as dielectric material is obtained as -18.4057 dB.The bandwidth is obtained as 64 MHz.Fig2(b) shows the 3D radiation pattern of the rectangular microstrip antenna with mica as the dielectric material.



Fig 2(b) 3D radiation pattern of rectangular microstrip patch antenna with mica as dielectric material

From fig2(b),we can observe that the gain of the rectangular microstrip antenna with mica as dielectric material is obtained as 3.888 dB.Fig 2(c) shows the electric field distribution of rectangular microstrip antenna with mica as dielectric material.

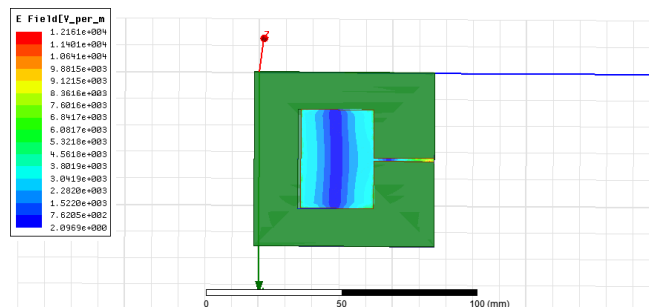


Fig.2©Electric Field distribution of rectangular microstrip antenna with mica as dielectric material

From fig 2©,we can observe the field distribution from the rectangular microstrip antenna with mica as dielectric material.

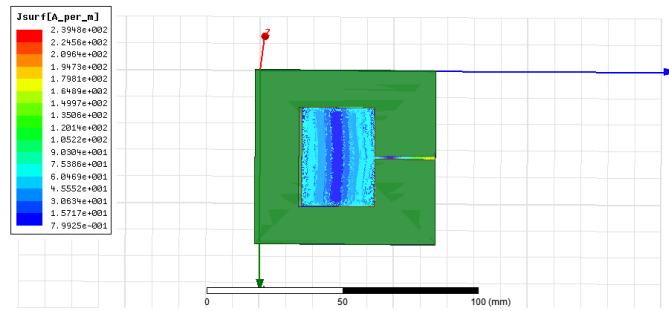


Fig.2(d)surface current distribution of rectangular microstrip with mica

Fig 2(d) shows the surface current distribution of rectangular microstrip antenna with mica as dielectric material.

From Fig 2(d),we can observe the uniform current distribution across the patch in a rectangular microstrip antenna with mica as the dielectric material.Fig 2(e) shows the VSWR plot of the rectangular microstrip antenna with mica as the dielectric material

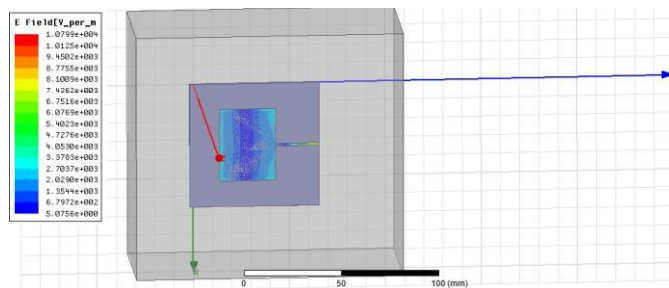


Fig.2(e)VSWR plot of rectangular microstrip with mica as dielectric material

From fig 2(e),we can observe that the VSWR of the rectangular microstrip antenna with mica as dielectric material is obtained as 1.2731.Fig 2(f) shows the 2D radiation pattern of the rectangular microstrip antenna with mica as the dielectric material.

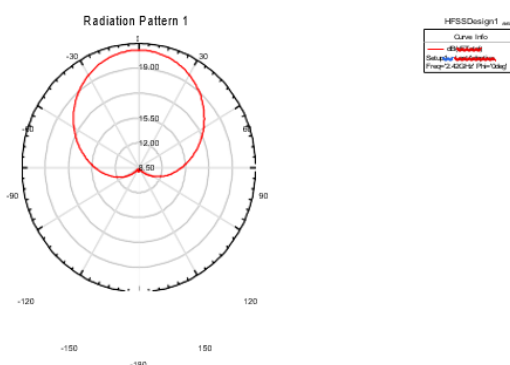


Fig.2(f) 2D radiation pattern of rectangular microstrip with mica as dielectric material

From fig 2(f),we can observe that the maximum power is radiated from the rectangular microstrip antenna with mica as the dielectric material.

II. Effect of Teflon on the performance of antenna:

The rectangular microstrip antenna is designed by considering FR4 substrate with a permittivity of 4.4. A slot is made on the FR4 substrate and filled with teflon material of dielectric constant 2.1. The performance of the rectangular microstrip antenna is analysed in terms of return loss, gain, bandwidth and VSWR. The rectangular microstrip antenna with teflon material is fabricated and the experimental results are also verified. A Conducting strip is placed on the teflon material and the dc voltage is applied. The performance of the antenna with teflon material is analysed by applying voltage and without applying voltage. Fig3(a) shows the fabricated rectangular microstrip antenna with teflon material and the experimental set up to measure the return loss of the antenna.



Fig 3(a) Experimental setup to measure the return loss of rectangular microstrip antenna with teflon material

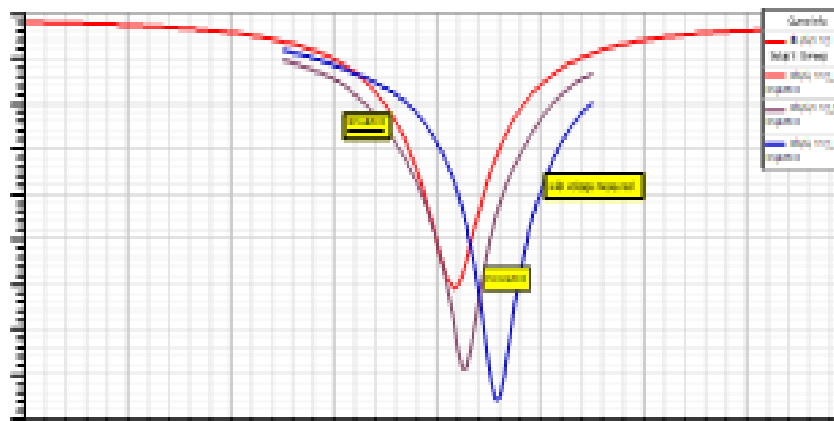


Fig 3(b) Simulated and measured return loss plot of rectangular microstrip antenna with teflon material

From fig 3(b), we can observe that the return loss of the simulated rectangular microstrip antenna with teflon material is -10.1293 dB. The measured return loss of the rectangular microstrip antenna with teflon material is found to be -19.71 dB. When the voltage is applied to the teflon material, the return loss is measured as -20.418 dB. The bandwidth of the simulated rectangular microstrip antenna with teflon material is 56 MHz. The bandwidth of the measured rectangular microstrip antenna with teflon material is obtained as 75 MHz. When the voltage is applied, the measured bandwidth is 79.5 MHz. The resonant frequency of the simulated rectangular microstrip antenna with teflon material is 2.4160 GHz. The resonant frequency of the measured rectangular microstrip antenna with teflon material is 2.4285 GHz. When the voltage is applied, the resonant frequency is shifted from 2.4160 GHz to 2.4600 GHz. This

shows that the antenna can be used as a frequency reconfigurable antenna which finds its application in wireless communication. Fig 3(c) shows the electric field distribution of rectangular microstrip antenna with teflon material.

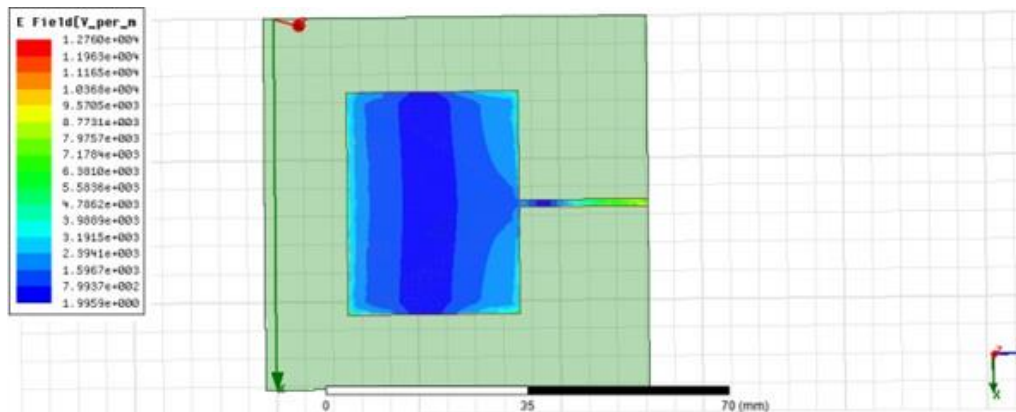


Fig.3© Electric Field distribution of rectangular microstrip antenna with teflon material

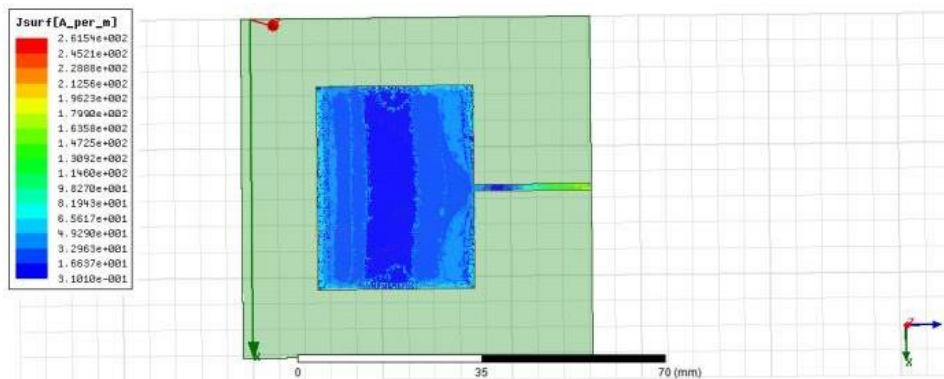


Fig 3(d) shows the surface current distribution of rectangular microstrip antenna with teflon material.

Fig.3(d) surface current distribution of rectangular microstrip antenna with Teflon material

From fig 3(d), we can observe that there is a uniform current distribution across the patch of a rectangular microstrip antenna with Teflon material. Fig 3(e) shows the 3D radiation pattern of the rectangular microstrip antenna with Teflon material.



Fig.3(e)3D radiation pattern of rectangular microstrip antenna with Teflon material

Fig 3(f) shows the 2D radiation pattern of the rectangular microstrip antenna with Teflon material.

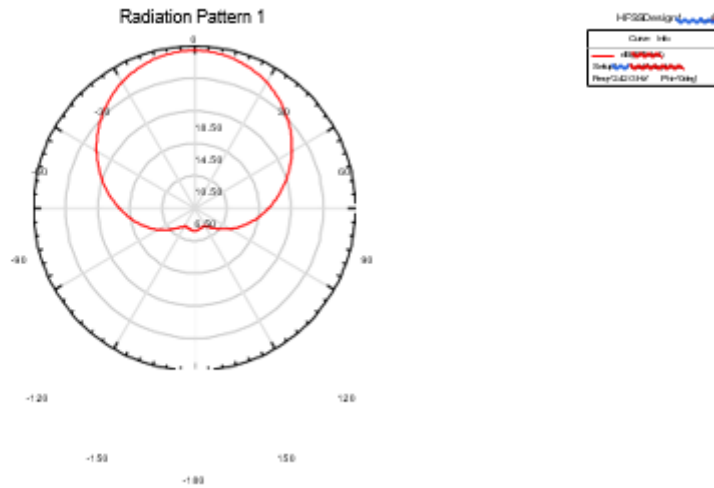


Fig.3(f) 2D radiation pattern of rectangular microstrip antenna with Teflon material

From fig 3(f),we can observe that the maximum radiation is obtained from the rectangular microstrip antenna with Teflon material.

III. Effect of paper on the performance of antenna:

The rectangular microstrip antenna is designed with FR4 substrate which has a dielectric constant of 4.4.A slot is made on the FR4 substrate and filled with paper as dielectric.The dielectric constant of paper is 3.1.Fig 4(a) shows the return loss plot of the rectangular microstrip antenna with paper material.

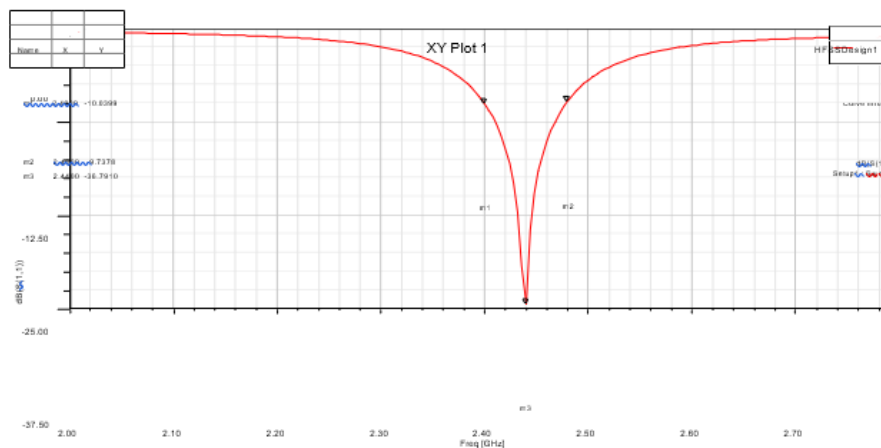


Fig.4(a)Return loss plot of rectangular microstrip antenna with paper material

From fig 4(a),we can observe that the return loss of the rectangular microstrip antenna with paper material is -36.79 dB.The bandwidth of the rectangular microstrip antenna with paper material is obtained as 80 MHz.Fig 4(b) shows the 3D radiation pattern of the rectangular microstrip antenna with paper material.



Fig.4(b)3D radiation pattern of rectangular microstrip antenna with paper material

From fig 4(b), we can observe that the gain of the rectangular microstrip antenna with paper as dielectric material is obtained as 2.6864 dB. Fig 4(c) shows the 2D radiation pattern of rectangular microstrip antenna with paper as dielectric material.

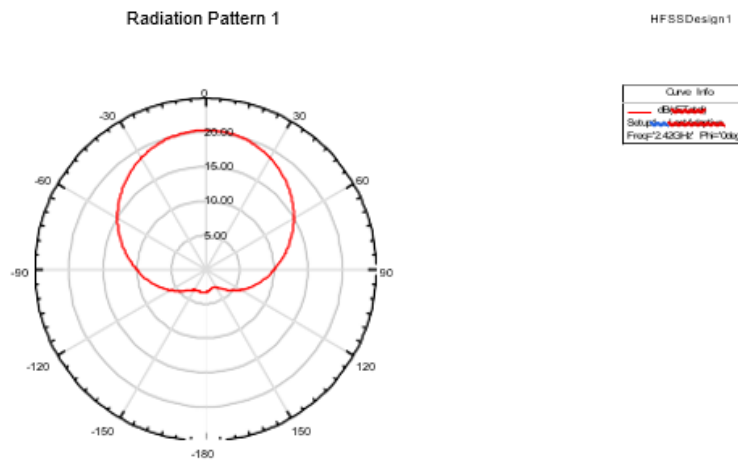


Fig.4(c)2D radiation pattern of rectangular microstrip antenna with paper material

Fig 4(d) shows the VSWR plot of the rectangular microstrip antenna with paper as the dielectric material.

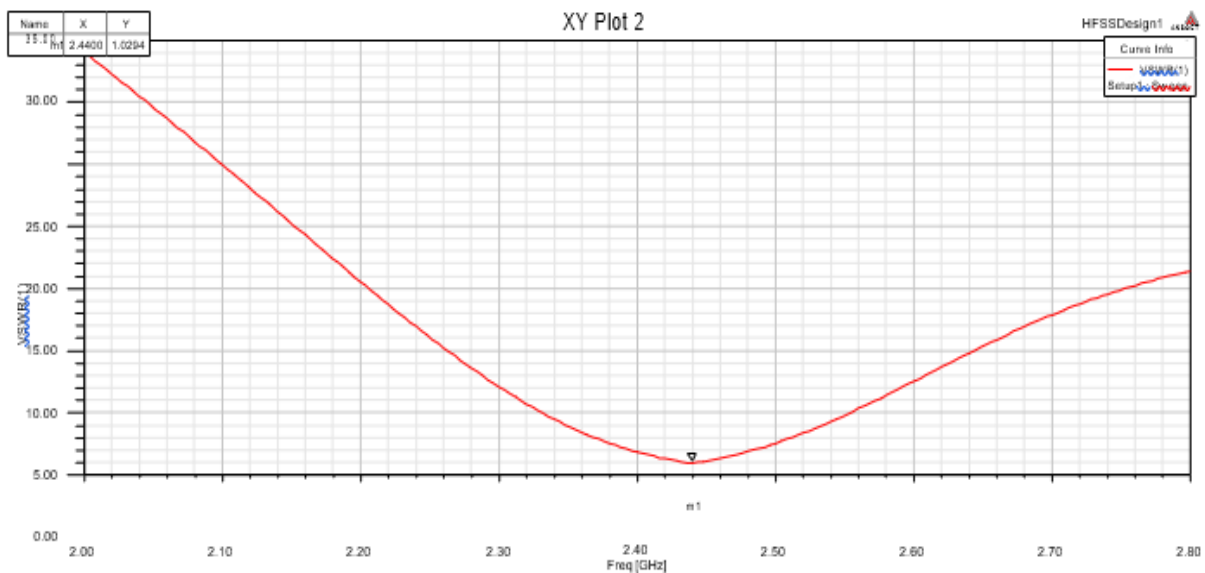


Fig.4(d) VSWR plot of rectangular microstrip antenna with paper material

From fig 4(d), we can observe that the VSWR of the rectangular microstrip antenna with paper as dielectric material is obtained as 1.0294. Fig 4(e) shows the electric field distribution of the rectangular microstrip antenna with paper as the dielectric material.

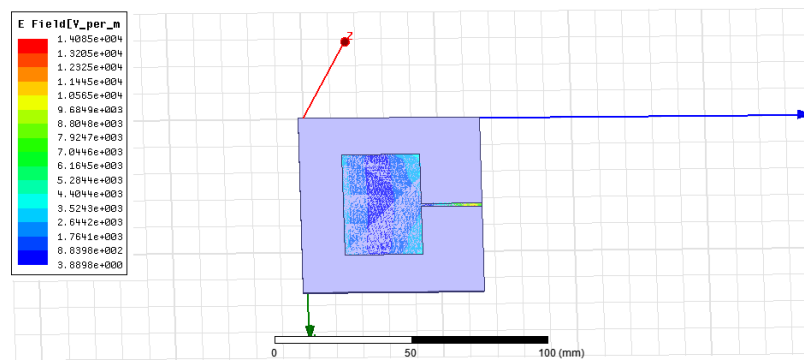


Fig. 4(e) Electric field distribution of rectangular microstrip antenna with paper material

Fig 4(f) shows the surface current distribution of rectangular microstrip antenna with paper material.

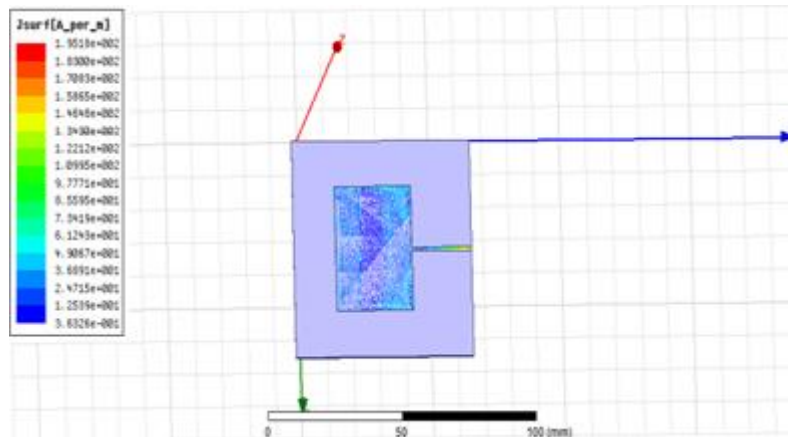


Fig.4(f) Surface current distribution of rectangular microstrip antenna with paper material

From fig 4(f), we can observe that there is a uniform current distribution across the patch of a rectangular microstrip antenna with paper material.

IV. Effect of rubber on the performance of antenna:

The rectangular microstrip antenna is designed by considering an FR4 substrate which has a dielectric constant of 4.4. A slot is made on the FR4 substrate and filled with rubber dielectric material which has a dielectric constant of

3. Fig 5(a) shows the return loss plot of the rectangular microstrip antenna with rubber as the dielectric material.

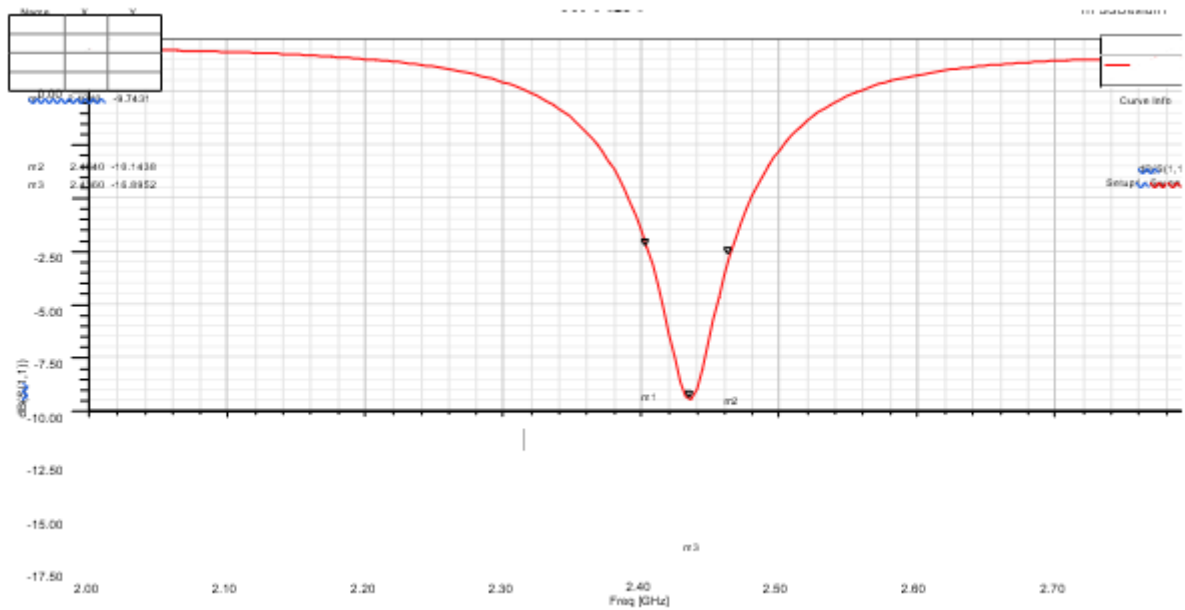


Fig.5(a)Return loss plot of rectangular microstrip antenna with rubber material

From fig 5(a),we can observe that the return loss of the rectangular microstrip antenna with rubber material is -16.89 dB.The bandwidth of the rectangular microstrip antenna with paper material is obtained as 60 MHz.Fig 5(b) shows the 3D radiation pattern of the rectangular microstrip antenna with rubber material.



Fig.5(b)3D radiation pattern of rectangular microstrip antenna plot with rubber material

From fig 5(b), ,we can observe that the gain of the rectangular microstrip antenna with rubber as dielectric material is obtained as 4.2007 dB.Fig 5(c) shows the VSWR plot of rectangular microstrip antenna with rubber as dielectric material.

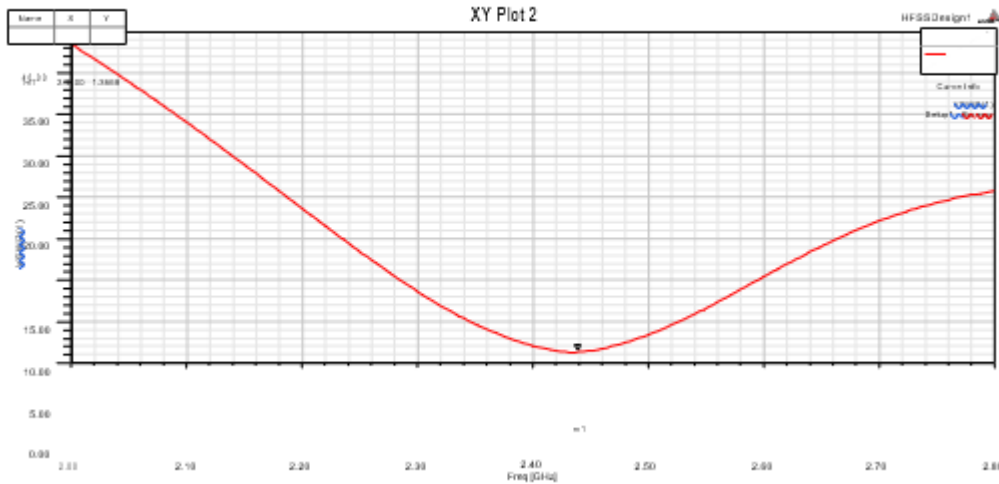


Fig.5©VSWR plot of rectangular microstrip antenna with rubber material

From fig 5(c),we can observe that the VSWR of the rectangular microstrip antenna with rubber as dielectric material is obtained as 1.3568.Fig 5(d) shows the 2D radiation pattern of the rectangular microstrip antenna with paper as the dielectric material.

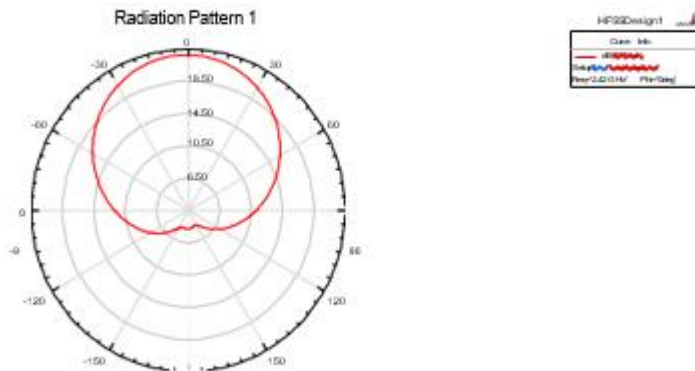


Fig.5(d)2D radiation pattern of rectangular microstrip antenna with rubber material

From fig 5(d),we can observe that the maximum radiation is obtained from the rectangular microstrip antenna with rubber material.Fig 5(e) shows the electric field distribution of rectangular microstrip antenna with rubber as dielectric material.

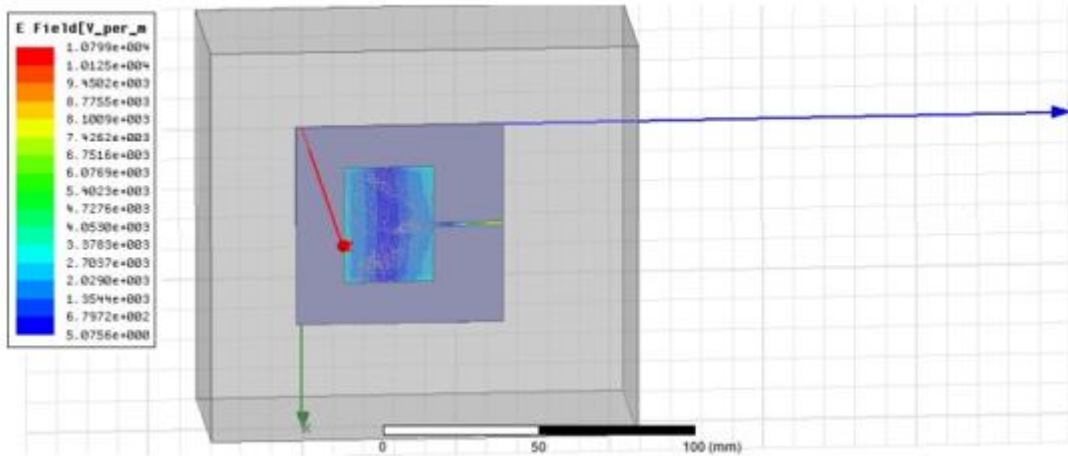


Fig.5(e)Electric Field distribution of rectangular microstrip antenna with rubber material

Fig 5(f) shows the surface current distribution of rectangular microstrip antenna with rubber material.

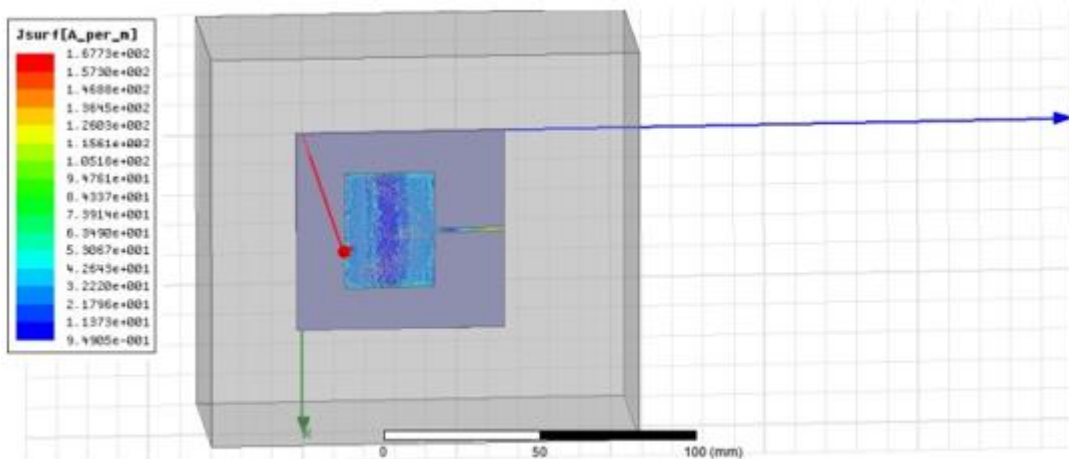


Fig.5(f)Surface current distribution of rectangular microstrip antenna with rubber material

From fig 5(f),we can observe that there is an uniform current distribution across the patch of a rectangular microstrip antenna with rubber material.

V. Effect of polyster on the performance of antenna:

The rectangular microstrip antenna is designed by considering an FR4 substrate which has a dielectric constant of 4.4.A slot is made on the FR4 substrate and filled with polyster dielectric material which has a dielectric constant of 3.2.Fig 6(a) shows the return loss plot of the rectangular microstrip antenna with polyster as the dielectric material.

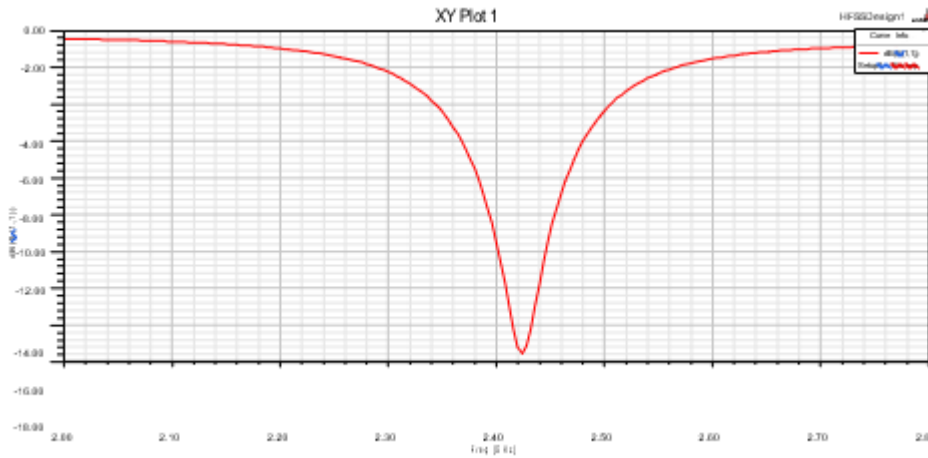


Fig.6(a)Return loss plot of rectangular microstrip antenna with polyster material

From fig 6(a),we can observe that the return loss of the rectangular microstrip antenna with polyster material is

-17.51 dB.The bandwidth of the rectangular microstrip antenna with polyster material is obtained as 64 MHz.Fig 6(b) shows the 3D radiation pattern of the rectangular microstrip antenna with polyster material.



Fig.6(b)3D radiation pattern of rectangular microstrip antenna with polyster material

Fig 6(c) shows the 2D radiation pattern of the rectangular microstrip antenna with polyster as the dielectric material.

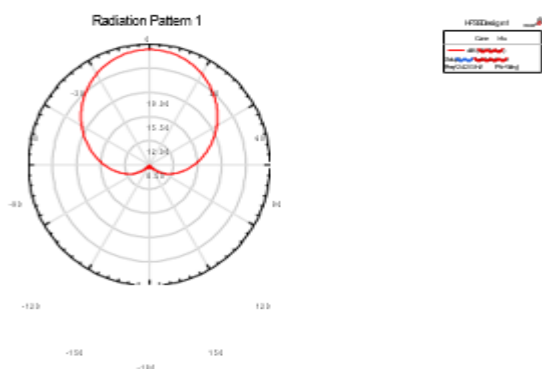


Fig.6©2D radiation pattern of rectangular microstrip antenna with polyster as dielectric material

Fig 6(d) shows the electric field distribution of rectangular microstrip antenna with polyster as dielectric material.

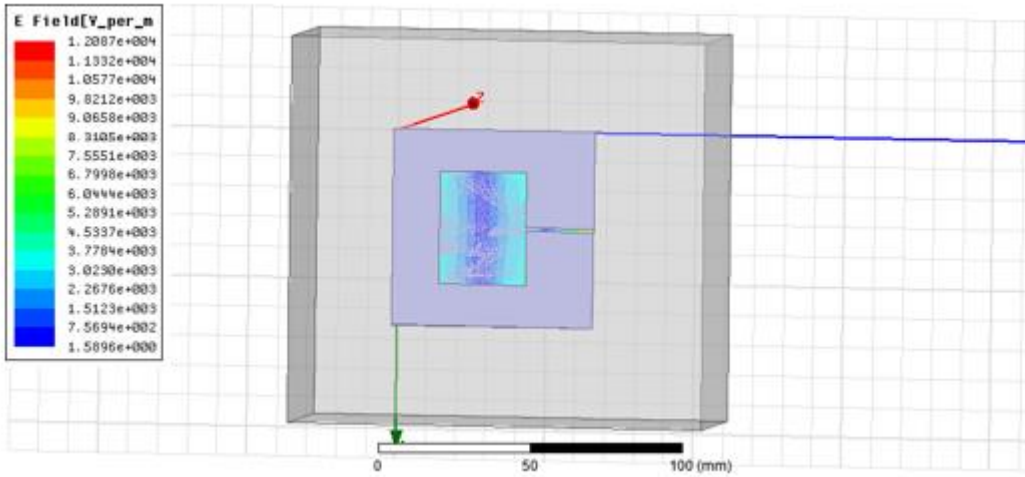


Fig.6(d) Electric Field distribution of rectangular microstrip antenna with polyster material

Fig 6(e) shows the surface current distribution of rectangular microstrip antenna with polyster dielectric material.

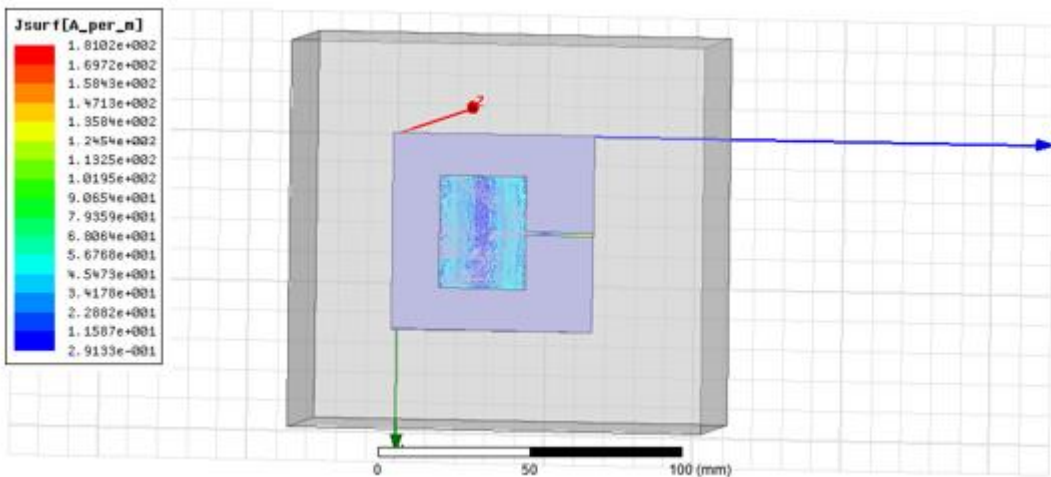


Fig.6(e)Surface current distribution of rectangular microstrip antenna with polyster material.

From fig 6(e),we can observe that there is an uniform current distribution across the patch of a rectangular microstrip antenna with polyster material

Table 1. shows the results obtained for different dielectric materials.From the results ,we can observe that when the paper material is integrated inside the FR4 substrate,the return loss is obtained as -36.79 dB .The gain of the antenna is increased to 4.351 dB when the Teflon material is digged inside the FR4 substrate and the bandwidth is also improved to 79.5 MHz.Since the loss of Teflon material is less and to improve the gain of the microstrip antenna,Teflon material can be used.

Table1.Results obtained for different dielectric materials

Sl. no	Name of the substrate	Dielectric constant	Return loss (dB)	Gain(dB)	Bandwidth(MHZ)	VSWR
1	Mica	5.7	-18.405	3.888	64	1.2731
2	Teflon	2.1	-20.4184	4.351	79.5	1.0294
3	Paper	3.1	-36.79	2.686	80	1.0294
4	Rubber	3	-16.89	4.2007	60	1.3568
5	Polyster	3.2	-17.516	4.0364	64	1.3226

Fig 7. Shows the return loss plot for different dielectric materials.

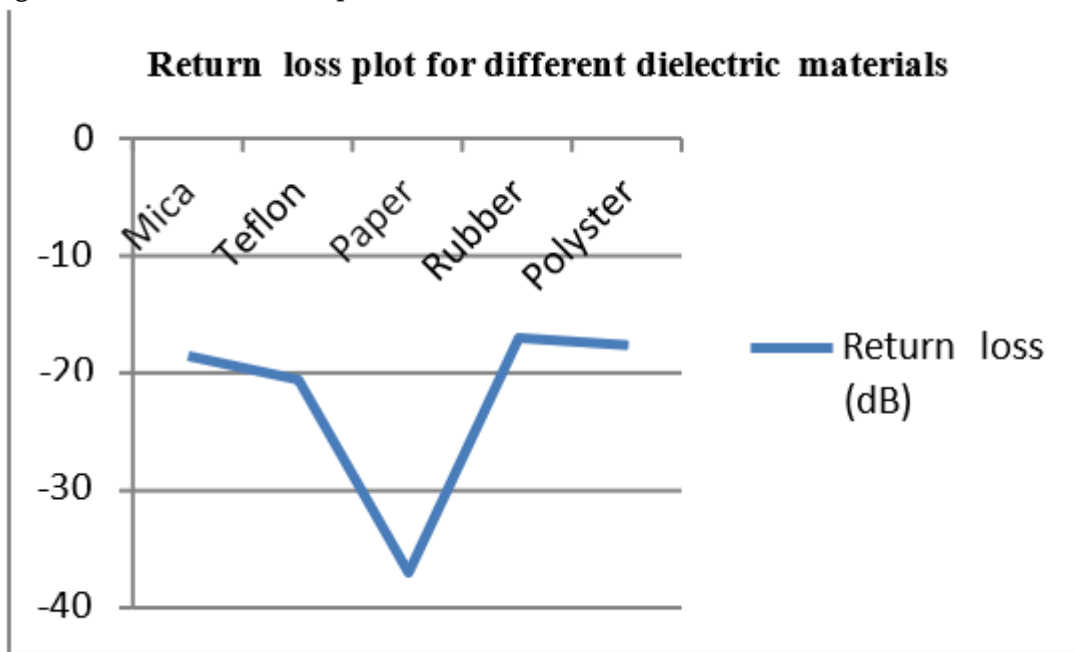


Fig 7. Return loss plot for different dielectric materials.

Fig 7. Shows the return loss obtained for different dielectric materials. From the graph, we can observe that the return loss obtained for paper is -36.79 dB which shows an improved performance, whereas the return loss obtained for rubber material is -16.89 dB which is not showing good performance compared to paper material.

Fig.8. shows the gain obtained for different dielectric materials.

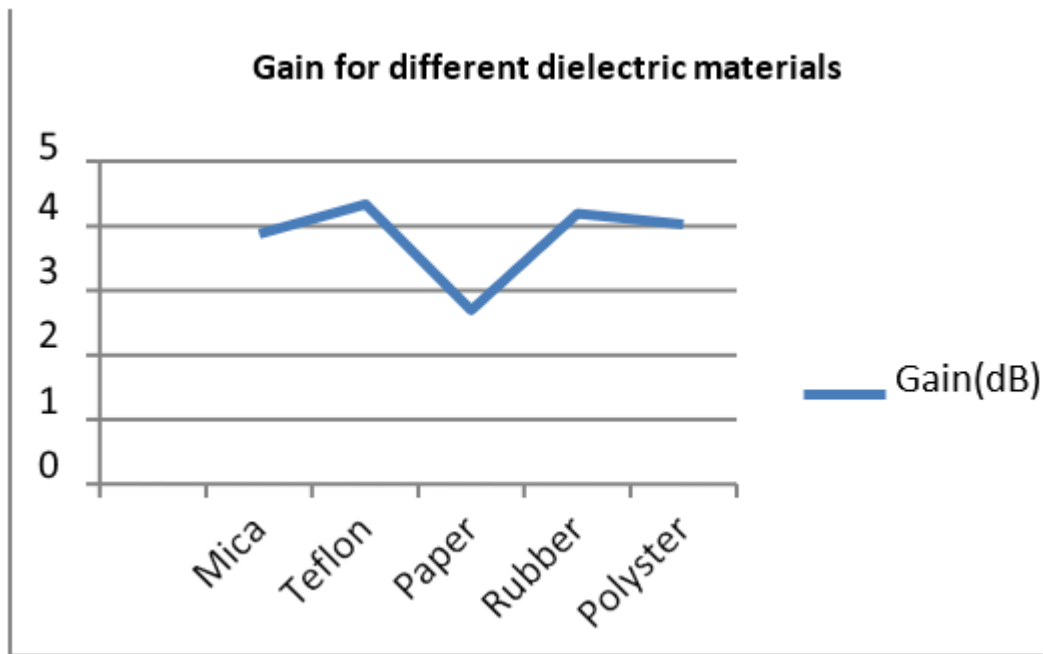


Fig 8. Gain plot for different dielectric materials

From fig 8, we can observe that the gain obtained for Teflon material is 4.351 dB, whereas the gain obtained for paper material is 2.686 dB. This shows that the performance of the antenna can be improved in terms of gain by considering Teflon material and the performance of the antenna can be improved in terms of return loss by considering paper as dielectric material.

IV. CONCLUSION

The rectangular microstrip patch antenna is designed at an operating frequency of 2.4 GHz. The rectangular microstrip antenna is designed and simulated using HFSS. The rectangular microstrip antenna is analysed by integrating different dielectric materials such as mica, Teflon, paper, rubber, polyster inside FR4 substrate. The rectangular microstrip antenna with different dielectric materials are fabricated and the experimental results are verified. The results show that the gain of the antenna is improved by considering a Teflon material which is obtained with a gain of 4.351 dB. The performance of the antenna is improved in terms of return loss by considering paper as dielectric material. The rectangular microstrip antenna with Teflon material can be considered for wireless applications as the loss of Teflon material is less compared to other dielectric materials.

III. REFERENCES

- [1]. Mrinmoy Chakrabortya , Biswarup Ranab , P.P. Sarkarc , Achintya Dasd, " Design and Analysis of a Compact Rectangular Microstrip Antenna with slots using Defective Ground Structure", Science direct, pp 411-416, 2012
- [2]. Indrasen Singh, Dr. V.S. Tripathi, Micro strip Patch Antenna and its Applications: a Survey, Indrasen Singh et al, Int. J. Comp. Tech. Appl., Vol 2 (5), 1595-1599.

- [3]. Md. Moidul Islam, Raja Rashidul Hasan, Md. Mostafizur Rahman, Kazi Saiful Islam, S.M. Al-Amin,” Design & Analysis of Microstrip Patch Antenna Using Different Dielectric Materials for WiMAX Communication System”, International Journal of Engineering and Science, vol.4, issue 1, 2016, pp 19-24
- [4]. Vivek Hanumante, Sahadev Roy; “Comparative Study of Microstrip Patch Antenna Using Different Dielectric Materials,” 9th International Conference On Microwaves, Antenna, Propagation & Remote Sensing ICMARS-2013
- [5]. Vivek Hanumante , Panchatapa Bhattacharjee , Sahadev Roy , Pinaki Chakraborty , Santanu Maity,” Performance Analysis of Rectangular Patch Antenna for Different Substrate Heights”, International Journal of innovative research in Electrical, Electronics, Instrumentation and Control Engineering vol 2, Issue 1, January 2014

A Short-circuit Model Based on Artificial Neural Network and Artificial Bee Colony Algorithm for SiC MOSFETs

Dr. Rajesh L, Praveen Kumar K C, Malini V L, Kavitha A

ABSTRACT

A short-circuit model for silicon carbide (SiC) metal-oxide semiconductor field effect transistors (MOS- FETs) using hybrid modeling method based on artificial neural network (ANN) and improved artificial bee colony (ABC) algorithm is proposed in this paper. In order to improve the search ability of the ABC, particle swarm optimization (PSO) is introduced to the scout bees' search strategy. The improved ABC is employed to find suitable initial parameters for ANN model, which can improve the accuracy of modeling results. Based on hybrid modeling method, the normal working model of SiC MOSFETs is established first. The modeling results of I-V characteristics, C-V characteristics and small signal parameters (gm, gd, etc.) are in good agreement with datasheet, which fully demonstrates the validity of the normal working model. Then the short-circuit model of SiC MOSFETs is further obtained based on the relationship between short-circuit current and junction temperature and normal working model. Eventually, the proposed short-circuit model is verified by device- and circuit-level tests. With its precision and simplicity, the proposed short-circuit model can be used to analyze short-circuit faults in SiC MOSFET simulation circuits and provide assistance for the design of protection circuits.

Keywords: Artificial bee colony (ABC) algorithm, artificial neural network (ANN), silicon carbide (SiC) metal-oxide semiconductor field effect transistors (MOSFETs)

I. INTRODUCTION

With the rapid development of process technologies of silicon carbide (SiC), SiC metal-oxide semiconductor field effect transistors (MOSFETs) have been commercialized in mass production and are popular in the design of high-power electronics [1]. Compared with traditional Si MOSFETs, SiC MOSFETs have lots of outstanding advantages, such as higher switching speed, higher switching frequency, smaller ON-state resistance, and better high temperature stability [2]. Due to the excellent characteristics of SiC MOSFETs, they are often used in harsh circuit conditions. Hence, it is necessary to ensure its reliability and safety to guarantee that SiC MOSFETs can operate normally under harsh conditions. One of the key reliability issues is the short-circuit capability of the SiC MOSFETs [3]. Therefore, an accurate and simple SiC MOSFET short-circuit simulation model is urgently needed to predict the characteristics of the faults caused by the short-circuit and provide guidance for the design of protection circuits.

In the past few decades, many SiC MOSFET models [4–6] have been proposed, but most of them only consider normal working scenarios. Recently, several models [7–9] describing the short-circuit characteristics of SiC MOSFETs have been reported. Physics-based models [7] can describe the internal physical characteristics of SiC MOSFETs and are usually considered to be accurate, but they are too complex to be suitable for power electronic circuit simulation [10]. The PSpice short-circuit model of SiC MOSFETs [8, 9] is simpler than the physics-based model, but it still has many parameters. The extraction of parameters is time-consuming and may lead to inaccurate results. In addition, the PSpice model only considers the short-circuit situation when the case temperature is 25°C, but different case temperatures have an impact on the short-circuit current. Data-oriented modeling methods can be quickly applied for the newly generated device data. Artificial neural network (ANN) is considered as a data-oriented modeling method [11] and can achieve an accurate model in a short time, which has been employed in the modeling of semiconductor devices [12, 13]. In order to reduce the developing time and obtain an accurate model, a short-circuit model of SiC MOSFETs considering case temperatures based on ANN is proposed in this paper.

In this work, a Multi-layer perceptron (MLP) [14] based on the levenberg-marquardt (LM) algorithm [15] is adopted to establish a short-circuit model for SiC MOSFETs. Since the LM algorithm is quite sensitive to the initial values, for the sake of overcoming the sensitivity of the LM to the initial values and get better modeling results, an improved artificial bee colony (IABC) algorithm [16] combined with particle swarm optimization (PSO) [17] (IABCPSO) is proposed and introduced into the training of MLP to find the appropriate initial weights and biases for the LM. In this paper, we first build the SiC MOSFET model under normal working conditions, and then the short-circuit model is developed based on the normal working model and junction temperature. A SiC MOSFET of type C2M0080120D (1200V/36A) [18] is chosen as the modeling object in this paper. Furthermore, the accuracy of the short-circuit model based on this hybrid modeling method is verified by both the device and circuit-level tests.

1. Normal Working ANN Model

Since the drain-source current I_{ds} under normal operating conditions also contributes to the short-circuit current, it is first modeled based on ANN modeling method, which takes into account the temperature characteristics. The ANN model contains the drain-source current I_{ds} , body diode D_b , gate-drain capacitor C_{gd} , gate-source capacitor C_{gs} , drain-source capacitor C_{ds} and internal gate resistor R_g , as shown in Fig. 1.

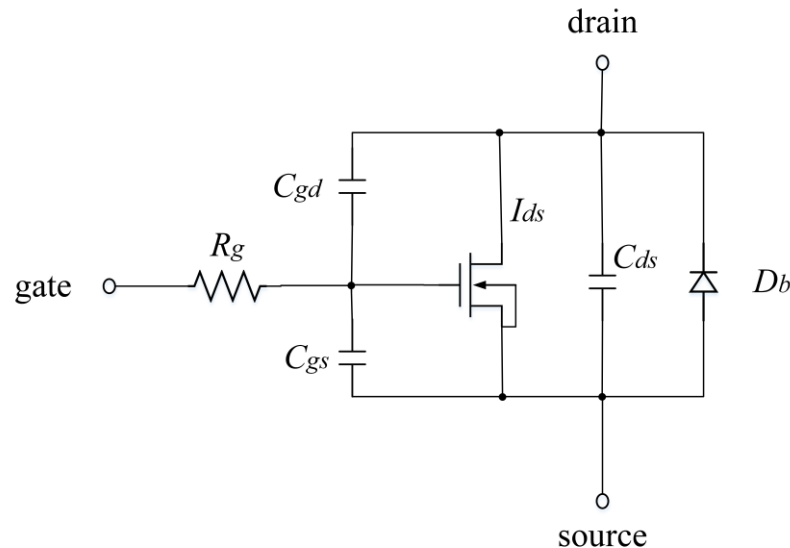


Fig. 1 The ANN model of SiC MOSFET

1.1 Improved artificial bee colony algorithm combined with particle swarm optimization

In our previous work [19], we used the MLP based on the LM algorithm for modeling SiC MOSFETs, which is also adopted as the basis of this paper. Different from [19], the ABC algorithm in this paper is improved by introducing PSO into the search strategy of the scout bees.

In PSO [17], each particle represents a possible solution, and the optimization process of the particle is related to two important factors: the individual optimal solution (pbest) and the swarm's optimal solution (gbest). And the fitness function of PSO will guide the particle swarm to find the optimal solution. In this paper, PSO is introduced into the optimization process of the scout bees of ABC. When the employed bees

and onlooker bees are converted to scout bees because their corresponding nectar sources aren't updated in

the limited times, they will restart the search for the best solution in the entire range set at the beginning, which is undoubtedly a waste of current information resources, such as the current best solution of the entire bee colony (Xbest) found by the employed bees and the onlooker bees. After introducing PSO into the optimization process of the scout bees, we can effectively use the Xbest information, and the optimization of the scout bees will be carried out in accordance with the idea of PSO, thereby improving the efficiency of the whole algorithm. The optimization process of the scout bees can be described as:

$$N_{ij} = w \cdot N_{ij} + r_{i1} \cdot c_1 (p_{best} - M_{ij}) + r_{i2} \cdot c_2 (g_{best} - M_{ij}) \quad (1)$$

$$M_{ij} = M_{ij} + N_{ij} \quad (2)$$

where N_{ij} and M_{ij} represent the velocity and position of the i th particle, respectively; w is an inertia factor describing the contribution rate of the particle's previous speed to its current speed, which helps particles to search a wider area in the previous direction. Moreover, r_{i1} and r_{i2} are random numbers in

the range of $[0,1]$; c_1 and c_2 are the acceleration factors. In order to use the X_{best} information, we set M_i as:

$$M_i = X_{best}. \quad (3)$$

Then, the particle swarm will use X_{best} as the initial position to help scout bees search for the best solution, which effectively enhances the search ability of the whole algorithm. After that, the mean square error of the I-V modeling results and the datasheet is set as the fitness function, and we compared modeling results of IABCPSO and IABC in [19] running 100 times respectively, the results of which are shown in Fig. 2. The conclusion can be drawn from Fig. 2 that, IABCPSO can get better results in a shorter time, which confirms the effectiveness of our proposed algorithm in this paper.

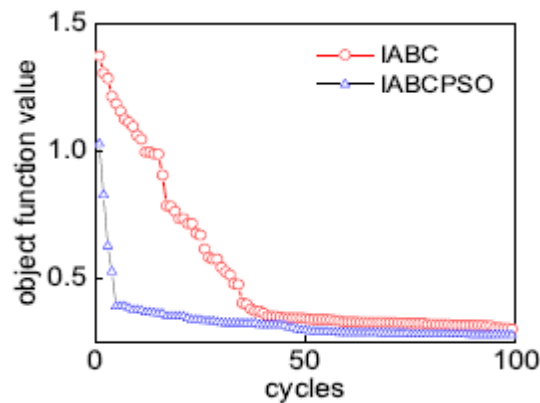


Fig. 2 Comparison results between IABCPSO and IABC

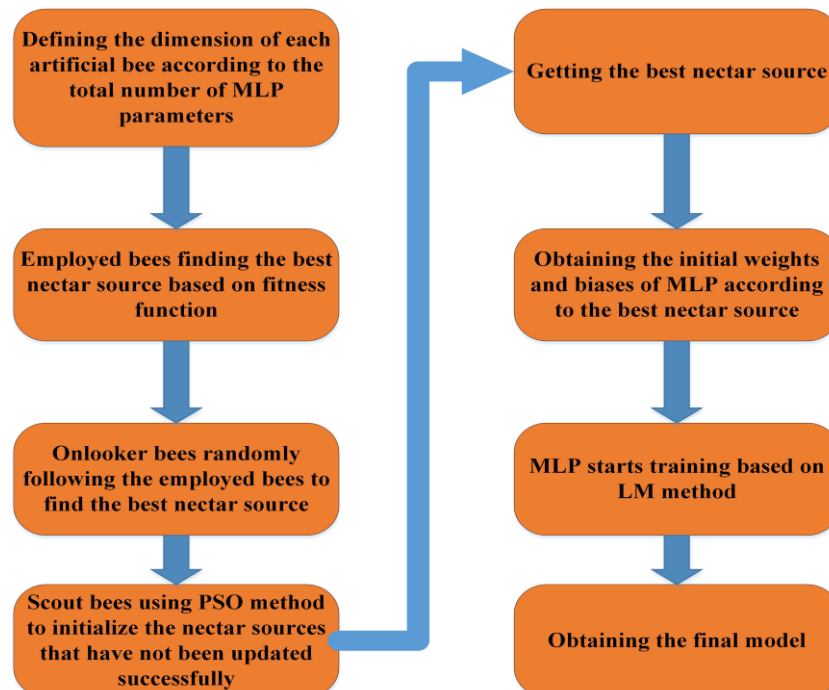


Fig. 3 The flow chart of a hybrid algorithm based on MLP and IABCPSO

2.3 Modeling of drain-source current I_{ds} , body diode I_{bd} and internal capacitors

In this paper, the drain-source current I_{ds} , body diode I_{bd} and internal capacitors are all modeled using our

proposed hybrid modeling method (IABCPSO-MLP). According to I-V curves provided by datasheet [18], the drain-source current I_{ds} can be modeled by an ANN with three inputs (drain-source voltage V_{ds} , gate-source voltage V_{gs} , and operating temperature T). In order to obtain a high-precision model, we use an ANN containing two hidden layers to model I_{ds} and each layer contains 8 neurons. The final modeling results can reach an accuracy of more than 99%.

From datasheet [18], we can find that the current of body diode I_{bd} , like I_{ds} , varies with V_{ds} , V_{gs} , and T . Therefore, the modeling of I_{bd} adopts the same ANN structure as that of I_{ds} and the accuracy of modeling

results of I_{bd} can also reach more than 99%.

According to the datasheet [18], both C_{ds} and C_{gs} vary nonlinearly with one variable, i.e., V_{ds} or V_{gs} . Hence, C_{ds} and C_{gs} can be modeled by same MLP structure with one input (V_{ds} or V_{gs}) and one output (C_{ds} or C_{gs}). Considering the simplicity and accuracy, the 1-5-5-1 MLP structure is finally selected among many tested structures, the accuracy of which can reach 98%.

3 Short-circuit model of SiC MOSFETs

When the short-circuit faults occur, the circuit power loop impedance will become extremely small, and the short-circuit current I_{sc} of the SiC MOSFETs will rise to a large amount. As the current of the circuit is very large, the power loss P_{loss} at this time will also become very large. Therefore, the junction temperature T_j begins to increase, leading to decrease of the channel carrier mobility and I_{sc} . However, T_j is still increasing, and the leakage current caused by thermal ionization is also gradually increasing. When the leakage current rate generated by thermal ionization is higher than the decrease rate of carrier mobility, I_{sc} starts to rise again. It can be concluded that the change of the short-circuit current of the SiC MOSFETs is mainly caused by the change of T_j . Therefore, to establish a short-circuit model, the change curve of T_j during the short-circuit process should be obtained first.

3.1 Thermal network model

In order to obtain the change curve of T_j during the short-circuit process, the thermal network of the SiC MOSFETs is established. The thermal network model based on the case-to-junction thermal impedance formed by a resistance-capacitance (RC) network [9] is the most commonly used, which is also used in this paper. As shown in Fig. 4, T_c and T_j are the case and junction temperatures of SiC MOSFETs, respectively. R_i and C_i are the thermal resistance and thermal capacitance, respectively.

After the development of the thermal network model, the transient thermal impedance Z_{th} can be obtained

by [9]:

$$Z_{th} = \sum_{i=1}^n R_i \cdot (1 - e^{-\frac{t}{R_i \cdot C_i}}). \quad (4)$$

The transient power loss P_{loss} is given by [9]:

$$P_{loss} = V_{ds} \cdot I_{ds} \quad (5)$$

After getting P_{loss} and Z_{th} , the junction temperature T_j of SiC MOSFETs can be obtained, which can be expressed as [9]:

$$T_j = P_{loss} \cdot Z_{th} + T_c \quad (6)$$

In this paper, the experimental data [20] is used as model reference. In [20], the DC bus voltage (V_{ds}) is set as 400V and the corresponding short-circuit current curves under different case temperatures are given.

In Fig. 5, the change of T_j is shown for $T_c=25^\circ\text{C}$ and $V_{ds}=400\text{V}$, which is obtained by Eq. (6) after substituting the transient power loss P_{loss} . When SiC MOSFETs work under normal conditions, the junction temperature is consistent with the case temperature, and when a short-circuit fault occurs, the junction temperature begins to rise.

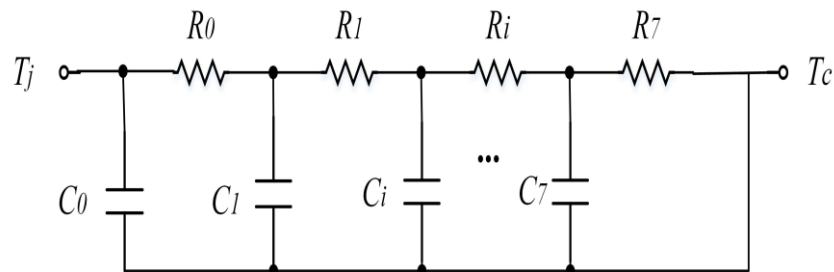


Fig. 4 Thermal network model between case and junction

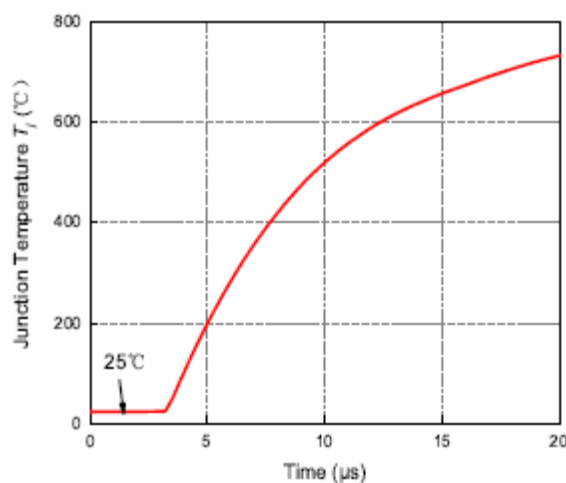


Fig. 5 The change curve of junction temperature T_j

3.2 Modeling of short-circuit current I_{sc}

After getting the instantaneous change curve of T_j , we can acquire the relationship between I_{sc} and T_j , as shown in Fig. 6, where the short-circuit current I_{sc} can be fitted based on T_j . Since when the short-circuit fault occurs, the current I_{ds} under normal working conditions also has output, I_{sc} needs to be fitted based on I_{ds} .

In this paper, the impact of different case temperatures on the short-circuit current is considered. Since the relationship between I_{sc} and T_j is various under different T_c , I_{sc} can be expressed as:

$$I_{sc} = I_{ds} \cdot f(T_j, T_c), \quad (7)$$

where $f(T_j, T_c)$ is a variable that changes with T_j and T_c . In this paper, $f(T_j, T_c)$ is fitted by a 2-5-5-1 ANN structure with hybrid modeling method, that is, ANN has two inputs (T_j and T_c), five neurons in two hidden layers and one output ($f(T_j, T_c)$). Hence, the final expression of I_{sc} can be rewritten as:

$$I_{sc} = \begin{cases} I_{ds_{ANN}} & T_j = T_c \\ I_{ds_{ANN}} \cdot f(T_j, T_c)_{ANN} & T_j > T_c. \end{cases} \quad (8)$$

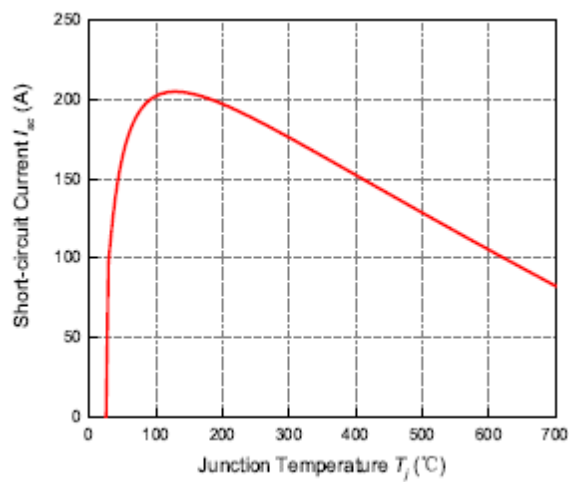


Fig. 6 The corresponding relationship between short-circuit current I_{sc} and junction temperature T_j

4. Conclusion

A short-circuit model based on IABCPSO-MLP modeling method for SiC MOSFETs is presented in this paper. In order to overcome the sensitivity of the basic algorithm (LM) of ANN to the initial values and enhance model accuracy, a scheme that uses IABCPSO to find the initial values for ANN is proposed and verified. The model under normal working conditions is verified by comparing the simulation results of the I-V characteristics, C-V characteristics and small signal parameters (g_d and g_m) that are not exposed in the training process with experimental data. And the short-circuit characteristics of the proposed model are proved by comparing short-circuit current waveforms predicted by our model and experimental data under different working conditions. Hence, our proposed SiC MOSFET short-circuit model can facilitate analysis of short-circuit faults and provide guidance for circuit design.

II. REFERENCES

- [1]. Mill'an, J., Godignon, P., Perpiñan, X., Tomas, A., Rebollo, J.: A survey of wide bandgap power semiconductor devices. *IEEE Transactions on Power Electronics*. 29(5), 2155-2163 (2014)
- [2]. Duan, Z., Fan, T., Wen, X., Zhang, D.: Improved SiC Power MOSFET model considering nonlinear junction capacitances. *IEEE Transactions on Power Electronics*. 33(3), 2509-2517 (2018)

- [3]. Sun, J., Xu, H., Wu, X., Sheng, K.: Comparison and analysis of short circuit capability of 1200V single-chip SiC MOSFET and Si IGBT. 2016 13th China International Forum on Solid State Lighting: International Forum on Wide Bandgap Semiconductors China (SSLChina: IFWS), 42-45 (2017)
- [4]. Fu, R., Grekov, A., Hudgins, J., Mantooth, A., Santi, E.: Power SiC DMOSFET model accounting for nonuniform current distribution in JFET region. *IEEE Transactions on Industry Applications*. 48(1), 181-190 (2011)
- [5]. Li, H., Zhao, X., Sun, K., Zhao, Z., Cao, G., Zheng, T.Q.: A Non-Segmented PSpice Model of SiC mosfet With Temperature-Dependent Parameters. *IEEE Transactions on Power Electronics*. 34(5), 4603-4612 (2019)
- [6]. Benedetto, D. L., Licciardo, D. G., Erlbacher, T., Bauer, A. J., Liguori, R., Rubino, A.: A model of electric field distribution in gate oxide and JFET-region of 4H-SiC DMOSFETs. *IEEE Transactions on Electron Devices*. 63(9), 3795-3799 (2016)
- [7]. Duong, T. H., Ortiz, J. M., Berning, D. W., Hefner, A. R., Ryu, S. H., Palmour, J. W.: Electro-thermal simulation of 1200V 4H-SiC MOSFET short-circuit SOA†. *IEEE 27th International Symposium on Power Semiconductor Devices & IC's (ISPSD)*. Hong Kong, 217-220 (2015)
- [8]. Zhao, X., Zhou, Z., Li, H., Sun, K., Zhao, Z.: A Temperature-dependent PSpice Short-circuit Model of SiC MOSFET. *IEEE Workshop on Wide Bandgap Power Devices and Applications in Asia (WiPDA Asia)*. (2019)
- [9]. Li, H., Wang, Y., Zhao, X., Sun, K., Zhou, Z., Xu, Y.: A Junction Temperature-based PSpice Short-circuit Model of SiC MOSFET Considering Leakage Current. *IECON 2019 - 45th Annual Conference of the IEEE Industrial Electronics Society*. (2019)
- [10]. Wang, Z., Shi, X., Leon, M., Fred, T., Wang, Z.: Temperature-Dependent Short-Circuit Capability of Silicon Carbide Power MOSFETs. *IEEE Transactions on Power Electronics*. 31(2), 1555-1566 (2016)

IOT based Contactless Temperature using Raspberry Pi

Anushree N R¹, Nilu Mishra², Kavitha L³, Dr. Nandini V L⁴

^{1,2,3}, Assistant Professor, Dept of ECE, East Point College of Engineering and Tecnology

ABSTRACT

In this paper we present the development of IOT based contactless body temperature monitoring using raspberry pi with camera and email alert. The proposed system offers the image of the person if the temperature of any particular person exceeds the set value. Experimental results of the suggested prototype show the measuring temperature and sending mail alert with PI.

Keywords : Raspberry pi3, pi camera, MLX90614-IR Temperature sensor, Temperature measurement, Electronic circuits.

I. INTRODUCTION

It has become truly challenging to recognize the individuals who are influenced by the infection or not. To tackle this issue, temperature gadgets are regularly used to gauge internal heat level. These gadgets have non-contact IR temperature sensors which can gauge the internal heat level with no actual contact. There are numerous temperature weapons accessible on the lookout, however none of them gives any ready or email warning to higher specialists to make fitting moves when the temperature surpasses a specific cut-off. In this undertaking, we will interface an IR temperature sensor and send the email alarms with the picture of the individual if the temperature of a specific individual surpasses the set is important. The Internet of Things is upsetting our life by fostering various frameworks which can be observed and controlled distantly. IoT can offer generous benefit across the whole life sciences esteem chain, from innovative work digitalization to upgrading the patient experience. This distant innovation dependent on IoT stage is particularly valid in Coronavirus-19 sickness, straightforwardly affecting general wellbeing measures on help clinical in friendly region. This exploration article proposes the contactless internal heat level checking of the in-patient division (IPD) utilizing the web of clinical advancement. IoT has begun to discover more extensive applications in the field of clinical material the executive's perception. Nodayway's, health monitoring is a global challenge in peoples life time solid condition which affected by natural and careful realities. The estimation of human body fundamental signs is an essential to recognize the wellbeing status. The exhibition of any work or exercise in hot conditions upsets the decent warm homeostasis condition of human body (HB). This equilibrium recognizes the HB about physiological and intellectual execution of body. The typical internal heat level reaches by 36.50C to 37.50C. The situation with wellbeing beneath this cut-off is expressed as hypothermia and the status above is alluded as fever and hyperthermia conditions. The hyperthermia likewise alluded as cancer contingent stage that ranges more than 38.5 0C. The singular body temperature estimation is reliant of various viewpoints for

example age, effort, contamination and spot of body at which estimation made. There are a few techniques to gauge the HBT for example oral, rental and axillary through inconsistent and contactless thermometers.

Literature Review

It utilizes high LM-35DZ temperature sensor for estimation of human internal heat level. It utilizes GSM innovation and its usefulness for versatile correspondence to communicate the physiological sign data to an approved individual's PDA. This framework has GPS innovation for area recognizable proof. By using this method, we can sense, send, display, and store the physiological parameter such as human body temperature.

Thermo-vision system is used to detect the overheated spots in electronic PCBs or integrated circuits in a non-destructive, contactless manner, in order to improve their thermal stability and reliability. It offers a low-cost solution for laboratory testing of electronic circuits that has good accuracy and flexibility.

3 IOT based health monitoring system using Raspberry Pi, it uses different sensors like Pulse/Heart beat sensor, Body temperature sensor, ECG sensor, Blood pressure sensor and Patient position sensor are attached to the patient and sensor output serially are sent to Raspberry Pi. It will be helpful for students, patients, athletes, gymnastics for their health analysis easily at any place.

4 The iRT incorporate a microcontroller with native Wi-Fi support, a Fire Beetle ESP8266 (DFRobot) and the sensor is connected using I2C interface. To make specialized upgrades, including the improvement of significant cautions and notices to inform the client when the temperature meets characterized setpoints. An embedded system using an infrared temperature sensor that works with an IoT-Wi fi controller on the NodeMCU ESP32 board and the detected data will be transferred to users via the internet network, and it will be stored on a cloud internet system. This method is helpful to reduce the contact, proximity between patients and healthcare professionals.

5 This system starts with initialization of temperature sensors for collection of real time temperature data in compare to environmental temperature values. The affectability of temperature sensors LM35 (S1) and MLX-90614 (S2) is customized in C++ language and access through Arduino CT-UNO regulator. The daily monitoring of body temperature can prevent the people from threaten of fever, hypothermia and hyperthermia illness.

6 A circuit consisting of a microcontroller, Bluetooth, LED, light-dependent resistor (LDR), and MLX 90615 IR temperature sensor has been designed. At the entrance of a building such as a university or a mall, the fever of the visitors can be detected safely, without contacting physically.

7 The temperature sensor type (MLX90614ESF) was used similarly as the usage of the beat sensor type (KY039), which related with Arduino Uno where the results were taken care of and sent by a nRF24L01 development to the far away end and ensuing to tolerating them in the far side are arranged using Arduino Uno. It will show the perusing of the heartbeat sensor and blood heat sensor in BPM (Beats Per Minute) and in Celsius or Fahrenheit.

8 To make a classifier that will differentiate between faces with masks and without masks. A Pre-prepared organization called mobileNetV2 which is prepared on the ImageNet dataset with our neural organization model. Various deep learning and computer vision frameworks are used for social distance finding with our proposed system on raspberry pi.

9 This system will help to identify people on image/ video stream wearing a facemask with the help of Deep Learning and Computer Vision algorithms by using various libraries such as OpenCV, Keras, TensorFlow etc. The images are downloaded from various open-source websites and are differentiated as “mask” and “no mask”. The pictures that we downloaded were of various sizes and various goals. Face Mask and internal heat level recognition can assist us with diminishing the enormous social affair of individuals in a single spot without veils, lessening the danger of getting contaminated.

Need of Temperature Monitoring System

The variation in human body temperature (HBT) can lead to different disease. It is essential to quantify the range of temperature as shown in body temperature measurement range (Fig1). As expressed by analysts that, while assessing and estimating the wellbeing status extraordinarily HBT, some crucial focuses are essential. Few measurement methods are shown in temperature measurements methods (Fig2), while some aspects are justified in sub-sections diurnal variations (2.1) and emotional status (2.2) respectively and linked are listed in variations in body temperature by age (Table 1).

2.1. Diurnal variations - This variety is reliant of human body digestion. During the sleep the metabolism is slower as decrement in contractions of muscles.

2.2. Emotional states- These variations frequently observed with young children during extreme anger and crying state which increase the body temperature.

MLX90614 IR Temperature Sensor: There are numerous sensors accessible in the market which can give us temperature and humidity. What makes this sensor unique in relation to any remaining sensors is that it can give us object temperature and different sensors give surrounding temperature. We have used DHT11 Sensor and LM35 extensively for many applications where atmospheric humidity or temperature has to be measured. But here for making a temperature gun which doesn't need physical contact and can measure the object temperature instead of ambient temperature, we use IR based MLX90614. MLX90614 sensor is made by Melexis Microelectronics Integrated frameworks, it chips away at the rule of InfraRed thermopile sensor for temperature estimation. These sensors comprise of two units inserted inside to give the temperature yield. The primary unit is the detecting unit which has an infrared identifier which is trailed constantly unit which plays out the calculation of the information with Digital sign preparing (DSP). This sensor deals with Stefan-Boltzmann law which clarifies power emanated by a dark body as far as its temperature. In straightforward terms, any item radiates IR energy and the power of that will be straightforwardly corresponding to the temperature of that article. MLX90614 sensor changes over the computational worth into 17-bit ADC and that can be gotten to utilizing the I2C correspondence convention. These sensors measure the ambient temperature as well as object temperature with the resolution calibration of 0.02°C. To find out about the elements of the MLX90614 sensor, allude to the MLX90614 Datasheet.

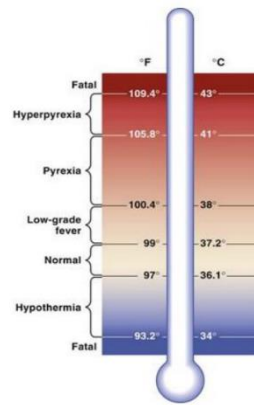


Figure 1. Body temperature measurement range

Features of MLX90614:

- Operating Voltage: 3.6V to 5V.
- Ambient Temperature Range: -40°C to 125°C.
- Object Temperature Range: -70°C to -382.2°C.
- Resolution/Calibration: 0.02°C.
- 17-bit ADC.
- I2C communication

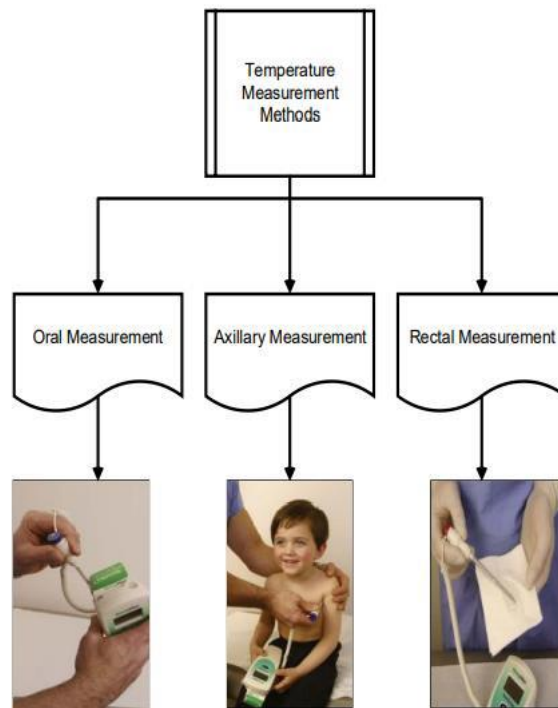
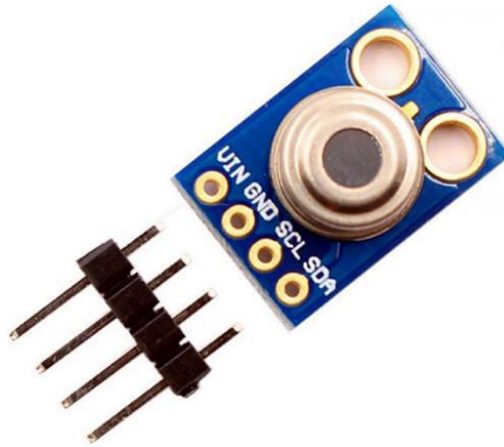


Figure 2. Temperature measurement methods



Methodology

Interfacing MLX90614 with raspberry pi

Step1: - Enabling the I2C from raspberry pi setting.

Step2: -Download the package/library of MLX90614 by going to [https://pypi.org/project/PyMLX90614/# files](https://pypi.org/project/PyMLX90614/#files) Pi camera interfacing with raspberry pi

Step1: -Enabling the camera from raspberry pi setting.

Step2: -To check if the camera to click a picture with the name image and store that on your desktop.

Setting up SMTP email with raspberry pi

Step1: -Go to the right corner and click on my manage your google account.

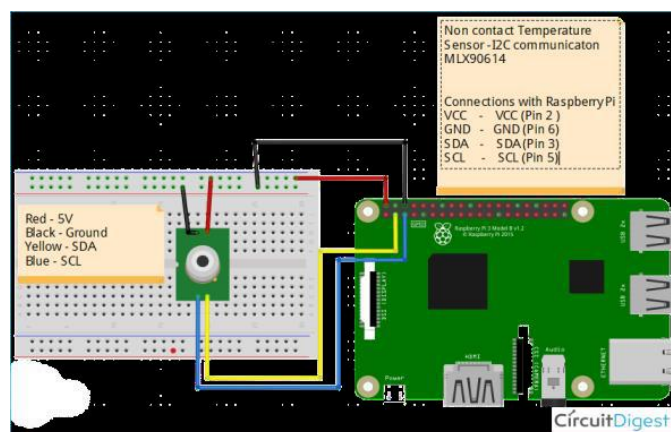
Step2: - Click on security and scroll down to “less secure app access”

Step3: - Enable the less secure app.

Step4: - Repeat with the other email id as well to send/receive the email from the python script.

Step5: -Download the required packages.

Step6: - After the establishment of the relative multitude of libraries is done, we need to make changes in the smtp.conf document where we need to enter the sender's email subtleties.



Steps to Send Mail with attachments using SMTP (smtp lib)

1. Create MIME.
2. Add sender, recipient address into the MIME.
3. Add the mail title into the MIME.
4. Attach the body into the MIME.
5. Start the SMTP meeting with legitimate port number with appropriate security highlights.
6. Login to the system.
7. Send mail and exit.

The Raspberry Pi Foundation explicitly chose Python as the fundamental language due to its force, flexibility, and convenience. Python comes preinstalled on Raspbian, so you'll be prepared to begin consistently. You have various choices for composing Python on the Raspberry Pi..

Raspberry Pi program is, without a doubt, an extremely insignificant beginning. A lot more impressive applications can be composed utilizing the Python programming language. Obviously, on the off chance that you simply need a modest \$35 Linux machine, the Raspberry Pi turns out extraordinary for that to.

Python is generally utilized for creating sites and programming, task computerization, information investigation, and information perception. Since it's moderately simple to learn, Python has been taken on by numerous non-developers like bookkeepers and researchers, for an assortment of ordinary undertakings, such as getting sorted out accounts.

Advantages and Disadvantages

Advantages

Smart sensors examine ailments, way of life decisions and the climate and suggest deterrent measures, which will diminish the event of sicknesses and intense states. Decrease of medical care costs: IoT lessens expensive visits to specialists and emergency clinic affirmations and makes testing more moderate.

1. Distant observing: Real-time far-off checking through associated IoT gadgets and savvy cautions can analyze ailments, treat infections and save lives in the event of a health-related crisis.
2. Prevention: Smart sensors dissect medical issue, way of life decisions and the climate and suggest protection measures, which will lessen the event of sicknesses and intense states.
3. Reduction of healthcare costs: IoT reduces costly visits to doctors and hospital admissions and makes testing more affordable.
4. Medical data accessibility: Accessibility of electronic medical records allow patients to receive quality care and help healthcare providers make the right medical decisions and prevent complications.
5. Improved treatment management: IoT devices help track the administration of drugs and the response to the treatment and reduce medical error.
6. Improved healthcare management: Utilizing IoT gadgets, medical services specialists can get significant data about hardware and staff adequacy and use it to recommend developments.

7. Research: Since IoT devices are able to collect and analyze a massive amount of data, they have a high potential for medical research purposes.

DISADVANTAGES

Security and privacy: Security and privacy remain a major concern deterring users from using IoT innovation for clinical purposes, as medical care checking arrangements can possibly be penetrated or hacked. The hole of touchy data about the patient's wellbeing and area and interfering with sensor information can have grave results, which would counter the advantages of IoT.

2. Risk of failure: Disappointment or bugs in the equipment or even force disappointment can affect the exhibition of sensors and associated gear putting medical services tasks in danger. Likewise, avoiding a planned programming update might be significantly more unsafe than skirting a specialist examination.

3. Integration: There's no agreement with respect to IoT conventions and norms, so gadgets delivered by various makers may not function admirably together. The absence of consistency forestalls full-scale coordination of IoT, thusly restricting its expected viability.

4. Cost: While IoT vows to lessen the expense of medical care in the long haul, the expense of its execution in clinics and staff preparing is very high.

CONCLUSION

When the hardware and software are ready, just run the python code on your pi. it will print the worth of temperature read from the sensor. If the object temperature, then our python program will take an image from the camera, save it on raspberry pi, and also share it via email.

REFERENCES

- [1] Sudhindra F 1, Annarao S.J2, Vani R.M3, Hunagund P.V4 “Development Of real time human body temperature [Hypothermia and Hyperthermia] monitoring and Alert Systems with GSM and GPS” 2016.
- [2] Miljana Milić and Miloš Ljubenočić “Arduino-based non-contact system for thermal-imaging of electronic circuits” 2018.
- [3] Sunil Kumar Laxman Bhai Rohit and Bharat V. Tank “IOT Based health monitoring system using raspberry pi” 2018.
- [4] Gonçalo Marques* and Rui Pitarma “Non-contact Infrared temperature acquisition system based on IOT for laboratory activities monitoring” 2019.
- [5] Wasana Boonsong1, Narongrit Senajit2, Piya Prasongchan3 “Contactless body Temperature Monitoring of In-patient department (IPD) Using 2.4GHZ microwave frequency via the IOT network” 2020.
- [6] Asif A. Rahimoon1, Mohd Noor Abdullah2, Ishkrizat Taib3 “Design of a Contactless body temperature system measurement using arduino” 2020.
- [7] Ahmet Remzi Ozcan1, Ahmet Mert1* “Low-cost android based telemonitoring System for body temperature measurement” 2021.
- [8] Shantilal Sen1, Manali Patil2, Sejal Ravankar3, Janhavi Sangoi4 “Survey of a symptoms Monitoring system for covid-19” 2021.

- [9] Sheetal Mahadik¹, Namrata J. Ravat², Kunal Y. Singh³, Suvita K. Yadav⁴ “Contactless system with mask and temperature detection” 2021.
- [10] NaveenKumar K, ²Surya.S, ³Mohammed Nihaal. S. S, ⁴Suranthar. S, ⁵Manoj Kumar. A “Automatic covid-19 face mask and body temperature detection with deep learning and computer vision” 2021

Blackfin Processor Boom to Embedded System

Nilu Mishra¹, Anushree N R², Kavitha L³, Chaitali Darode⁴

^{1,2,3}Assistant Professor, Dept of ECE, East Point College of Engineering and Tecnology

⁴Assistant Professor, Dept of ECE, SBJain Institute of Technology, Nagpur

ABSTRACT

Digital signal processing (DSP) is a key requirement in a variety of industries and applications. It offer an assortment of digital signal processing solutions for applications including automotive, portable, motor/power control, security, test and measurement, and beyond it also meet design needs. Processor provides scalable low-latency audio performance, featuring large on-chip SRAM with many options including on-chip ASRCs and multi-channel IIR/FIR/FFT accelerators to facilitate real-time audio processing. System connectivity includes TDM/I2S, Ethernet, MLB, CAN, SPI, I2C, UART, and many others, making them a fit for a wide variety of embedded applications.

I. INTRODUCTION

Blackfin processor was designed, developed, & marketed through Analog Devices & Intel as Micro Signal Architecture (MSA). The architecture of this processor was announced in December 2000 & demonstrated first at the ESC (Embedded Systems Conference) in June 2001. This Blackfin processor was mainly designed to reach the power constraints & computational demands of present embedded audio, video & communications applications. This article discusses an overview of a Blackfin processor – architecture and its applications.

II. Architecture

The Blackfin processor provides both the functionalities of a micro-controller unit & digital signal processing within a single processor by allowing flexibility. So this processor includes a SIMD (single instruction multiple data) processor including some features like variable-length RISC instructions, watchdog timer, on-chip PLL, memory management unit, real-time clock, serial ports with 100 Mbps, UART controllers & SPI ports.

The MMU supports multiple DMA channels to transfer data between peripherals & FLASH, SDRAM, and SRAM memory subsystems. It also supports data caches & configurable on-chip instruction. The Blackfin processor is a simple hardware which supports 8, 16, and 32-bit arithmetic operations.

The Blackfin architecture is mainly based on the architecture of micro signal and this was jointly developed by ADI (Analog Devices) & Intel, which includes a 32-bit RISC instruction set and 8-bit video instruction set with dual 16-bit multiply-accumulate (MAC) units.

Analog devices are capable of achieving a balance between the DSP & MCU requirements through the instruction set architecture of Blackfin. Generally, the Blackfin processor is coupled with the powerful Visual DSP++ software development tools but now by using C or C++, it is possible to produce highly efficient code very easily than before. For real-time requirements, operating system support becomes critical, so the Blackfin supports a no. of operating systems & memory protection. Blackfin processor comes in both single-core like BF533, BF535 & BF537, and dual-core like BF561 models.

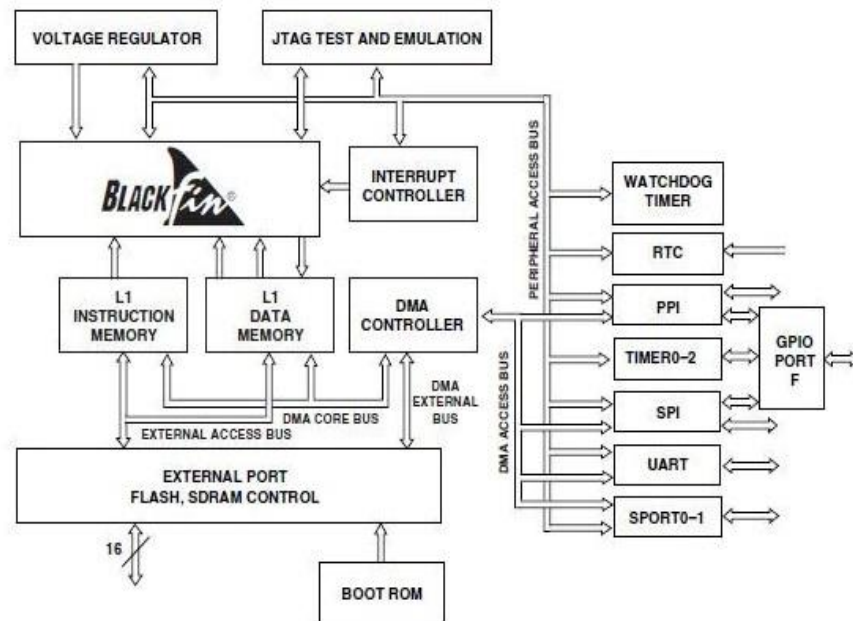


Figure 1.1 Blackfin Processor Architecture

The Blackfin processor architecture includes different on-chip peripherals like a PPI (Parallel Peripheral Interface), SPORTS (Serial Ports), SPI (Serial Peripheral Interface), UART (Universal Asynchronous Receiver Transmitter), General-purpose timers, RTC (Real-Time Clock), Watchdog timer, General-purpose I/O (programmable flags), Controller Area Network (CAN) Interface, Ethernet MAC, Peripheral DMAs -12, Memory to Memory DMAs -2 including Handshake DMA, TWI (Two-Wire Interface) Controller, a Debug or JTAG Interface & Event Handler 32 Interrupt Inputs. All these peripherals in the architecture are simply connected through different high-bandwidth buses to the core.

III. IMAGE PROCESSING APPLICATION OF BLACKFIN PROCESSORS

As high definition (HD) cameras and displays become commonplace, the need to quickly process large images increases. The embedded processors found in such devices have, for the most part, not followed the trend of increasingly faster clock speeds seen in general-purpose processors. High clock speeds translate to higher power usage, which in turn requires cooling systems to maintain reliable performance.

Such requirements are ill-suited to the constrained environments of embedded systems. For this reason, and because embedded processors tend to be geared more to specific classes of applications, embedded chips have specialized hardware resources to do more per cycle, rather than reducing the cycle time. Many image processing routines can be expressed as a set of instructions, called compute kernels, which transform raw image data into meaningful information. Vector processing units, special-purpose hardware such as video ALUs (vALUs), and convergent cores have extended some embedded architectures to allow multiple pixels to be transformed at once. But because of the vast amounts of data needing to be processed, memory performance is critical. Researchers have examined the memory hierarchy and proposed methods to minimize the latency associated with accessing high-capacity, slow off-chip SDRAM (called the Memory Wall effect). This need to feed the computational units which may otherwise be starved for data motivates our work and our examination of the stream model of computing.

The software modules are fully optimized for the Blackfin processor family and include image processing task level primitives to enable faster development cycles for video analytics applications. The free software modules, available in object code or a C source wrapper, provide advanced video design functionality such as video filtering, transforms, color operations and utilities suitable for a wide range of applications, including video surveillance, automotive vision systems and industrial vision.

A scheduling algorithm for image processing tasks which have two computations steps both of them depend of noise power. The scheduling algorithm trades off between the quality of the restored image and the constraint to meet the deadlines. The framework for real time implementation of such image processing algorithms that ensure a reasonable quality of the videoclips in systems prone to impulsive noise but meeting deadlines.[1]

Figure 1.2 proposed steps for Image processing

Video surveillance systems [VSS] are digital today due to advancement of processing capabilities of DSP compared to analog. Video surveillance technology is necessary and indispensable around the world for public safety and law enforcement control. The advantage of video surveillance is to monitor and provides the real-time protection for investigation and evidence preservation. Largely, it depends on the quality of the images transmitted by digital video surveillance cameras and networks. Image quality is paramount. Digital VSS provides various advantages such as viewing the video or images immediately as soon the incident captured by the VSS either near or remote locations. So, action for the captured incident will be address immediately to to apply intelligence and swift response [3-4].

VSS is a kind of any video surveillance technology which has features of enabling (videotapes, photographs or digital images) for continuous or periodic recording and viewing or monitoring of public areas. Monitoring and tracking will provide the safety for lives. A variety of applications are emerging to leverage the power of DSPs in products like video surveillance cameras and video servers. A surveillance is one of the major verticals that is witnessing exponential growth. The threat to security globally is the major driver for the growth in security surveillance market.[8-9]

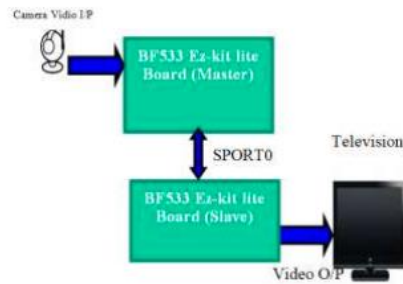


Figure 1. Block diagram of VSS

The various parameters for VSS are analyzed, how it will be implemented on the embedded processor. ADSP Blackfin processor BF533 is suitable for the video application. It can be developed on BF533 at low cost and low power consumption. The VSS is designed based on available ADSP BF533 Ez-kit lite. The concept is developed and verified on the Ez-kit lite. The application video signal processing is facilitating and achieved through the parallel peripheral interface (PPI) of the Blackfin processor which is connecting to both of video encoder and video decoder in the Ez-kit lite. Hence, two boards are used to prove the real time design as master and slave transfer mode. The VSS block diagram is shown in the below Figure. It gives the concept of system at the top level and interconnection. Two BF533 Ez-kit lite boards are interconnected through SPORT to transfer the data. The detailed technical design is described in the next section.

Video interfaces. The Video interfaces will be discussed in System on the BF533 Ez-kit lite board's features and how it is implemented. Also, it contains the block diagram, and flowchart representation for the design and implementation of the logic. The system architecture is discussed with the top-level block diagram. The board hardware configurations, setups and interfaces with respect to video processing are described though BF533 Ez-kit lite supports other features like Audio interface, UART. The basic configuration will be discussed for each section except detail as separate sections include memory and peripheral interfaces, power and clock signals, LED, pushbutton switch and video interfaces.

Audio compression (data), a type of lossy compression in which the amount of data in a recorded waveform is reduced for transmission with some loss of quality Dynamic range compression, also called audio level compression, in which the dynamic range, the difference between loud and quiet, of an audio waveform is reduced. Dynamic range compression, also called DRC (often seen in DVD and car CD player settings) or simply compression reduces the volume of loud sounds or amplifies quiet sounds by narrowing or "compressing" an audio signal's dynamic range.

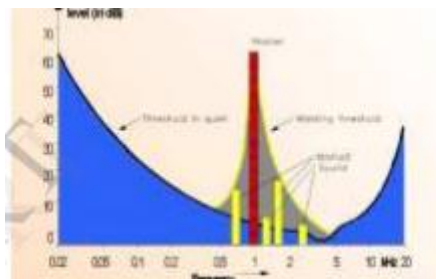


Figure shows the threshold of energy required in the 20Hz-20 KHz range for an average human to perceive sound in quiet, measured in deci-Bells (dBs)

Goals Of audio Compression:

Reduced bandwidth or storage make decoded signal as close as possible lowest implementation complexity reasonable arithmetic requirement. Application to as many signal type as possible robust, scalable extensible an `audio CODEC' is a system for the Needs of audio compression: Audio compression (data), a type of lossy compression in which the amount of data in a recorded waveform is reduced for transmission with some loss of quality Dynamic range compression, also called audio level compression, in which the dynamic range, the difference between loud and quiet, of an audio waveform is reduced. Dynamic range compression, also called DRC (often seen in DVD and car CD player settings) or simply compression reduces the volume of loud sounds or amplifies quiet sounds by narrowing or "compressing" an audio signal's dynamic range Goals Of audio Compression: Reduced bandwidth or storage make decoded signal as close as possible lowest implementation complexity reasonable arithmetic requirement. Application to as many signal type as possible robust, scalable extensible an `audio CODEC' i s a system for the encoding, and Decoding of audio data for use in digital systems The term `Lossy' refers to the fact that once audio data have gone through this process and been reconstructed, some information will be lost and the resulting signal will not be identical to that sampled. The key to successful CODEC is being able to identify where the redundant information in the signal is and being able to remove it, while at the same Time minimizing the perceived impact on the listener of the reconstructed signal. [10]

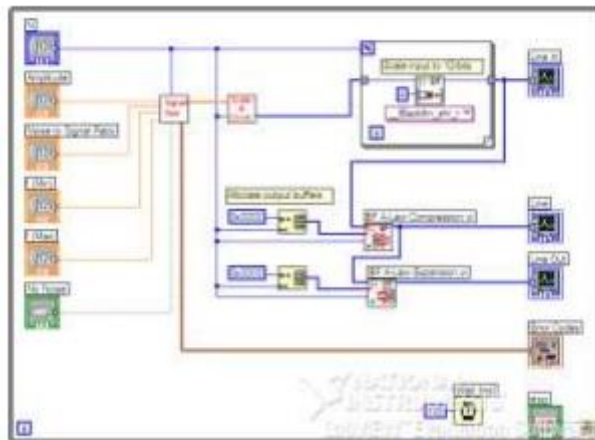


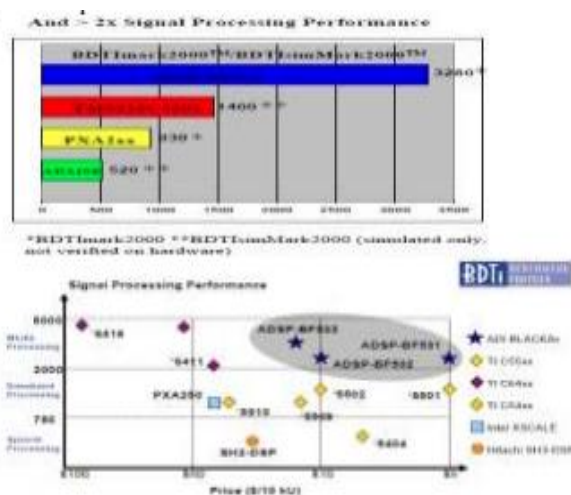
Figure Audio compression using Blackfin

Arbitrary bit and bit-field manipulation, insertion and extraction Integer operations on 8/16/32-bit data-types Memory protection and separate user and supervisor stack pointers Scratch SRAM for context switching Population and leading digit counting Byte addressing DAGs Compact Code Density.

Types of Audio Codec:

Non-compression formats: LPCM, generally only described as PCM is the format for uncompressed audio in media files and it is also the standard for CD DA note that in computers, LPCM is usually stored in Container Formats such as WAV FF mpeg Pulse Density Modulation (PDM) Pulse Amplitude Modulation (PAM) Lossless data compression: APPLE Lossless Audio Codec (ALAC) FF mpeg QuickTime ATRAC Advanced lossless (AAL) Direct Steam Transfer (DST) MPEG-4 DST reference software (ISO/IEC

14496-5:2001/Amd.10:2007) MLP but adds higher sample rates, bit rates, and more channels FF mpeg. (decoding only)



CONCLUSION

We have compared Video, Audio, Image and data coding using blackfin processors, only video and Audio reference we have taken in this paper. From above same it is clear that blackfin processor are very efficient, cost, effective and best suited for above applications.

IV. REFERENCES

- [1]. Use of an Embedded Configurable Memory for Stream Image Processing, Michael G. Benjamin and David Kaeli Northeastern University Computer Architecture Research Group Department of Electrical and Computer Engineering Northeastern University, Boston, MA 02115 {mbenjami, kaeli}@ece.neu.ed
- [2]. Blackfin processor based secure Audio, Video and image transmission, Ardina Aurthur, V Saravanan, Department of Embedded system technologies, Procedia Engineering 38(2012), 359-365.
- [3]. ADSP BF533 Ez-kit lite Specification, Analog Devices, 2010. [Online].
- [4]. A. Seema and M. Reisslein, "Towards efficient wireless video sensor networks: A HW/SW cross layer approach to enabling sensor node platforms," IEEE COMSOC MMTCE-Letter, vol. 7, no. 4, pp. 6-9, 2012. [5] Ahrenberg. L. Ihrke. I., Magnor.M, "A mobile system for multi-video recording," CVMP, 1st European Conference Visual Media Production, 2004, pp, 127-132.
- [5]. A. Bouyahya, Y. Manai and J. Haggege, "Application of new approach of design flow for hardware/software embedded systems with use of design patterns in fuzzy control system," International Journal of Reconfigurable and Embedded Systems, vol. 4, no. 2, pp. 142-160, 2015.
- [6]. S. Dessai and K. Ramakrishna, "Implementation of video capture and playback in mobile systems," International Journal of Reconfigurable and Embedded Systems, vol. 2, no. 3, pp. 106-115, 2013.
- [7]. S. Dessai and K. Ramakrishna, "Implementation of video capture and playback in mobile systems," International Journal of Reconfigurable and Embedded Systems, vol. 2, no. 3, pp. 106-115, 2013. [6] D. Fronczak and D. Seltz, "Motion JPEG and MPEG solutions for multimedia," IEEE transaction on Multimedia published in 2002, pp. 2-4.
- [8]. F. Gaarder, "Video streaming into virtual worlds" M.S. thesis, Department of Informatics, University of Oslo, Norway, 2009
- [9]. New Algorithms for Implementing Audio Compression Techniques Using Embedded System, Mr. A. V. Warhade, Prof A. D. Bijwe Prof. A. P. Deshpande, International Journal of Engineering Research & Technology (IJERT) Vol. 2 Issue 5, May - 2013

Selection of Suitable Filter Parameters for Denoising Breast Thermograms Using Anisotropic Diffusion Filter

Vijaya Madhavi M*, Vetrikani R, Malini V L

Department of Electronics and Communication Engineering, East Point College of Engineering and Technology, Bengaluru, India

ABSTRACT

The most common form of cancer among women is breast cancer. Breast thermography is the new technology employing infrared camera to detect heat emissions from the breast region. The acquired thermal images are of low contrast and are corrupted to a greater extent by quantum noise. The objective of the proposed work is to effectively denoise breast thermograms using anisotropic diffusion filter. In the proposed work, frontal breast thermograms are processed using anisotropic diffusion filter which preserves sharp edges and also effectively removes noise. The selection of optimum parameters to perform anisotropic diffusion determine the quality of denoised images. Two crucial parameters for filtering are gradient threshold parameter (k) and number of iterations (itr). The number of iterations is chosen based on subjective evaluation whereas the gradient threshold parameter is determined by selecting knee point from the plot of k versus Peak Signal to Noise Ratio (PSNR). The filtered output is evaluated using PSNR and Mean Structural Similarity Index (MSSIM). The values obtained are PSNR of 39.74 dB and MSSIM of 0.9859 indicating the usefulness of anisotropic diffusion filtering.

Keywords— Thermography, breast cancer, anisotropic diffusion filter, PSNR, MSSIM

Introduction

In all of the world's female population, breast cancer is the most prevalent cancer type. It effects women majorly from low- and middle-income countries. Five-year survival rate of high-income country is 90% whereas for middle-income country it is 66% and for low-income country it is 40%. World Health Organization (WHO) has taken initiative to save 2.5 million lives over a period of 20 years by means of health promotion, timely diagnosis and comprehensive breast cancer management [1].

Breast cancer is due to aberrant cell proliferation in the breast region. It occurs due to numerous factors such as family history of breast cancer, genetic mutation, obesity, smoking, alcohol consumption or due to higher levels of certain hormones. Various symptoms for breast cancer include development of lump, changes in breast shape, dimpling of the skin and so on [2]. By the time any one of the above-mentioned symptoms are identified by the patient, the cancer would have reached stage II or stage III. Nowadays the existence of breast cancer is more in young women especially from the age of 35 [3]. Thus, in order to increase the survival rate, early identification of breast cancer becomes crucial. Mammogram is a gold standard modality that helps to identify suspicious

findings in the breast but has limitation in imaging dense breast tissues. Thermography is a new technique proven to identify breast cancer in its initial stages. It has an advantage over mammogram by identifying abnormalities in dense breast tissues. Thus, breast cancer can be detected in initial stages using thermography. Several authors have asserted usage of pre-processing as an initial task before segmentation or classification of breast thermal images. Fractional-order derivative filter was used to improve the texture and denoise the image [4], median filter was used to remove noise [5], Gaussian filtering was used for denoising and Contrast Limited Adaptive Histogram Equalization (CLAHE) was used to enhance the image [6], combination of Gaussian and bilateral filter was employed for denoising thermograms [7]. The objective of image denoising is to remove noise and at the same time preserve the edge information of the objects in an image. Anisotropic diffusion filter is one of the popularly used filter for denoising of thermograms but authors failed to mention the procedure for selection of filter parameters [8-9]. The anisotropic diffusion filter was applied for denoising images of different modalities such as mammogram, brain MRI, ultrasound, microscopic and nature images [10-13]. Thus, in the proposed method procedure for selection of anisotropic diffusion filter parameters is explored.

Methodology

Image Database

In the proposed work, the frontal thermograms from Database of Mastology Research (DMR) recorded using FLIR SC-620 IR camera are taken into account for analysis. These images are recorded using static protocol and has a spatial resolution of 640x480 pixels. In static thermal image acquisition, the patient has to rest for 10 minutes in order to achieve thermal stability inside the temperature-controlled environment. After the patient has rested, 5 images (1 frontal, 2 lateral images of left breast at 45° and 90° and 2 lateral images of right breast at 45° and 90°) were acquired [14].

Thermogram Preprocessing

The acquired thermal images are color images, hence color to gray scale conversion is performed. These images contain undesired regions such as thoracic, arms, waist region along with the complete breast region as depicted in Figure 1. Hence, for the acquired image of size $M \times N$, the image was roughly cropped such that the coordinates of the cropped image were $x1 = 10$; $x2 = N - 40$; $y1 = 76 M/4$; $y2 = M - 0.3 * M$ resulting in removal of certain undesired regions.

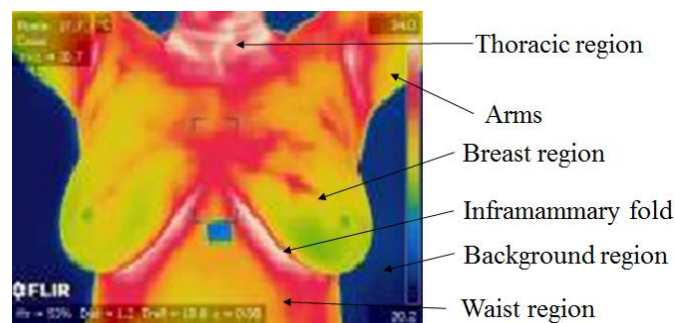


Figure 1. Breast thermogram with marked areas

Anisotropic Diffusion Filtering

The infrared cameras used in breast cancer detection are LWIR (Long Wave InfraRed) cameras with FPA (Focal Plane Array) uncooled microbolometers. The noise in IR images is not only determined by the detector but also by background and emissivity fluctuations of the object.

The major source of noise in infrared images is due to non-uniformity of FPA and read-out circuits of IR cameras [15].

The acquired breast thermal images are of low contrast and low Signal to Noise (S/N) ratio, hence denoising are carried out to enhance the image quality. Anisotropic Diffusion (AD) is a nonlinear filter utilizing diffusion approach that helps to reduce the noise and conserving the edges in an image. It reduces diffusion at strong image gradients (edges) and increases diffusion in other sections of the image. AD is represented by

$$f_t = \text{div}(c(x, y, t)\nabla f) = c(x, y, t)\Delta f + \nabla c \cdot \nabla f \quad (1)$$

where Δf is the gradient of an image f , div represents divergence, c is the conduction constant and ∇f is the Laplacian of an image f . The conduction constant is expressed as

$$c = \frac{1}{[1 + (\nabla f / \kappa)^2]} \quad (2)$$

where κ is a gradient threshold parameter that controls conduction as a function of gradient. Four nearest neighbour discretization of Laplacian operator is

$$f_{i,j}^{t+1} = f_{i,j}^t + \lambda [c_N \nabla_N f + c_S \nabla_S f + c_E \nabla_E f + c_W \nabla_W f]_{i,j}^t \quad (3)$$

Here, λ controls the speed of diffusion and takes value of 0.25; ∇ is the nearest neighbor difference in north (N), south (S), east (E) and west (W) direction [16].

AD filtering is implemented by computing the amount of differences ∇ in N, S, E and W directions, determining values of conduction in N, S, E and W directions using eq. 1, computing the diffused image using eq. 2 and repeating the above process for number of iterations (itr) times. The parameters κ and itr are important parameters that influence the quality of de-noised images. A low value of κ indicates that the diffusion process stops in early iterations yielding output image to be similar to input image whereas high values of κ over smoothens the image resulting in blurred image. Hence, optimum value of κ has to be selected. Initially, the set of images obtained by varying itr were subjected to subjective quality assessment followed by selection of optimum value of itr. For the obtained optimum number of iterations, κ value is varied from 5 to 100 in steps of 5 and the value of PSNR value was computed using the formulae

$$PSNR = 20 \log_{10} \left(\frac{255}{\sqrt{\frac{1}{M \times N} \sum_{i=1}^N \sum_{j=1}^M [f - f_t]^2}} \right) \quad (4)$$

Where f is the processed image and f_t is the filtered image. A graph has been plotted for κ versus PSNR and knee point is computed from the graph which determines the optimum value of κ . MSSIM is a quality measure that computes similarity between degraded and filtered image. MSSIM is computed to estimate the performance of the algorithm given by

$$MSSIM(f, f_t) = \frac{1}{MN} \sum_{i=1}^m \sum_{j=1}^n SSIM[f(i, j), f_t(i, j)] \quad (5)$$

$$SSIM = \frac{(2\mu_f\mu_{ft}+C_1)(2\sigma_f\sigma_{ft}+C_2)}{(\mu_f^2+\mu_{ft}^2+C_1)(\sigma_f^2+\sigma_{ft}^2+C_2)} \quad (6)$$

where, C_1 and C_2 are constants described as $C_1 = (M_1L)^2$ and $C_2 = (M_2L)^2$, M_1 and M_2 are constants taking value less than 1, L is the image's dynamic range, μ is the mean and σ is the SD [14]. In eq. 6, local statistics are calculated in 11x11 Gaussian window of standard deviation 1.5; with constants $M_1 = 0.01$, $M_2 = 0.03$ and dynamic range, $L = 255$ [17].

Results and Discussion

Figure 2(a) depicts the acquired frontal thermal breast image and Figure 2(b) depicts the corresponding gray scale converted image. It is perceived that various colors in the acquired image are represented in different shades of gray.

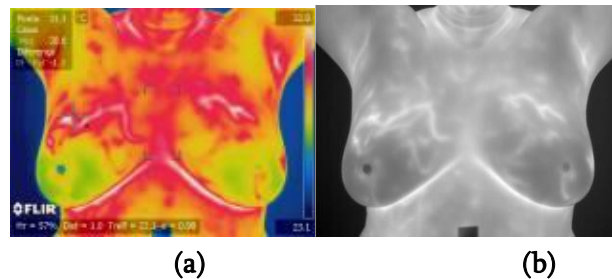


Figure 2. Breast thermogram (a) Color image (b) Gray scale image

To perform denoising of images, the parameters itr and κ have to be carefully selected. First the number of iterations is chosen by visualizing the results obtained for different values of itr . Figure 3(a) represents gray scale image, figure 3 (b)-(d) represents AD filtered images for $itr=5$, 15 and 100 respectively. We can perceive that for $itr=5$, the resultant filtered image is not completely free from noise, for $itr=100$ the filtered image is over smoothed and for $itr=15$, noise is removed and also edges are preserved. Hence $itr=15$ is employed in AD filter.

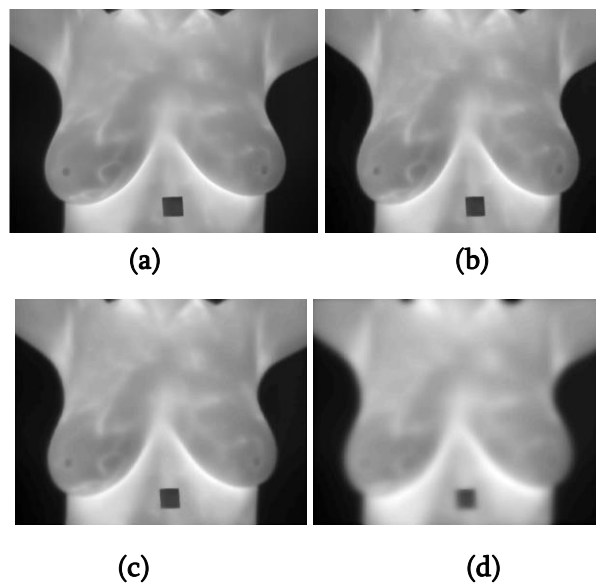


Figure 3. Selection of number of iterations (a) Gray scale image (b) AD filtered image ($itr=5$) (c) AD filtered image ($itr=15$) (d) AD filtered image ($itr=100$)

The value of parameter κ is determined by computing PSNR for κ varying from 5 to 100 in steps of 5 and the obtained results are represented as line plot in figure 4. Knee point is computed from the graph and the obtained knee point value is considered as the gradient threshold parameter. From the graph, the gradient threshold parameter obtained is $\kappa = 25$. Hence all the images considered in the dataset are filtered using itr as 15 and κ as 25.

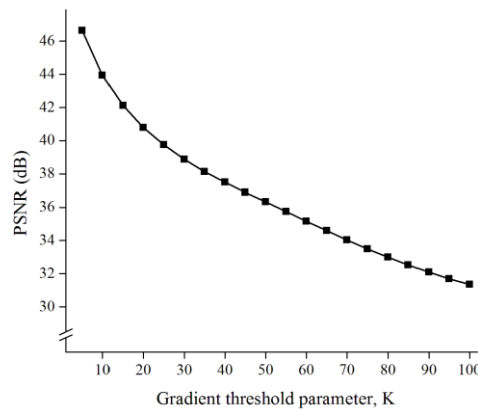


Figure 4. Line plot for determination of κ

Cropped image is shown in figure 5(a) wherein undesired regions are eliminated to some extent. AD filtered image employing the obtained optimal parameters is shown in figure 5(b) and from the obtained image we can observe that the image is smoothed as a result of noise removal and at the same time the edges are clearly visible.

The image quality assessment metrics obtained for de-noised thermograms are $PSNR_{avg}=39.74$ dB, $MSSIM_{avg}=0.9859$. The average value of PSNR above 30 dB represents good quality of de-noised image [18] and average MSSIM close to 1 indicates that the structural information is well retained [17].

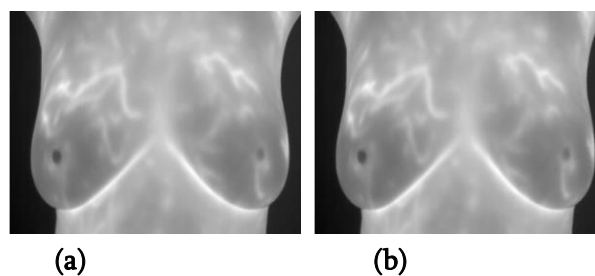


Figure 5. Breast thermogram (a) Cropped image (b) AD filtered image

Table 1 describes comparison of proposed work with other works employing images of different modalities. From the obtained results it is evident that the methodology employed for selection of filter parameters produced better results in terms of PSNR and comparable results in terms of MSSIM when compared to other methods applied on different categories of images.

TABLE 1. COMPARISON OF PROPOSED WORK WITH OTHER WORKS

Sl. No	Methodology	Category of images	Total number of images	PSNR (dB)	MSSIM
1	Enhanced anisotropic diffusion (EADF) based method for Unsharp masking and crispening of images [11]	MRI brain images	10	36.85	0.9921
2	Speckle reduction anisotropic diffusion filter [12]	Uterus ultrasound images	-	28.19	-
3	Anisotropic diffusion filtering [13]	Medical images (5), Satellite images (5), nature images (5) and microscopic images (5)	20	30.42	0.9079
4	Proposed work	Breast thermography images	70	39.74	0.9859

Conclusion

Breast cancer is a common cancer among women and when identified in early stages can save lives. Thermogram is a modality that aids in early detection of cancer. The acquired thermal images are corrupted by noise and are low contrast images. The images need to be processed prior to segmentation or classification. Anisotropic diffusion filter has capability of removing noise along with preserving edges and is hence the preferred type of filter. There are two key filter parameters, number of iterations, *itr* and global threshold parameter, κ that need to be optimally selected. *Itr* is determined by subjective evaluation whereas for κ , knee point is determined from the plot of κ vs PSNR. The above procedure is evaluated by calculating Mean Structural Similarity Index Measure (MSSIM) and the average value obtained is 0.9859 justifying the retainment of structural information in the image. Hence in order to diagnose breast cancer, Computer Aided Diagnosis (CAD) systems can employ the recommended method of parameter selection for an anisotropic diffusion filter.

References

- [1] <https://www.who.int/initiatives/global-breast-cancer-initiative>. [last accessed 5th July 2023]
- [2] <https://medicalnewstoday.com/articles/322832> [last accessed 5th July 2023]
- [3] C. A. Gabriel and S. M. Domchek, "Breast cancer in young women", *Breast Cancer Research*, vol. 12, no. 212, 2010. doi: 10.1186/bcr2647
- [4] R. Sharma, J. B. Sharma, R. Maheshwari and P. Agarwal, "Thermogram Adaptive Efficient Model for Breast Cancer Detection Using Fractional Derivative Mask and Hybrid Feature Set in the IoT Environment",

- Computer Modeling in Engineering & Sciences, Vol. 13, Issue 2, pp. 923-947, 2022. doi: 10.32604/cmcs.2022.016065
- [5] B. V. Solanki and N. Patel, "Thermographic imaging-based breast cancer diagnosis using deep learning", *International Journal of Current Science*, Vol. 13, No. 2, 2023, pp. 938-948. <https://www.ijcspub.org/download.php?file=IJCSP23B1115.pdf>
- [6] R. Gonzalez-Leal, M. Kurban, L.D. López-Sánchez, and F.J. Gonzalez, "Automatic breast cancer detection on breast thermograms", in *15th Quantitative InfraRed Thermography Conference*, Mexico, 2020. doi: 10.21611/qirt.2020.100
- [7] A. A. Edwin Raj, A. Sundaram and T. Jaya, "Advanced framework for effective denoising the enhanced thermal breast image", *IETE Journal of Research*, Vol. 69, No. 1, 2021, pp. 59-72. Doi: 10.1080/03772063.2021.1898481
- [8] Vijaya Madhavi and T. Christy Bobby, "Assessment of asymmetry in bilateral static frontal breast thermograms using difference image and radiomic features", *Biomedical Sciences Instrumentation*, Vol. 57, no. 2, pp. 256-263, 2021. doi: 10.34107/YHPN9422.04256
- [9] J. S. Jeyanathan and A. Shenbagavalli, "The Efficacy of Capturing Lateral View Breast Thermograms," *2019 IEEE International Conference on Clean Energy and Energy Efficient Electronics Circuit for Sustainable Development (INCCES)*, Krishnankoil, India, December 2019, pp. 1-4, doi: 10.1109/INCCES47820.2019.9167722.
- [10] Y. Gherghout, Y. Tlili and L. Souici, "Classification of breast mass in mammography using anisotropic diffusion filter by selecting and aggregating morphological and textural features", *Evolving systems*, Vol. 12, pp. 273-302, 2021. doi: 10.1007/s12530-019-09270-z
- [11] R. R. Kumar, A. Kumar and S. Srivastava, "Anisotropic diffusion based unsharp masking and crispening for denoising and enhancement of MRI images" in *2020 International Conference on Emerging Frontiers in Electrical and Electronic Technologies (ICEFEET)*, Patna, India, 10-11 July 2020, pp. 1-6, doi: 10.1109/ICEFEET49149.2020.9186966.
- [12] K. T. Dina and D. J. Hemanth, "Novel image enhancement approaches for despeckling in ultrasound images for fibroid detection in human uterus", *Open Computer science*, Vol. 11, pp.399-410, 2021. doi: 10.1515/comp-2020-0140.
- [13] S. S. Filwa and S. Nithya Selvakumari "Analysis and Comparison of Edge Preserving Filtering using Bilateral Filtering of Images with Gaussian Kernels and Anisotropic Diffusion Filtering", *European Chemical Bulletin*, Vol. 15, No. S1, pp. 3855-3867, 2023. <https://www.eurchembull.com/uploads/paper/01d5ccda8eb8f0008720818fc0c228ae.pdf>
- [14] L. F. Silva, D. C. M Saade, G. O. Sequeiros, A. C. Silva, A. C. Paiva, R. S. Bravo and A. Conci, "A New Database for Breast Research with Infrared Image", *J. Med. Imaging Health Inf.*, vol. 4, no. 1, pp. 92-100, 2014, doi:10.1166/jmihi.2014.1226.
- [15] [15] S. Budzan and R. Wyzgolik, "Remarks on noise removal in infrared images", *Measurement Automation Monitoring*, Vol. 61, No. 06, 2015. https://yadda.icm.edu.pl/baztech/element/bwmeta1.element.baztech-6a63485c-1dbe-4a00-83e2-4449e3e66210/c/Budzan_remarks_MAM_6_2015.pdf

- [16] P. Perona and J. Malik, "Scale-space and edge detection using anisotropic diffusion", *IEEE Trans. Pattern Anal. Mach. Intell.*, pp. 629- 639, July 1990. doi: 10.1109/34.56205
- [17] Z. Wang, A.C. Bovik, H.R. Sheikh and E.P. Simoncelli, "Image quality assessment: from error visibility to structural similarity", *IEEE Transactions on Image Processing*, vol. 13, no. 4, 2004, pp. 600-612. doi:10.1109/TIP.2003.819861.
- [18] M. Talha, G.B. Sulong and A. Jaffar, Preprocessing digital breast mammograms using adaptive weighted frost filter, *Biomedical Research*, vol. 27, no. 4, 2016, pp.1407-1412.

Sign Language Recognition System based on posture using Seer pipe

Radhamani R, Praveen Kumar K C

Department of ECE, East Point College of Engineering and Technology, Bangalore.

ABSTRACT

Sign language is a visual language that uses hand motions, changes in hand shape, and track information to convey meaning. It is the primary mode of communication for those with hearing and language impairments. The use of sign language for communication is limited, despite the fact that sign language recognition can help a large number of such persons deal with regular people. As a result, there is a need to create a more comfortable approach for people with hearing and language impairments to learn and work in order to improve their lives. Therefore, the basic idea behind this article is to make the communication between normal human beings and deaf people much easier. In order to recognize static postures associated with sign language alphabet and a few commonly used words, we conducted a comprehensive research study employing the hand tracking technique Seerpipe and a posture classification model based on Support Vector Machine (SVM). The results of the experiments are validated using Recall, F1 Score and Precision. Based on the validated results, we recommend the application of the discussed techniques for such communication. The suggested methods have high generalization qualities and deliver a classification accuracy of around 99 percent on 26 alphabet letters, numerical digits, and some regularly used words.

Keywords : Machine Learning, Seerpipe, SVM, Sign Language, Posture recognition, Assistive technology.

I. INTRODUCTION

Humans communicate with one another using natural language channels such as words and writing, or by body language (postures) such as hand motions, head postures, facial expression, lip motion, and so forth.

Comprehending sign language is equally as vital as understanding natural language [13]. People with hearing impairment use sign language as their preferred mode of communication. Without a translation, people with hearing impairments have difficulty speaking with other hearing people. As a result, implementing a system that understands sign language would have a substantial positive impact on the social lives of deaf people. According to the World Health Organization, 466 million individuals worldwide (more than 5 percent of the population) have impaired hearing, with 34 million of them being teens (WHO). According to studies, by 2050, these numbers will have surpassed 900 million. Furthermore, the majority of cases of profound hearing loss, which afflict millions of individuals, occur in low and middle-income nations [2]. Furthermore, the majority of cases of substantial hearing loss, which affects millions of individuals, occur in low- and middle-income nations.

There are more than 135 distinct sign languages spoken worldwide, including American Sign Language (ASL), British Sign Language (BSL), and Indian Sign Language (ISL) [15].

Machine learning enables the development of systems that accurately interpret sign language, which can greatly improve communication and social lives of deaf people. These technologies are particularly important for those living in low and middle-income nations where the majority of hearing impairments occur. The growing prevalence of hearing loss worldwide highlights the urgent need for technological solutions to help bridge the communication gap between hearing-impaired individuals and the rest of society. Machine learning is a branch of artificial intelligence that deals with the methods that let computers extract meaning from data and create AI applications. In the meanwhile, deep learning is a subset of machine learning that enables computers to resolve increasingly challenging issues [11]. As deep learning develops transferable answers, it is more powerful than traditional machine learning. Through neural networks, or layers of neurons/units, deep learning algorithms are able to produce transferable solutions [12]. Deep learning is a subset of machine learning where a computer program learns to carry out classification operations on complex input such as images, text, or sound. These algorithms are able to execute at a state-of-the-art (SOTA) level of accuracy and, in certain situations, even surpass humans. Numerous labeled data points and intricate neural network topologies are used to learn them. It is a vital part of modern innovations like self-driving cars, virtual assistants, and face recognition. In our research, we have thoroughly examined the existing literature on Sign language recognition. We will now focus on the most notable research papers and discuss their methods for feature extraction, image pre processing, and image classification, which employ a variety of algorithms including SVM, KNN, and CNN.

Additionally, we have examined several image- processing techniques, including Canny-edge detection, Convex-hull algorithm, and Gaussian blur filter, among others. A Microsoft Kinect camera was used to create a sign language recognition system in [6]. This was chosen to allow the whole programme to be independent of restrictions such as poor illumination, loud input, and so on. Depth and Motion were the two main feature capturing modules used in their methodology. In fact, a feature vector was calculated for each frame of the video series, and some pre processing was applied to each frame to eliminate undesired noise and provide a clean image of the depth map. They used the Gaussian blur filter 15 and the Erosion filter to do this and also presented the depth information using a 256-bin histogram for a depth image. They were able to create the feature matrix for that particular video sequence or posture using the combined array of feature vectors from all of the frames in the video sequence. Following this pre-processing, the feature matrix was given as an input to a multi-class SVM classifier to construct an appropriate Machine Learning model for classification of the test files using kernel functions, with the linear and RBF kernels being specifically employed. The total accuracy achieved was between 81.48 and 87.67 percent. However, this work was unable to investigate other high-level characteristics such as optical flow information, motion gradient information, and so on, which may have improved accuracy performance. A more precise real-time Hand Posture Recognition (HGR) system based on American Sign Language is the primary goal of [8], which is to illustrate (ASL). The combination of K-curvature and convex hull approaches is proposed as a novel feature extraction technique. This method, known as the "K Convex Hull" technique, can recognize fingers with extreme precision. An ANN is used in this system together with feed forward and reverse propagation techniques to train a network with 30 feature vectors to accurately identify 37 indications of American alphanumeric letters, which is beneficial for HCI applications. The entire posture recognition rate of this system in a real-time scenario is 94.32 percent. [19] reviews and compares

several algorithms and techniques for creating single hand posture detection systems utilizing various vision-based methodologies. The research uses the hand's fundamental structure as well as properties like centroid to identify the pattern the fingers and thumb generate and assign code bits, i.e., changing each posture into a set of 5 digits representation. Motion is recognized using centroid movement in each frame. The study uses techniques like K-means clustering or thresholding for background removal, Convex Hull or a custom peak identification algorithm, and text to voice API to translate posture-related words and phrases into speech. The Convex Hull algorithm is used to identify the smallest convex polygon that contains every point from the frame.

II. Dataset

In this work, we have utilized the ASL dataset [20] consisting of 51 classes, with approximately 4000 images per class. The classes comprise the alphabet, numbers, and commonly used words such as 'Hello', 'Help', and 'Stop'. The alphabet class enables the formation of new words through fingerspelling, where individual letters are used to represent words without a designated sign symbol. A Python script was employed to efficiently convert the image class folders into a .csv file, which stores the (x, y, z) coordinates of all landmark points of each sign with their respective outputs. An 80:20 train-test split was implemented to improve the model's feature extraction process.



Fig1: Various Sign symbols

III. Seerpipeline

Sign language recognition has the potential to improve the situation of a large number of disabled people while dealing with normal human beings but the use of sign language for communication is limited. As a result, there is a need to create a more convenient approach for persons with hearing impairments to learn and work in order to improve their lives. Posture recognition has been studied extensively utilizing traditional techniques such as body component tracking, different color glove-based tracking, Kinect depth sensor tracking, and skeleton tracking. Multiple methods have been used to solve this problem like modified CNN, image segmentation, SVM and deep

learning. Many machine learning algorithms have been developed for hand posture recognition so as to create AI-based applications. Out of them, Seerpipe can be used for hand posture recognition. Google supported Seerpipe framework can be used for solving several problems like face-recognition, face-map, eye, hand, poseestimator, holistic, hair, object-detection, box tracking and KIFT. With the help of the Seerpipe framework, we can develop an algorithm or model for the application, then help the application by providing results that can be cloned across different platforms. The Seerpipe framework is composed of three major components: (1) performance evaluation, (2) a mechanism for collecting data from the sensor (3) an assembly of reusable parts. A graph consisting of all the parts called the calculators is known as pipeline, wherein every calculator is interconnected by channels through which the data flows. Developers can create their required application by removing or delineating

user defined calculators anywhere in the graph. This result of calculators and channels creates a data-flow diagram.

Hand posture recognition with the Seerpipe framework is a dependable and high-fidelity hand and finger tracking system. Seerpipe hands uses an integrated ML pipe of several models working together [18]: (1) A palm recognizer processes the captured hand image, (2) A hand landmark model takes processed image as input and returns hand with 3D key points as output. (3) A posture recognition model which processes the 3D hand key-points and classifies them into a discrete set of postures.

The palm detection model outputs a precisely cropped picture of the palm that is then sent to the landmark model. This method does away with data augmentation, which is used in deep learning models [5] to rotate, flip, and scale images. The technique of detecting hands is time-consuming and difficult since it involves working with different hand sizes, thresholding, and image processing. Prior to identifying hands with connected fingers, a palm detector is trained, which estimates bounding boxes around hard objects like fists and the palm. The second method is to utilize an encoder-decoder as an extractor for a larger scene context [14].

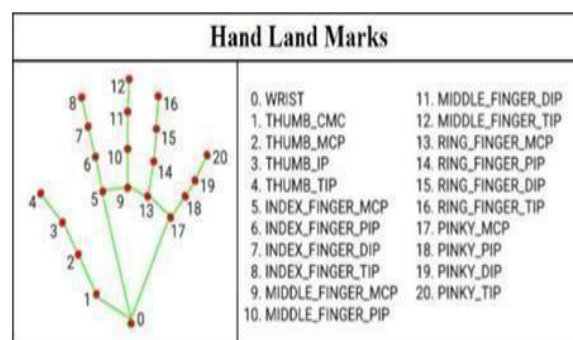


Fig2: Hand Landmark

Hand-knuckles of the landmark have x, y, and z coordinates where x and y are normalized to [0, 1] as width and height of the image, while z represents the depth of the landmark. The closer the landmark to the camera, the value of z becomes smaller.

IV. Experimentation

In order to achieve our desired objective, we have created an end-to-end web application that allows real-time communication between common people and deaf people without any use of hardware technologies like sensors, microcontrollers, etc. This website makes user interaction comfortable as it consists of combined

application of Sign to Text and Text to Sign conversion, along with other essential features. To create this application, we have made use of multiple technologies and frameworks. HTML, CSS and JavaScript tools are used for Frontend and Flask (a Python web framework) is used for Backend. In Backend, the machine learning model is loaded in the form of a pickle (.pkl) file. This .pkl file allows easy serialization and deserialization of any ML model.

The functionality of our website is that it takes the webcam video as the input which captures our hand image. Later, Seerpipe technique is applied to this extracted image and key points are marked accordingly which then stores the (x, y, z) coordinates of the landmarks. Last but not least, this data is sent into the Support Vector Machine classifier, a supervised machine learning classifier (SVM). Regression and classification studies both use the SVM model. Finding the most important dividing line is done using it. The primary objective of this approach is to identify the best hyperplane for dividing and separating training vectors. Using gamma as the RBF parameter, SVC is an SVM classifier (Radial basis function kernel). To determine if a model is overfitting, underfitting, or providing the optimum fit, one uses the gamma value. The pickle (.pkl) module was utilized to load the two files, X and y, which are data files used for training the SVM model. The X file contains a list of image pixels, while the Y file contains labels for the list of pixels. After loading the dataset, it is passed to the model for training purposes.

The SVM model is represented by the equation:

$$f(x) = \text{sign}(\text{sum}(\alpha_i * y_i * \exp(-\text{gamma} * \|x_i - x\|^2)) + b) \quad \dots\dots\dots (1)$$

where α_i are the Lagrange multipliers, y_i are the corresponding labels, $\exp(-\text{gamma} * \|x_i - x\|^2)$ is the RBF kernel function, x represents the input feature vector, and b is the bias term. The hyperparameters C and gamma are typically determined through a grid search or cross-validation process. Once the model is trained, the webcam images are passed to the model for testing. The model recognizes the corresponding letter/word and outputs it on the screen.

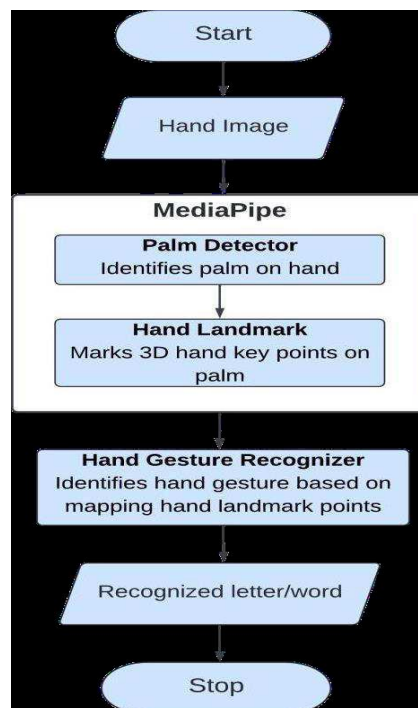


Fig3: Methodology

V. Results

Various machine learning models are used for sign detection. These models are evaluated based on parameters like accuracy, recall, F1 score, etc. Among the utilized models, it is observed that SVM outperformed other machine learning techniques such as Naive Bayes, KNN, Decision Tree, etc. by achieving an accuracy of 98.65% (training) and 98.35% (testing) as shown in table 0. The reason it outperformed is because of its effectiveness in high- dimensional spaces where it draws a hyperplane boundary in order to classify the labels. The below table shows the values of training and testing accuracy along with Recall, F1Score and Precision for different tried models:

The below confusion matrix for SVM algorithm prints the correct and incorrect values in number count which gives us a good data visualization.

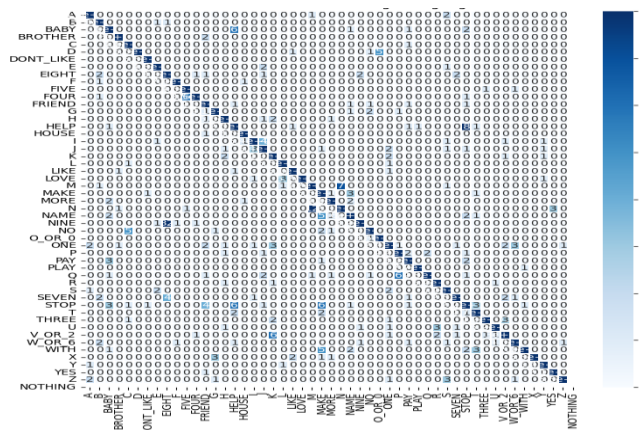


Fig4: Confusion Matrix for SVM Model

The output images captured for some of the real time inputs are shown below:

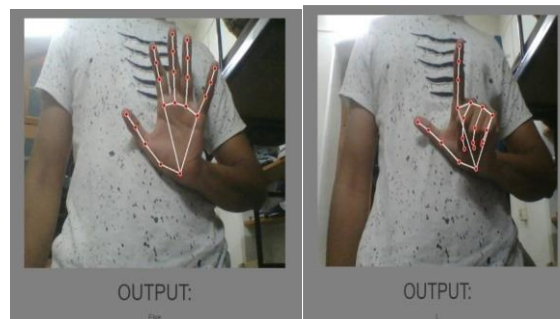


Fig5: Output 5 and L

Results obtained in [12] and [5] are less accurate due to the use of ineffective feature extraction approaches and inappropriate models. Despite using the same dataset, accuracy mentioned in [22] is around 94.88%. Additionally, some of the research papers have attained an accuracy of about 99%, however these articles employ a small dataset with a small number of classes. Our machine learning approach is suitable for use in mobile applications since the learned model is deliberately light. Our methodology’s real-time sign language identification makes it quick, reliable, and especially flexible for smart devices. Seerpipe makes feature extraction simple by deconstructing and analyzing challenging hand-tracking data. This strategy uses less computer resources and takes less time to train the model than other cutting-edge approaches.

This table compares the effectiveness of different preprocessing techniques and algorithms on our dataset and simpler datasets. It includes the preprocessing technique and algorithm used, along with the training accuracy and validation/test accuracy achieved by each technique. As shown in table 1, several preprocessing techniques were tested, including convex hull, Gaussian blur, and Canny edge detection. The algorithms used included CNN, VGG, ResNet, and EfficientNet. After analyzing the results from the experiments using the techniques and algorithms presented in the above table, we found that they did not yield satisfactory performance on our dataset. Therefore, we decided to discard these techniques and algorithms and explore other approaches to achieve better results.

Table 1 : Comparative Analysis of Accuracy for Various Models and Preprocessing Techniques with Simpler Datasets

Preprocessing & Algorithm	Training Accuracy	Validation/ Test Accuracy
Convex Hull + CNN	99.54%	91%
Gaussian Blur + CNN	89.8%	91%
Gaussian Blur + VGG	84.66%	84.92%
Canny Edge Detection + VGG	93.71%	93.69%
Convex Hull + ResNet	94.03%	91.98%
Convex Hull + EfficientNet	90.68%	90%

Table 2 : Performance Comparison with Similar Techniques

Type of Dataset	Our Accuracy	Existing/Others Accuracy
Alphabets only	99.43%	99.15% [7]
Alphabets, Numbers, and Words	98.975%	98.62% [7]

Based on our analysis, we could improve the accuracy of the model by adjusting the parameters. The improvement in accuracy was found to be around 0.28% to 0.35%. Our experiments also revealed that the model tends to overfit at higher values of C, and the choice boundary's curvature weight decreases with lower values of gamma. As a result, the areas separating different classes become more generic. After tuning the parameters, we were able to identify the optimal decision boundary for our dataset at C = 52 and gamma = 0.6.

VI. CONCLUSION

Individuals with hearing disabilities often face significant challenges in communicating with people who can hear. One of the most effective ways for them to communicate is through sign language. However, for people who do not know sign language, understanding what is being communicated can be a significant challenge.

This communication gap can have a detrimental impact on the social and emotional well-being of individuals with hearing disabilities, making it difficult for them to engage fully in society.

The proposed Sign Language Recognition system offers an innovative solution to the communication gap between individuals with hearing disabilities and those who can hear. The proposed system successfully recognizes sign language with high accuracy, with an SVM model achieving a classification accuracy of 98.975%. Moreover, the use of Google's Seerpipe palm detector method has made the system accessible to people without any special hardware, which is a significant advantage.

The proposed method's potential for practical applications is considerable, and it has the capacity to improve the quality of life for individuals with hearing disabilities, helping to bridge the communication gap between them and the rest of the world. Future work will expand the current system to add more indicators and create complete and reliable system for mobile platforms. Additionally, the proposed method can be adapted for use in other Indian regional languages, such as Hindi, Kannada, Malayalam, Telugu, and more.

Although there are still some research gaps that need to be addressed, such as improving the system's accuracy in recognizing signs for complex phrases and developing a portable and affordable device for practical use in daily life, the proposed Sign Language Recognition system offers a promising step towards creating a more inclusive society. With further development and refinement, this system can play a significant role in breaking down communication barriers and facilitating greater accessibility and understanding for individuals with hearing disabilities.

REFERENCES

- [1] Akoum, Alhussain, and Nour Al Mawla. "Hand gesture recognition approach for ASL language using hand extraction algorithm." *Journal of Software Engineering and Applications* 8.08 (2015): 419.
- [2] Bandgar, Bapurao. "Implementation of Image Processing Tools for Real-Time Applications." *International Journal of Engineering Research & Technology (IJERT)* 10.07 (2021).
- [3] Bazarevsky, Valentin, and G R Fan Zhang. "On-Device MediaPipe for Real-Time Hand Tracking." (2019).
- [4] Brahmankar, Vipul, et al. "Indian Sign Language Recognition Using Canny Edge Detection." *International Journal* 10.3 (2021).
- [5] Das, P., T. Ahmed, and M. F. Ali. "Static Hand Gesture Recognition for American Sign Language Using Deep Convolutional Neural Network." *2020 IEEE Region 10 Symposium (TENSYP)* (2020): 1762-1765.
- [6] Devineau, G., F. Moutarde, W. Xi, and J. Yang. "Deep Learning for Hand Gesture Recognition on Skeletal Data." *2018 13th IEEE International Conference on Automatic Face & Gesture Recognition (FG 2018)* (2018): 106-113.
- [7] Halder, Arpita, and Akshit Tayade. "Real-Time Vernacular Sign Language Recognition Using MediaPipe and Machine Learning." *International Journal of Recent Technology and Engineering (IJRTE)* 10.2 (2021): 7421.
- [8] Islam, M. M., S. Siddiqua, and J. Afnan. "Real-Time Hand Gesture Recognition Using Different Algorithms Based on American Sign Language." *2017 IEEE International Conference on Imaging, Vision & Pattern Recognition (icIVPR)* (2017): 1-6.
- [9] Jin, C. M., Z. Omar, and M. H. Jaward. "A Mobile Application of American Sign Language Translation via Image Processing Algorithms." *2016 IEEE Region 10 Symposium (TENSYP)* (2016): 104-109.
- [10] Khan, Rafiqul Zaman, and Noor Adnan Ibraheem. "Hand Gesture Recognition: A Literature Review." *International Journal of Artificial Intelligence & Applications* 3.4 (2012): 161.

- [11] Li, Y., X. Wang, W. Liu, and B. Feng. "Pose Anchor: A Single-Stage Hand Key Point Detection Network." *IEEE Transactions on Circuits and Systems for Video Technology* 30.7 (2020): 2104-2113.
- [12] Martinez-Martin, Ester, and Francisco Morillas-Espejo. "Deep Learning Techniques for Spanish Sign Language Interpretation." *Computational Intelligence and Neuroscience* 2021 (2021).
- [13] Pal, D. H., and S. M. Kakade. "Dynamic Hand Gesture Recognition Using Kinect Sensor." 2016 *International Conference on Global Trends in Signal Processing, Information Computing and Communication (ICGTSPICCC)* (2016): 448-453.
- [14] Raheja, J. L., Anand Mishra, and Ankit Chaudhary. "Indian Sign Language Recognition Using SVM." *Pattern Recognition and Image Analysis* 26.2 (2016): 434-441.
- [15]. Shriram, S., Nagaraj, B., Jaya, J., Shankar, S., & Ajay, P. (2021). Deep Learning Based Real-Time AI Virtual Mouse System Using Computer Vision to Avoid COVID-19 Spread. *Journal of Healthcare Engineering*, 2021, 8133076.
- [16]. Singha, J., & Das, K. (2013). Hand gesture recognition based on Karhunen-Loeve transform. *arXiv preprint arXiv:1306.2599*.
- [17]. Trigueiros, P., Ribeiro, F., & Reis, L. P. (2012). A comparison of machine learning algorithms applied to hand gesture recognition. In *7th Iberian Conference on Information Systems and Technologies (CISTI 2012)* (pp. 1-6).
- [18]. Zhang, F., Bazarevsky, V., Vakunov, A., Tkachenka, A., Sung, G., Chang, C. L., & Grundmann, M. (2020). *MediaPipe Hands: On-device Real-time Hand Tracking*. *arXiv preprint arXiv:2006.10214*.
- [19]. Zivkovic, Z., & Van Der Heijden, F. (2006). Efficient adaptive density estimation per image pixel for the task of background subtraction. *Pattern recognition letters*, 27(7), 773-780.
- [20]. <https://www.kaggle.com/datasets/belalelwikel/asl-and-some-words?select=ASL>.
- [21]. <https://google.github.io/mediapipe/solutions/hands.html>.
- [22]. <https://www.kaggle.com/code/vaishnaviasonawane/asl-recognition-model-training-revisited>.

Energy Conservation through Energy Audit in LT2 Consumers

Avinash B C, Kiran Kumar Kommu, Rajesh K

Assistant Professor, Department of Electronics & Communication Engineering, East Point College of Engineering and Technology Bengaluru

ABSTRACT

Electricity bill or consumption rate is growing at exponential rate in Low Tension i.e 230V ,1 phase consumers because of various reasons like modern life style, inductive loading, improper knowledge of consumption.

Energy audit in LT-2 consumers gives scope of setting benchmark of consuming around 100 units kwh energy or reduction of around 20 percent of kWH consumption, low cast and safe compensation of reactive power KVAR through pf capacitor at consumer premises without affecting comfort and security of the consumer and also we emphasis on right use of illumination as the standard level and maintenance factor.

Keywords— KWH, KVAR, energy audit, illumination, maintenance factor, pf capacitor.

I. INTRODUCTION

Energy Audit is an inspection, survey and analysis of energy flows for energy conservation in a building or system to reduce the amount of energy input to the system without negatively affecting the output..

As per the Energy Conservation Act, 2001, Energy Audit is defined as “the verification, monitoring and analysis of use of energy including submission of technical report containing recommendations for improving energy efficiency with cost benefit analysis and an action plan to reduce energy consumption”.

It is an effective and concrete method to achieve rapid improvement in energy efficiency in buildings and industrial process First step in identifying opportunities to reduce energy expense. Which is a Systematic procedu.re includes some steps. Energy auditing is also called as Energy assessment, Energy survey etc...

The objectives are production & quality

- To minimize energy costs / waste without affecting
- To minimize environmental effects.

The primary objective of Energy Audit is to determine ways to reduce energy consumption per unit of product output or to lower operating costs. Energy Audit provides a “bench-mark” for managing energy in the organization and also provides the basis for planning a more effective use of energy throughout the organization.

Statistical review of world energy

Focus/Methodology : Percentage increase in power consumption and carbon emission in India

Published : August 8,2020

Conclusion : Indian Power Consumption Growth rate per annum:

- From the year 2008-18 – 5.2%
- From the year 2019 - 2.3%
- Power share on year 2019 – 5.8%

Carbon dioxide emission in India , Growth rate per annum:

- From the year 2008-18 – 5.3%
- From the year 2019 - 1.1%
- Share on the year 2019 – 7.3%

The lighting hand book Focus/Methodology : lighting technology Published : August 8,2013

Conclusion : Basic parameters used in lighting:

Luminous flux- Luminous intensity – Illuminance –Luminance Quality Characteristics of Lighting: Glare – glare limitation

1. Direct glare 2. Reflected glare

I. cause

-Luminaries without glare control -Reflective surfaces

-Very bright surface -Incorrect luminaire arrangement

-Incorrect workstation position

II. Effect

-Loss of concentration-More frequent mistakes -Fatigue

III. Remedy

-Luminaires with limited -Matching luminaire to luminance level workstation (layout)

-Blinds on windows -Indirect lighting

-Matt surface

Preliminary Energy Audit Flowchart

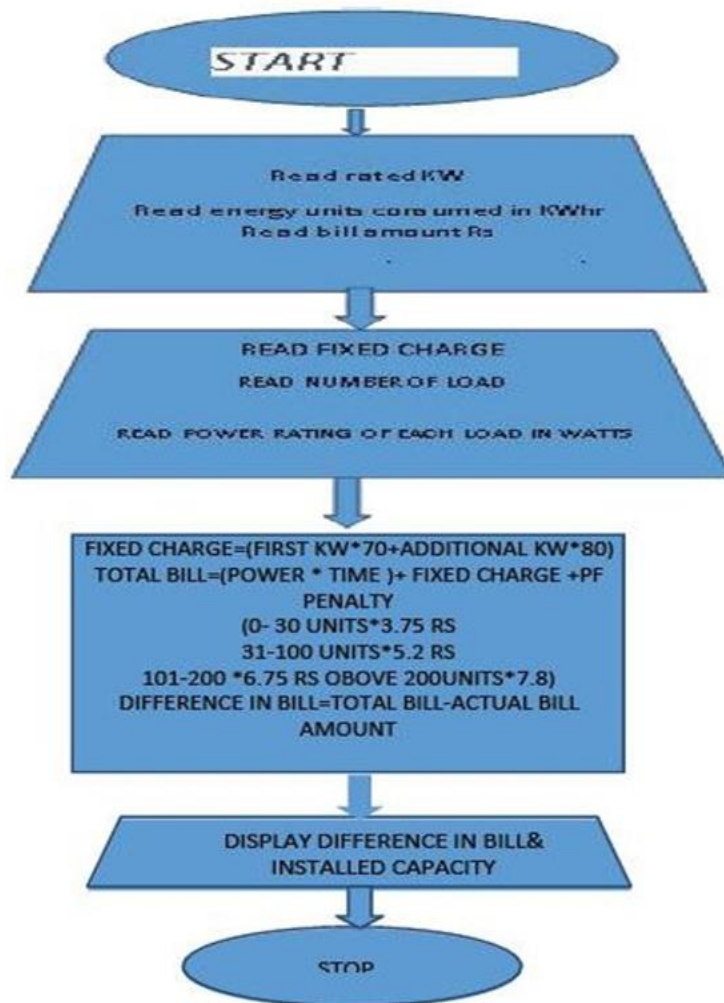
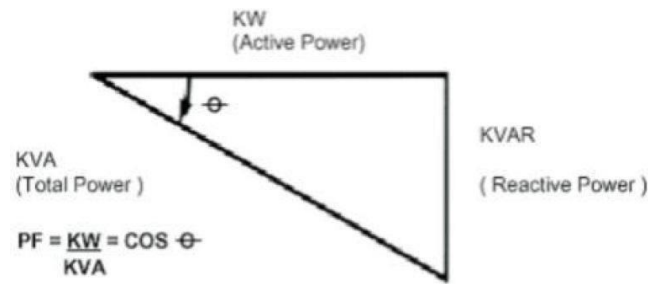


Fig 1: preliminary audit calculation

POWER FACTOR CALCULATION In all industrial electrical distribution systems, the major loads are resistive and inductive. Resistive loads are incandescent lighting and resistance heating. In case of pure resistive loads, the voltage (V), current (I), resistance (R) relations are linearly related, i.e. $V = I \times R$ and Power (kW) = $V \times I$

Typical inductive loads are A.C. Motors, induction furnaces, transformers and ballast type lighting. Inductive loads require two kinds of power: a) active (or working) power to perform the work a b) reactive power to create and maintain electromagnetic fields. Active power is measured in kW (Kilo Watts). Reactive power is measured in KVAR (Kilo Volt- Amperes Reactive). The vector sum of the active power and reactive power make up the total (or apparent) power used.

This is the power generated by the SEBs for the user to perform a given amount of work. Total Power is measured in KVA (Kilo Volts-Amperes) Managers and Energy Auditors conducted by Bureau of Energy Efficiency, Government of India.

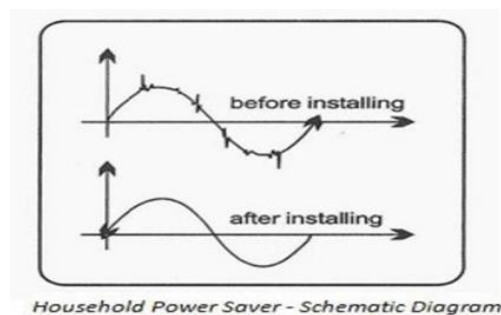


The active power (shaft power required or true power required) in kW and the reactive power required (KVAR) are 90° apart vertically in a pure inductive circuit i.e., reactive power KVAR lagging the active KW. The vector sum of the two is called the apparent power or KVA, as illustrated above and the KVA reflects the actual electrical load on distribution system.

SCOPE OF PROJECT

It is known that the electricity that comes to our homes is not stable in nature. There are many fluctuations, raise and falls, and surges/spikes in this current. This unstable current cannot be used by any of the household appliances. Moreover, the fluctuating current wastes the electric current from the circuit by converting electrical energy into heat energy. This heat energy not only gets wasted to the atmosphere, but also harms the appliances and wiring circuit.

Power Saver stores the electricity inside of it using a system of capacitors and they release it in a smoother way to normal without the spikes.



1) Cost Saving (Improve the P.F)

Reactive power control can regulate the voltage. But installation of reactive power equipment required investment.

Consider a simple two-part tariff given by,

$$T = x \cdot \text{KVA} + y \cdot \text{kwh}$$

here x is charge for KVA, y is charge for kwh.

Let us draw an active power P_1 at a power factor $\cos \phi_1$

the KVA is $P_1 / (\cos \phi_1)$

If now the power factor is improved to $\cos \phi_2$ the new KVA is $P_1 / (\cos \phi_2)$

The saving in cost is $x[(P_1 / \cos \phi_1) - (P_1 / \cos \phi_2)]$

The reactive power required to change the power factor is $[P_1 \tan \Phi_1 - P_1 \tan \Phi_2] (\text{KVAR})$

If the cost of installation is Rs C/(KVAR) Then total cost of installation is

$CP_1 [\tan \Phi_1 - \tan \Phi_2]$ hence the net saving is given by $\text{Saving} = x P_1 [(1/\cos \Phi_1) - (1/\cos \Phi_2)] - CP_1 [\tan \Phi_1 - \tan \Phi_2]$ Rs

Maximum saving is obtained when $d[\text{saving}]/(d\Phi_2) = 0$

or $\sin \Phi_2 = C/x$

2) INSTRUMENTS USED IN THE ENERGY AUDIT

- Lux Meters
- CLAMP on METER
- ENERGY METER 1 phase and 3

DETAILED ENERGY AUDIT ANALYSIS

3) Data collected from domestic load 1

CONCLUSION

From above analysis, energy conservation through energy audit has shown tremendous improved results. During lighting audit, the main objective is to improve the lighting efficiency without affecting the productivity and visual comfort. For improvement of lighting efficiency we have improve luminous efficiency and for greater luminous efficiency LED is the best option. For energy conservation we replace old luminaries with new efficient LED lamps and by replacing luminaries we can save the energy up to 3.536kW. By replacing old luminaries

we can reduce lighting load by 40.47%. For that we have invest Rs.2,30,740 and from that we can save Rs.12237.39 per month. Payback period for this investment is 18 months

i.e. 1 year 6 months. Also during load management audit, we calculated that how much and what type of load is available in industry, and duration of working hours for one day and one month. Also calculate load curve of one day which defines how energy is used in industry. Load curve

also shows peak load hours are at 9am to 1pm and non-peak load hours is at 11pm to 6am.

Electric load management helps to reduce unnecessary load, also separate metering helps to evaluate production cost.

DATA COLLECTION

Consumer Type	Sl.No	Light Load	Power Rating	Actual Power Consumption	Time of Consumption in hr	Illuminance in Lux (without msc)	Illuminance in Lux (with msc)	Power Factor	HVAC Load	Power Rating	Time of Consumption in hr	Power Factor
LT2(1)	1	LED Lamp	40	38.9	4	98	105	0.7	1	Ceiling fan	4	0.9
Allotted KW	2	Incandescent	60	62	1	49	53	0.94	2	Ceiling fan	6	0.91
0.48kw	3	LED	40	39	1	96	103	0.7	3	Ceiling fan	7	0.9
Unit Consumed	4	Incandescent	60	61	1	46	51	0.93	4	Water Heater	1/2	0.95
108	5	LED	9	7	0	42	51	0.7	5	Television	9	0.7
	6	LED	40	39	2	99	105	0.71	6	Refrigerator	24	0.6
	7	LED	9	14	1	47	54	0.71	7	Sump pump	5	0.86
	8	LED	18	21	2	72	79	0.68				
	9	CFL	12	16	2	43	47	0.84				



Fig.-2. Audit data collection

Billing Before and After Implementation

Fig: Glimpse of electricity bill before and after energy audit

Result

Load curve

also shows peak load hours are at 9am to 1pm and non-peak load hours is at 11pm to 6am.

Electric load management helps to reduce unnecessary load, also separate metering helps to evaluate production cost.



Illumination level before and after maintenance



Reference

- [1] Bureau of energy efficiency guide books, book 1, chapter 03 "Energy Management and Audit", page no. 54-78.
- [2] Sandip Ballal, "Energy Performance Important and Energy Cost Reductions at Baltic Place Commercial Office Complex", thesis published in STAFFORDSHIRE University, February 2016, page no.1- 64.
- [3] Rakiba Rayhana, "Electric and Lighting Energy Audit: A Case Study of Selective Commercial Buildings in Dhaka", 2015 IEEE international WIE conference on 20 December 2015, page no 1-4.

- [4] Barney L. Capehart, "Guide to Energy Management", Book published by The Fairmont Press, Inc 2003, Chapter no 5.
- [5] Rajesh Tilwani, "Energy saving potentials in building through energy audit – A case study in an Indian building", published in 2015 IEEE International Conference on Technological Advancement in Power & Energy, June 2015 page no 289-293.
- [6] Sonal Desai, "Handbook of Energy Audit", Book published by McGraw Hill (India) Private Limited, 2015, chapter 1 & 2.
- [7] Shailesh K. R., "Energy consumption optimization in classrooms using lighting energy audit", Research and technology in coming decades (CRT 2013), IEEE National Conference, 27-28 Sept. 2013, page no.1-5.
- [8] Muhammad Usman Khalid, "Energy Conservation through Lighting Audit", 2012 IEEE International Conference on Power and Energy, 2-5 December 2012, page no.840-845.
- [9] G. Paris, "Combined electric light and day light systems Ecodesign", IEEE Industry Applications Society Annual Meeting (IAS), 2011, page no. 1-5.
- [10] Jian Zhang, "How to Reduce Energy Consumption by Energy Audits and Energy Management: The Case of Province Jilin in China", Technology Management in the Energy Smart World (PICMET), 2011 Proceedings of PICMET '11, September 2011, page no. 1-5.
- [11] J. A. Qureshi, et al., "Demand Side Management through innovative load control" in TENCON 2010 - 2010 IEEE Region 10 Conference, 2010, page no. 580-585.